Understanding the hydrological performance of a permeable pavement

Majed Alsubih

Submitted for the degree of Doctor of Philosophy

Heriot-Watt University

School of Energy, Geoscience, Infrastructure & Society

March 2016

ABSTRACT

Permeable pavements play an essential role in urban drainage systems, making them the subject of great interest to both researchers and practitioners. However, previous studies have demonstrated a significant degree of uncertainty regarding both the hydrological performance and the maintenance requirements of this type of pavement. Within this context, a one metre square surface area of permeable pavement and a laboratory rainfall simulator were constructed to investigate the influence of rainfall intensity on the hydrologic response of permeable pavements. The hydrological performance of permeable pavement was tested under clean laboratory conditions and under the influence of sedimentation. The design of the permeable pavement test rig complied with the SuDS manual guidance and British Standards (BS 7533-13:2009). Simulated rainfall event results demonstrate that the hydrologic performance of the pavement varied according to the rainfall intensity and duration. More than 40% of the total rainfall from all rain events was temporarily detained within the structure. The total volume of discharge from the permeable pavement ranged from 8% to 60% of the inflow, illustrating the storage capacity of the pavement. The results of the simulation showed that the outflow reduction due to the application of sediment was 6.4% within the first ten years. The reduction in outflow volume was a result of the increasing water content within the pavement structure over time. The impact of sediment addition on the pavement surface was evident in the third year of the simulation. The concentration of suspended solids in the outflow showed a slight variation following the addition of the sediment, but remained low. Further analysis showed the outflow duration increased over time and no temporary ponding occurred on the surface during the ten-year simulation.

Acknowledgments

I am forever in debt to my primary supervisor, Dr Scott Arthur. He was and always there, whenever I need help. When I started my PhD, my daughter diagnosed with a bilateral profound sensorineural hearing loss, and this diagnosis has required much of my time to look after my little girl. I remembered he said ‘’family first ‘’, so these two words gave me a great motivation that I could finish my study and at the same time as looking after my daughter. It is no understatement to say that without his support, guidance and continual encouragement, this thesis would not have been completed.

I am very thankful for the support and assistance I received from my co-supervisor, Dr Grant Wright, also my supervisor during my MSc. He has been very helpful and source of inspiration. During my PhD, he has added valuable contribution to this research.

I would like also to extend my thanks to Mr Alistair McFarlane for his interest and support, especially in the geotechnical lab, software and electrical issues associated with this research equipment. I would also express my thanks to the technical staff of the built environment at Heriot-Watt University for their support. Many thanks go to Mr Tom Stenhouse for his assistance in resolving operational problems with my experiment, to Mr David Marry for his assistance during the construction and operating the research rig, and to Mr Hugh Barras for his support and provision of equipment.

Many thanks go to King Abdullah Foreign Scholarship Program and Royal Embassy of Saudi Arabia Cultural Bureau in London for generous funding. Also, I would like to thank my relatives and friends for all support and love. Also, I would like to thank Mrs Deonie Allen for her support, advice, valuable comment through my writing up stage.

Finally and most importantly, I would also like to say a heartfelt thank: to my parents Mr Abdullah and Slma Alsubih and to my siblings for their love and support through my life. To my children, Mayas, Wasn, and Abdullah for being patient while I was busy during weekends and holidays. To my wife Amal who has been by my side throughout this PhD, living every single minute of it, I really couldn’t have done it without her costly scarifies.

ACADEMIC REGISTRY

Research Thesis Submission

Name*:*	Majed Alsubih		
School/PGI:	School of the built Environment IIE		
Version: *(i.e. First, Resubmission, Final)*	Final	Degree Sought (Award **and** Subject area)	Doctor of Philosophy (Civil Engineering)

Declaration

In accordance with the appropriate regulations I hereby submit my thesis and I declare that:

1) The thesis embodies the results of my own work and has been composed by myself
2) Where appropriate, I have made acknowledgement of the work of others and have made reference to work carried out in collaboration with other persons
3) The thesis is the correct version of the thesis for submission and is the same version as any electronic versions submitted*.
4) my thesis for the award referred to, deposited in the Heriot-Watt University Library, should be made available for loan or photocopying and be available via the Institutional Repository, subject to such conditions as the Librarian may require
5) I understand that as a student of the University I am required to abide by the Regulations of the University and to conform to its discipline.

* *Please note that it is the responsibility of the candidate to ensure that the correct version of the thesis is submitted.*

Signature of Candidate*:*		Date:	

Submission

Submitted By *(name in capitals):*	
Signature of Individual Submitting:	
Date Submitted:	

For Completion in the Student Service Centre (SSC)

Received in the SSC by *(name in capitals):*			
Method of Submission (Handed in to SSC; posted through internal/external mail):			
E-thesis Submitted (mandatory for final theses)			
Signature:		Date:	

TABLE OF CONTENTS

LISTS OF TABLES AND FIGURES

List of Tables

List of Figures

List of publications

Journal papers

Alsubih, M., Arthur, S, Wright, G, Allen, D, 2015. Experimental study on the Hydrological Performance of a Permeable Pavement. Urban Water Journal, in press.

Alsubih, M., Arthur, S, Wright, G, Allen, D, 2015. Influence of Sediment on the Hydrological Performance of a Permeable Pavement. Water Science and technology journal, under review.

Conference papers

Alsubih, M., Arthur, S, Wright, G, 2015. Experimental study on the Hydrological Performance of a Permeable Pavement . 8th International Conference Novatech Planning and Technology for Sustainable Water Urban Management, 24-27 July 2013, Lyon , France.

Alsubih, M., Arthur, S, Wright, G, Allen, D, 2015. Influence of Sediment on the Hydrological Performance of a Permeable Pavement.13th International Conference on Urban Drainage, 7-12 September 2014, Sarawak, Malaysia.

Oral presentations

Peter Wolf Early Career Hydrologist's Event, 25-26 March 2013 at Imperial College, London, UK

Infrastructure and environment Scotland 1st postgraduate conference, 03-Jun-2013- School of the Built Environment, Heriot-Watt University, Edinburgh, UK

Infrastructure and environment Scotland 2nd postgraduate conference, 02 September 2014 School of Engineering, Hudson Beare Building, King's Buildings, Edinburgh, UK

List of abbreviations

BS	British Standards
BMPs	Best Management Practices
CBPP	Concrete Block Permeable Paving
CGP	Concrete Grid Pavers
CIRIA	Construction Industry Research and Information Association
EA	Environment Agency
EC	European Commission
EPA	Environmental Protection Agency
MC	Moisture Content
VWC	Volumetric Water Content
PA	Porous Asphalt
PC	Porous Concrete
PICP	Permeable Interlocking Concrete Pavements
PGP	Plastic Grid Pavers
SEPA	Scottish Environment Protection Agency
SS	Suspended Solids
SuDS	Sustainable Urban Drainage Systems
TSS	Total Suspended Solids
USEPA	United State Environmental Agency

CHAPTER 1 – INTRODUCTION

1.1 Overview

In order to improve quality of life and protect urban areas from flooding, it is necessary to examine approaches to dealing with the effects of heavy rainfall. Throughout history, engineers have built complex infrastructure and drainage systems to improve the quality of living within civilizations (Burian & Edwards 2002) . The building of urban drainage was originally intended to convey storm water away from developed areas (Fletcher et al., 2014). However, over the recent two decades these urban drainage systems have been found to be both ineffective and inefficient (Ellis et al., 2002, Balmforth et al., 2006, Dickie et al., 2010, Poleto and Tassi, 2012, Barbosa et al., 2012).

A number of impediments have caused failures in the system, including:

- rapid population growth;
- inadequate government planning and management;
- insufficient investment;
- Climate change.

These factors have led engineers to move their attention away from traditional drainage systems to consider alternative techniques to overcoming these challenges and thus ensure that urban drainage systems become sustainable (Scholz and Grabowiecki, 2007). Such alternative techniques include: improvements in conventional engineering practices; and implementation of Sustainable Urban Drainage Systems (SuDS) (Martin, 2001), i.e. management, planning and facilities designed to drain urban runoff through sustainable and environmentally-friendly methods. The main objectives of SuDS are to reduce the negative impact of urban developments on the quantity and quality of surface runoff while also increasing local amenity and biodiversity (Woods-Ballard et al., 2007). Figure 1-1 demonstrates the three objectives of the SuDS approach. The success of each of these objectives depends on characteristics and constraints of the local environment. The philosophy

of SuDS is to drain surface runoff in a similar manner to natural drainage (Woods-Ballard et al., 2007).

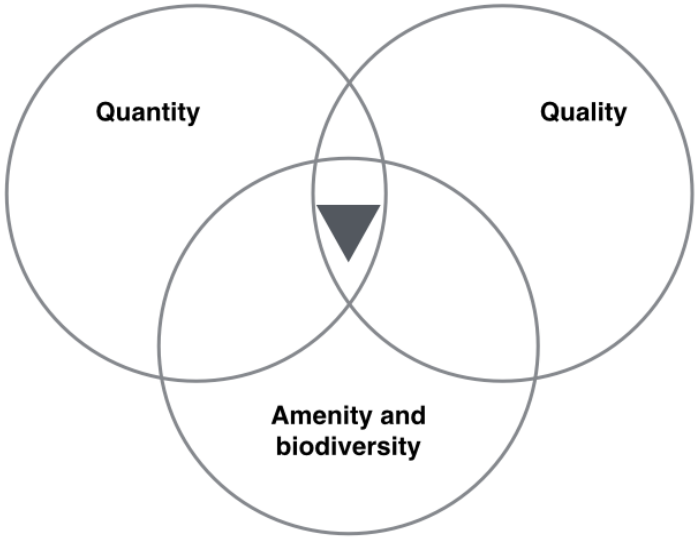

Figure 1-1: SuDS objectives (Woods-ballard et al, 2007).

The management of storm water runoff is the main factor in the potential effectiveness of sustainable urban drainage. Thus SuDS are designed to deal with runoff at source (i.e. close to the area where rain falls), and therefore the management technique can be defined as source control as it stores water temporarily close to the source in order to reduce the runoff volume during rainstorms (Pratt et al., 1995). In addition, SuDS also cover further method control such as site control, regional control; this concept known as "SUDS management train" which uses drainage techniques in series to achieve:

- Flow rate reduction;
- Volume reduction;
- Pollution reduction.

The hierarchy of techniques that involved in the the management train are; prevention (i.e., to prevent runoff and pollution by applying policies within the site management plan), source control, site control, and regional control.

The control structure investigated in this research project is the permeable pavement. This is principally a means of rapid rainfall and runoff infiltration through a pavement, using the gaps between paving blocks as the conveyance flow path and storing surface runoff within the three dimensional pavement structure. The stored water is eventually released into the receiving watercourse or allowed to percolate underground. Permeable pavements can be used for car parks, pedestrian paths, driveways and areas of low traffic speed and intensity of use. The SuDS Manual CIRIA C697 (Woods-Ballard et al., 2007) demonstrates a number of permeable pavement design options, varying according to the site specific hydrological and structural requirements (Woods-Ballard et al., 2007).

Despite their proven ability to attenuate surface runoff, there remains a lack of detailed understanding of the hydrological performance of permeable pavements, and there are consequently no firm design guidelines to assist designers and other stormwater professionals (Mullaney and Lucke, 2014). There is also some uncertainty regarding the influence of sediment on a pavement's operational performance and maintenance requirements (Abbott and Comino-Mateos, 2003, Newman et al., 2013). Thus, the research has been designed to define the hydrological performance of permeable paving in detail by relating it to rainfall characteristics and the influence of sediment on the hydrological performance of a permeable pavement.

The following indicators will be used to evaluate the hydrological performance of permeable pavements following a rainfall input:

- Discharge, as a rainfall equivalent (mm)
- Discharge Duration (h)
- Retention (mm)
- Start delay to discharge (min)
- Moisture Content (%)
- Concentration of Suspend Solid

This research study involved a full-scale permeable pavement structure built in the hydraulic laboratory at Heriot Watt University. A rainfall simulator was designed to mimic a range of rainfall events, and appropriate monitoring equipment was installed and calibrated for the purposes of the study. The performance of the permeable pavement was examined twice: (1) a hydrology test was conducted, in order to study the response of the permeable pavement under a variety of rainfall intensities; (2) a sediment test was conducted to study the hydrological response to 10 years of accumulated sediment across the pavement surface.

The current work was undertaken to provide answers to the following questions:

- How do permeable pavements respond to different storms characteristics?
- What is the influence of sediment accumulation on the hydrological performance of a permeable pavement?

1.2 Aims and objectives

The study focuses on the potential change in hydrological performance during the lifespan of a permeable pavement that associated with the permeability of pavement when it deteriorated due to a build-up of sediment into the structure. Thus, the aim was to investigate the influence of sediment on the hydrological performance. This was supported by a number of objectives to:

- Design and construct a permeable pavement that can be used for academic research purposes.
- Quantify the ability of permeable pavements to reduce surface runoff in response to different rainfall conditions.
- To assess the influence of sediment on hydrological performance of a permeable pavement.
- To determine the way in which permeable pavement can filter suspended solids.

1.3 Overview of Thesis

Chapter 1 introduces the thesis topic, the main aim and objectives of the research, and thesis structure.

Chapter 2 describes the pervious pavement and establishes the distinction between porous and permeable pavements. In addition, a complete illustration of permeable pavement systems is presented. Section 2.3 of the critical literature review covers the hydrological performance of permeable pavements and highlights the main studies under discussion in this field. Section 2.4 forms a discussion of the current issues associated with the hydrological performance of permeable pavements.

Chapter 3 is divided into three sections. Firstly, a description of the research methodology is provided, presenting the phases of the experiment, i.e. data collection and analysis; monitoring equipment; the size of rig. Secondly, a description of the experimental design, the rig, the materials employed, along with the development of monitoring equipment used in the laboratory, is provided. Finally, a summary of both the hydrology and sediment experiments are provided.

Chapter 4 presents the hydrological performance of a permeable pavement. Three rainfall intensities were applied on the test rig in order to examine the influence of rainfall characteristics on the response of permeable pavement. This chapter presents detailed discussion focussed on the following: rainfall; outflow; volumetric water content (VWC); and atmospheric conditions during this experiment and the pavement performance findings from the laboratory studies.

Chapter 5 presents the results of the sediment experiment, which was conducted after completion of the hydrology experiment, to assess the influence of sediment on the hydrological performance of permeable pavement. The extensive experimental programme was carried out over six months to simulate 12-year performance. The findings of sediment influence on hydrological performance of the pavement are presented and discussed in detail.

Chapter 6 highlights the main conclusions from the research and their implications to the water quality and quantity. Lastly, recommendations for further work are suggested.

CHAPTER 2 – CRITICAL LITERATURE REVIEW OF PERMEABLE PAVEMENTS

2.1 Introduction

Urban areas classically rely heavily upon the use of impermeable surfaces, such as concrete and asphalt. These surfaces do not allow surface water to soak into the ground, which results in a host of attendant problems. In particular, the widespread use of impermeable surfaces has accelerated the run-off of surface water, increasing flood risks. Impermeable surfaces also collect pollutants, such as oil, petrol or dust, which are then washed into the drains and ultimately into streams or rivers, adversely affecting wildlife and the wider environment (Huang et al., 2008, Jacobson, 2011, Hawley and Bledsoe, 2011, Fletcher et al., 2013, Newman et al., 2013, Miller et al., 2014).

Globally, urban areas account for approximately 4% of the total land area (around 471 million ha), which continues to grow with increasing population and housing pressures, employment and other socio-economic factors (Perry & Nawaz 2008). In the UK, urbanisation has advanced to the extent that recent estimates suggest that around 7% of the land area in England is now covered by cities and towns (Shaffer et al., 2009). This rapid urbanisation is necessarily accompanied by the construction of impermeable surfaces that lead to a reduction of vegetation and natural permeable surfacing. This change negatively impacts upon the local environment, with effects like increased storm water runoff, increased pollutant loads to streams destroying natural habitats, higher peak stream flows, bank erosion, and increased sediment transport and reduction of infiltration. This leads to the consequence of lowering groundwater recharge and potentially also lowering stream base-flows (Brattebo and Booth, 2003).

Increased flood risks occur when surface water runs off more quickly and in greater volumes than in naturally permeable areas, such as grasslands and forests (Collins et al., 2006). This increased water quantity can overload piping and drainage systems, causing an increase in overland flows and stream-bank erosion caused by the rapid

transit of water. Streams then experience irregular flow rates and higher sediment loadings, potentially causing significant damage to aquatic habitats (Collins et al., 2006).

The most common types of stormwater pollutants include fertilizers, nutrients, sediment and suspended solids, hydrocarbons, bacteria, and heavy metals (USEPA, 2003). When there are elevated concentrations of nutrients in runoff, such as nitrogen and phosphorous, in rural catchments this can result in eutrophication. This is an effect that results in cyanobacterial blooms, oxygen depletion, as well as the death of aquatic animals in local water receiving bodies (Collins et al., 2006).

The environmentally friendly alternative to traditional impermeable paved areas is the use of pervious surfaces, which enable surface water to drain through them into the ground. This kind of surface has a number of important benefits, including the reduction of runoff, recharging of groundwater, the ability to save water through recycling, and ultimately the reduction of pollution (Scholz & Grabowiecki 2007), as well as a reduced need for curbing and storm sewers (USEPA, 1999).

2.2 Current best practice design

In the 1980's, drainage engineers were concerned by the frequent flooding caused by overloading of the existing infrastructure (Andoh & Iwugo 2002). Their attention was paid to temporary techniques in that they sought temporary measures that would work in parallel with urban drainage systems, such as oversized pipes to serve small developments, using detention tanks, and constructing ponds on main rivers downstream of urban areas (Pratt, 1997). Thus, this change in thinking led to a move away from the traditional drainage system designs to look for new ways to mitigate flooding in urban areas. Recently, the idea of source control is widely favoured to be the solution for failing urban drainage systems. Source control functions by storing rainfall close to the point of collection and in addition captures pollutants at source(Pratt et al., 1995, USEPA, 1999).

SuDS in the United Kingdom and the use of best management practices (BMPs) in the United States are both alternative approaches used over conventional urban

drainage. The aim is to limit the impact of urbanization and stormwater on urban areas as well as to provide a quality treatment prior to discharge into receiving water (Lampe et al., 2004). SuDS consist of structural elements that address pollutant reduction and flow control, while providing amenity. On the other hand, the BMP's focus is on water quality rather than in handling quantity. It can be either structural such as ponds, swales or other constructed features designed for the pollutant removal, or non-structural, such as education programmes for the public. (Lampe et al., 2004).

Current design and construction practices are increasingly seeking to focus on more natural sustainable developments using the infiltration and storage capacity of natural systems (Butler and Davies, 2004). This can be seen through the move towards designing more environmentally sustainable urban drainage systems, using pervious or permeable pavement systems as part of sustainable urban drainage design (Nnadi et al., 2008). Sustainable design seeks to control runoff at the source, enabling the natural drainage of water into the local environment. This approach attempts to place responsibility for water control on those causing the runoff and to prevent problems occurring, rather than implementing mitigation measures to control runoff water quality and quantity (Pratt et al., 2002).

A key publication — Source Control using Constructed Pervious Surfaces CIRIA C582 (Pratt et al., 2002); this discusses the critical issues that should be considered when designing and manufacturing pervious pavements. To date, there is no established standard for pervious pavements, although, the CIRIA publication, The SuDS manual C697 (Woods-Ballard et al., 2007) offers technical information for designing pervious pavements.

Interpave works closely with CIRIA and other organisations to develop innovative concrete block permeable paving products and systems; it represents all the major precast concrete paving manufacturers in the UK and has established documents intended to support those engaged in the development process to understand concrete block permeable paving – including designers and developers, and planning, building control and adoption officers. Some of their publications are *Permeable Pavement* -

Guide to The Design Construction and Maintenance of Concrete Block Permeable Pavements Edition 6 (Intepave, 2010). The final publication in the list offers technical details and is considered to offer a definitive design. British standards have also introduced reference standard BS7533 part 13: 2009 (BSI, 2009), which works alongside *The SuDS Manual* and Interpave's technical support. The design of permeable pavements is an area that is continuing to develop.

The SuDS manual CIRIA C697 describes types of pervious pavement systems and their potential uses. It also details the structure and substructure of the varying systems with detailed descriptions of several of those most widely used. The manual provides guidance on associated elements such as vegetation, landscaping, pre-treatment and outlets. The manual also recommends considering the following key criteria:

Hydraulic design

- Confirmation of adequate rates of infiltration of rainwater through the pavement surface.
- Storage volume required for rainfall event management.
- Adequacy of outfall capacity to convey water from the pavement structure.
- Management of events exceeding design.

Structural design

- The subgrade must be able to sustain traffic loading without excessive deformation.
- The bedding course and sub-base layer must afford sufficient load spreading to provide an adequate consideration platform and base for the overlaying pavement layers.
- Pavement materials must be structurally fit for intended use.

There is also a flow chart (see Figure 2-1) referred to in the CIRIA (Intepave, 2010) document, to assist in the design of concrete block pavements. The SuDS manual recommends observance of the design flow chart during manufacture.

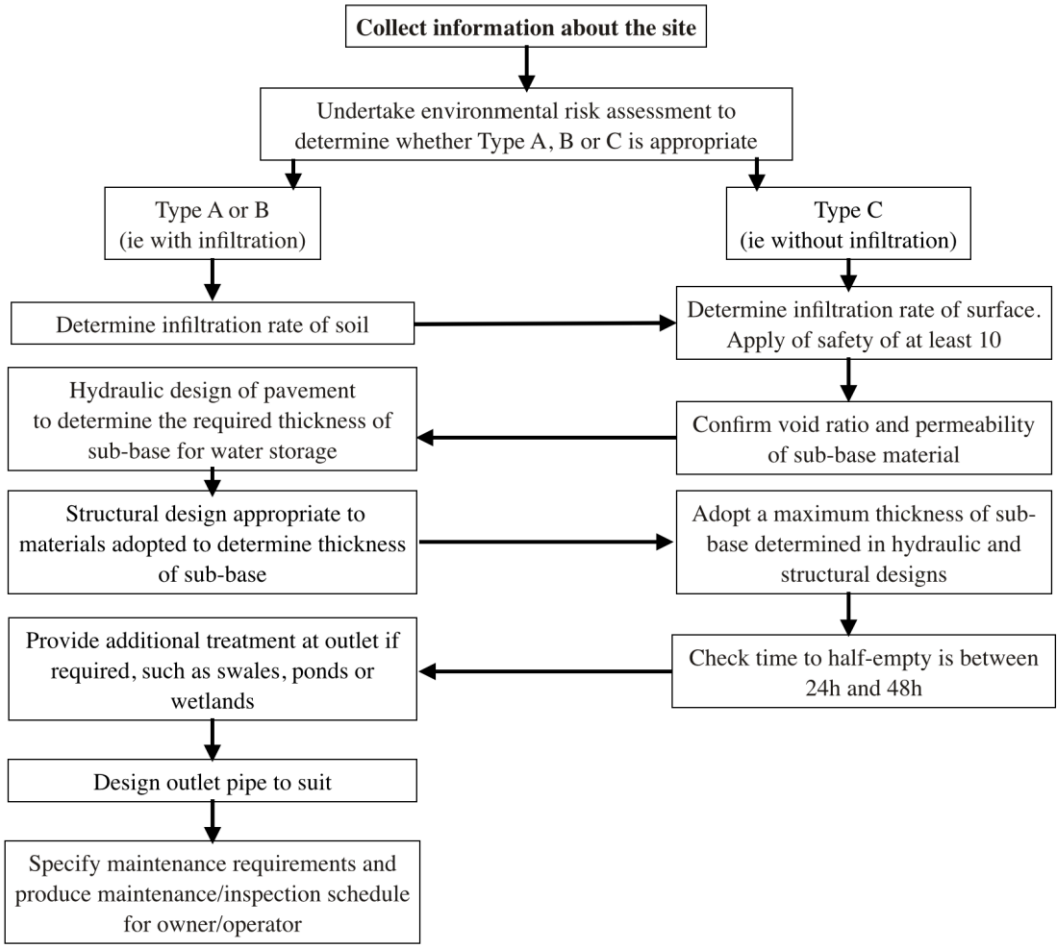

Figure 2-1: Design of permeable pavement system (Source from CIRIA C582, Pratt et al, 2001).

2.3 Pervious surfaces

2.3.1 Background

SuDS come in a variety of forms, such as permeable and porous pavements, with both porous and permeable surfacing being generally classified as pervious surfacing. The surface of a porous pavement (see Figure 2-2) is composed of porous materials that enable the infiltration of rainfall into the ground across the entire surface of the pavement. A permeable pavement is surfaced with non-porous materials, instead allowing infiltration of water through specially designed inlets (Pratt, 1997). Permeable surfaces significantly reduce the amount of water leaving (or shedding) from the surface of the pavement after rainfall.

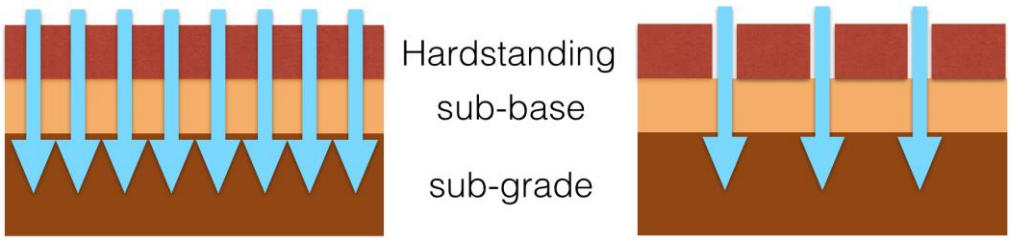

Figure 2-2: Porous (*left*) and permeable (*right*) hard-standing (Wright, 2010).

Japan was one of the first countries to deal with these pervious pavements, as they were already using 494,000 square meters of pervious pavements by 1984 (Fujita, 1997). This vast quantity sought to play a significant role in urban storm water management through the reduction of water runoff, protecting against flood risk in densely populated areas. These pavements also have other advantages, such as raising the level of groundwater, maintaining the temperature, and conservation of urban ecology (Fujita et al., 1996, Pratt, 1997).

The proliferation of these pavements was not limited only to Japan, with countries like the United States using porous surfaces from 1970, when they were adopted in Portland, Clearwater, Naples and Sarasota, Florida. The sandy soil of these locations made it an appropriate place for applying these types of pavements (Booth and Leavitt, 1999, Dreelin et al., 2006). In addition, the US began to lay down a system to provide comprehensive guidance on the design and maintenance of pervious pavements (Schueler, 1987).

In Sweden, the use of pervious pavements took place as a part of a 'Unit Superstructure' approach that was presented to cope with storm water, instead of total dependence on conventional drainage. This approach is up to 25% cheaper, when taking all contracture and drainage costs into consideration, and resulted in an approximate reduction of peak flow by 80% (Hogland and Niemczynowicz, 1986).

In the UK, pervious pavements also have been in development and use since the 1980s, where small-element concrete blocks where used to form permeable surfaces at Nottingham Trent and Coventry universities. These projects were undertaken to monitor water quality and quantity. In addition, a significant number of pervious

pavement systems were installed in Scotland prior to 2002 (Lampe et al., 2004), with the SEPA database Wild *et al.* (2002) demonstrating that about 25% of all SuDS sites in Scotland include permeable paving (Wild et al., 2002). Pervious pavements have also been installed in the National Air Traffic Services and Royal Bank of Scotland in Edinburgh (Pratt et al., 2002).

2.3.2 Porous pavement

Porous pavements are covered by porous paver materials that enable the movement of water through the entire surface. These kinds of surfaces primarily comprise grass/gravel surface pavements, porous concrete or porous asphalt. Grass/gravel surfaces are typically used in locations where the traffic is light and which therefore only require a simple design, such as pedestrian areas, driveways or temporary car parks.

Porous concrete (PC) consists of coarse aggregate bound together by cement (see Figure 2-3 (a)), which creates a 15- 25% void content due to the omission of the vast majority of the fine aggregate. These void spaces can admit from 3 to 5 gallons of water per minute for each square foot of surface area (2.04×10^{-3} to 3.40×10^{-3} $m^3/sec/m^2$). Porous concrete (PC) surfaces are therefore suitable for locations that have low traffic loads, such as driveways and walkways, in addition to certain medium traffic load areas, like commercial parking and residential streets. Finally, porous asphalt (see Figure 2-3 (b)) consists of course aggregate bound with asphalt cement, creating void space ranges between 15 to 20% (Hunt and Collins, 2008). The mixture volume of porous asphalt can comprise from 60 to 90% of the aggregate (Ferguson, 2005). The thickness of the asphalt layer generally ranges from 75 to 180 mm depending on the traffic loading (Hunt and Collins, 2008). Superficially, porous asphalt or macadam pavements resemble conventional asphalt, although they are evidently relatively porous (Scholz and Grabowiecki, 2007).

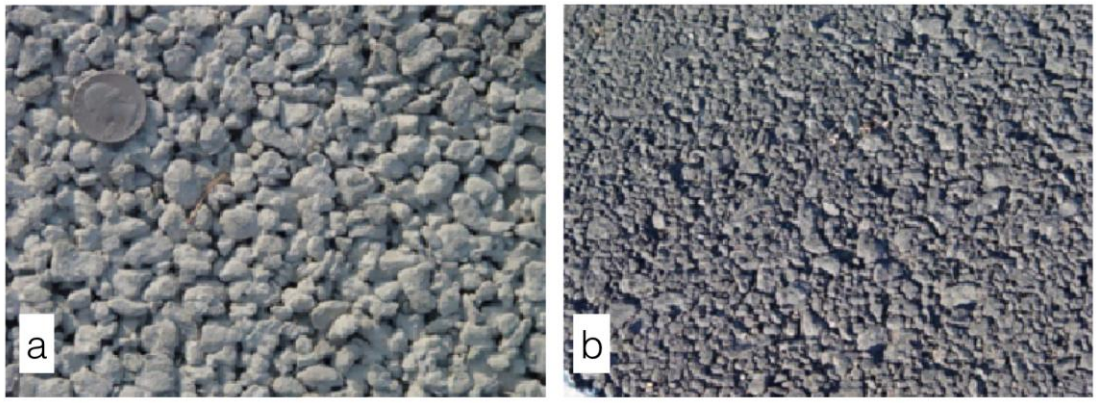

Figure 2-3: Showing (a) Porous concrete, (b) Porous Asphalt, (Collins et al. 2008).

2.3.3 Permeable pavement

The surfaces of permeable pavements consist of multiple, inter-connected impermeable units that are paved by geometric shapes. These create openings that allow water to infiltrate through into the soil. The materials filling the gaps between these units are usually similar to the contents of sub-base layer, but are of different aggregate size. The voids range between 8 to 20% of the surface area (Hunt and Collins, 2008). There are three types of permeable pavements: Concrete Block Permeable Paving (CBPP), concrete grid pavers, and plastic grid pavers.

The first of these, CBPP (see Figure 2-4), is the most widespread of all permeable pavement systems and is also known as Permeable Interlocking Concrete Paving (PICP) in North America. CBPP consists of small units made from concrete, clay, natural stone or wood. These units can be designed in many different shapes, colours, and sizes, and when placed together interlock to create a hard surface for roads or pavements (Intepave, 2010). The joint filling media tend to be porous aggregate or soil. CBPP performs comparably to concrete pavement in terms of bearing traffic loads, but differs from traditional impermeable surfaces in that it is possible for water to infiltrate through their open joints.

Figure 2-4: Concrete Block Permeable Paving (CBPP). (Interpave, 2010)

The next form of permeable surface is concrete grid paver (CGP) (see Figure 2-5 (a)), which can be further categorised into lattice and castellated versions, with opening area ranges between 20 to 50%. The void space can be filled by topsoil and grass, sand, or aggregate (Smith, 2006). Finally, plastic reinforcement grid pavers (PG) (see Figure 2-5 (b)**)** consist of interlocking plastic units. These units facilitate the infiltration through large gaps that generally account for 90 to 98% of the overall surface area and are typically filled with gravel or topsoil planted with grass (Hunt and Collins, 2008, Mullaney and Lucke, 2014). Otherwise known as plastic geo-cells, these surfaces are adaptable to sites where a small portion of the surface area needs to be covered. The presence of either topsoil or aggregate adds significant permeability to the surface and enhances the visual appearance (Ferguson, 2006).

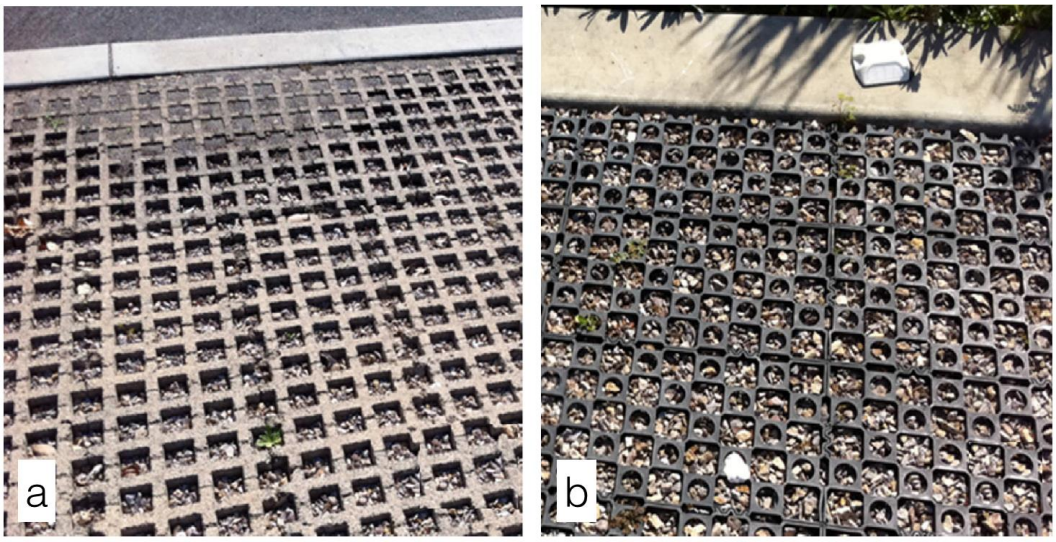

Figure 2-5: Showing, (a) Concrete Grid Pavers (CGP), (b) plastic reinforcement grid pavers (PGP) (Mullaney and Luke , 2014).

2.3.4 Hydraulic function of pervious surfaces

There is no difference between pervious pavement types in relation to which surface reduces runoff better than the other (Hunt and Collins, 2008). Field studies carried out by Brattebo and Booth (2003) examined PICP, CGP, and PG. They found there was no substantial difference in reduction of surface runoff. A similar result was confirmed by another study, which showed no difference in the performance with regard to surface runoff reduction, with the exception of CGP, where there was a slight increase in runoff (Collins et al., 2008). Hunt and Collins (2008) state that the curve number CN (CN is a measure of direct runoff from storm rainfall (Ponce and Hawkins, 1996)) for a standard impervious surface is 98, where a pervious surface has a range of from 45 to 89. Bean et al. (2007) found that the PICP curve number ranged between 37 and 45, CGP ranged between 70 and 89, and PC ranged between 77 and 89.

Runoff coefficient (a ratio of rainfall to runoff) can provide an indication of the functionality of a pervious pavement. Abbott et al. (2003) examined a car park where they found that the runoff coefficient ranged between 0.3 and 1.2, with an average value of 0.67. They inferred that runoff greater than 100% of the rainfall, maybe due to high detention existing from the previous events. Ferguson (2005) found that coefficients for most types of pervious pavements are below 0.5, meaning that these

pavements are more similar to the natural surface than to the impermeable surface. Table 2-1 illustrate the runoff coefficients for variety of pervious pavements.

Table 2-1: Runoff coefficients of pervious pavements (Source from Ferguson, 2005)

Surface Type	**Runoff Coefficient**
Aggregate	0.30 to 0.70
Turf, grass cover greater than 50 percent	0.05 to 0.53
Open-jointed blocks: with 0.80" to 0.20" aggregate fill	0.30 to 0.50
Open-celled Checkerblock and Monoslab grids: with topsoil and Kentucky bluegrass	0.00 to 0.27
Open-celled Turfstone (Turfblock) grids: with :sandy loam and Bermuda grass	0.18 to 0.36
Open-celled Turfstone (Turfblock) grids: with topsoil and Kentucky bluegrass	0.00 to 0.56
Porous asphalt:newly installed	0.12 to 0.40
Porous asphalt: 3 to 4 years after installation	0.18 to 0.29
Dense asphalt	0.73 to 0.95
Dense concrete	0.75 to 0.97

Surface infiltration rates might vary slightly among the four types of pervious pavement. However, this depends on materials used, system design, site characteristics and construction. Table 2-2 shows the infiltration rates found from a mix of field and laboratory studies. Most research has found that there is no considerable difference in infiltration rate between pavement types, with the exception of CGP, which showed a low infiltration rate compared to other types. In some cases PC showed higher infiltration rates than other pavements. The infiltration rate for all pavements was high, especially when they were new, the infiltration rate showed a decline after few years but it maintained an acceptable level. From the literature review, it can be concluded that the pervious pavements do not differ significantly in hydraulic performance due to the similar performance in their infiltration rate.

Table 2-2: Previous studies on infiltration rate and surface runoff reduction of four types of pervious pavements

No	Author	Testing	Location	Pavement age	Pavement description	Main findings
1	Pratt *et al*, 1995	Field	UK	9 years	**Area study = 40 x 4.6 m** **PICP Depth**: Surface 80 mm Sub-base 300 mm	▪ Infiltration rate still excess of 1000 mm / h ▪ Pavement reduced runoff and peak flow rate up to 60% compared to traditional pavement
2	Brattebo and Booth, 2003	Field	USA	6 years	**Study area for each : 3 x 6 m** Grasspave (PGP) filled with sand Grasspave (PGP) filled with gravel Turfstone (PICP) filled with soil + grass UNI Eco-Stone (CGP) filled with **Depth :** not reported gravel	▪ After 6 years, 4 pavements had a positive performance compared to traditional asphalt. ▪ Water quality showed positive sign. ▪ PGP produced runoff. ▪ No runoff was produced from PICP and CGP. ▪ Infiltration not reported
3	Collins , 2008	Field	USA	Not reported	Total study area = 6 m x 18 m **CGP Depth**: Surface 80 mm Bedding 100 mm Sub-base 225 mm **2 x PICP Depth**: Surface 80 mm Bedding 100 mm Sub-base 250 mm **PC Depth**: Surface 150 mm Bedding 50 mm Sub-base 230 mm **2 x asphalt Depth**: Surface 80 mm Sub-base 200 mm	▪ All pavements reduced surface runoff and peak flow, average reductions were 67.1%, 73.5%, 77.1%, and60.3% for PC, PICP1, CGP, and PICP2 respectively. ▪ Infiltration rate approximately (July 2007): o PC = 49410 mm/h o PICP1 = 15360 mm/h o CGP = 1010 mm/h o PICP2 = 2670 mm/h

No	Author	Testing	Location	Pavement age	Pavement description	Main findings
4	Pezzaniti *et al*, 2009	Laboratory	Australia		**Block paving PP 1 and PP2:** Surface 80 mm Bedding 50 mm Geotextile Sub-base 280 mm Geotextile Sub-grade 20 mm	**Laboratory results:** ▪ Over 35-year simulated the hydraulic conductivity declined of 59%, 68%, and 75% for the block paving (PP1, 2, and 3). ▪ PP1 = 60000 mm / h (laboratory test). ▪ PP2 = 34000 mm / h (laboratory test). ▪ PP 3 = 4000 mm / h (laboratory test). ▪ **Field result:** ▪ Grass paving site, infiltration rate was dropped to 8% of initial rate over two months of testing. ▪ Block paving sites, infiltration rate was dropped between 19-23% of initial rate over two months of testing. ▪ Infiltration rate after testing: o Block paving sites between 200 and 600 mm / h o For Grass paving site , 5 mm / h
					Grass paving PP3: Surface 25mm Geotextile Sub-base 280 mm Geotextile Sub-grade 20 mm	
		Filed			**3 sites of block paving :** Surface 80 mm Bedding 50 mm Geotextile Sub-base 350-550 mm Geotextile	
					1 site of Grass paving : Surface 20 mm Bedding 200 mm Geotextile Sub-base 300 mm Geotextile Sub-grade 50mm	

No	Author	Testing	Location	Pavement age	Pavement description	Main findings
5	Lucke and Beecham 2011	Field	Australia	8 years	Car park area 700 m^2 (40.5 m x 17.3 m) consisting of 225 m of PICP + 470 m^2 of Impermeable Asphalt	▪ PICP was very effective at filtering sediment ▪ Infiltration rate representing fully blocked site = 10 mm / h ▪ Infiltration rate representing medium blocked site = 293 mm / h ▪ Infiltration rate representing unblocked site = 972 mm / h
6	Welker *et al*, 2012	Field	USA	1 years	Pervious concrete = 9 m x 15 m Porous asphalt area = 9 mx 15 m The depth range between 0.5m to 1.5 m (because slope)	▪ The pavements were nearly identical in terms of water quality infiltration rate up to 39600 mm / h.
7	Fassman and Blackbourn, 2010	Field	Auckland, New Zealand	1 years	A standard asphalt area = 850 m^2 permeable pavement area = 395 m^2 depth was not reported	▪ Infiltration rate did not substantially deteriorate after 1 year of operation. ▪ Infiltration rate above 1200 mm / h
8	Yong *et al.*, 2013	laboratory	Australia	-	Porous asphalt area = 0.9 x .45 m2 **Depth**: Surface 75mm Bedding 40 mm Sub-base 570 mm Hydrapave area = 0.9 x .45 m2 **Depth**: Surface 80 mm Bedding 50 mm Upper Sub-base 100 mm Lower Sub-base 250 mm	▪ PS ponding occurred above the pavement ▪ Clogging behaviour and lifespan of porous pavement varied according to their design ▪ Ponding occurred above geotextile ▪ No ponding occurred

No	Author	Testing	Location	Pavement age	Pavement description	Main findings
					Permapave area = 0.9 x .45 m2 / **Depth**: Surface 50mm Sub-base 350 mm	
9	Abbott & Comino-Mateos , 2003	Field	UK	0.83 years	Formapave (PICP) area = 6250 m2 **Depth:** bedding = 50 mm geotextile sub-base =350 mm impermeable geotextile	▪ The peaks of storm events were reduced ▪ The infiltration rate remained high. ▪ In 1999, infiltration rate ranged between 1100 and 22900 with average 5100 mm / h ▪ In 2000, infiltration rate ranged between 1030 and 3880 mm / h , with average 1300 mm /h.
10	Dreelin *et al.*, 2006	Field	USA	>3 years	PGP /asphalt PGP area is 187 m2 Traditional Asphalt area is 64 m2	▪ PGP generated 93% less surface runoff than the asphalt ▪ Infiltration rate is still effective, not reported
11	Gilbert and Clausen, 2006	Field	USA	1 year	**Asphalt driveway depth:** 50 mm of asphalt Subsoil **Paver (UNI Ecostone 115 x 230 mm) driveway depth:** 50 mm of coarse sand 150 mm of gravel **Crushed Stone driveway depth:** 120 mm of crushed stone 75 mm of sand PICP / crushed stone	▪ Asphalt was highest in runoff and pollutant loads ▪ PICP had lowest pollutants ▪ Crushed stone has similar concentration of pollutants of Asphalt ▪ Infiltration rates at both Crushed Stone and Paver declined over time but acceptable level. ▪ Reduction in infiltration due to fine particles. ▪ Paver: Infiltration rate ranged between 59 and 114 mm/h. ▪ Crushed Stone: Infiltration rate ranged between 31 and 113 mm/h.

No	Author	Testing	Location	Pavement age	Pavement description	Main findings
12	Bean *et al.*, 2007	Field	USA	>2 years	2 X PICP **Depth**: Surface 75 mm Bedding 75mm Sub-base 200 mm Sub-grade = sand soil CGP **Depth**: Surface 90 mm Bedding 50 mm Sub-base 200 mm Sub-grade = sand soil PC **Depth**: Surface 200 mm Sub-grade = sand soil	▪ No runoff produced ▪ **CGP:** infiltration rate was 49 mm/h and 86 mm/h after maintenance ▪ **PICP:** infiltration rate was 20000 mm/h without fines and 800 mm/h with fines ▪ **PC:** infiltration rate was 40000 mm/h without fines and 130 mm/h with fines
13	Ball and Rankin 2010	Field	Australia	Not reported	Rocla Ecoloc pavers (PICP)	▪ Outflow from the PICP and PC occurred less frequently, in smaller volumes, at slower rates, and for longer durations than the runoff from the asphalt control. ▪ All system functioned well under the site condition. ▪ Peak flows were reduced by at least 50%.
14	Bill *et al.*, 2002	Field	USA	I year	PGP	▪ The infiltration was acceptable ▪ The runoff was decreased ▪ Runoff coefficients ranged from 0.20 to 0.50

Research studies have demonstrated that the hydraulic performance of permeable pavement generates less runoff than other conventional pavement, and discharged volume is comparable to an urban green area (Bond et al., 1999, Andersen et al., 1999, Dreelin et al., 2006, Fassman et al., 2010). Pratt et *al.,* (1995, 1997) found that the permeable pavement reduced surface runoff by up to 60% compared to conventional asphalt pavements, while Rushton (2001) found that the permeable pavement reduced surface runoff between 40-50%. However, Dreelin *et al.,* 2006 claimed that the permeable pavement could reduce the surface runoff by up to as much as 93%, and Gilbert and Clausen (2006) claimed that 72% of rainfall could be reduced through permeable pavements.

At Nottingham Trent University, Pratt *et al.,* (1989, 1995) studied the performance of a full-scale permeable pavement car park (pavement depth 300-400 mm). Impervious partitions separated the base of car park into four sections which were filled with different materials. The results indicated that the average discharge from the pavement was 37 % (gravel); 34% (blast furnace slag); 47% (granite); and 45% (limestone). This study found that the lowest runoff was created by the blast furnace slag, which was explained as being a result of the shape of the blast furnace slag, which has a void space of 48% and therefore offers numerous storage sites for storm water. The peak discharge for all sub-bases was 30%. The delayed time was 5 to 10 minutes from peak rainfall. Overall, the performance of permeable pavements is governed by a large number of factors, including the type of materials used in their construction and the particle size distribution. These factors can directly affect permeability, then leading to the reduction of hydraulic conductivity for permeable pavement systems.

The observations of Pratt *et al.,* (1989, 1995) were confirmed by a field study that was carried out by Abbott and Comino-Mateos (2003). They investigated the in-situ hydraulic performance of a permeable pavement system. The pavement structure was 480 mm deep, consisting of 80 mm of block paving and 50 mm of bedding course and 350 mm of sub-grade. The results indicate that 67% of rainfall percolated through the pavement. The observations show that the start delay ranged between 5 minutes to two hours and average discharge lasted 14 times longer than the rainfall; therefore the system showed an effective degree of attenuation. The volume discharge was similar to Pratt observations, but the start delay was longer due to the sub-base materials.

A recent laboratory study was carried out by Palla *et al.*, (2015) to study the hydrological response of a permeable pavement with different rainfall intensities and slopes. The study examined two types of pervious pavements, concrete cell (CC) of depth 210 mm and previous brick (PB) of depth 190 mm, with two filter layers made of recycled glass aggregate and a mix of gravel and coarse sand. The hydrological response was analysed by calculating the discharge coefficient for each pavement, which was defined as the ratio between the discharge volume and the inflow volume measured at the end of the rainfall event, corresponding to 15 minutes of constant rainfall intensity. The results of the study confirmed that no surface runoff occurred for all the tests. The discharge coefficient of CC and PB ranged between 0.55-0.75 during high rainfall intensity (98 mm/h in 15 minutes), and 0.01-0.12 during low rainfall intensity (17 mm/h in duration 15 min). The results also indicate that the higher drainage results from a higher slops. The study confirmed that recycled aggregate turns out to be a valid solution to replace sand and gravel in permeable pavement (Palla et al., 2015).

2.4 Permeable Pavement Systems

2.4.1 Types of Permeable Paving Systems

It is possible to categorize permeable pavements into three main types, in terms of their infiltration capacity. These types are described here as Systems A, B and C (Interpave, 2010). These types and the situations to which they are best suited will be briefly discussed in this section.

2.4.1.1 Total Infiltration System (A)

The first permeable pavement type under consideration, System A, allows rainwater to pass through its constructed layers and into the sub-grade (see Figure 2-6). A proportion of the water will temporarily remain in the sub-base, enabling initial storage before its transferral to the sub-grade.

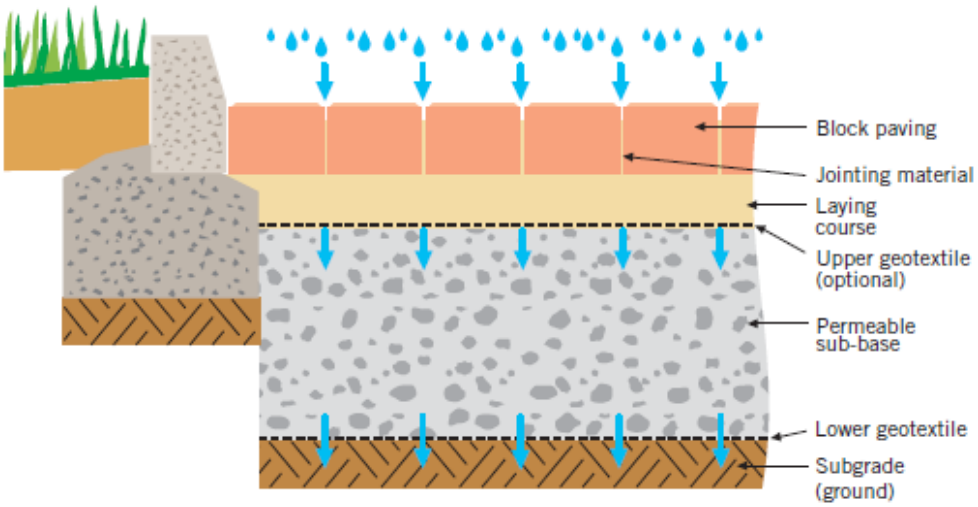

Figure 2-6: System A – Total Infiltration (Interpave, 2010).

2.4.1.2 Partial Infiltration System (B)

The next pavement type, System B (see Figure 2-7), is commonly employed where the sub-grade is unable to absorb all of the water that falls onto the pervious surface. This system is therefore intended to stabilize the soil by discharging an appropriate amount of water using traditional drainage techniques.

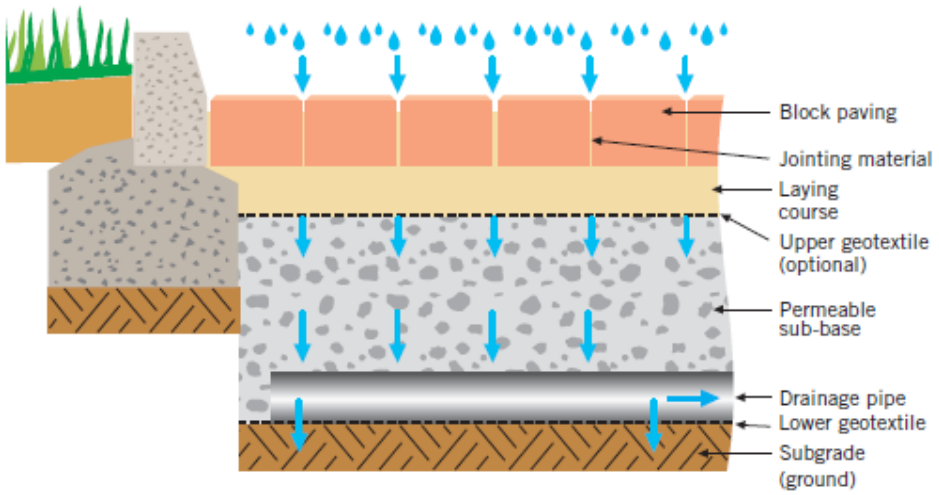

Figure 2-7: System B – Partial Infiltration (Interpave, 2010).

2.4.1.3 No infiltration system (C)

The third pavement type, System C (see Figure 2-8), uses an impermeable flexible layer composed of an impermeable geo-textile in order to keep all the rainwater on the surface. The surface is placed over the sub-grade, as well as through the specifically raised sides of the sub-base. This category of pavement system is utilized where the sub-grade has either low permeability or low strength, meaning the introduction of additional water would profoundly adversely affect the system. It can also be used for the purpose of rainwater harvesting or in order to prevent water infiltrating into the ground in sensitive sites, such as water extraction areas.

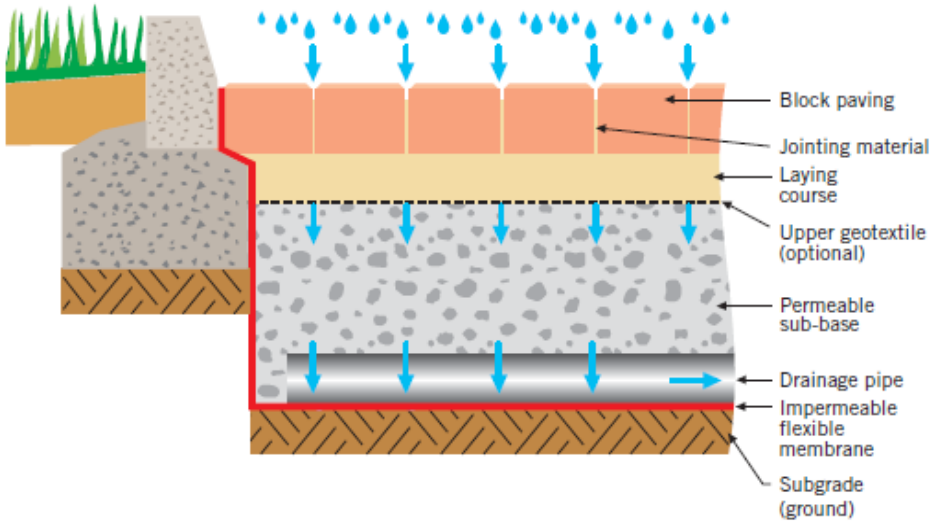

Figure 2-8: System C - No Infiltration (Interpave, 2010).

The design of this surface also makes it particularly suitable for use contaminated sites, as pollutants are kept from entering the groundwater. In addition, the polluted water can even be safely stored and used for other purposes, such as irrigation or flushing toilets, although it may require treatment before being used for other purposes.

2.4.2 Pavement thickness design

It is important to consider a number of factors in the design of permeable construction. These aspects include both structural and hydrological characteristics, such as structural strength under the expected loading from traffic, hydrological inputs, hydraulic response, and pollution impacts (Pratt, 1997). These aspects are often interrelated,

meaning that the importance of each aspect must be assessed depending on the location. For example, the discharge of stormwater through the construction base can negatively affect the bearing capacity of its underlying sub-grade, which has direct structural design implications.

To date, only limited non-specific guidance is available on the design and construction of permeable surfaces. The most comprehensive guidance available is provided by Interpave, the precast concrete paving and kerb association, or by individual manufacturers providing advice with regards to their specific products (Shaffer et al., 2009). Generally, the minimum depth of sub-base for most car parking sites is likely to be 150mm to 350mm. Impermeable surfaces will normally be "hardcore", with a depth of 100mm to 150mm thick, unless there is unusually soft ground that requires a stronger construction (Shaffer et al., 2009). A higher depth is required for permeable construction in comparison to impermeable surfaces because the strength of the surface will be reduced by the presence of water in the pavement layers.

The movement of water through permeable pavements occurs in a variety of ways: surface runoff, infiltration, lateral drainage at the base, and percolation through both the unsaturated zone and the sub-grade (Scholz and Grabowiecki, 2007). Therefore, one crucial consideration during the design of a permeable pavement is the provision and maintenance of sufficient surface infiltration and storage capacity to facilitate the capture and treatment of the specified quantities of stormwater. The hydraulic design normally employs the HR Wallingford procedure based on statistical rainfall events for different regions, the depth of the sub-base storing the water is determined (Wright et al., 2010). The accuracy can be improved through the use of various modelling software, such as InfoWorks and Micro Drainage.

2.4.3 The water quantity improvement function of permeable pavement

Permeable pavements reduce runoff quantity and peak runoff rates by allowing the water to quickly infiltrate through the system (Pratt et al., 1989). For example, the use of porous macadam for car parking and highways in Sweden has shown approximately 80% peak flow reductions (Pratt, 1997). It should be noted that some studies have found that porous asphalt surfaces can double runoff durations in comparison to impermeable

asphalt surfaces (Pagotto et al., 2000). This may be a result of the infiltration capacity of the porous pavement, which serves to delay the evacuation of the water.

The use of permeable surfaces enables water to infiltrate into the pavement during rainfall events and in some system, by temporarily storing water in the sub-base. The storage capacity of the sub-base can be as high as 100-200mm rainfall, for a 30% void in the sub-base, which is approximately equivalent to two months rain for many lowland parts of the UK. This means that there is a possibility to effectively delay the discharge from the sub-base, in order to prevent downstream flooding, or to allow the water to be directed to treatment areas without undue loading of the reclamation works (Pratt, 1997).

Permeable pavements are not only effective in the reduction of stormwater rates and volumes, but also provide numerous other benefits including groundwater recharge, decreasing groundwater salinity and improving the water quality received by water courses. Permeable pavements therefore play a crucial role in sustainable urban drainage system design, allowing disadvantages associated with impermeable surfacing to be either partially or completely overcome. As mentioned, permeable pavement systems offer a number of benefits over traditional impermeable construction in terms of both water quality and quantity.

Various studies have confirmed that by reducing peak runoffs, permeable pavements are able to reduce the volume of rainfall runoff that is discharged into a drainage system or a local watercourse (Pratt et al., 1995, Bond et al., 1999, Backstorm, 2000, Schluter and Jefferies, 2002, Brattebo and Booth, 2003, Gilbert and Clausen, 2006). Pratt *et al*. (2002) agrees with this argument, explaining that a permeable pavement is an infiltration system where surface water runoff is filtered into the ground through a permeable layer. Therefore, in a permeable pavement, the surface layer must be laid on a suitable porous material. Permeable pavements can directly manage the quantity and quality of runoff, through storage, infiltration, recycling and conveyance of runoff (Pratt et al., 2002).

Permeable pavements can positively affect the flow rate and volume of runoff through the provision of storage for runoff and slowing the time taken to discharge. Pratt et al.

(2002) state that one of the main methods for achieving source control is through the use of permeable pavements to minimise the volume of runoff discharged into watercourses, as well as improving the quality of runoff water and potentially enhancing the health and diversity of the local environment. Novotny (2003) cites a study in New York that demonstrated that permeable pavements could reduce peak runoff rates by approximately 83%.

Novotny (2003) maintains that the principle benefit of permeable pavements is the reduction or even elimination of surface runoff rate and volume. If the system is properly designed and maintained then the "*runoff can be stored and allowed to infiltrate the ground naturally"* (Novotny, 2003, p 445). Furthermore, reduction of the volume of runoff and time to peak flow also means that permeable pavements reduce the need for piped surface water drainage systems. Dzurik (2003) explains that passing the surface water runoff through a permeable pavement means that the water is stored in the voids of the filtered permeable layer, which reduces the volume of runoff discharged to the watercourse.

Performance studies carried out by (Francey, 2005) assessed the effect of permeable pavements on runoff flow rates. The study concluded that permeable pavements could reduce peak flow rates and total volume of runoff through infiltration, storage and evaporation. The effect on flow was also shown to be largely dependent on the volume of storage and the infiltration capacity of the permeable pavement material, the base material, the use of geotextiles and the type of subsoil. The study concluded that the choice of porous material used could potentially yield a reduction in runoff coefficient from approximately 0.95 for traditional pavement types to approximately 0.4 for permeable pavements.

The individual properties of permeable surfaces, such as their evaporation rates, drainage rates, and retention characteristics, depend to a large extent upon the particle size distribution of the bedding material (Collins et al., 2006). For example, in highly permeable soils, the captured water can infiltrate gradually into the sub-soil, while in areas containing soils of lower permeability, it may be necessary for the water to leave the structure though an underdrain system. Despite the differing performances of construction materials, however, it can generally be said that permeable pavements are

sustainable alternatives to traditional impermeable surfaces for the purpose of reducing the rate and volume of runoff.

Most literary sources agree that a permeable pavement allows a measure of filtration at the source of the runoff (Bean et al., 2007, Ball and Rankin, 2010, Gomez-Ullate et al., 2011, Roseen et al., 2012, Beecham et al., 2012). Marsalek and Schreier (2009) argue that the ability of permeable pavements to reduce surface water runoff through the infiltration process can be particularly beneficial in small developments over soils with adequate percolation rates and deep groundwater (Marsalek and Schreier, 2009). These changes in turn reduce pressure on drainage systems and improve soil erosion at discharge points, as the lowered velocity of runoff is less likely to cause erosion of the riverbank. It has therefore been argued that one of the chief motivations for using this type of pavement is to reduce runoff rates to streams, rivers and lakes (Dawson, 2008).

As discussed earlier, the high proportion of impermeable surfaces in the current built, means that pavement runoff reaches local watercourses more rapidly than it does in natural environments where the water is delayed by vegetation and soil. This increased rate of runoff results in a greater risk of flooding, because the watercourse deals with peak rainfall runoff (Bean et al., 2007). Therefore, Dawson (2008) argues that the provision of storage within the pavement serves to delay the movement of surface water runoff into the watercourse, which in turn reduces the risk of flooding. The fact that the runoff seeps into the permeable pavement also means that less standing water is left on surfaces, leading to reduced spray and improved traction for vehicles.

The above literature review has shown evidence to show that permeable pavements reduce the size and volume of storm water drainage through the storage the runoff in the porous material, thus potentially avoiding the peak flows that can overload existing drainage systems. It can also be inferred that permeable pavements are effective in recharging groundwater by allowing the surface water runoff to filter back into the ground.

2.4.4 Pollutant Characteristic

Surface water runoff is major recharging source for receiving water. It is essential to ensure that surface water runoff containing high concentrations of pollutants does not

discharge into a water course, as these can damage any life present in the body of receiving water. Any pollutants and deposits on surfaces can be conveyed into water courses as a consequence of runoff. The level of pollutants in the water depends on activities that occur at or near these surfaces, and the impact of the pollutants on surface runoff depends on the quantity of pollutants, their concentration, and the runoff volume (Pratt et al., 2002). Contaminants in surface water runoff can be generated from numerous sources, such as the presence of open land areas, public use of chemicals, air-deposited substances, ice control chemicals, dirt and contaminants washed off vehicles (Sartor et al., 1974).

Paved urban surfaces are major contributors to surface runoff pollution, as sediments accumulate on these surfaces during dry periods. When the rain falls, deposits wash off and into wastewater treatment plants or open receiving water. As runoff from paved urban surfaces is associated with a build-up and washing off process, rates vary between sites. The rate of runoff depends on rainfall intensity and duration, and deposits and pollutants are affected by the length of any preceding dry period. Urban environments with permeable pavements, assure that deposits and pollutants are filtered inside the sediment structure as the rain falls. In regard to the performance of permeable surfaces, the presence of any pollutants may raise a concern about permeable performance over the lifetime of the pavement; any monitoring of performance should account for operational conditions long term.

In reference to contaminants in surface water runoff in urban environments, CIRIA C582 (Pratt et al., 2002) identified specific pollutants of concern present in road, pavement and car park runoff:

- Sediments;
- metals (zinc, copper, cadmium);
- Hydrocarbons (oil and fuel) including polycyclic aromatic hydrocarbons (PAH);
- Pesticides and herbicides (from landscaping and maintenance); and
- Chloride (from de-icing).

The sediments found in surface water runoff can be categorized into dissolved sediments, suspended sediments, and bed load; they can be further classified according

to particle size, which distinguished between dissolved sediment and suspended sediment(Sansalone and Buchberger, 1997, Sansalone and Cristina, 2004). In terms of soil classification, British Standard 1377:1:1990 (BSI, 1990a) states that sand particles range between 2000 μm and 60 μm, whereas silt particles are between 60 μm and 2 μm. Any particles smaller than 2 μm are clay. Further distinctions have been suggested to separate fine and coarse grains, using a cut off of 63 μm. Suspended sediments are also characterized according to concentration, sediments load, specific gravity, and optical properties. Concentration of suspended solids is a parameter used to measure water quality in stormwater for regulatory and removal efficiency (Herngren et al., 2005). Sedimentary load is a parameter used to determine the quantity of sediment deposited on a surface resulting from different activities, the unit is usually expressed according to weight by unit area.

A number of studies have investigated sediment loads on road surfaces. For example, Sartor *et al.*, (1974) also reported that average sediment loading varies between 3 and 749 g/m^2/year. Deletic and Orr (2005) investigated sediments on an urban road in Aberdeen (UK) over a period of 17 months. The authors found that sediment load ranges between 834.8 and 77.1 g/m^2. Sixty six per cent of the sediments were found within the area up to 0.5 m from the curb. The authors also found the median diameter of sediments (d_{50}) was around 400 μm. (Vaze and Chiew, 2002) investigated build-up and wash-off rates for urban road surfaces in Melbourne, Australia over a period of 36 days. He found that surface pollutants stood at 30 g/m^2 and a maximum of 70 g/m^2. Ellis (1996) estimated that sediment load in car parks in the UK ranged between 124-762 kg / ha/year with an average 440 kg/ha/year.

It is crucial to study the size distribution of particles of any sediment in surface runoff, as this helps to identify any metals present in the particles. Selbig and Banneman (2011) reported that 74 percent of metals were found in particulates, with the remaining 26 percent of the metals in dissolved form. Sedimentary deposits are comprised of coarse and fine particles. Metals are attached to fine particles, because they have a relatively large surface area and contain negative charges as an aspect of their chemical composition (Opher and Friedler, 2010). This means that coarse particles are of lesser importance when studying metal contaminants (Stone and Marsalek, 1996, Sutherland, 2003).

The principal metals of interest are Zinc, Copper and Lead. It has been found that quantities increase relative to a decrease on sediment particle size. High concentrations of these metals have been associated with particle fractions <250 μm (Ellis and Revitt, 1982, Sansalone and Buchberger, 1997). Zhao and Li (2013) reported that 80% of total metal loads was found in particle sizes smaller than <250 μm, while particle sizes <44 μm accounted for greater than 70% of the metals present. It has also been found that particle sizes of less than 50 μm comprise between 70 and 80% of runoff sediments (Vignoles and Herremans, 1995, Roger and Montrejaud-Vignoles, 1998, Andral et al., 1999, Zanders, 2005, Kayhanian et al., 2008, Zhao and Li, 2013).

As stated above, urban stormwater is a major delivery source of contaminants into receiving water, transporting a large quantity of sediment. Thus, sustainable urban drainage system (SuDS) devices have been introduced to control and limit the sediments discharged without treatment into receiving water. However, as all SuDS devices filter the surface runoff that transports the sediments, they are subject to failure, as the sediments affect their performance (Kayhanian et al., 2012). In order to select a suitable SuDS device for sediment control in a given area, gathering data about particle size distribution is critical for each site at which a device is to be placed (Selbig and Bannerman, 2011).

2.4.5 The water quality improvement function of permeable pavement

The quality of rainfall runoff and the pollution of local watercourses and groundwater is a major concern in the UK. The runoff from impermeable areas contains pollutants that adversely affect the watercourses into which the water discharges (Pratt, 1999). The quality of the runoff is affected by contaminants picked up from the impermeable surfaces, such as roads, footpaths, car-parking areas that ultimately pollute the sub soil, ground water and local watercourses. In large storms, the highest pollutant level is found at the early stages of a storm, during the initial period of rainfall which is known as the “first flush” (Campbell, 2004).

Road traffic is one of the largest sources of zinc, polycyclic aromatic hydrocarbons (PAHs) and lead in the UK (Wilson et al., 2005, Napier et al., 2008). These pollutants are washed into local watercourses, where they adversely affect the quality of the water

through the reduction of the oxygen content of the water, the nitrates and phosphates; promote the growth of algae; and supply heavy metals which are toxic to marine life.

Expert opinion is supported by studies carried out on permeable pavements, which confirm that permeable pavements reduce the volume of surface water discharged into watercourses and improve the quality of that discharged water. Brattebo and Booth (2003) evaluated four different permeable pavement types over a six-year period, looking at their structural durability, infiltration rates and the measurable impact that they had on water quality. This study established that almost all rainwater infiltrated the permeable pavements, with minimal surface runoff. In addition, the infiltrated water was shown to have significantly lower levels of metals than direct surface runoff from the asphalt area, with contaminants found in up to 89% of samples from the asphalt runoff, but none in samples from the permeable pavement.

A study by Francey (2005) assessed the effect of permeable pavements on water quality. The study also showed that permeable pavements improve the quality of runoff through the filtration of water through the permeable material; through biological activity within the pavement and the sub-base; and finally through the reduction of the overall level of pollutants reaching watercourses through reduction of the runoff volumes. It can also be predicted that water quality can be improved through the reduction of pollutant levels. Potentially permeable pavements were predicted to have a possible 80% reduction in total suspended solids, 65% reduction in nitrogen, 85% reduction in hydrocarbons and approximately 75% reduction in metals such as lead, zinc and nickel (Francey, 2005).

Permeable pavement systems have the capacity to reduce suspended solids and nitrogen. Permeable pavement systems with an infiltration elemnt have higher denitrify potential than system with underdrain system. (Scholz and Grabowiecki, 2007). Infiltrated water has been shown to have significantly lower levels of copper and zinc than the direct surface runoff from impermeable asphalt pavements (Brattebo and Booth, 2003). In addition, hydrocarbons has been detected in 89% of samples from the impermeable asphalt runoff, unlike in samples infiltrated through permeable pavement systems (Brattebo and Booth, 2003). Research also suggests that permeable pavements are effectively bioreactors, lowering contamination from hydrocarbons by up to 98.7% (Scholz and Grabowiecki, 2007).

The quality of the surface water runoff from permeable pavements was tested by (Nnadi et al., 2008). They sought to establish whether water runoff from pervious pavements was suitable for use in crop irrigation, which was assessed through the addition of oil to a model pervious pavement comprised of non-porous concrete blocks. The chemical content of the runoff was monitored, after which an assessment was made of its suitability for re-use in crop irrigation. The chosen porous concrete block system was constructed of blocks laid on 10mm bed of split pea gravel, a stone sub-base and a geotextile. The geotextile was shown to improve the retention of the system, as well as to affect the biodegradation of the hydrocarbons. The study concluded that the permeable pavement effectively filtered out the contaminants and that the resulting runoff was therefore suitable for plant growth.

Coventry University conducted a study into the quality of storm water discharge for Tarmac, with the aim of investigating the effectiveness of porous pavements in improving surface water runoff quality. Five different types of Tarmac Dry pavements were tested, representing a range of different porous asphalt layers on unbound aggregate sub-bases (Beddow, 2010). The three year study used two sets of pavements: the first loaded with sediment containing heavy metals and clean engine oil, subjected to rainfall equivalent to three years operational life; and the second subjected to solute of heavy metals and used engine oil and rainfall equivalent to ten years operational life. The pollutants used were collected from highway street sweepings. The samples were tested for total suspended solids, hydrocarbons and heavy metal concentrations. This study concluded that it was possible for porous pavement construction to reduce the peak outflow after peak rainfall by attenuating the storm water. These systems were also shown to be able to reduce the volume of the water discharged to the drainage system by increasing the volume of water infiltrated to the sub-grade, as well as by internal storage.

A study carried out by Beddow (2010) maintains that permeable pavements can improve the quality of discharge through sedimentation, adsorption and bio-degradation. This reduces the volume and velocity of water discharged downstream and improves the quality of water discharged into local watercourses. Beddow (2010) found that permeable pavements limited the infiltration of hydrocarbons to below 1mg/l, with up to 99% retention, meaning that heavy metal concentrations were below the World

Health Organisation permitted levels for drinking water. In addition, total suspended solids were limited to 30mg/l, which is within the limits permitted by the Environment Agency. Sediment and hydrocarbons were also found to be retained in the top 3cm of the porous asphalt surfacing material. The hydrocarbons were shown to be biologically degraded by the distribution of microorganisms near the surface of the pavement, where oil and sediment accumulated (Beddow, 2010).

Ball and Rankin (2010) argue that the use of a permeable pavement can improve the quality of rainfall runoff through the increased filtration of the runoff through the permeable pavement. Pollutants are removed from the surface water runoff, through filtration and microbiological degradation as the water seeps through the pavement voids to the sub-surface material. A permeable pavement must contain sufficient void space to allow water to infiltrate into the underlying soil. It has been argued that permeable pavements can improve the quality of the surface water through the removal of 80% of pollutants such as sediment, trace metals and organic matter (Sipes, 2010). In addition, as heavy metals and hydrocarbons are often attached to sediment, these pollutants are reduced as the runoff water is filtered through the permeable pavement material (Ball and Rankin, 2010). As the filtration process slows the flow of runoff discharging into a watercourse, the sediments drop out of the flow before they are able to contaminate the watercourse, while percolation simultaneously reduces the level of contaminants in the surface water runoff (Dawson, 2008, Dzurik, 2003). Scholz (2013) argue that pervious surfaces can reduce the risk of contamination of watercourses by reducing the level of contaminants during filtration (Scholz, 2013).

2.4.6 Hydrological Performance

Although permeable pavements have demonstrated an ability to attenuate runoff, their hydrological performance is still not sufficiently understood. The key component in permeable pavement structure is the aggregate used, which has been shown to affect the characteristics of both hydrology and hydraulics. Pratt *et al*, (1989) studied four different sub base materials were examined: 10 mm round gravel, 40 mm blast furnace slag, 5-40 mm granite, and 5-40 mm limestone. This study found that the lowest runoff was created by the blast furnace slag, which was explained as being a result of the shape

of the blast furnace slag, which has a void space of 48% and therefore offers numerous storage sites for storm water.

The size of the aggregate can affect evaporation, drainage and the storage (Andersen et al., 1999). Investigations into the gradual movement of water through the structure of permeable pavements have examined the relationship between rainfall input, storm water drainage, and evaporation over time. This was supplemented with an examination of different types of bedding course with a variety of grain size stones and in different rainfall intensities and durations. Anderson *et al*. (1999) found that 55% of rainfall (15 mm/hr for one hour duration) can be retained in a previously dry pavement with a grain size of bedding stone ranging from 1-10 mm.

The grain size of the materials was also shown to exert a considerable influence over the movement of water. For instance, small aggregate size demonstrated the ability to prolong the lag time and lower drainage from the rig pavement, suggesting that decisions about the size and shape of aggregate may be critical in the design of permeable pavements. These findings were supported by Cooley *et al.* (2002), who showed that permeability seems to be extremely dependent on particle size distribution. In other words, they state that the density of aggregate influences the permeability, meaning that the higher the density of aggregate, the lower the permeability it should be expected to have.

A high degree of permeability in pavements can potentially interfere with their structural integrity. Therefore, in order to ensure that pavement retains a desirable level of performance, a compromise needs to be found between stiffness and permeability (Pratt et al., 2002). Continuously graded materials create a stiffer structure that is less permeable, which could potentially be explained by the fact that continuously graded soil normally has a range of particles that are less than 2 mm in size, which decreases the void space and results in low permeability (Moulton, 1980). In comparison, the single size aggregate creates structures that have large open voids, which makes the construction less dense but provides higher permeability. Infiltrations and structural tests have been conducted to test the extent to which a change in the grading of the materials alters the permeability and stiffness (Shackel et al., 2008). Results indicate

that the use of a clean 2-5 mm aggregate seems to be the best way of combining high water infiltration and good structural performance.

The volume of runoff water stored and therefore the overall performance of the permeable pavement has been shown to be profoundly influenced by the porosity of the construction materials and the base upon which the pavement is built. Most pavements consist of a surface layer that is supported by a sub-base, laid on a prepared sub-grade material. The materials chosen will tend to depend on the levels of predicted traffic, as well as the type of traffic expected to use the pavement. The decision will also be influenced by the bearing capacity of the existing ground, the type of existing soil and the local water table (Pratt et al., 2002).

A study by Collins *et al.* (2008) examined the performance of four types of permeable pavements against a standard asphalt pavement. Two types of permeable interlocking concrete pavements were studied, one with 12.9% open surface area and the other with 8.5% open surface area. In addition, the study examined a permeable pavement of concrete grid pavers filled with sand and a permeable pavement of pervious concrete. All the pavements were used as car parking areas, which were carefully monitored over eighteen months, taking account of volumes of surface runoff and total outflow, peak flow rates and time to peak flow rates. The conclusion of the investigation was that the four types of permeable pavement types significantly reduced runoff volumes and peak flow rates in comparison to the standard impermeable asphalt pavement. The high open surface area interlocking pavers and the concrete grid pavers were shown to perform better than the other two permeable pavement types, yielding noticeable lower runoff volumes and lower peak flows (Collins et al., 2008).

The chosen sub-base material will ultimately depend on the particular surface layer that has been selected and the proposed end-use of the pavement. For example if the surface layer is open graded asphalt then it can be recommended that a sub-base be selected which is composed of high void material such as a bed of stone recharge (Gopalakrishnan, 2011). The bed of stone should be single sized stone with a large percentage, approximately 40% voids, for infiltration purposes. Gopalakrishnan (2011) also recommends that a separator material, such as a geotextile, be placed beneath the sub-base. This will help to prevent contamination of the stone bed by the sub-grade

material, while simultaneously allowing the runoff water to filter through to the sub-grade material. However, the precise level of filtration will depend on the type and compaction of the sub-grade material (Dawson, 2008). In cases where the sub-grade is impermeable, like clay for example, then the pavement must be designed to allow horizontal runoff in order to prevent degradation of the sub-grade. In permeable sub-grade, it may be possible to construct vertical drains to the water table.

Overall, the hydrological performance of permeable pavements is governed by a large number of factors, including the type of materials used in their construction and the particle size distribution. These factors can directly affect permeability, then leading to the reduction of hydraulic conductivity for permeable pavement systems. A review of previous studies summarised that hydraulic conductivity could be a primary driver in the improvement of the performance of permeable pavements, and for this reason hydraulic performance needs further investigation.

2.5 Operating life and maintenance

2.5.1 Clogging

The infiltration rate of permeable pavement reduces over the lifespan of a pavement because of the sediments that accumulate through its structure (Interpave, 2010). This may be due to the accumulation of fine sediments in the void spaces over time, leading to a gradual reduction in the void ratio of the structure, with a resultant decrease in permeability. The effective life of a permeable pavement is the length of time the pavement remains in service until the rate of infiltration of storm water is reduced to an unacceptable level (Pezzaniti et al., 2009, Lucke and Beecham, 2011, Yong et al., 2013). The end of effective life occurs when the pavement behaves as an impermeable surface, meaning the permeable pavement is unable to reduce peak flow volume and to trap pollutants. This process is known as clogging. Siriwardene (2007) defines clogging as the process of eliminating the porosity and permeability of permeable pavement due to physical, biological and chemical processes. Mullaney and Lucke (2014) define clogging as the result of many particles such as fines, organic matters, and traffic-caused abraded particles that block pore spaces due to physical, biological, and chemical process.

A number of studies have studied the clogging within the structure, including (Pratt, 1990, Dierkes et al., 2002, Davies et al., 2002, Borgwardt, 2006, Pezzaniti et al., 2009, Yong et al., 2013, Boogaard et al., 2014). Research suggests that blockages in the pavement structure do not completely fill the voids, instead forming a clogging layer at the bottom of the pavement. The failure in a permeable pavement can be referred to poor construction, bad design, low permeability soil or poor maintenance (Pratt, 1997). Sediment erosion during construction can sometimes be lead to the failure of permeable pavement (Cahill, 1994). Pratt (1990) conducted a laboratory experiment on small-scale model in order to examine pollutant retention within permeable pavement for long-term performance. The rig consisted of a series of interlocking plastic rings 110 mm by 350 mm. The materials used were blast furnace slag, granite, and limestone. Urban stormwater from surrounding impermeable surfaces was applied to the model in order to simulate ten years of sediment loading. Pratt found that the sediment and organic materials accumulated in the upper layers of the bedding materials and on the upper geotextile layer.

Davies et al. (2002) conducted a laboratory study on the infiltration performance of permeable pavement, both with silt and without silt, at a range of surface gradients up to 10%. They demonstrated that the addition of silt can result in high levels of blockage because of the infiltration. The increase of gradient was also found to slightly worsen the infiltration. Borgwardt (2006) investigated the long-term infiltration performance of PICP. He concluded that infiltration rate decreased significantly within a few years of the life span of the pavement. The reduction in infiltration was attributed to the mineral and organic particles (less than 63 μm in diameter) that were retained in the upper 20 mm of the surface.

Siriwardene et al. (2007) investigated this phenomenon in order to understand the role that sediments play in the clogging process. Their test rig was formed from detachable Perspex segments, with 90 cm of gravel built on top of 70 cm of soil. An infiltration system operated at a constant water level was shown to be likely to slow the clogging process by acting as barrier, meaning that the particles are partially prevented from reaching the clogging layer. In contrast, a fluctuating water level does not create a barrier, resulting in the sediments being rapidly dragged to the clogging layer. In reality, the fluctuating water level system is widely used, which explains why storm water

infiltration systems tend to suffer from the issue of clogging after time, when they would normally be expected to regularly empty. A sediment particle size of less than 6 µm was shown to be the main driver in the development of the clogging layer.

Davies et al. (2002) state that infiltration rates through permeable surfaces tend to be high, especially in newly laid pavements, with rates in excess of 10000 mm/h. Although these rates will reduce over time, potentially by as much as 10% over the life of the pavement, the rate of infiltration is influenced by the materials used, as well as by the presence and type of geotextile. Therefore, in order for permeable pavements to function efficiently, they must be regularly maintained. Studies have shown that when these pavements are properly maintained, they can have an effective operational life of up to 15 years (Pratt, 1997).

2.5.2 Maintenance

A number of key design factors affect the performance of permeable pavement design and reduce attendant risks. These include the conditions of the local site, the materials used in the construction, and the particular methods used in design and installation of the surface (USEPA, 1999). Pervious pavement systems, including porous concrete or porous asphalt, also have a tendency to become clogged within three years after installation (Scholz and Grabowiecki, 2007). When the voids become clogged, this reduces the porosity of the system. Scholz and Grabowiecki (2007) explain that the main causes of clogging are:

- Sediment being ground into the porous pavement by traffic;
- Waterborne sediment which drains onto pavements;
- Shear stress from repeated breaking actions of vehicles, resulting in damaging pores;
- Transport via wind and runoff from local disturbed soil.

Once severely clogged, these surfaces have to be removed and replaced, emphasising the need to minimize this occurring through the maintenance of pavement areas and locating them away from areas with surface soil disturbance (Hunt and Collins, 2008). There is increasing evidence that surfaces do not clog completely, however, even without regular maintenance (Shaffer et al., 2009). This suggests that correctly designed

and constructed permeable pavements may have an operational life comparable to impermeable surfaces. Because they are not displaced by the weight or movement of vehicles, porous concrete and asphalt constructions tend to have a longer lifespan than mobile surfaces such as gravel, however. The limitation of gravel to lightly trafficked situations makes it possible to assume a similar design life for gravel driveways under the right conditions (Shaffer et al., 2009).

As stated earlier, permeable pavements are likely to become less efficient at reducing volume of rainfall runoff over time, as solid particles block the voids (Dawson 2008). This has been confirmed by Bean et al. (2007) on the surface infiltration of twenty-five permeable pavement sites in North Carolina, Maryland and Delaware. The study sought to ascertain the rates of runoff infiltration on different types and ages of permeable pavement types, looking at pavements aged six months to twenty-one years. An evaluation was conducted of twelve permeable concrete grid pavers with sand, which were tested under two conditions: existing state and after maintenance. In the second scenario, approximately 15 mm of the top layer of residue build up was removed from the pavement to simulate maintenance. The results showed that maintenance improved the rates of infiltration on 92% of the sites, with infiltration increasing from an average of 53.34 mm/h (2.1in/hr) in the existing state to 88.9 mm/h (3.5 in/hr) post maintenance. The study also tested permeable interlocking concrete pavers and found that the infiltration rates were dependent on the location of the pavement. Rates of infiltration were shown to be considerably slower in areas where the pavers were located near loose fine material. The study concluded that permeable pavements can provide greater infiltration rates of surface runoff into the subsoil material, with the rate of infiltration tending to be largely dependent on the maintenance levels and the presence of loose fine (Bean et al., 2007). Finally, all the permeable pavement types tested in sandy soil environments had relatively high surface infiltration rates, with the minimum rates comparable to those of a grassed sandy loam soil.

Due to the build-up of detritus in the jointing material, the infiltration rate of a permeable concrete block pavement will usually decrease with age; however infiltration rates seem to stay above rainfall intensity (Interpave, 2010). If true, this suggests that there should be sufficient infiltration to cater for rainfall events even without regular maintenance. Water ponding on the surface is a clear indication of the insufficient

infiltration and the joints/voids will need to be cleaned, even they need to be replaced. As with conventional pavements, depressions, rutting and cracked or broken blocks will tend to be detrimental to the performance of the pavement or a hazard to users, and will therefore require corrective actions to be taken (Interpave, 2010). The corresponding maintenance requirements can vary, although they typically include the removal of clogging, in the form of leaves, mud or litter; brushing the surface to stop weeds from growing and reduce blocking; and removal of any weeds that have grown.

It is clear from the literature review that the sediment was main cause of clogging; however, there is lack of understanding on the effect of maintenance on the clogging rate.

2.5.3 The effect of frost

In cold climates, the temperature can fall below freezing and the soil moisture migrates, freezes and expands. Varying moisture levels mean varying ice formation, thus the "Frost Heave" may give an uneven surface to pavements. This phenomenon leads to soil being moved upward, and consequently an uneven surface pavement appears. Additionally, during spring, the ice melts and leaving voids in the soil structure. This lessens the density and thus ability of the soil to support the upper layers.

Studies show that permeable pavement has performed effectively in cold climate conditions (Bäckström and Bergström, 2000, Duin et al., 2008, Roseen et al., 2009, Gomez-Ullate et al., 2010, Roseen et al., 2012). Pratt (1997) suggests that the air inside the permeable pavement structure could act as a ''night storage heater''. Backstorm (2000) agrees that the air stored within the pavement delays the freezing point in the soil below the pavement, compared to conventional road constructions. Ferguson (2005) points out that ice formation does not happen in well-drained structures such as coarse-grained soils; this is due to large pores, which usually contain insufficient water to grow an ice mass. Tyner *et al.* (2009) investigated twelve porous concrete pavements and reported that the temperature of porous concrete dropped below freezing point, water was not present in the storage volume; maybe because the presence of water is likely to raise the specific heat capacity of the system, which delays the freezing of the pavement until it drains (Tyner et al., 2009). Al-Rubaei *et al.* (2013) studied infiltration on porous

asphalt under Swedish conditions. Their finding showed that the infiltration rate continued high during wintertime, despite heavy frost (Al-Rubaei et al., 2013).

From the above studies, it can be concluded that the pervious pavements were shown to be more resistant to frost than conventional pavement, in cold climates. This is due to the features of their structure (1) sub-base material (e.g. aggregates) forms larger pores than soil, (2) the specific heat capacity of air stored in the structure delays the freezing point.

2.5.4 The research gap

Permeable pavements play a vital role in sustainable urban drainage systems, making them a subject of considerable interest to both specialists and engineers. The review of literature clearly indicates that permeable pavements have proven their usefulness regard to the management of storms (Pratt et al., 1989, Schluter and Jefferies, 2002). However, previous studies have revealed a relatively significant degree of uncertainty regarding both their operational performance and maintenance requirements (Abbott and Comino-Mateos, 2003, Scholz and Grabowiecki, 2007, Newman et al., 2013). The performance variation may be attributable to the length of case study monitoring and influence of sediment across the pavement surface, thus the necessity for ongoing pavement maintenance. The lack of clear information and understanding of these pavement performance factors is the key driver behind this research experimental design. This suggests a need for further investigation into this form of pavement system, in order to address the gaps existing in the literature and understanding, as well as ensuring that the body of available knowledge remains up to date.

2.6 Chapter summary

With growing urbanisation, impervious pavement has become major issue worldwide creating a diverse range of problems, such as flooding risks and danger to natural habitats. The function of this phase of the project was to critically review and present permeable pavements and their impacts on water quality and quantity. It has identified that the use of permeable surfaces brings many benefits and that many countries recognise and promote the use of permeable pavement in controlling stormwater more

effectively towards a sustainable environment. Most literary sources agree that pervious pavements are able to attenuate excess runoff as well as capturing pollutants (Pratt, 1990, Pratt et al., 1995, Pratt et al., 2002, Abbott and Comino-Mateos, 2003, Novotny, 2003, Francey, 2005, Gopalakrishnan, 2011). Current practice have been reviewed to assist the direction of the research. The aim of the research is to investigate the possibility for attenuation of any excess run-off and measuring the potential clogging which can occur in the structure of the pervious pavement from sediments.

CHAPTER 3 – EXPERIMENTAL DESIGN

3.1 Introduction

This research will study the hydrological performance of a permeable pavement that mimics a car park. The research will also investigate the impact of sediment particulates on the hydrological performance of a permeable pavement. The data required to achieve the research objectives included:

- Rainfall data (inflow);
- Outflow rate and volume;
- Retention volume;
- Additional data: such as moisture content, temperature, and relative humidity;
- Sediment loading
- Concentration of suspended solids in the outflow.

Three types of equipment have been designed and developed in order to gather the above data:

- A laboratory based permeable pavement rig, with a model structure following current best practice engineering design;
- A water delivery system (artificial rain simulator); and
- A water collection system (post infiltration).

Additional equipment has been utilised during the experiment to monitor the external and internal condition of the pavement's structure; that is, to measure moisture content, temperature and relative humidity.

This chapter is divided into three sections that describe the research methodology, experimental approach, and the experimental procedure.

3.2 Research methodology

The research was conducted in the hydraulics laboratory at Heriot-Watt University. The overall purpose of the investigation was to gather data that can be used to understand the performance of a permeable pavement in terms of water quality and quantity. For this study, the laboratory involved the following considerations: structural and hydraulic design of permeable pavement, construction of the rig, selection of materials and measuring instruments. The experiment was divided into two phases: firstly to investigate the hydrological performance of the original test rig, secondly to examine the influence of sediment on the hydrological performance of permeable pavement.

3.2.1 Hydrological performance phase

The hydrological phase was designed to investigate two stages; the short-term and the long-term hydrologic performance of the pavement (as shown in Figure 3-1). The former will consider the period a few hours after rainfall cessation. This stage will include data such as rainfall duration, rainfall volume, and drainage volume. Through monitoring the input and output flow characteristics, it is possible to calculate the retention time and storage volume of the pavement. The impact of evaporation from the permeable surface was considered to be negligible during rainfall event, given that air temperature and relative humidity (RH) was less variation because it was indoors and not subject to varying weather conditions. In the field this would obviously not be the case. Consideration was given to monitoring the mass changes in the rig, to account for fluctuations resulting from evaporation loss. However, due to the weight of the model structure (approximately 2 tonnes dry), continuous monitoring of the structure weight for very fine fluctuations was not feasible. However, small-scale hydrology experiments on the surface component of permeable pavement were undertaken in order to estimate the evaporation from surface (basic hydrology experiment will be discussed in Section 3.5.1)

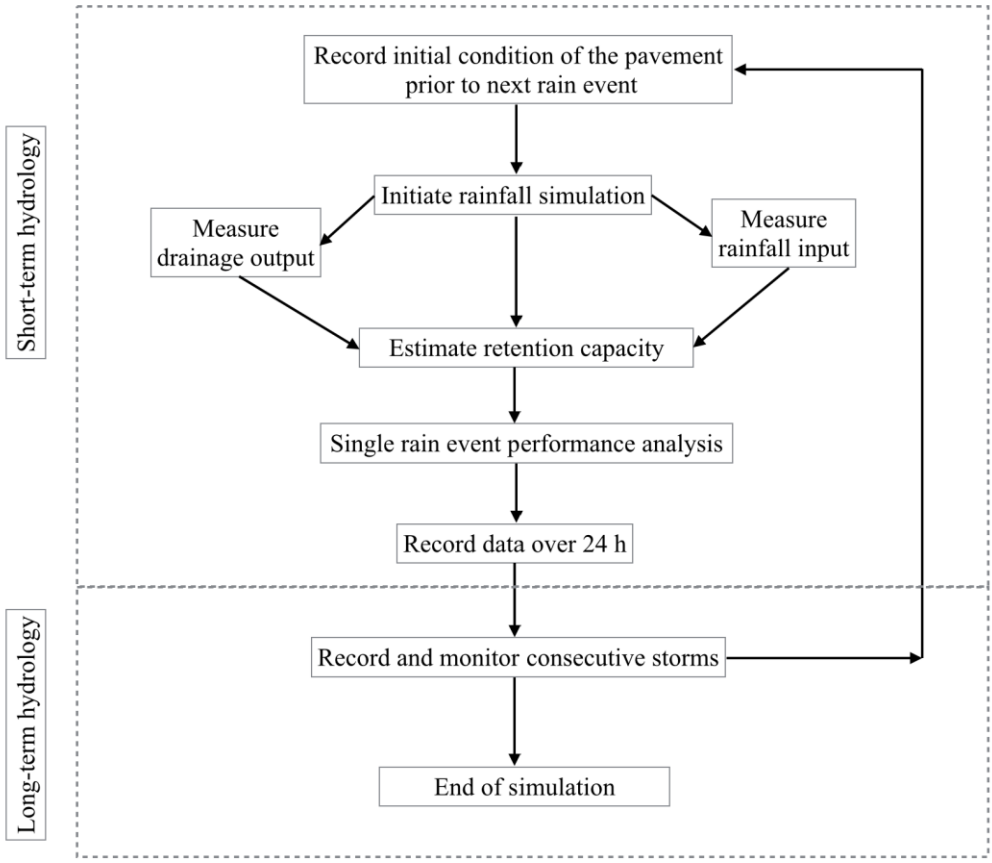

Figure 3-1: A procedure for the hydrological investigation.

3.2.2 Sedimentation phase

This second phase of the research was to evaluate the process of sediment accumulation within the structure overtime and to monitor the change in drainage volume after the addition of sediment to the pavement surface.

Figure 3-2 presents the procedure of this stage. The sediment phase was designed to describe a one year simulation that included rainfall simulation and sediment application representative of an average annual occurrence. However, there were a number of points that required consideration before beginning this phase:

- The input concentration of sediment;
- Particle size of input sediment;
- Information from the hydrological phase;
- Type of sediment; and
- Analysis of output concentration.

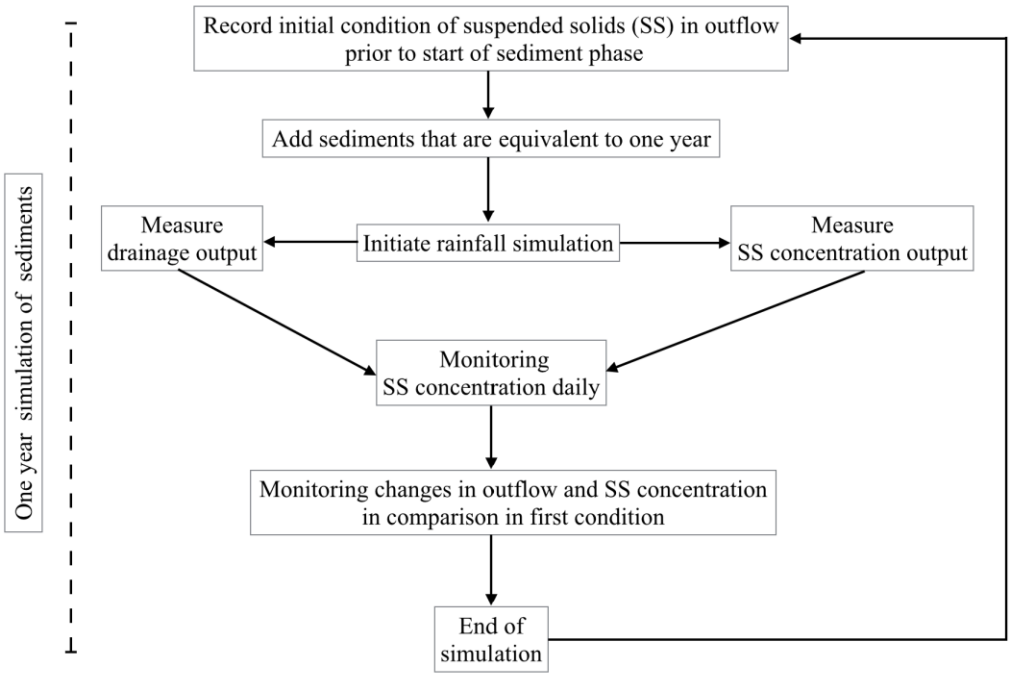

Figure 3-2: A procedure for application of sediment for one year simulation.

3.2.3 Design method

The basic permeable pavement design seeks to capture and store rainwater, infiltrate the stored water into the subgrade, while simultaneously withstanding an active traffic load. As discussed in Section 2.4.1, a permeable pavement consists of three systems, which have been introduced in Interpave guidance (Intepave, 2010). This guidance has been adopted in British Standards and The SuDS Manual (CIRIA C697) (Woods-Ballard et al., 2007). The laboratory pavement was designed to represent a full scale car park surface. It was intended that the laboratory pavement rig would mimic the functionality of an appropriately located permeable pavement in the urban environment, i.e. in an area of appropriate soil infiltration capacity and a water table of at least 1m in depth below surface level. Therefore, the pavement design used in this research was permeable pavement system (A) (see Figure 2-6). The timescale of the experiment was selected to simulate both short and long hydrology performance and the impact of sediment on hydrology performance. The sediment experiment was designed to evaluate the first 10 years of the lifespan of permeable pavement.

3.2.4 Data collection and analysis

The data collected in this study was divided into four main types, as shown in Figure 3-3. Data was gathered from all the equipment by a data logger and analysed in order to assess the hydrological process. The data collected included:

- The input (rainfall intensity) during the test, in order to produce a hydrograph;
- The output (outflow volume) to observe changes before and after rainfall start;
- The moisture content of the sub-grade before and after storm commencement; and
- The surface and air temperature and relative humidity during the length of the experiment.

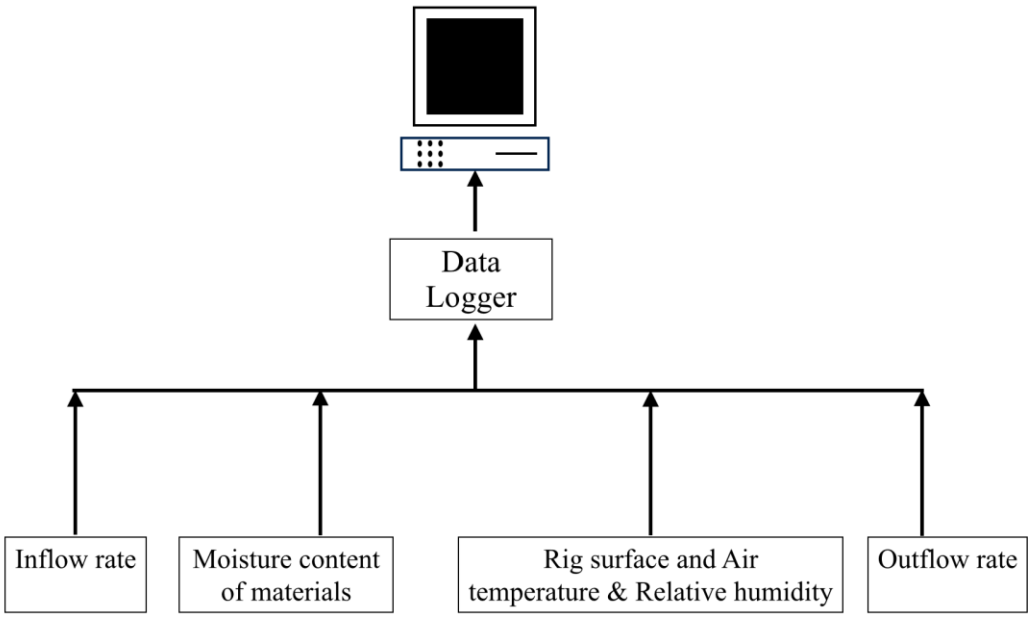

Figure 3-3: A flow diagram representing the data collected.

3.3 Permeable Pavement Components

3.3.1 Model structure

The model structure will represent a car park surface at 1 to 1 scale. It was designed:

- To be representative of the typical size of a car park ($1m^2$).

- To follow technical guidance that is provided by the SuDS manual, British Standard and manufacturer.
- To be a model structure that can effectively represent and replicate the performance of permeable pavement for long period.

The physical structure was constructed in the hydraulics laboratory at Heriot-Watt University. It was made of strong polypropylene walls within a welded steel frame. The dimensions of the pavement rig were 1000 mm x 1000 mm x 1600 mm, with one side made of Perspex to allow visual inspection of the subsurface material as shown in Figure 3-4. At the base of the rig, a stainless steel mesh was provided to support the base of the structure. The metallic and polypropylene structure was design to provide enough space for all (3 dimensional) constituents of permeable pavement. These include:

- Concrete block paving;
- Bedding course materials;
- Sub-base materials;
- Geo-textile; and
- Sub-grade material.

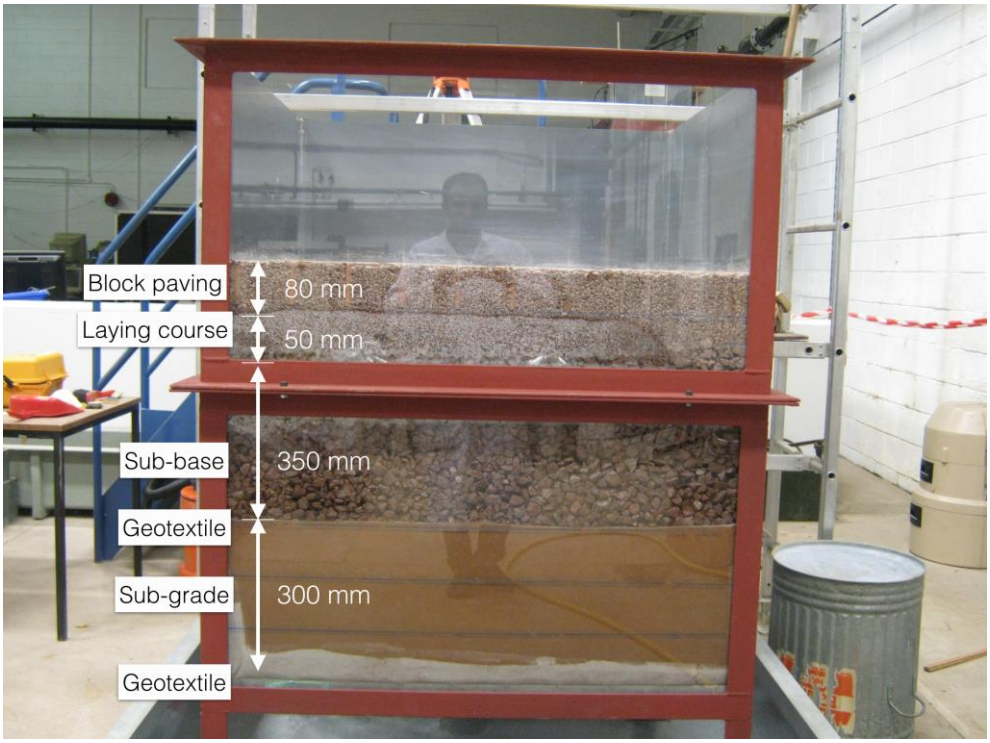

Figure 3-4: Cross section of model structure.

The depth of the permeable pavement was designed in accordance with the SuDS Manual CIRIA C697 (Woods-Ballard et al., 2007) and British Standard 7533-13-2009 (BSI, 2009). It consisted of 80 mm of block paving, a course substrate bedding layer of 50 mm, a sub-base layer of 350 mm, and subgrade layer of 300 mm (see Figure 3-5). The following list offers a brief description of the components of the materials from the base up:

- Geotextile was placed over the stainless steel mesh, preventing sub-grade materials from washing into the lower container.
- The sub-grade layer was filled with 300 mm of clean sand.
- The second geotextile layer was positioned between the sub-grade and sub-base layer, to prevent the migration of the sand particles to the aggregate;
- The sub-base layer comprised of 350 mm of coarse aggregate (size 20-4 mm);
- The bedding course layer comprised of 50 mm of fine aggregate (6-2 mm); and
- The paving blocks were then placed on the top.

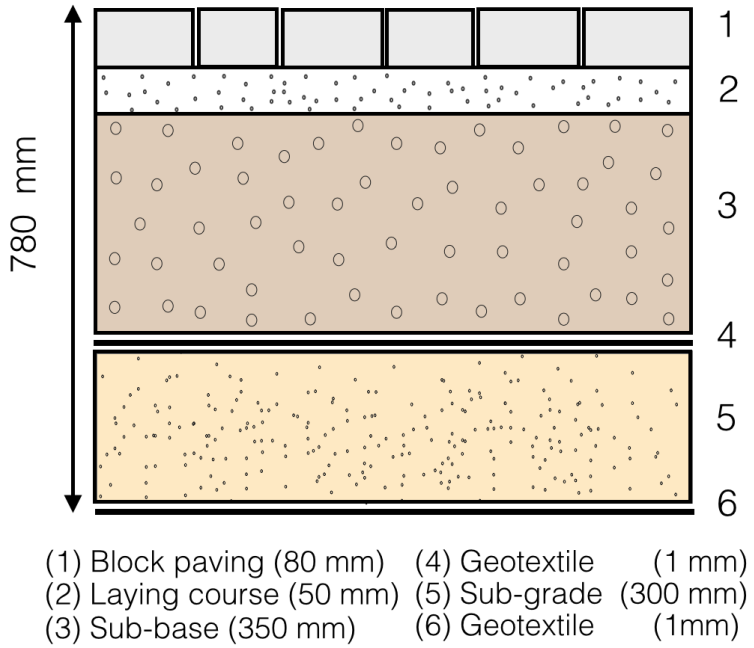

Figure 3-5: A Schematic illustrating the layers comprising the permeable pavement and thickness of each layer.

3.3.2 Block surface

The block surface layer forms the upper layer of the permeable pavement. The function of this is to allow the water to infiltrate the layer and at the same time transport the traffic load into the lower layer reducing the traffic abrasion effects. The block concrete paving was provided by Marshall (a commercial permeable paving block provider located within the UK). The Priora block paving (see Figure 3-6 a) has dimensions of 200 x 100 x 80 mm. Block paving are designed with a nib, a protrusion along the block edge creating a void between adjacent blocks. The unique patented Priora nib leaves a space between the bricks to allow water to infiltrate (see Figure 3-6 b) The design permeability of the Priora blocks 18750 l/sec/ha (6750 l/hr/m^2 = 6750 mm/hr) (Marshalls, 2013).

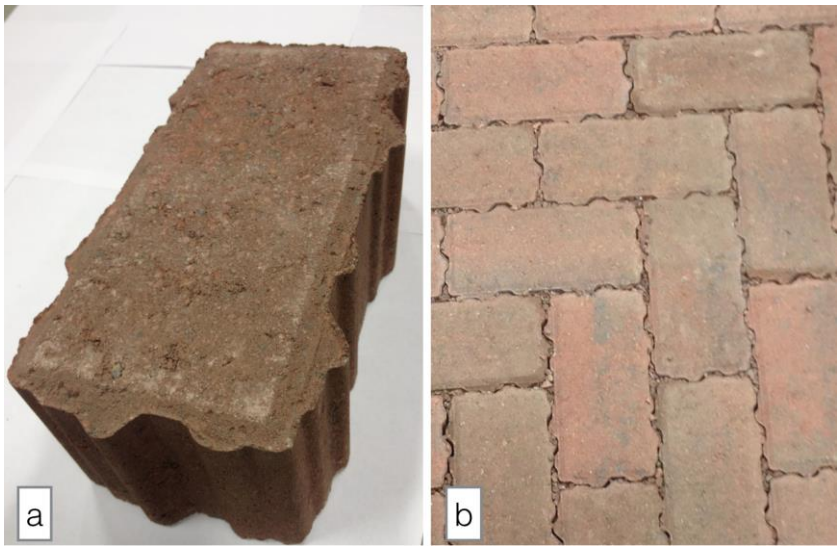

Figure 3-6: (a) Marshall block paving (Priora); (b) details of completed permeable pavement surface, showing layout of block paving.

3.3.3 Bedding course layer

A layer 50 mm of fine aggregate (6 mm Priora Aggregate, by Marshall) formed the bedding course layer. The grading of the fine aggregate was guaranteed to fall within the particle size distribution recommended by the manufacture (see Figure 3-7), and the construction was in accordance with BS EN 13242 (BSI, 2002).

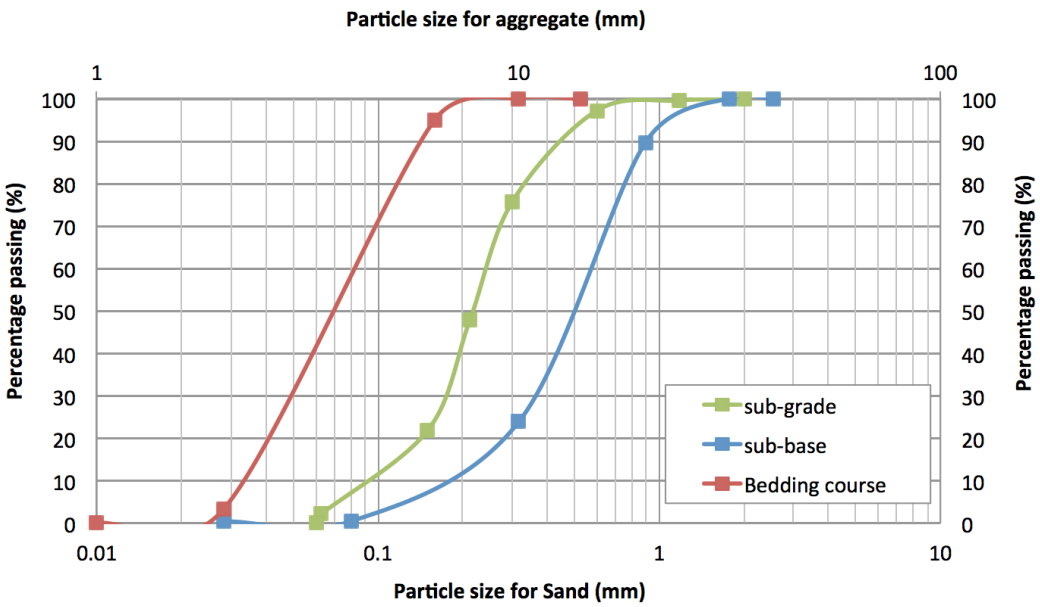

Figure 3-7: The particle size distribution curves for bedding course (6 mm Priora Aggregate), sub-base (20 mm Priora Aggregate), and sub-grade (sand).

3.3.4 Sub-base layer

The sub-base layer was the main structural element of the pavement, offering significant temporary storage capacity for the water. The material within this layer should be designed with sufficient porosity to allow water to pass through. The material is also required to handle the design traffic load on the pavement. The sub-base was made up of 350 mm of coarse aggregate (20 mm Priora Aggregate, provided by Marshall). The grading of the coarse aggregate, as shown in Figure 3-7, was determined in accordance with British Standards BS EN 13242 (BSI, 2002).

3.3.5 Sub grade

To fit permeable pavement system requirements, the sub-grade material should achieve suitable permeability consistent with the Californian bearing ratio (CBR) over 5 per cent (Woods-Ballard et al., 2007). The sub-grade was filled with clean sand with a particle size distribution as illustrated in Figure 3-7. The sand was classified as uniform graded sand, according to the British soil classification system for engineering purposes BS 5930 (BSI, 1981).

The constant head method BS 1377-5 (BSI, 1990c) was used to measure the permeability (hydraulic conductivity) of the sand. Full details of test data are in Appendix A (see Table A - 2 and Table A - 3 of Appendix A). The permeability for the sand was 219.15 mm/hr (609 l/ha/sec); and the accepted minimum permeability of subgrade is 13 mm/hr (36.11 l/ha/sec) (USEPA, 1999). The material therefore fell within the acceptable limits appropriate for permeable paving construction.

During the construction phase, the sub-grade material must be compacted, to improve the paving structures strength by increasing the unit weight (Intepave, 2010). Therefore, the Proctor Test BS 1377- 4 (BSI, 1990b) was carried out on a sample of sand, in order to obtain the degree of compaction required to obtain the desired design strength. The Proctor test also measures the optimum moisture content at which maximum dry unit weight is attained. Figure 3-8 shows the optimum moisture content to be 12.87% at maximum dry density 1011.21 kg/m^3 (see Table A - 1 in Appendix A). The soil sample was prepared with the addition of a known volume of water to known weight of sand, in order to achieve a compaction degree with optimal moisture content.

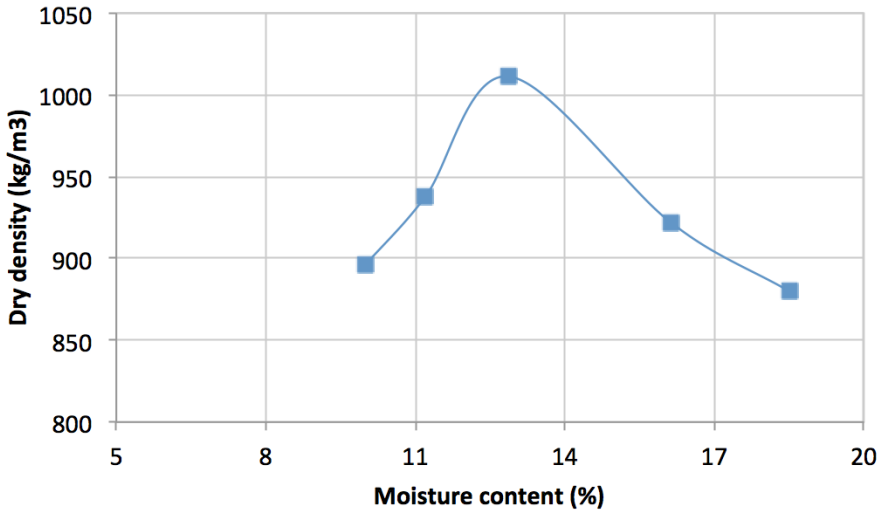

Figure 3-8: Standard Proctor Curve for sub-grade materials

3.3.6 Geotextile

Non-woven Geotextile was placed in two positions within the permeable pavement structure. One layer was positioned between the sub-grade and sub-base to prevent the sub-grade (sand) from moving into the sub-base (coarse aggregate). The other layer

was added above the base support mesh to prevent the sand from washing into the lower container. Geotextile (Terram T900) was used; it is made of 70% polypropylene and 30% polyethylene. It has a pore size of 75 µm and a tensile strength of 7.5 KN/m. The permeability is 95 l/m^2/sec (TRERRAM, 2012).

3.4 Experimental Equipment

3.4.1 Water delivery system

The function of the water delivery system is to deliver water into the surface pavement mimicking a natural rainfall event. Therefore, a rainfall simulator was designed to generate rain droplets that emulate the characteristics of natural rainfall. The challenge in this design was finding a suitable rainfall simulator that achieves research and experiment requirements. The simulation of known and specified rainfall intensity and volume was key to the rain simulator design and laboratory research. A further key element was the generation of a sufficient range of rainfall intensities as well as volumes for the experimental testing purposes. For this reason, simulation of identical rainfall intensities and durations were required prior to rig experimentation commencement.

3.4.1.1 Design of a rainfall simulator

The design of the rainfall simulator should be determined according to the needs of each individual researcher (Bowyer-Bower and Burt, 1989, Andersen et al., 1999). The design of rainfall simulators discussed in the literature review consists of three systems (Andersen et al., 1999): spray system, spray rotating system, and drip system. This research adopted a spray system because it is effective in terms of consistent coverage and distribution across a small surface area, such as over one metre square.

Spray nozzle

The nozzle is a key component of a rainfall simulator. Therefore, the process of choosing a nozzle depends on the rainfall application rate as well as the number of nozzles intended to cover the plot study area. The rainfall application rate was based upon the Flood Estimation Handbook. The design storm event selected for this research was the 1 in 5 year, 1 in 10 year and 1 in 10 year average return interval storm events.

The rainfall depth and duration of these events for Edinburgh were calculated using the FEH CD-ROM software (CEH, 2009). Thus, the storm events chosen for the study were: 6.39, 7.78, and 10.85 mm; these were applied over 15, 15, and 30 minutes respectively.

The design surface study area was one meter square. Despite the small area, it was difficult to find a single nozzle to fit the requirement in terms of the range of intensities and consistent coverage; therefore, it was decided to use more than one nozzle. The chosen nozzle was manufactured by Delavan Spray Technologies, (see Figure 3-9). This nozzle produces discharge rates ranging between 2.87 to 7.63 l/hr at pressure ranges between 5 to 35 bars respectively. The nozzle produces a solid cone spray pattern.

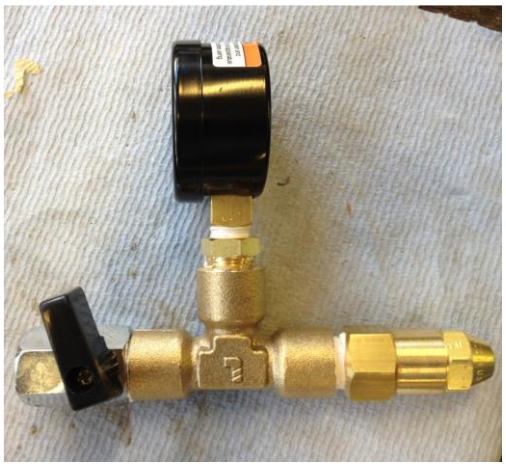

Figure 3-9: Assembled Spray nozzle consists of spray nozzle, pressure gauge, and valve (spray type: WDB 12, 0-60° Stainless Steel).

Structural design

The rainfall simulator frame structure was designed to be a simple, portable, and lightweight structure that would be easy to assemble and disassemble for maintenance. The frame was made of 150 mm diameter lightweight copper pipe. The frame structure included additional components; push-fit fittings (push-fit connectors), a pressure gauge (0 to 7 bar), and valves, as shown in Figure 3-10. There were nine orifices located on the frame for the spray nozzles. These orifices, and therefore the spray nozzles, were located in a grid pattern. The entire structure was mounted above the permeable pavement surface (see Figure 3-11). The mesh was introduced into the design to

increase the droplet size, as the current spray nozzles produce mist sprays and natural rainfall droplet size is larger than mist droplet size.

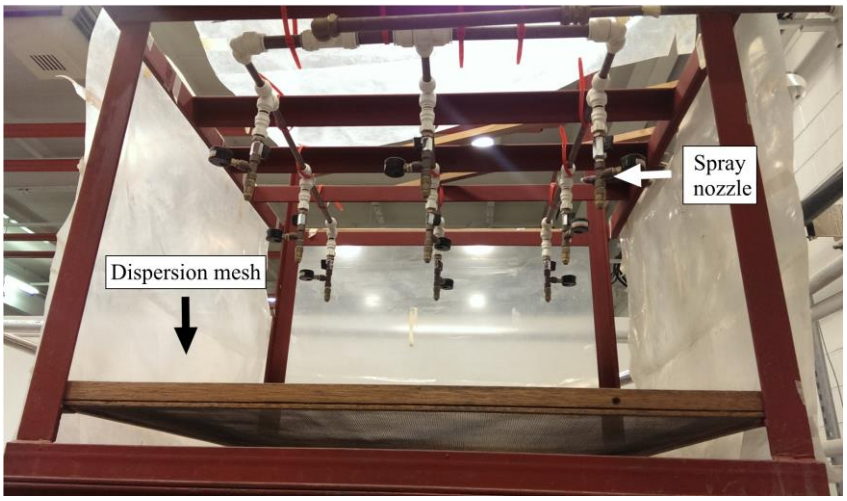

Figure 3-10: Assembled rainfall simulator.

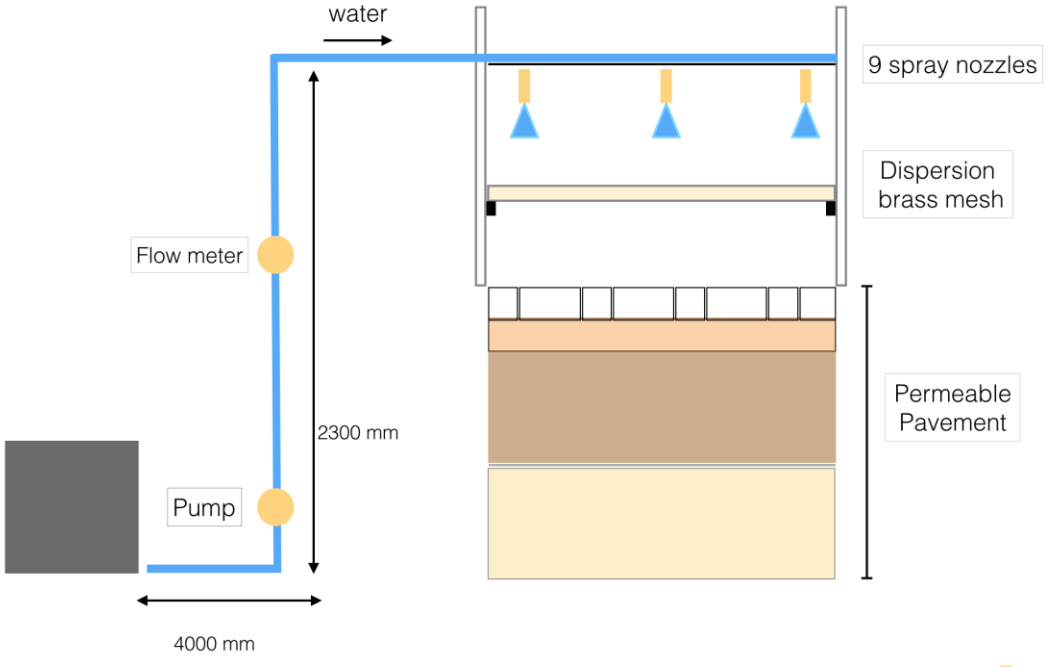

Figure 3-11: Schematic layout of the rainfall simulator.

3.4.1.2 Performance calibration of the rainfall simulator

Flow meter calibration

A flow meter was placed in the main pipe before the rainfall simulator. It was connected to a data logger in order to record the inflow rate over time, throughout the test. The FLR1000 Omega flow meter was used in the experiment. It was calibrated by the manufacture. The flow meter can measure from 3.33×10^{-6} to 3.33×10^{-5} m^3/s (3.33×10^{-3} to 3.33×10^{-2} litres per second).

While the original calibration certificate was provided by the meter manufacturer, an in line calibration process was undertaken to obtain actual performance details of the flow meter. Calibrating the flow meter using the same liquid and conditions to be used in the research tests provided a more applicable and appropriate analysis of the systems performance. Four flow tests were conducted to identify the relationship between the flow-meter output and the actual flow rate. Figure 3-12 illustrates the linear regression relationship between flow output (voltage reading) and measured flow, R^2 value of 0.91. The calibration equation is presented as follows, where Q is flow rate in litre per hour and V is voltage reading in volts:

$$Q = 0.0232 \times v + 0.3576 \quad \textbf{(1)}$$

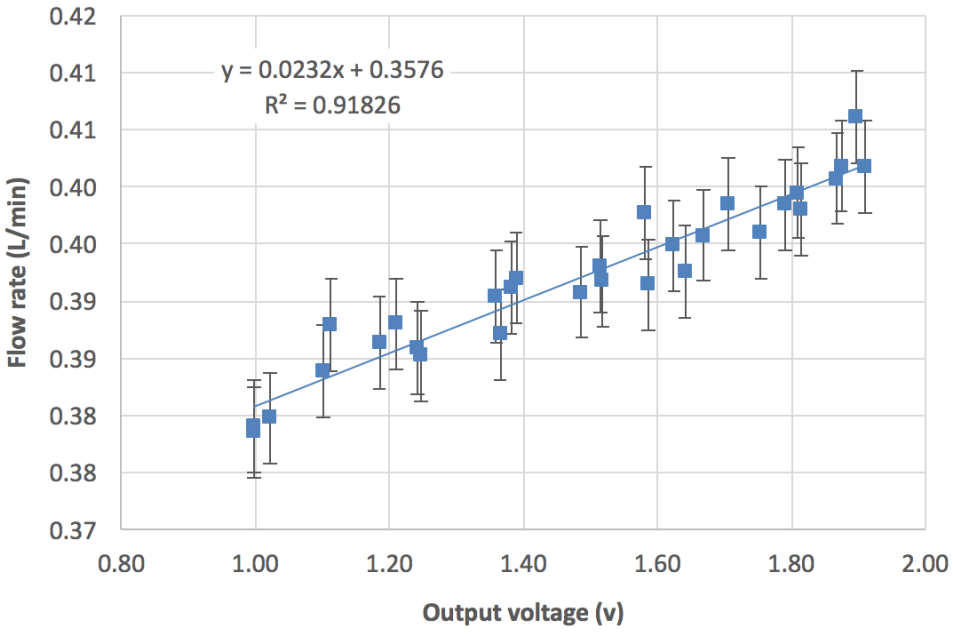

Figure 3-12: Calibration data for the flow meter.

Full details of the results obtained from four tests can be found in Table B- 6 to Table B- 9, in Appendix B.

Nozzle discharge

The performance of the spray nozzles flow rate was adjustable. Individual nozzles, due to the nozzle location, were able to be modified to meet specific flow rate requirements. Therefore, the flow rate was measured to facilitate estimation of the percentage change in flow rate among the spray nozzles. The flow rate was measured using a container placed underneath the nozzles, as shown in Figure 3-13. The test was run for 15 minutes and repeated 14 times. The collected water was weighed and the flow rate calculated for each nozzle. The average flow rates from the nine nozzles are shown in Figure 3-14. The mean flow rate is 2.93 l/hr (SD dev. 0.09), varying between 2.65 to 3.26 l/hr. The coefficient of variation is 6.71%, meaning that applied rainfall intensity will vary only +/- 6.71% from the target. Full details of flow rate measurements can be found in Table B - 1, in Appendix B.

Figure 3-13: Plastic containers to collect water from the spray nozzles.

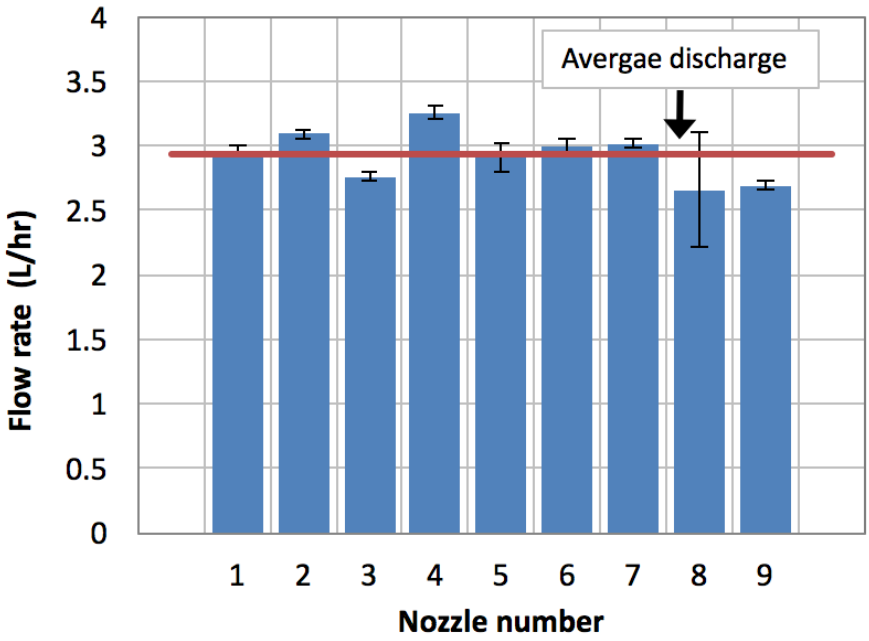

Figure 3-14: Average discharge for nine nozzles at 5 bars.

Nozzle coverage

Distribution uniformity (DU) is a key factor when investigating the efficiency of the rainfall simulator. DU is calculated by dividing the lower quartile average rainfall depth by the total average rainfall depth. To estimate the change of distribution uniformity over time tests were conducted over four selected durations. 81 plastic containers were placed in a grid pattern (9x9) on the surface, as shown in Figure 3-15. The spacing between each container was 100 mm. The test was run for periods of 15, 30, 45, and 60 minutes to provide an understanding of the distribution.

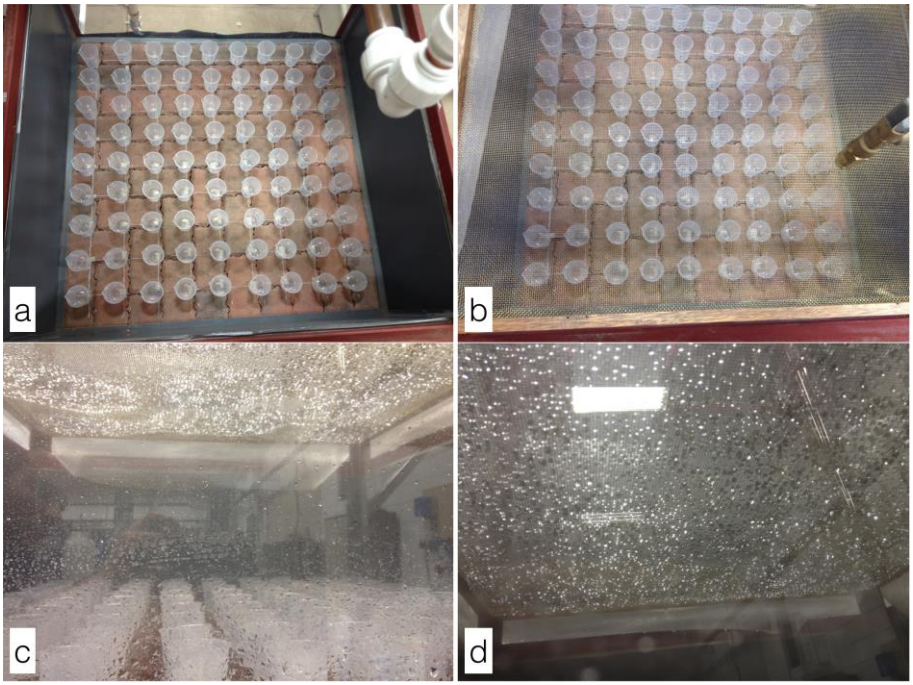

Figure 3-15: showing (a) layout of the 81 containers during the DU tests, (b) Brass mesh is on, (c) and (d) rain droplets were formed on brass mesh.

Figure 3-16 to Figure 3-19 show the collected water from the 81 containers for test duration 15, 30, 45, and 60 minutes (respectively). The results showed that the DU was 49.83%, 51.52%, 56.88%, and 63.97% respectively. It can be seen that there is an increasing uniformity as the duration of flow increases. Full details of the results obtained from the 81 containers from the selected testing durations are presented in in (Table B- 2 to Table B- 5 in Appendix B).

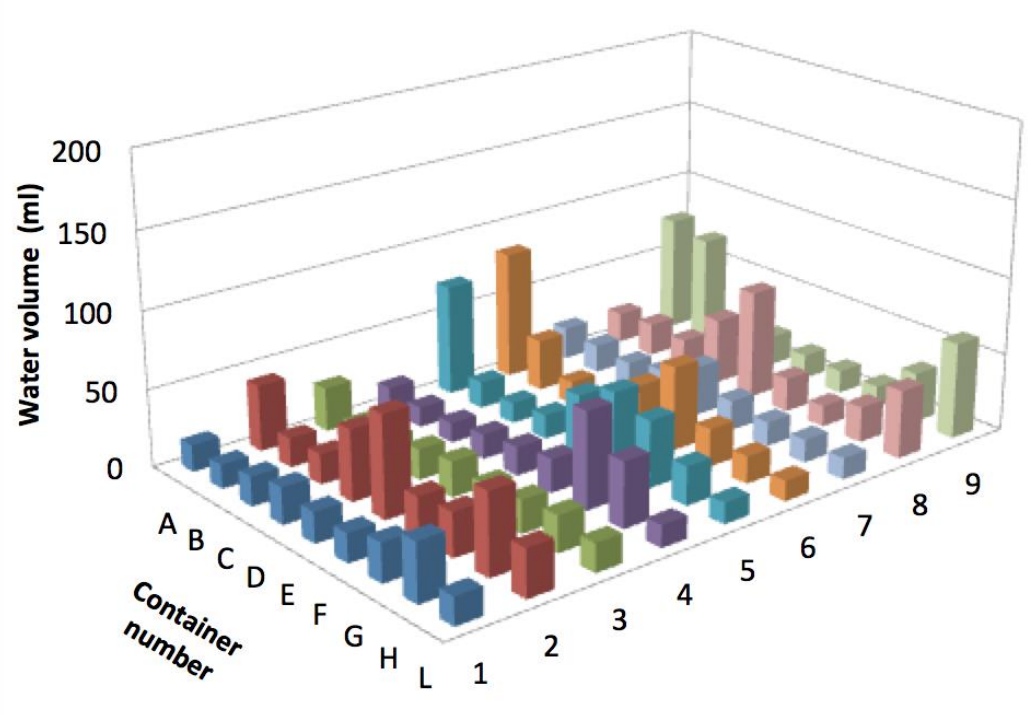

Figure 3-16: Average volume from 81 containers resulting from the 15 minutes flow test.

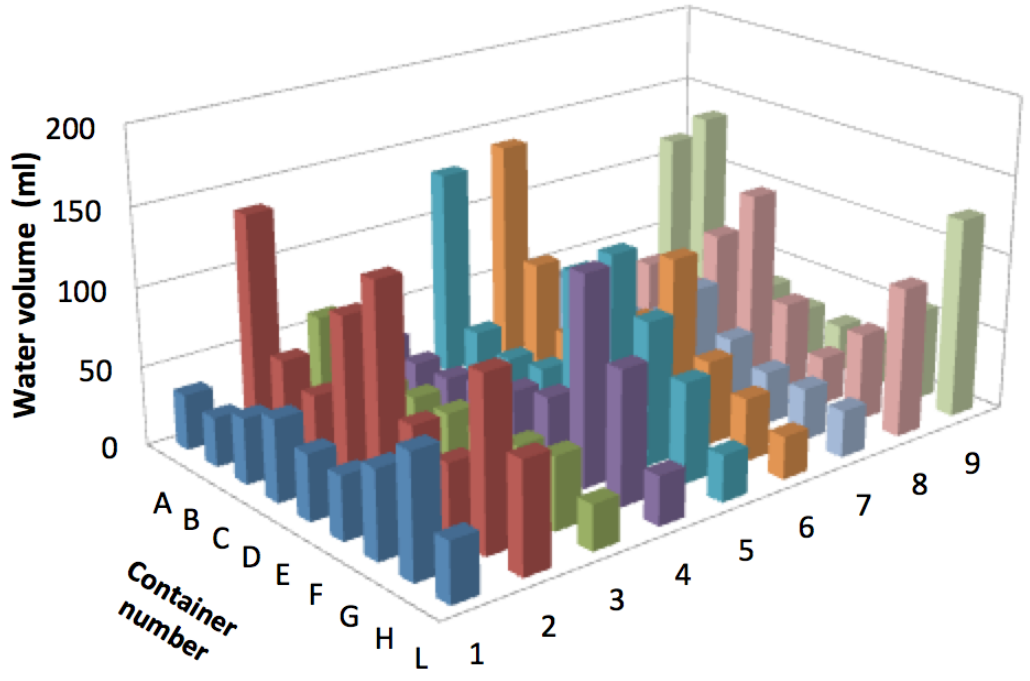

Figure 3-17: Average volume from 81 containers resulting from the 30 minute flow test.

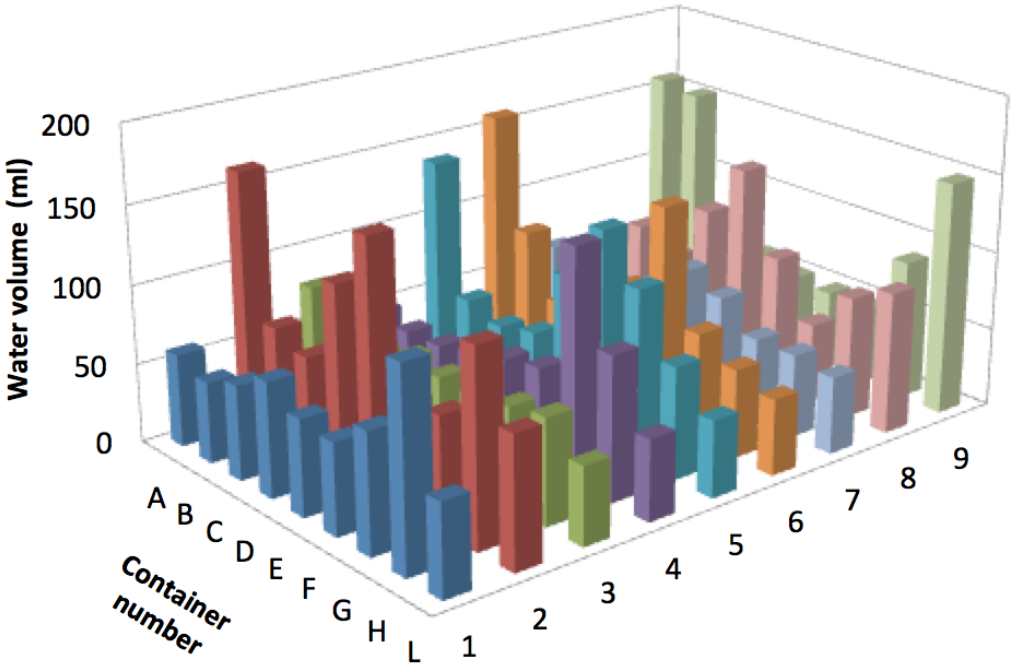

Figure 3-18: Average volume from 81 containers resulting from the 45 minute flow test.

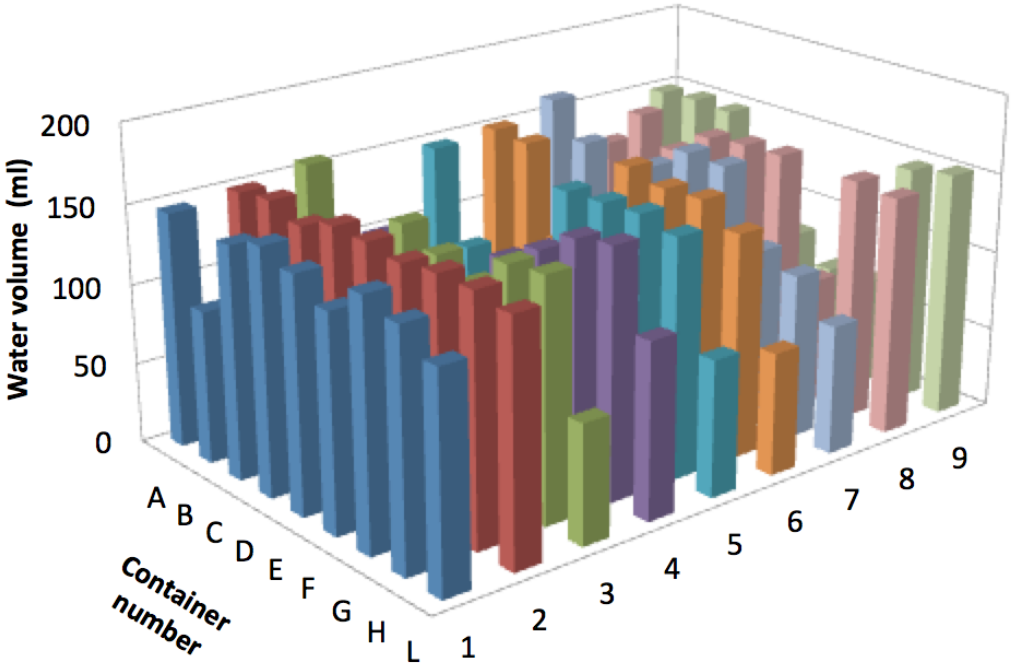

Figure 3-19: Average volume from 81 containers resulting from the60 minute flow test.

3.4.2 Outflow collection

The water collection system was designed to capture drainage from the model structure over a certain period of time. It was necessary to capture and monitor the outflow from the pavement rig over a long period as well as recording the fluctuation of the outflow rate during the specific rainfall tests. Practically, there were a number of considerations required for attenuation of the outflow: accuracy of the measurement, the potential volume of water needing to be measured, and the ability to monitor a variety of outflows.

The method for collecting water from permeable pavements depends on outflow characteristics, such as the discharge volume during a rainfall event, the duration of the outflow, and the variation in the discharge rate over time. Furthermore, an outflow collection system should be designed to collect water at a low flow rate for a specified duration, as the outflow from pavement is expected to decrease over time. The system should be capable of accommodating a variety of precipitation volumes. There are two methods for measuring discharge water volumes from permeable pavements; these are either by monitoring water pressure or weight. Different types of transducers, such as pressure and displacement (see Figure 3-20 a, c), use the pressure method and float transducers. However, these are unsuitable for use in this research test case because the measurements may be affected by atmospheric pressure when measured at low rates only. The weighing method can be facilitated using an electronic load cell or a weighing scale (see Figure 3-20 b, d). However, both types of equipment are suitable for the weighing method, although the load cell system is more expensive. Therefore, after consideration of the benefits and limitations of these two systems, the weighing scale was selected for this research.

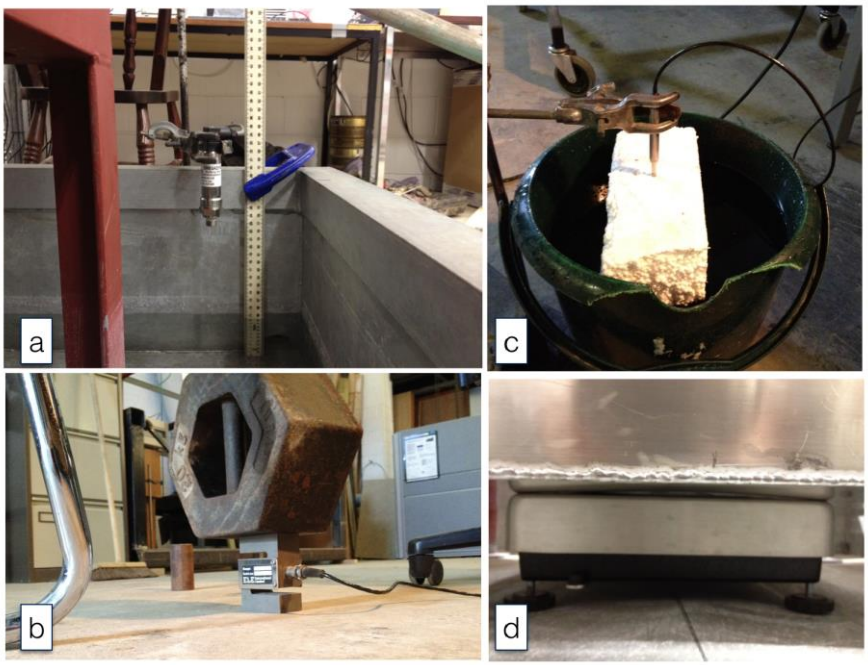

Figure 3-20: (a) pressure transducer; (b) displacement transducer (c); load cell; (d) weighing scale.

The weighing scale design consists of a scale, a container and data acquisition system. A Kern scale (Model: DS 60K0.2) was used for the collection system, and the maximum measurable is 60,000 grams, with a fine scale of 0.2 grams. The dimensions of the stainless steel weighing plate were 450 x 350 x115 mm. The container was made of aluminium so that it was light weight. The dimensions were 800x800x150 mm. The container had a maximum capacity of 150 litres of discharged water.

3.4.3 Monitoring equipment

Monitoring equipment consisted of two types of data collection systems:

- Atmosphere condition monitoring, monitoring the environment surrounding the model structure
- Water content monitoring, recording the water content of the internal model structure materials.

The moisture content of the internal materials of model structure, such as gravel and block, was more difficult to monitor. However, the sand layer of the structure could be monitored, due to its media characteristics allowing probes to exchange electromagnetic waves between the rods inserted into the layer. Therefore, the sand water content was

measured to provide a representative water content database and an opportunity to generate a moisture content profile for subgrade during the wet and dry phase of the experiments.

3.4.3.1 Moisture content

Measuring the moisture content of the subgrade provides an estimation of water movement through the layers of the pavement, which also provides an estimation of the dry period as it affects the whole structure. Not all pavement materials moisture content can be easily estimated. For example, composition of aggregate, block paving does not easily permit the monitoring of moisture content using available moisture content probes. Thus, only the subgrade material could be measured easily, because it consisted of media in which moisture content is readily detectable.

The chosen moisture monitoring method involved installing a number of probes in the top and bottom position of the subgrade layer. This was to generate a profile of moisture content change during the test. The monitoring design measured the volumetric water content in the sand surrounding each probe. The data generated from the probes was then stored in the data logger, after which it was transferred to the PC for analysis. Different types of curves could be created to depict the following data:

- The change in moisture content over a single rain event;
- The change in moisture content following a consecutive rain event;
- The change in moisture content over a long period; and
- Dry periods of short or long duration.

The CS650 is a Water Content Reflectometer that can be used to measure volumetric water content and other parameters related to porous media (see Figure 3-21). The stainless steel probe has two parallel rods 300 mm length and 32 mm in diameter, with spacing 32 mm. The types of readings available from the probe cover bulk electrical conductivity, soil temperature, and bulk dielectric permittivity. The volumetric water content can be derived from the bulk dielectric permittivity. Therefore, a relationship between these figures is needed. This can be found from the probe calibration for sand, using the following equation:

$$\boldsymbol{\theta_V = C_0 + C_1 \times K_a + C_2 \times K_a^2} \quad \textbf{(2)}$$

Where θ_v is the volumetric water content, K_a is the bulk dielectric permittivity of the subgrade material, and Cn, is the calibration coefficient (Campbell-Scientific, 2012).

Figure 3-21: CS650 TDR probe.

3.4.3.2 Installation

The method used to install the probe must be applied sensitively, as it can impact on the measurement. The probe rods should be installed in the media so that it is positioned parallel, in order to not to cause problems with the wave transport. Proper installation minimises the occurrence of any air voids around the rods and therefore the potential for invalid or inaccurate results. The insertion tool is provided by Campbell Scientific, see Figure 3-22, and it was used install the probes into the sand media of the research test rig.

Figure 3-22: Insert tool was used to create path for volumetric water content probe.

The probes were positioned at two depths, as shown in Figure 3-23. The first depth was 75 mm from the bottom of the subgrade, where three probes were inserted. The second depth was 225 mm from the bottom subgrade, and included the use of five probes. The number of probes increased at this depth because the water was more variable at the top of the sub-grade than at the bottom. The sphere of influence for the measurement of the sensors was 75 mm around the rods along their length (75 mm radius around each probe rods) and 45 mm at each end (Campbell-Scientific, 2012).

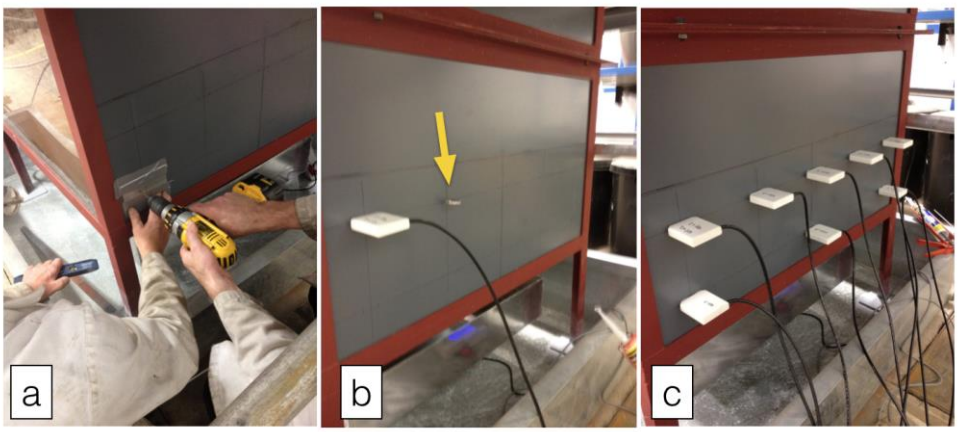

Figure 3-23: Installation process, showing the two probe depths. (a) Layout of the probes location and making two holes for each probe; (b) Insert tool which was used to create path for probe; (c) illustrating the 8 probe locations.

3.4.3.3 Calibration

The manual for the probes recommended using three samples to derive the calibration equation. The use of a 20 cm diameter container (PVC cylinder) with a 35 cm length is also recommended. The CS650 probe was calibrated using material with a volumetric water content of 5%, 7%, 10%,12%, 15%, 18%, 20%, and 23%. Figure 3-24 shows the sample prepared to meet these proposed moisture contents. After monitor readings were recorded by the CS650 probe. After the completion of the test, three samples were taken from each cylinder from top, middle, and bottom, to estimate the change in moisture content along the cylinder (because the probes were orientated vertically). The moisture content was calculated for each sample using the oven method.

Figure 3-24: An example of sample preparation; (a) prepare dry sand;(b) add an known volume of water; (c) mix sample manually;(d) compact sand into container on three layers;(e) create path for probe and then insert probe inside the sample;(f) cover the top of container to prevent evaporation.

The relationship between the dielectric permittivity and the known water content can be described using a linear equation:

$$\boldsymbol{\theta_V = C_0 + C_1 \times K_a + C_2 \times K_a^2} \quad \textbf{(3)}$$

Where θ_v is the volumetric water content, K_a is the bulk dielectric permittivity of the subgrade material, and Cn, is the calibration coefficient (Campbell-Scientific, 2012). Full details of associated tests for calibration can be found in Table C-1 and Table C-2 of Appendix C present the bulk dielectric permittivity results (K_a).

Through these tests and with consideration of data, the calibration equation was generated (see Equation 8). Figure 3-25 shows bulk dielectric permittivity versus the actual volumetric water content (VWC), which was obtained from PVC Cylinder. The average calibration equation is presented, where θ is the volumetric water content and K_a represents bulk dielectric permittivity:

$$\boldsymbol{\theta_V = 0.0248 + 0.0051 K_a - 0.0006 K_a^2} \quad \textbf{(4)}$$

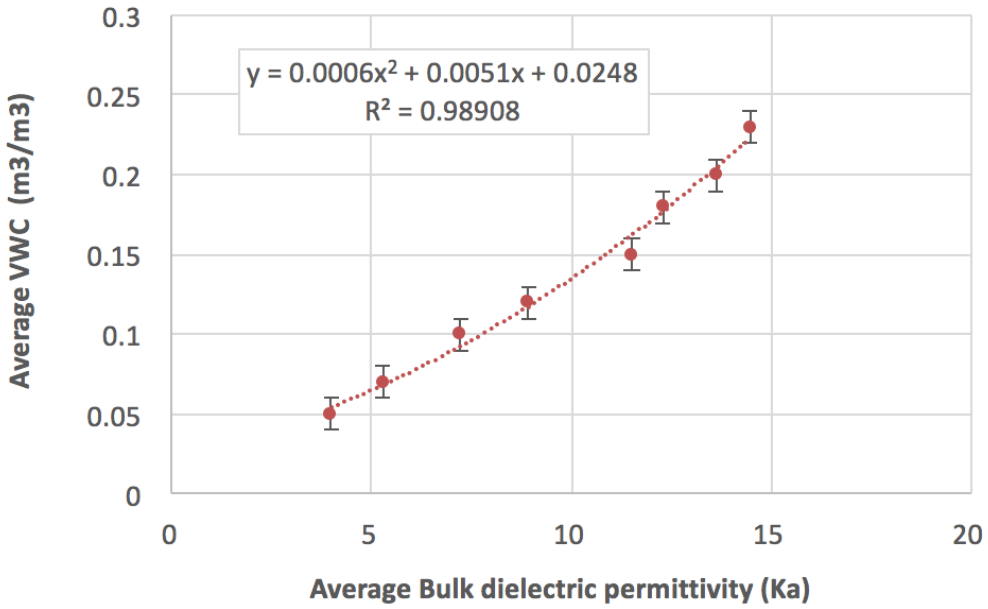

Figure 3-25: Two calibration tests showing the relationship between bulk dielectric permittivity and actual VWC in PVC Cylinder.

3.4.3.4 Temperature and humidity probes

The atmospheric conditions surrounding the model structure (rig) were observed using probes that continuously measured the air temperature and relative humidity. The humidity was measured using probes (CS215 Campbell Scientific Temperature and RH probe) and at temperatures was measured using a T107 Campbell Scientific Thermistor (which has a range of-55°C to +70°C). The temperature was measured in terms of the surface pavement temperature and the air temperature. All the data was then stored in the Campbell scientific data logger.

3.4.4 Data logger & PC

Windmill software

Windmill software is used for data acquisition. This software gathers data from a scale, which collects and weighs the discharged water.

The CR 800 data logger

The CR 800 data logger was responsible for collecting the data from four device types: eight moisture content probes, the temperature and humidity probe, the surface

temperature probe, and the flow meter. Measurements were taken every 30 seconds. The communication device between the data logger and probes was a SDI-12 communication. The data was processed using Data logger support software and then transferred onto an Excel Spread sheet for analysis.

3.5 Experimental procedure

The previous sections have explained how the permeable pavement was constructed and how the rainfall simulator and monitoring equipment was designed and developed in order to obtain the appropriate data to analyse the hydrological performance. Figure 3-26 displays the full layout of the rig and associated equipment.

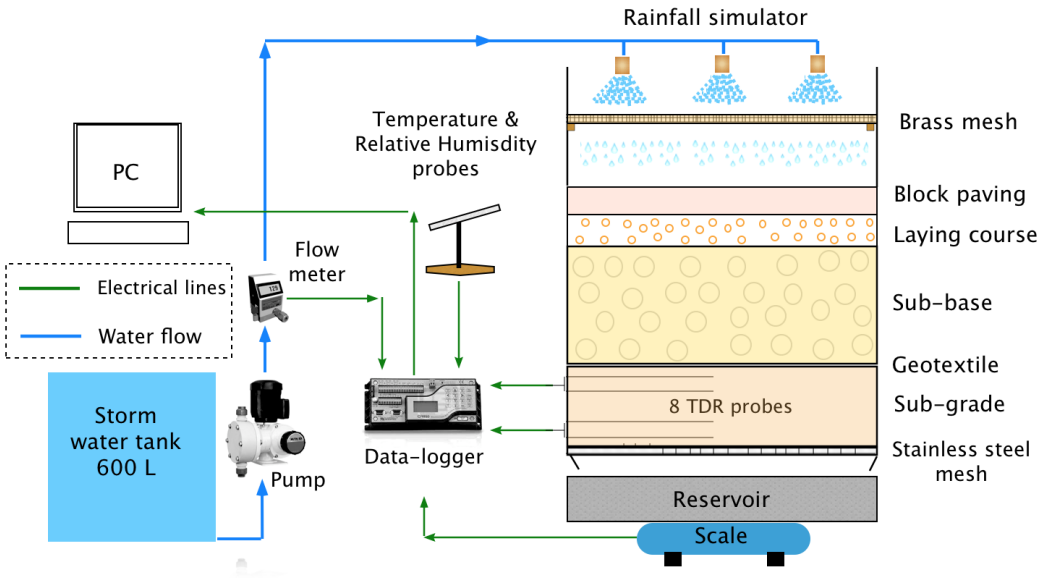

Figure 3-26: Layout of the permeable pavement and associated equipment.

3.5.1 The surface pavement components test

The permeable pavement consists of three components (block concrete, gravel, and sand), each with their own physical characteristics. It was anticipated that these physical characteristics would influence certain test parameters, such as absorption and evaporation rate. Therefore, it was considered essential to measure absorption and evaporation rate for blocks and the gravel.

The hydrological test was carried out for the block and gravel to obtain data to assess the hydrological performance. Basic hydrology, such as absorption and evaporation

rate, is known for each element of the structure. For example, the block paving absorbs some water during a rainfall event and then absorbed water evaporates over time. Therefore, knowing these water loss figures is potentially beneficial to understanding the internal infiltration and detention process of the permeable pavement.

3.5.1.1 The paving blocks

The amount of water that can be absorbed by the block can be measured using an absorption test. The test is simple and allows the blocks to be submerged in a container and then the weight measured over time. The first measurement represents the initial rate of absorption. Twenty paving blocks were examined to estimate the average results. Initially the blocks were put in an oven for three weeks at 40 C° to dry and then allowed to cool down for a week in the laboratory conditions. After this they were then submerged in water for three weeks and the weight of bricks were taken every hour on the first day and then daily thereafter. The total surface area of block paving was approximately 880 cm^2 (including the base). In order to obtain the evaporation rate, the same blocks used in the absorption tests were allowed to dry in laboratory conditions (20-22C°). They were weighed hourly for the first 10 hours then daily for 13 days. The surface area of block was 680 cm (the base not included).

3.5.1.2 Joint filling material

In order to estimate the absorption rate and evaporation the similar procedure was carried out for the joint filling material. The test was conducted on fine aggregate (it is the same as will be used in the test rig). The amount of fine aggregate was spread on a container of surface 250 × 250 mm, the sample depth was 150 mm (see Figure 3-27). Fine aggregate was dried for 24 hours and then left to cool down in the laboratory condition, and then submerged in water for one hour. Ten samples were used to estimate the average absorption.

For evaporation test, a sample was submerged for one hour. The base of the box was sealed; allowing water loss only via the surface (see Figure 3-27). Therefore, the sample was only exposed to a surface of 625 cm^2 so any change in the weight it would be referred to loss water via evaporation. The weight was recorded every 30 sec for 72 hours.

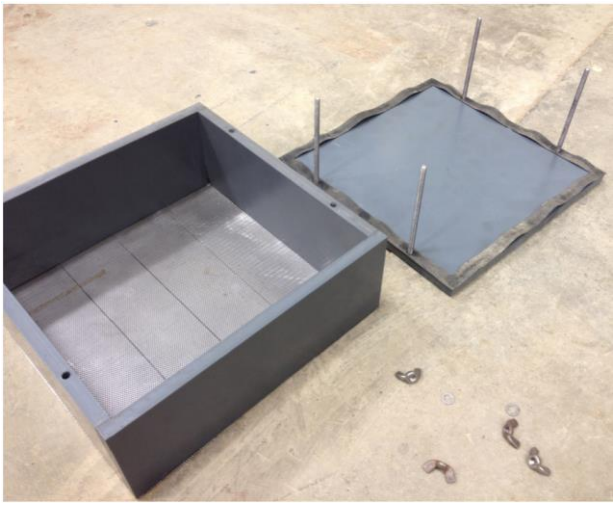

Figure 3-27: A container with stainless steel mesh was designed for absorption test and including an extra base to seal it during evaporation test

3.5.2 Surface infiltration of permeable pavement

The infiltration rate of a permeable pavement is one of the fundamental parameters that influence its ability to manage stormwater. Permeable pavement must be designed with enough infiltration capacity and structural integrity to maintain an acceptable level of function in the long term. Therefore, both initial and long-term infiltration capacities must be compared in order to estimate the degradation of the infiltration rate.

The permeability of each layer is known: the block surface layer was constructed by Priora block paving, which was provided by Marshall. According to their information, the permeability of the blocks is 6742.8 L/m^2.h (18750 l/sec/ha). The course bedding and sub-base layer were constructed from 6 mm Priora Aggregate and 20 mm Priora Aggregate (provided by Marshall in compliance with BS EN 13242, 2002) respectively. The permeability of the sub-base was as 25200 L/m^2.h (70000 l/sec/ha). The sub-grade was constructed from clean sand, classified as uniform graded sand, according to the British soil classification system for engineering purposes (BS5930: 1981). The permeability of the sand was 218 L/m^2.h (605.55 l/sec/ha), measured by the constant head method (BS 1377-5:1990).

In this study, it is difficult to measure the permeability of permeable pavement; due to the dimensions of the rig (surface area of one meter square and the depth is 0.78

meters). Therefore it was decided to measure the surface infiltration rate of the pavement instead.

A radial-flow falling-head permeameter (see Figure 3-28) was used to measure the infiltration rate of the permeable pavement (BSI, 1996). This test determines the time taken for two litres of water to infiltrate though a known area of surface. The hydraulic conductivity, K (m/sec), can be calculated from the following equation:

$$\boldsymbol{K = \frac{(R)2 \times v}{2d(t-r)} \log_e \frac{H_1}{H_2} \log_e \frac{D_1}{D_2}} \quad \textbf{(5)}$$

Where;

K = hydraulic conductivity (m/sec),
R is the effective radius of the standpipe (m),

H_1 is the initial water head (m),

H_2 is the final water head (m),

D_1 is the inner diameter of the sponge rubber annular disc (m),

D_2 is the outer diameter of the sponge rubber annular disc (m),

d is the thickness of the porous surfacing (m),

υ is the viscosity of water at the test temperature (Pa .s),

t is the outflow time (sec),and

r is the series resistance time (sec) is outflow time (in second), corrected to 20 °C, when the outlet is not restricted by a surfacing.

By combining the dimensional constants, the Equation (9) can be reduced to:

$$\boldsymbol{K = \frac{c}{d(t-r)}} \quad \textbf{(6)}$$

Where,
K = hydraulic conductivity (in m/day), and
C is a constant for a particular design of apparatus and for results normalized to a standard test temperature.

C can be derived by inspection from the Equation in (9) as:

$$C = 0.5 + 2Rv \log_e \frac{H_1}{H_2} \log_e \frac{D_1}{D_2} \quad (7)$$

For the design of this permeameter, C is typically assumed to be 65 m/day.

Figure 3-28: Permeameter and standing board.

3.5.3 Outflow samples

The outflow sample was collected from the base of the collection reservoir and placed in 1000 ml Reagent bottle (see Figure 3-29). A grab sample was taken during the rainfall event as there was a possibility that sediment accumulation could occur on the bed surface of the reservoir (catching pan under the rig), Thus it was considered appropriate to take the sample two hours from the start of the rainfall to avoid particle accumulation.

Figure 3-29: An example of outflow sample was kept in 1000 ml Reagent bottle

In order to obtain a homogenous sample the water in reservoir was stirred for 60 second using a rubber bladed brush (see Figure 3-30). This was done to reduce the possibility of the sediment settlement within the reservoir prior to sample acquisition.

Figure 3-30: A sweep water with rubber bladed brush (Squeegee).

Daily observations were made of the outflow using the suspended solids test method in accordance to British Standard BS EN 872:2005. 100 ml of outflow was filtered through a pre-weighed glass microfiber filter paper (Whatman G/FC) (1.2 µm), dried at 105 degree Celsius for 24 hours and then weighed to determine the sediments weight within the sample (see Figure 3-31 and Figure **3-32**). This provided an indication of

any change in suspended solid concentration in the outflow which may have been caused by the addition of sediment on the pavement surface.

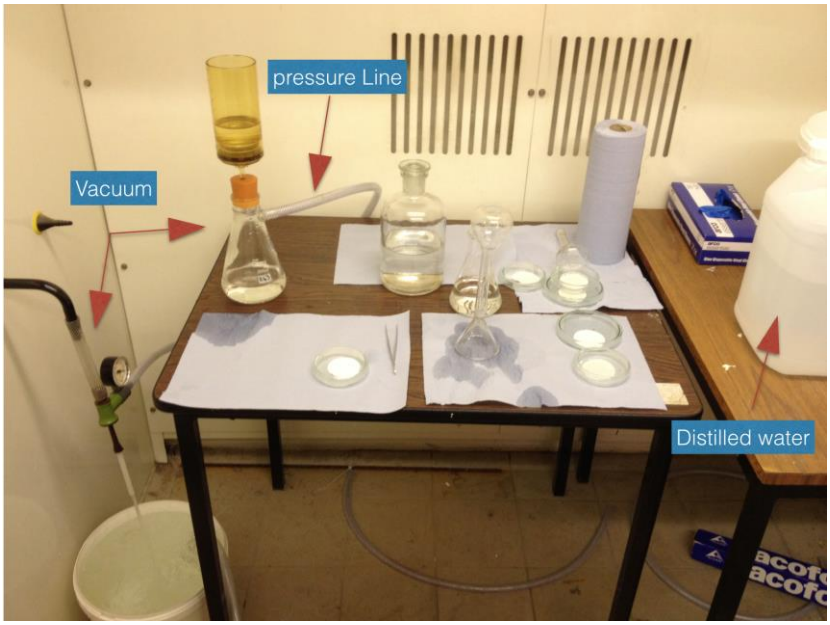

Figure 3-31: Suspended solids apparatus: including vacuum, vacuum flask, distilled water, petri dishes, and tweezers.

Figure 3-32**: (a) analytical balance; (b) drying oven (105 °C) ; (c) desiccator to allow filter to attain moisture equilibrium with the air near the balance;(d) Filter paper.**

The suspended solids concentration can be calculated from the expression:

$$\boldsymbol{\rho = \frac{1000 \times (b - a)}{v}} \quad \textbf{(8)}$$

Where,

ρ is the content of suspended solids, in milligrams per litre, mg/l;

b is the mass of the filter after the filtration, in milligrams, mg;

a is the mass of the filter before the filtration, in milligrams, mg;

v is the volume of the sample, in millilitres, ml.

3.5.4 Hydrological experiment

The permeable pavement was subjected to three storm events, as shown in Table 3-1. The storm event design was based on the Flood Estimation Handbook Software (FEH CD-ROM 3) (CEH, 2009) for Edinburgh City in the United Kingdom. A depth of rainfall of 6.39, 7.78, and 10.85 mm were applied over 15, 15, and 30 minutes respectively. These rainfall intensities and durations were representative for return periods of 5, 10, and 10 annual return periods respectively.

Table 3-1: Rainfall data applied for the hydrology experiment

Storm Event No.	Rainfall depth (mm)	Duration (minutes)	Return period (year)	Rainfall intensity (mm /h)
1	6.39	15	5	25.56
2	7.78	15	10	31.12
3	10.85	30	10	21.7

The experimental procedure involved applying three different rainfall intensities/duration combinations three times. The sequence of three rainfall storms with different duration and intensities allowed collection of data that can be analysed from different perspectives of pavement response. Each rainfall storm event was repeated over three cycle simulations. Table 3-2 details the timeline of the hydrological experiments which were conducted over 9 weeks. Typically, the simulated rainfall

events occurred over a cycle of seven days. Rainfall was simulated, at one event per day, for the first five days (days 1 to 5). No rainfall was simulated on days 6 and 7. The repetition over three weeks gave an average trend of the structure response as well as increasing the reliability of the results via repetition.

Table 3-2: Detailed schedule of the hydrology experiments

Storm event No.	**Simulation cycle No.**	**Cycle days (Rainfall days)**						
		1	**2**	**3**	**4**	**5**	**6**	**7**
1	1	■	□□	■	□□	■	□	□
	2	■	■	■	■	■	□	□
	3	■	■	■	■	■	□	□
2	1	■	■	■	■	■	□	□
	2	■	■	■	■	■	□	□
	3	■	■	■	■	■	□	□
3	1	■	■	■	■	■	□	□
	2	■	■	■	■	■	□	□
	3	■	■	■	■	■	□	□

■ Rainfall
□No rainfall due to the laboratory because closed for safety issue.
□□ No rainfall simulation was applied on this day due to wait for outflow from previous day.

In the short-term, the following hydrological data can be collected:

- Rainfall volume;
- Discharge volume; and
- Volumetric water content (VWC).

The water retention of the permeable pavement structure was calculated using a water balance equation: The mass balance approach was applied to calculate the change in water volume in the rig pavement. The change in water flux in the rig pavement can be described by the following formula:

$$\mathbf{I - O = \Delta}\boldsymbol{S} \qquad \textbf{(9)}$$

Where *I* is the input volume into the system, *O* is the output from the system, and $\boldsymbol{\Delta S}$ is the change in storage at certain time which represents retention volume within permeable pavement. The input was represented by rainfall volume while the output comprises the discharge volume and the evaporation loss.

The amount of retention equals the discharge output and evaporation subtracted from rainfall input, whereas, long term hydrological data is calculated according to the changes in the retention over a period of time. The volumetric water content (VWC) data indicate the level of water retention in the rig. From this data, it is not difficult to monitor pre-storm retention levels during the experiment period. Furthermore, the experiment has initial pre-storm retention, which was calculated prior to the experiment, and the pre-storm retention, which is created during the weekends (day 6 and 7). The pre-storm conditions were expected to influence the outflow during the consecutive rainfall events.

An analysis of the results generated from these tests can be found in Section 4.3 and 4.4

3.5.5 Sedimentation experiment

The experiment was designed to investigate the impact of the sediment on the hydrology performance of the permeable pavement. The experiments were intended to simulate a 12 year life cycle for the pavement. The application of rainfall and sediment was described in Table 3-3. No sediment was added for the first two simulated years. Sediment was progressively added for the subsequent 10 year simulation. The amount of sediment load applied to the surface per year was based on a study carried out by Ellis (1996) who estimated that a car park in the United Kingdom receives a range of 124 – 762 kg/ha/year with an average 440 kg/ha/year. Sand, with a d_{50} of 250µm was selected to represent the natural sediment load (Deletic and Orr, 2005, Selbig and Bannerman, 2011), and was applied manually to the surface using a distribution device, as shown in Figure 3-33.

Figure 3-33: A distribution device which was used to apply the sediment.

To run a one year simulation, 704 mm of precipitation (Met-Office, 2013) was applied to the pavement which converted into 704 litres (1 mm of rainfall per meter square equals 1 litre). This volume of water was applied to the pavement surface over ten rain events (five rainfall days followed by 2 dry days, repeated for two consecutive weeks). The design storm event duration was 2 hours and 45 minutes with a rainfall intensity of 25.56 mm per hour. The 440 kg/ha/year of sediments were applied on the first day of each test, with 9 more consecutive rain events applied to allow the sediment to be transported into the structure. The entire duration of the experiment was 24 weeks, simulating 12 years. During the rainfall event a sample was taken daily of the flow discharge rate to measure the concentration of suspended solids (SS). This method allowed for monitoring and discovery of the discharge rate from the pavement and evidence of any change in suspended solids concentration. The application of rainfall and sediment loading is shown in Table 3-3, which shows the weeks reflecting the year-long simulation of the permeable pavement's lifecycle.

Table 3-3: Schedule of the sediment experiments, showing equivalent simulated years and application of rainfall and sediment loading

Simulation cycle No.	Cycles days (Rainfall days)							Hydrology simulation years	Sediment simulation years
	1	2	3	4	5	6	7		
1	■	■	■	■	■	□	□	1	*
2	■	■	■	■	■	□	□		
3	■	■	■	■	■	□	□	2	*
4	■	■	■	■	■	□	□		
5	■	■	■	■	■	□	□	3	1**
6	■	■	■	■	■	□	□		
7	■	■	■	■	■	□	□	4	2**
8	■	■	■	■	■	□	□		
9	■	■	■	■	■	□	□	5	3**
10	■	■	■	■	■	□	□		
11	■	■	■	■	■	□	□	6	4**
12	■	■	■	■	■	□	□		
Three weeks dry period (Christmas Break)									
13	■	■	■	■	■	□	□	7	5**
14	■	■	■	■	■	□	□		
15	■	■	■	■	■	□	□	8	6**
16	■	■	■	■	■	□	□		
17	■	■	■	■	■	□	□	9	7**
18	■	■	■	■	■	□	□		
19	■	■	■	■	■	□	□	10	8**
20	■	■	■	■	■	□	□		
21	■	■	■	■	■	□	□	11	9**
22	■	■	■	■	■	□	□		
23	■	■	■	■	■	□	□	12	10**
24	■	■	■	■	■	□	□		

■ 25.56 mm/h and 165 minutes duration
□ No rainfall
* No sediment addition
** Applied sediment loading 440 kg/ha/year

In summary, this resulted in 120 rain event simulations and outflows, comprised of:

- 24 outflows before adding sediment;
- 95 outflows since the start of sediment addition; and
- 1 outflow was counted as the first day of the experiment period.

It is usefull to explain why the annual rainfall volume was delivered ten days on each year simualtion. As the expriment was aimed at investagating the influnce of sediment

on the hydrological performance, it was nessary to introduce annual rainfall into number of rain events, allowing sediment to be distributed within the structure. However, this will not mimic field conditions, but it will provide a good indcation of the influnce of sediment on water movement. With regards to the annual rainfall of Edinburgh, delivering the amount of water in one event would requre 27.5 hours, which is an impracticable. Thus, the application of rainfall and sediment represents a compromise between what is practible in the labortory-based test and the reality of the field conditions.

3.6 Potential error and uncertainties

In laboratory experiment there is no perfect certainty in the measurements. There is always the potential for errors and uncertainty in data collected and thus results. In the study the uncertainties in physical measurements can be described in the following:

3.6.1 Flow meter

Although the flow meter was calibrated by the manufacturer and also calibrated within the laboratory prior to experimental use, error in data may still occur due to measurement of the voltage across an inappropriate portion of electrical circuit and resulted in potential errors in the measurements of inflow. The potential errors in the measurements were minor and unlikely to have a significant impact on the results.

3.6.2 Probes

Moisture content was measured using a CS650 Probe. The manufacturer stated accuracy of moisture content readings is ±3% of measured value. The use of these probes resulted in a potential source of experimental error where the experimental method required exact moisture content.

The calibration in the laboratory was carried out for the probes and the installation was undertaken in accordance with the technical manual recommendation as discussed in (Section 3.4.3). However, some errors may occur as a result of the formation of air voids around rod surface that indicate lower water content than actual and lead to errors in measurements. Thus, the calibration and installation in laboratory aimed to

reduce the potential inaccuracies in measurements were minor and unlikely to have a significant impact on the results.

It can be concluded that the source of potential errors have been identified in this study. A number of steps were taken to minimise potential errors including calibration equipment and repeating the experiment. The uncertainty of the results would not be found to have a significant impact on the results.

3.7 Chapter summary

The purpose of this chapter was to describe the hydrological testing of the permeable pavement rig utilised in this project, with particular reference to the process of building the pavement and the specific pavement materials. A description has also been provided for the data that this approach gathers and the chosen methods of analysis. The results of the experiment will be discussed in the following chapters.

CHAPTER 4 – HYDROLOGICAL EXPERIMENT

4.1 Introduction

This chapter describes the hydrological experiment that was conducted between October and December 2012. The experiment was essential in order to understand the hydrological behaviour of this particular pavement. It also needed to be carried out prior to start of the main experiment for this research (sediment experiment) to provide appropriate pre-event conditions. The hydrology experiment was divided into three phases, based on designed storms. The aim was to monitor the response of the permeable pavement to three storm characteristics. The three storms were chosen to simulate natural rainfall that occurs in Edinburgh, UK. The experimental method was described previously in Section 3.5.2 (see Table 3-2). The chapter includes the following sections:

- Introduction,
- The small-scale experiment,
- The condition of the permeable pavement prior to starting the experiment,
- Hydrological performance of the permeable pavement,
- The relationship between outflow and other variables,
- Summary.

To analyse the hydrological performance, the following results were monitored and calculated from the raw data produced by the data-logger:

- Rainfall (mm),
- Rainfall intensity (mm h^{-1}),
- Outflow, as a rainfall equivalent (mm),
- Volumetric water content (m^3 m^{-3}), and
- Temperature (°C) and relative humidity (%).

From these elements, the hydrological performance was analysed. Table 4-1 includes all the variables that were used in the calculation of these elements in order to produce final information for analysis.

Table 4-1: variables and calculations were used for data analysis

Variable	Calculation	Units
Time	Time is recorded for every 30 seconds and transported from data logger to PC	(h)
Rainfall intensity	Rainfall intensity ($mm.h^{-1}$) = 0.0239 × voltage (v) + 0.357 (Chapter 3)	($mm\ h^{-1}$)
Rainfall volume	= Rainfall intensity× area ($1m^2$)× time (0.5 / 60)	($mm\ m^2$)
Rainfall depth	= Rainfall volume / area (m^2) × (1000 / 1000)	(mm)
Volumetric water content (ω)	Measured by dielectric permittivity and then converted	($m^3\ m^{-3}$)
Volumetric water content (θ_v)	$\theta_v = -0.0005Ka^2 + 0.0208Ka - 0.0321$ (Chapter 3)	($m^3\ m^{-3}$)
Outflow mass	Outflow weight	(g)
Outflow rate	= ((weight $_2$ (g) – weight $_1$ (g))/1000)/((time $_2$-time $_1$) / 60)	($L\ h^{-1}$)
Outflow volume	= Outflow rate ($L\ h^{-1}$) × time (0.5 / 60)	(L)
Outflow volume expressed as a rainfall equivalent	= Outflow volume (L) / area (m^2) X (1000 /1000)	(mm)

It should be noted that during the experiment there was no direct measurement of water volume retained within the structure layers. This was because the volume of water within the pavement as a whole could not be quantified. The sub-grade was the only layer in which the water content could be estimated (Section 4.3.2).

4.2 Small-scale experiments

Due to the size of the rig, it was difficult to measure the water content of the pavement blocks and aggregate. It was necessary to conduct a small-scale experiment to investigate the basic hydrology of the surface of permeable pavement components (block paving and joint materials). The experiment covers the retention and evaporation for the components of the permeable pavement surface. The result of this experiment is representative of the pavement's function in the laboratory, rather than in the field, and

thus provides a baseline understanding of this pavement research rig performance in the laboratory environment.

The test included consideration of the basic hydrology for the top layer of the pavement (80 mm). This included the block paving and the joint materials. The top layer is considered by the author to be responsible for the most water loss that occurs in the pavement, due to evaporation. This does not mean to say that the lower layers do not have any water loss, some water loss by sub-grade evaporation is expected, but there is uncertainty regarding the influence of the sub-grade layer on the evaporation from permeable pavement (Ferguson, 2005, Starke et al., 2011). Therefore, in this research, deep evaporation was assumed to be insignificant. In addition, the evaporation from the surface depends on atmospheric conditions and the retention capacity of the material. Thus, the experiment outlined in Section 4.2.1 on both blocks and fine aggregate indicates the general trend of the retention and evaporation from the surface of permeable pavement under laboratory conditions.

4.2.1 The paving blocks

4.2.1.1 Absorption

The test was conducted on twenty concrete blocks in order to estimate the average absorption rate of the blocks, as shown in Figure 4-1.

Figure 4-1: Showing 20 blocks of paving during the immersion stage.

Table 4-2 details the average and cumulative absorption of water by the pavement blocks over 24 hours, in grams per square metre, and mm equivalent depth of rainfall. It can be seen from Table 4-2 that the amount of absorbed water was 103.75 g (76% of the total water) within the first hour. However, there was no significant increase in the second hour of the test; the amount absorbed reached 112 g (82% of the total water). This indicates that the rainfall in the first hour is an important factor when considering potential retention during an event.

Table 4-2: Average absorption of water by block paving for duration 24 hours

Time period (h)	Average water absorbed (g)	SD dev.	Cumulative water absorbed (g)	Cumulative water absorb (g/cm^2)	Cumulative water absorbed – (rainfall equivalent) (mm/m^2)	Amount absorbed (%)*
0 - 1	103.75	0.051	103.75	0.118	1.179	76.1
1 - 2	8.20	0.039	111.95	0.127	1.272	82.1
2 - 3	3.85	0.039	115.80	0.132	1.316	84.9
3 - 4	3.30	0.039	119.10	0.135	1.353	87.4
4 - 5	1.90	0.039	121.00	0.138	1.375	88.8
5 - 6	1.90	0.039	122.90	0.140	1.397	90.1
6 - 7	1.90	0.039	124.80	0.142	1.418	91.5
7 - 8	2.40	0.040	127.20	0.145	1.445	93.3
8 - 9	1.45	0.040	128.65	0.146	1.462	94.4
9 - 10	1.00	0.040	129.65	0.147	1.473	95.1
10 – 24	6.65	0.040	136.30	0.155	1.549	100.0
*Amount absorbed as a percentage of the total absorbed in 24 hours						

Table 4-3 shows the water absorption over a longer time period of 336 hours (20 days). 136.3 g was absorbed in the first day (83.75%). Absorption continued; however, after 72 hours the bulk of the total water content had been absorbed, leaving just 9.43% to be absorbed over the remaining 264 hours. This indicates that a rapid absorption occurred at the commencement of the wetting period. The results (see Table 4-2) suggest that 1.179 mm of rainfall can be stored as detention in every square metre of the paved surface during the first hour. Anderson et al. (2001) found that concrete blocks

absorbed rainfall of up to 4 – 6% of the block weight. When the obtained result (103.75g) was compared with the total weight of the block paving, 3400 g, then the percentage absorbed was 3.05% of block weight.

Table 4-3: The average absorption of water by block paving for duration 336 hours

Time period (h)	Average water absorbed (g)	SD dev.	Cumulative water absorbed (g)	Cumulative water absorbed (g/cm^2)	Cumulative water absorbed – (rainfall equivalent) (mm/m^2)	Amount absorbed (%)*
0 - 24	136.3	0.042	136.30	0.12	1.55	83.75
24 - 48	4.5	0.043	140.80	0.15	1.60	86.51
48 - 72	6.6	0.043	147.40	0.16	1.68	90.57
72 - 96	1.35	0.043	148.75	0.17	1.69	91.40
96 - 120	1.1	0.043	149.85	0.17	1.70	92.07
120 - 144	1.2	0.043	151.05	0.17	1.72	92.81
144 - 168	1.15	0.043	152.20	0.17	1.73	93.52
168 - 192	1.87	0.043	154.08	0.17	1.75	94.67
192 - 216	1.67	0.043	155.74	0.18	1.77	95.69
216 - 240	1.81	0.043	157.55	0.18	1.79	96.81
240 - 264	1.45	0.043	159.00	0.18	1.81	97.70
264 - 288	1.3	0.043	160.30	0.18	1.82	98.49
288 - 312	0.55	0.043	160.85	0.18	1.83	98.83
312 – 336	1.9	0.042	162.75	0.18	1.85	100.00
*Amount absorbed as a percentage of the total absorbed in 336 hours (%)						

4.2.1.2 Evaporation

Evaporation was measured from the same samples (see Figure 4-2) used in the absorption test (absorbing on average 162.75g of water per block paving, with a standard deviation of 0.43 g). The blocks were allowed to dry in laboratory conditions (20-22 C°). Measurements were taken hourly in the first 10 hours and then daily over 13 days. The permeable pavement block surface area was 680 cm^2 (the base was not included).

Figure 4-2: Showing 20 blocks of paving during the evaporation test.

Table 4-4 illustrates the water loss via evaporation from block paving during 24 hours. It shows that more evaporation occurred in the first two hours of the experiment: 7.3 g was evaporated during the first hour, the equivalent of 0.1074 mm rainfall depth. The amount of water loss was 12.85 g (7.9% of total 162.75 g absorbed water) during the first two hours. After 24 hours the total amount of water loss was 22.04 g. This was evidence that the highest evaporation rate occurred within the first few hours after the rainfall event.

Table 4-4: Measured loss of water by evaporation from a concrete block surface over 24 h

Time period (h)	Average water loss (g)	SD dev.	Cumulative water loss (g)	Cumulative water loss (g cm^{-2})	Cumulative water loss (rainfall equivalent) (mm m^{-2})	*	**
0 - 1	7.30	0.043	7.30	0.0107	0.1074	0.0107	4.49
1 - 2	5.55	0.042	12.85	0.0189	0.1890	0.0082	7.90
2 - 3	2.30	0.043	15.15	0.0223	0.2228	0.0034	9.31
3 - 4	2.65	0.043	17.80	0.0262	0.2618	0.0039	10.94
4 - 5	1.95	0.043	19.75	0.0290	0.2904	0.0029	12.14
5 - 6	2.15	0.043	21.90	0.0322	0.3221	0.0032	13.46
6 - 7	1.26	0.043	23.16	0.0341	0.3406	0.0019	14.23
7 - 8	1.49	0.043	24.65	0.0363	0.3625	0.0022	15.15
8 - 9	1.31	0.043	25.97	0.0382	0.3818	0.0019	15.95
9 -10	1.17	0.043	27.14	0.0399	0.3991	0.0017	16.68
10 -24	22.04	0.043	49.18	0.0723	0.7232	0.0023	30.22
* Evaporation rate (mm h^{-1}) **Evaporation loss as a percentage of the total absorbed (%)							

Table 4-5 illustrates the water loss via evaporation from block paving during 264 hours. It can be seen that the greatest water loss occurred during first day, 49.18 g; this indicates that after 24 hours, 0.72 mm of water can be lost by evaporation from one square metre of block surface area. During the experimental period the total amount of water loss was 94.2 g (representing 58 % of total absorbed water). This result shows that the 1.39 mm of rainfall can be lost by evaporation after 11days (264 hours). Overall, the evaporation rate was higher during the first two hours and then decreased significantly, maintaining a constant between 0.003 and 0.001 mm h^{-1}. It can be concluded that, when considering short-term behaviour, evaporation has an insignificant influence on retained water in block paving.

Table 4-5: Measured loss of water by evaporation from a concrete block surface over 264 h (time interval 24 h)

Time period (h)	Average water loss (g)	SD dev.	Cumulative water loss (g)	Cumulative water loss (g cm^{-2})	Cumulative water loss -(Rainfall equivalent) (mm m^{-2})	*	**
0 – 24	49.18	0.043	49.18	0.0723	0.72	0.030	30.22
24 –48	14.35	0.047	63.53	0.0934	0.93	0.009	39.04
48 – 72	7.55	0.050	71.08	0.1045	1.05	0.005	43.67
72 –96	5.3	0.051	76.38	0.1123	1.12	0.003	46.93
96 – 120	4.28	0.051	80.66	0.1186	1.19	0.003	49.56
120 –144	2.92	0.052	83.58	0.1229	1.23	0.002	51.35
144 –168	3.55	0.052	87.13	0.1281	1.28	0.002	53.54
168 – 192	2.56	0.053	89.69	0.1319	1.32	0.002	55.11
192 – 216	1.69	0.053	91.38	0.1344	1.34	0.001	56.15
216 – 240	1.45	0.052	92.83	0.1365	1.37	0.001	57.04
240 – 264	1.37	0.052	94.2	0.1385	1.39	0.001	57.88
***** Evaporation rate (mm h^{-1}) **Evaporation loss as a percentage of the total absorbed (162.75 g) (%)							

4.2.2 Joint filling materials

4.2.2.1 Absorption

The test was conducted on fine aggregate, as shown in Figure 4-3. The results of the test are presented in Table 4-6. The results show that 1 kg of fine aggregate absorbed 0.104 kg of water, on average, within one hour (0.104 mm equivalent depth of rainfall).

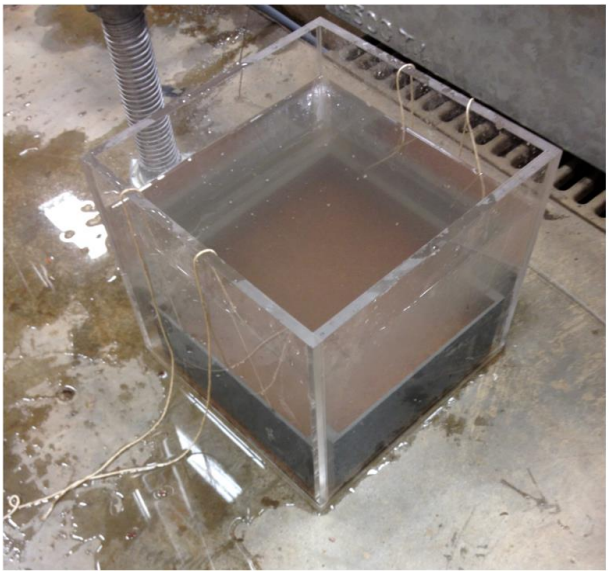

Figure 4-3: showing a container with stainless steel mesh which was designed for the absorption test and including an extra base to seal it during the evaporation test.

Table 4-6: Water absorbed from fine aggregate during 1 hour

Test No.	Water absorbed by 6820 g of fine aggregate in 1 hour (g)	Water absorbed (g) (for 1000 g of fine aggregate)
1	709.34	104.01
2	708.70	103.91
3	710.12	104.12
4	708.50	103.89
5	709.09	103.97
6	709.30	104.00
7	710.30	104.15
8	708.50	103.89
9	707.60	103.75
10	709.80	104.08
Average	765.29	103.98
SD	0.83	0.12

4.2.2.2 Evaporation

The results of the evaporation test are presented in Table 4-7. The observed water loss was obtained from the surface area, which represented 6.25 % (625 cm^2) of materials in the constructed permeable pavement. Table 4-7 shows the results as a cumulative water loss (rainfall equivalent mm) and evaporation rate (mm h^{-1}). It can be seen from the table that the greatest amount of evaporation occurred in the first hour, 10 g. During the first ten hours 52 g was evaporated. The evaporation rate was higher during the first three hours and then decreased gradually. After 24 hours, only 1.3 mm of rainfall had evaporated. The results show that the evaporation has limited impact on the rain event and resulting discharge rate.

Table 4-7: Measured loss of water by evaporation from fine aggregate over 72 h

Time period (h)	Time Interval (h)	Water loss (g)	Cumulative water loss (g)	Cumulative water loss (equivalent rainfall) (mm)	Water loss rate (mm h^{-1})
0-1	1	10	10.0	0.160	0.160
1-2	1	6	16.0	0.256	0.096
2-3	1	6	22.0	0.352	0.096
3-4	1	5	27.0	0.432	0.080
4-5	1	5	32.0	0.512	0.080
5-6	1	5	37.0	0.592	0.080
6-7	1	4	41.0	0.656	0.064
7-8	1	4	45.0	0.720	0.064
8-9	1	4	49.0	0.784	0.064
9-10	1	3	52.0	0.832	0.048
10-24	14	31	83.0	1.328	0.021
24-48	24	40	123.0	1.968	0.027
48-72	24	6	129.0	2.064	0.004

4.3 The condition of permeable pavement prior to starting the experiment

4.3.1 Temperature and relative humidity

The pavement construction was completed in the summer of 2012. During the construction phase, the base material received a certain amount of water, necessary to compact the pavement layer to the required density. After a period following the construction, the rainfall simulator was tested in order to measure the distribution of spray from nozzles. Therefore, there was some water retention in the structure and that could only be lost by evaporation. However, the evaporation rate is slow and depends on the temperature and relative humidity, which was less variation for the course of the experiment. Table 4-8 details the air temperature and the relative humidity. It can be seen that the air temperature ranged between 18.5 and 27 °C, and the difference was 8.5 °C, over three months.

Table 4-8: Statistical data for Atmosphere conditions surrounding the rig during three months

	Air Temperature (°C)	**Relative humidity (%)**
Max	27.09	47.43
Min	18.51	21.24
Average	23.52	33.58
SD	1.51	4.81

A brief summary of the atmospheric data is presented in Figure 4-4. This shows the air temperature and relative humidity distribution from September to December 2012. The fluctuation in temperature seems to be a limited process in the laboratory, with average temperatures of 23.5°C (SD 1.5) and average relative humidity of 33.6 % (SD 4.8) for the duration of experiment. It was deemed unnecessary to wait until the rig was completely dry, as it replicated moisture contents similar to those that would be expected under real conditions.

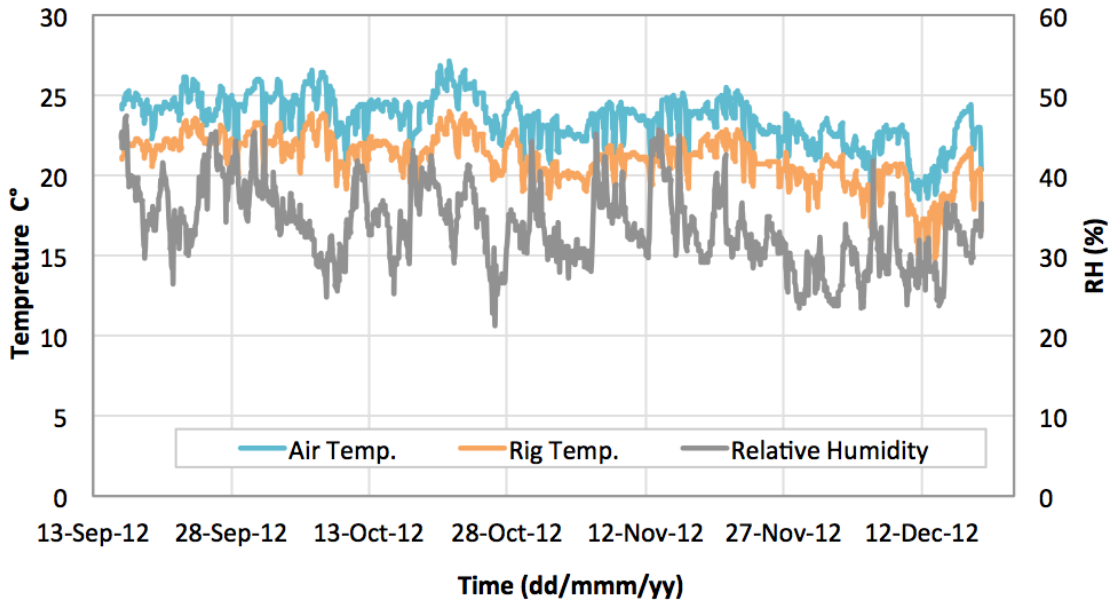

Figure 4-4: Air and rig temperature & relative humidity data over the three months (from 16/09/2012 to 18/12/2012).

4.3.2 Volumetric water content

The pavement was not totally dry prior to starting the experiment in October 2012. Figure 4-5 shows the trend for volumetric water content (VWC) of the sub-grade from September to December 2012. Over the two months prior to the commencing the experiment, the VWC gradually decreased. The percentage reduction in VWC was approximately 6.85% and 1.11% for top and bottom probes respectively. The minor reduction at both levels would indicate that the process of drying was very slow during these two months. When the experiment commenced and the first rain event was applied, the volumetric water content (VWC) increased gradually over the ensuing 24 hours. The percentage increase was 1.11% and 0.35% for top and bottom probes respectively. The largest variation was noted to consistently occur in the top layer. This is a result of gravity, as the top layer is able to infiltrate water to the lower subgrade vertically below. In light of this analysis, the VWC profile for two months prior to start the experiment may provide a qualitative indication of the degree of the pavement dryness.

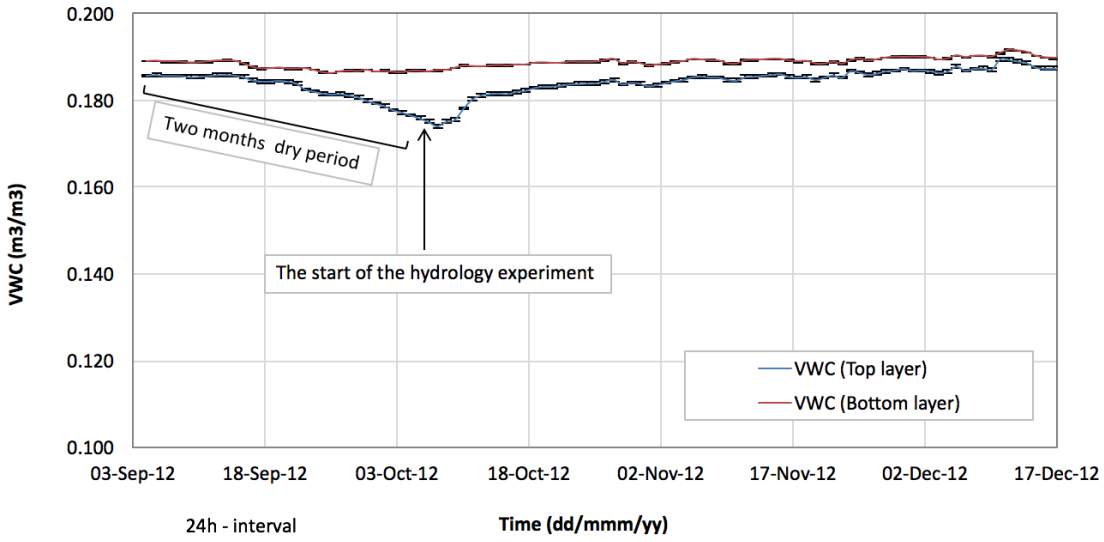

Figure 4-5: Average volumetric water content for both top and bottom layer of sub-grade.

4.4 Hydrological performance of permeable pavement

This section discusses the influence of both the condition of the sub-grade and rainfall intensity on the response of the outflow. This analysis has been undertaken in order to obtain data that can provide a picture of the hydrological performance of the designed permeable pavement. The key points of importance in this analysis are:

- The influence of the moisture content of the sub-grade on outflow; and
- The influence of rainfall intensity on the response of the outflow.

4.4.1 The influence of the moisture content of the sub-grade on outflow

4.4.1.1 Short-term condition

To discuss this point, three conditions of the sub-grade were considered for analysis. These are: the relative dry condition (prior to the start of the experiment); the Day1 condition (prior to the weekly start of the new cycle of rain events); and the Day2-5 condition throughout day 2 to 5 of the experimental rainfall cycle.

The simulated rainfall events occurred over a cycle of seven days. Rainfall was simulated, at one event per day, for the first five days (days 1 to 5). No rainfall was simulated on days 6 and 7 (as mentioned previously in Table 3-2). Rainfall simulations were performed using three rainfall intensities: 25.56, 31.12, and 21.7 mm/h (Rainfall

Intensity 1, 2, and 3 respectively). A total of 43 rain events were applied with only 41 resulting in any outflow (the first two events had no outflow).

Relatively dry condition (initial condition)

At the start of the series of experiments (relatively dry condition), there were three rainfall events that were carried out on days 1, 3, and 5 of the initial week. There was no outflow during day 1 or 3, as the two rainfall events were fully absorbed by the structure. Figure 4-6 illustrates the percentage increase in VWC within the sub-grade for days 1, 3, and 5 for the top layer. It shows the increase in VWC over two hours after the start of the rainfall event. The first two rain events caused a sharp increase in the VWC, seen at 15 minutes. This increase was a response to the rainfall event, after which the percentage change in VWC continued increasing slowly. Conversely, the day 5 event shows there was an increase in VWC within 15 minutes, followed by a gradual decrease in the VWC, because there was a discharge in this event.

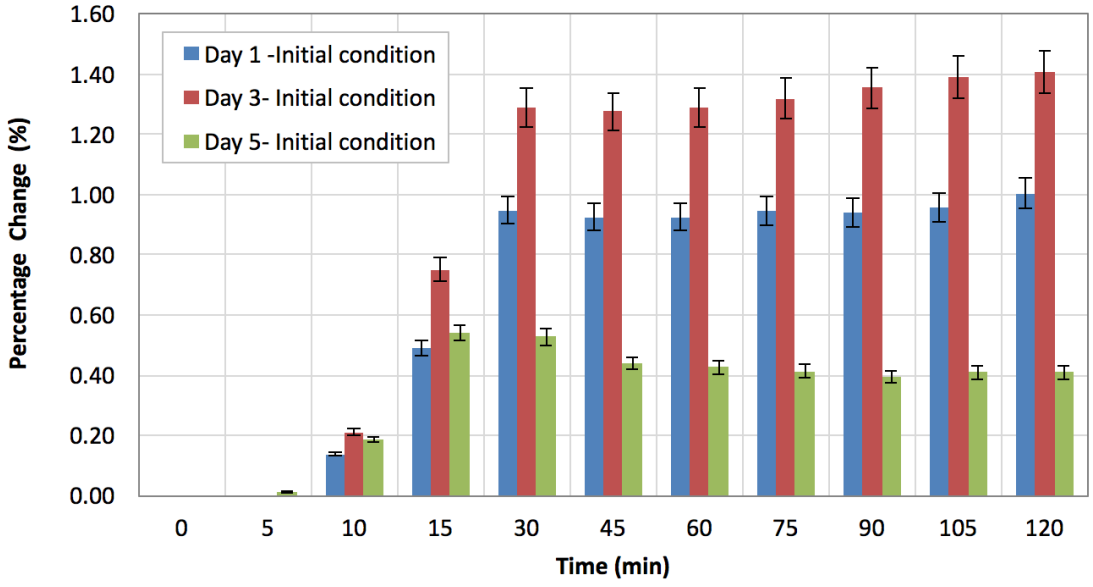

Figure 4-6: The percentage change in volumetric water content of the sub-grade from the start of the rainfall – during relatively dry condition (Initial condition), for top layer- the measured from start of daily rainfall event.

VWC for the bottom layer performed similarly to the top layer (see Figure **4-7**). The response in the bottom layer mirrored the response in the top layer in terms of time

action, but has a lower percentage change than the top layer. This is because there was more water retained in the bottom layer than the top layer prior to the start of the experiment.

The VWC percentage increase in the bottom layer did not exceed 0.4%, whereas that in the top layer increased up to 1.4%. The lower percentage can be explained by the fact that most of the rainfall was absorbed by the materials in the upper layers (i.e. block paving, aggregate). Thus only a small amount of rainfall infiltrated to the sub-grade during the first rain event (day 1). Moreover, the event on day 3 had a similar percentage increase to day 1. This was because of two reasons. Firstly, the upper layer became more saturated after the first rainfall event started. The saturation level in the upper layers was higher as a result of the first rainfall, thus unabsorbed water moved down to the sub-grade. Secondly, no outflow occurred from the pavement during days 1 and 3. The structure materials reached saturation level such that any additional water was discharged from the sub-grade. Conversely, the event on day 5 showed a lower percentage change; this was because the pavement produced outflow after 10 minutes from the start of the rainfall. The discharge shows a reduced ability to retain more water. It was also noticed that the percentage change on day 5 increased within 30 minutes and then decreased, in contrast days 1 and 3 showed an increase consistently. Thus, the outflow response was different on days 1, 3, and 5.

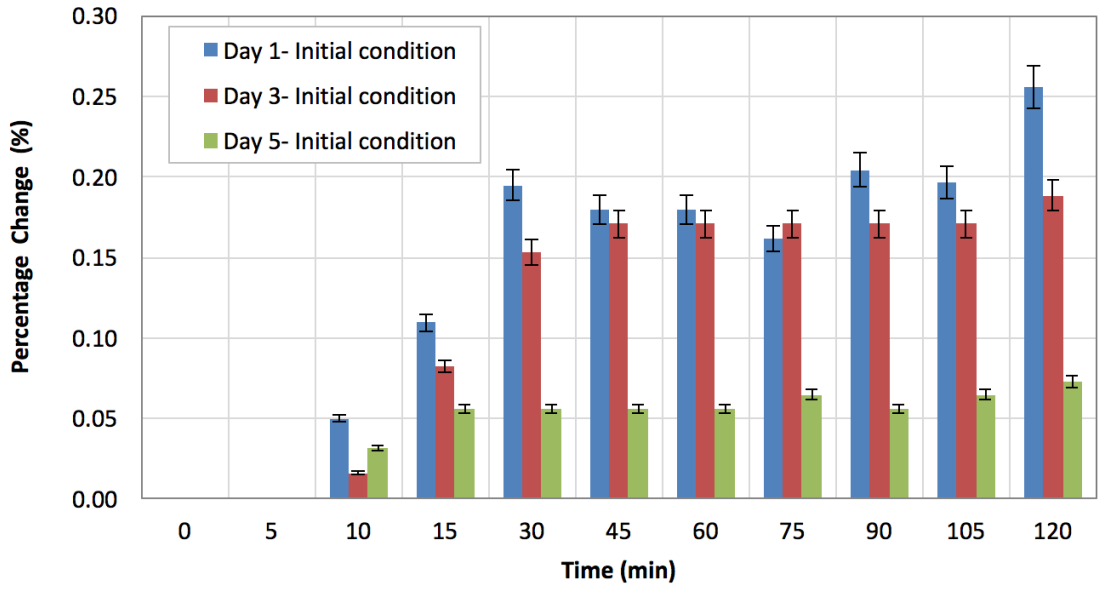

Figure 4-7: The percentage change in volumetric water content of the sub-grade since the start of the rainfall – during relatively dry conditions (Initial condition), bottom layer.

Day1 condition

The Day-1 condition describes the volumetric water content level of the sub-grade on day 1(from each cycle after the initial simulation cycle). Prior to start of the rainfall, the pavement was exposed to dry periods during days 6 and 7 (Saturday and Sunday), and then the pavement was exposed to another series of rainfall events over 5 days (Monday –Friday). Figure 4-8 and Figure 4-9 illustrate the average percentage of change in VWC during day 1 over three rainfall intensities, for top and bottom layer, respectively. Within the top layer there was an increase in VWC level, followed by a decrease, as shown in Figure 4-8. The increase in VWC reached a peak during the first 15mins of rainfall for both Rainfall Intensity 1 and 2, and during the first 30 minutes for Rainfall Intensity 3. The largest increase in VWC occurred in Rainfall Intensity 1, due to the retention condition of the pavement being low at the beginning of the experiment. The change in VWC since the rainfall start (delay in peak) decreased respectively over Rainfall Intensity 1, 2, and 3 as a result of increased pavement saturation over time. Figure 4-9 shows a similar magnitude in the percentage change; however, the change in VWC level is very small.

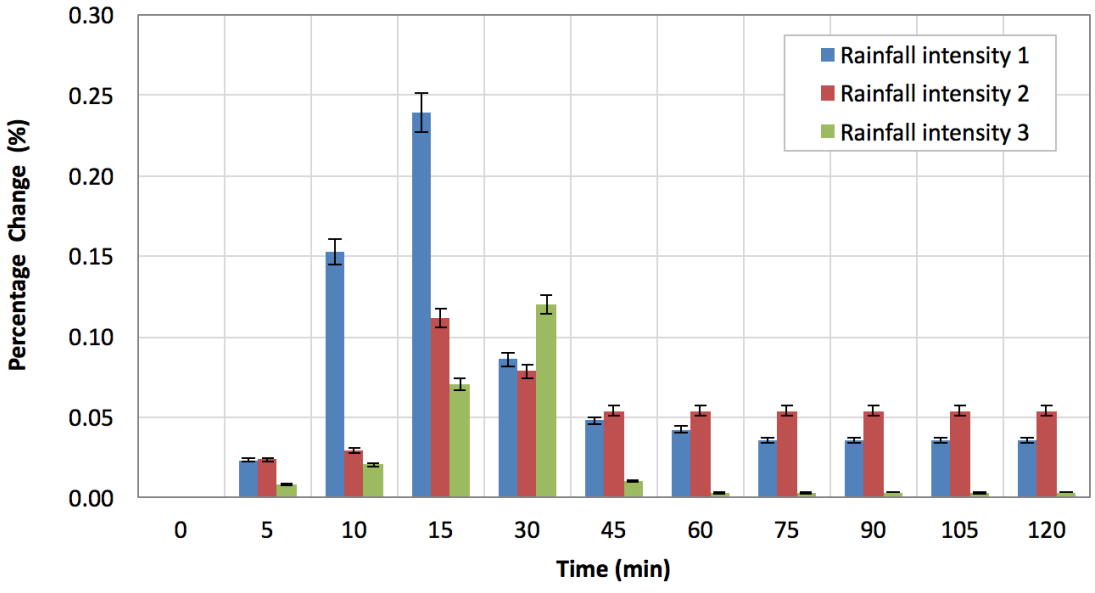

Figure 4-8: The percentage change in volumetric water content of the sub-grade since the start of the rainfall – during Day-1 conditions, top layer.

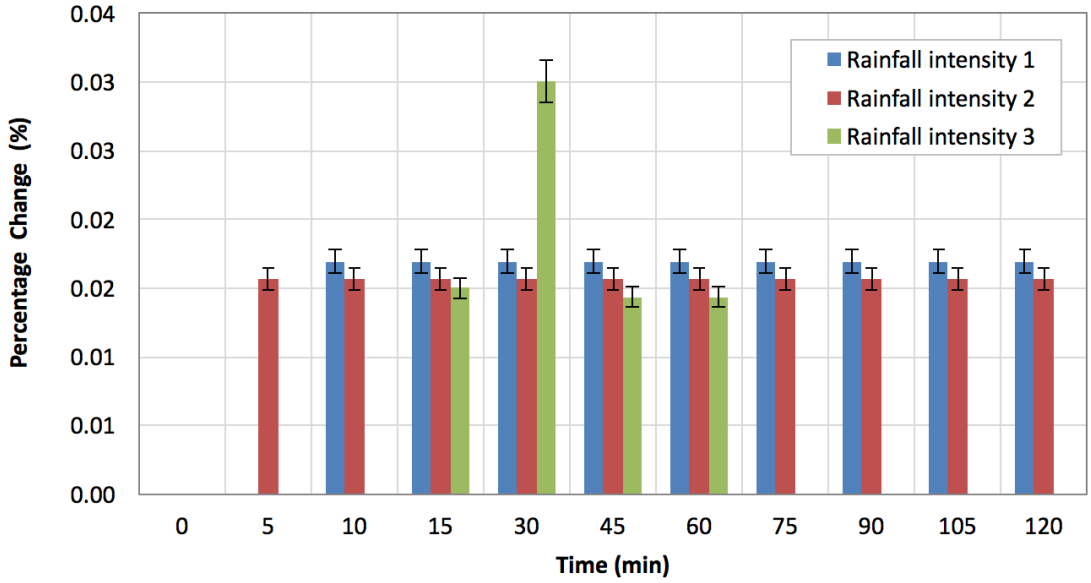

Figure 4-9: The percentage change in volumetric water content of the sub-grade since the start of the rainfall – during Day1 conditions, bottom layer.

Day2-5 condition

The Day2-5 condition (days 2 to 5) response is illustrated in Figure 4-10 and Figure 4-11 , which show the average percentage change in VWC within the sub-grade during Rainfall Intensity 1, 2, and 3, for top and bottom layer respectively. The maximum increase in VWC was in Rainfall Intensity 1, due to lower water content in the sub-grade at the beginning of the experiment. It was similar in magnitude to a Day1 condition (day 1), but the increase in VWC on days 2 to 5 is more than that on Day 1.

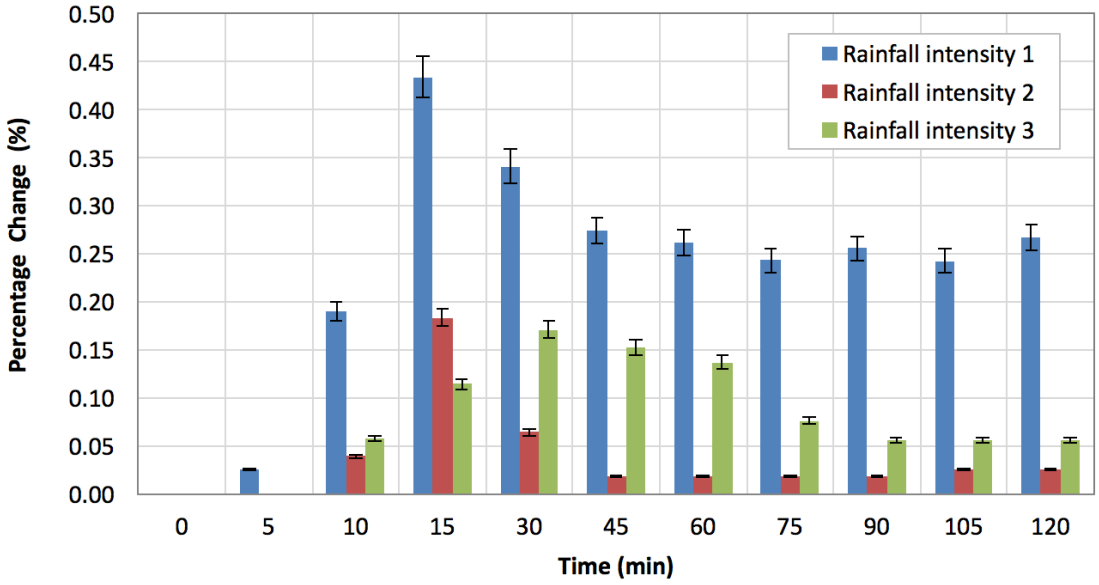

Figure 4-10: The percentage change in volumetric water content of the sub-grade since the start of the rainfall – during Day2-5 conditions, top layer.

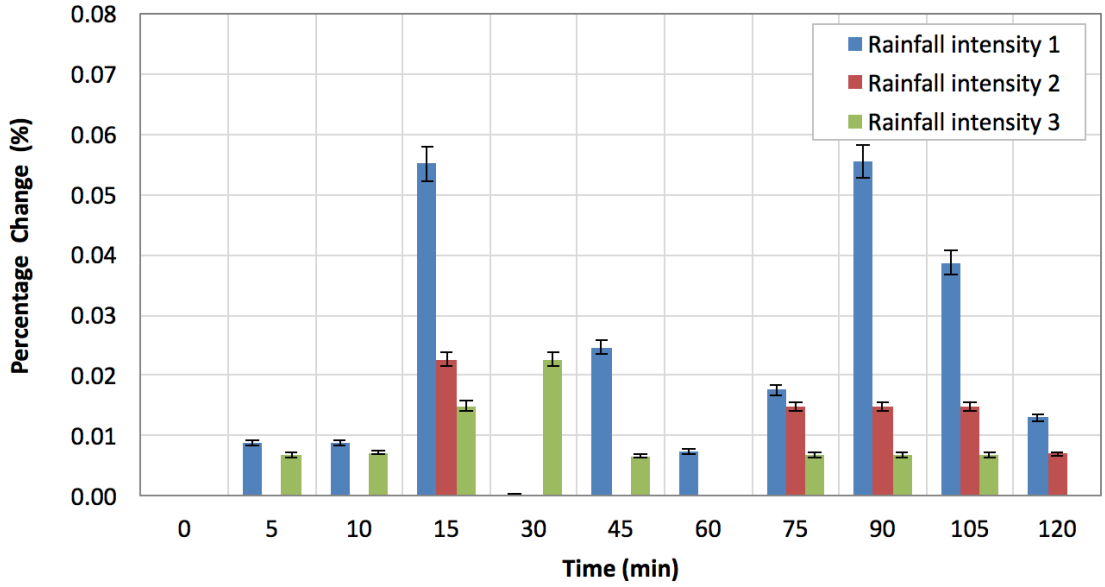

Figure 4-11: The percentage change in volumetric water content of the sub-grade since the start of the rainfall – during Day2-5 conditions, bottom layer.

4.4.1.2 Long-term condition

Section 4.4.1.1 discussed the change in volumetric water content after rainfall events, and the sub-grade response to rainfall intensities. This provided evidence of how the lower pavement structure responds to each rainfall intensity. It was useful to observe the influence of the rainfall intensity on the sub-grade relative to the amount of change in VWC since the start of the experiment, for all rain events.

First Rainfall Intensity (25.56 mm/h)

Figure **4-12** shows the volumetric water content (VWC) since the start of the experiment for the top and bottom layer of sub-grade for Rainfall Intensity 1, 2, and 3. It can be seen that the VWC increased gradually after the start of the experiment. Although the pavement structure has been exposed to two months of dry period, the bottom layer did not show a substantial increase in the level of VWC. Figure 4-13 shows the VWC during the initial week (first simulation), where the pavement was subjected to relatively dry conditions. Obviously, due to the percolation, the bottom layer shows higher values than the top layer. In contrast, the top layer shows a greater increase than the bottom layer, by 4.75% and 0.60 % for top and bottom layer respectively.

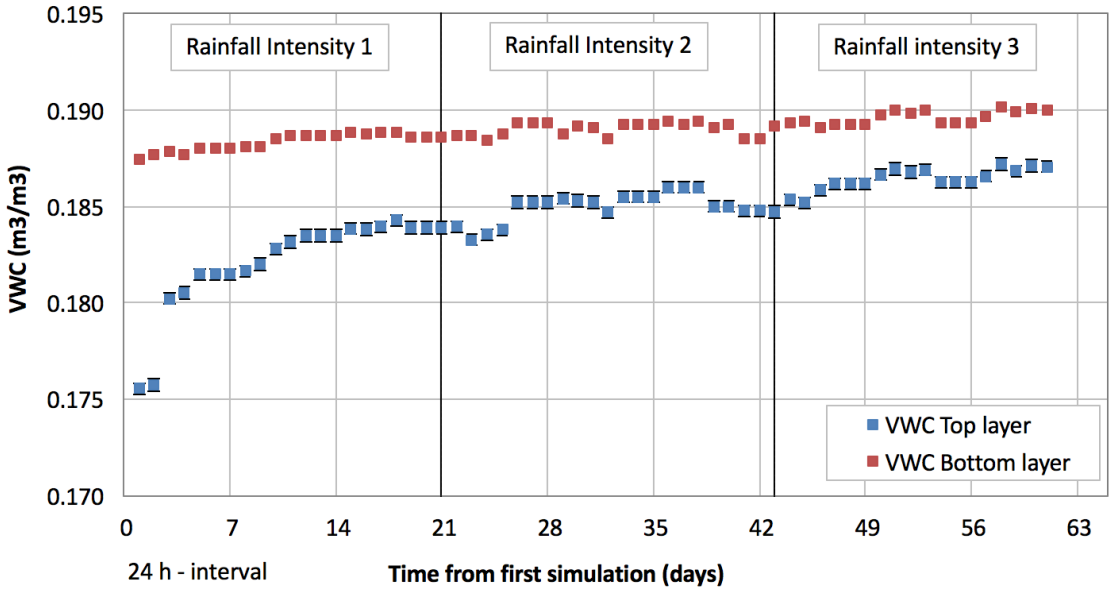

Figure 4-12**: Showing the value of the volumetric water content since the start of the experiment- for Rainfall Intensity 1, 2, and 3 - top and bottom layers.**

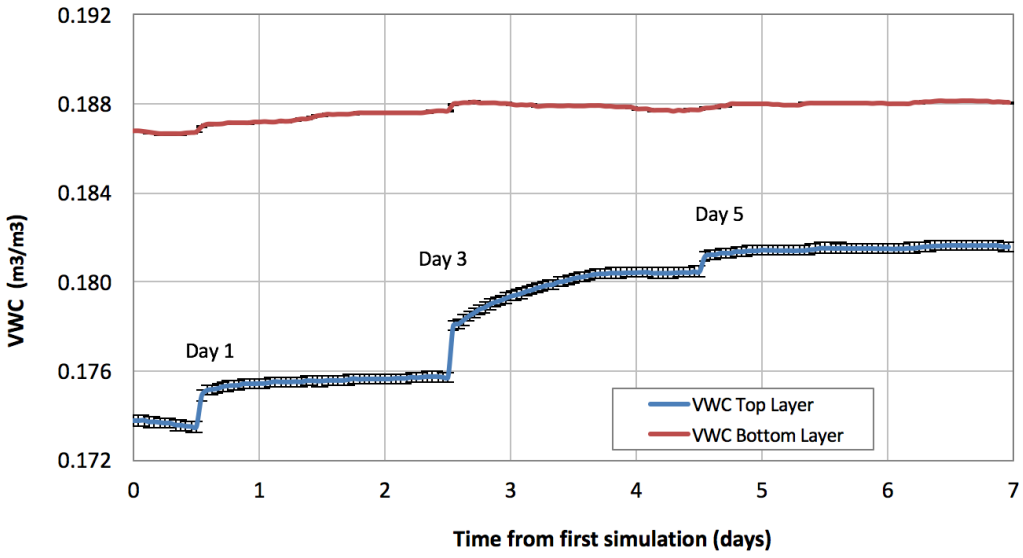

Figure 4-13: The initial value of the volumetric water content during the initial simulation cycle - relatively dry condition, top and bottom layer.

Second Rainfall Intensity (31.12 mm/h)

Prior to the start of Rainfall Intensity 2, the pavement shows no saturation. Figure **4-12** illustrates the volumetric water content (VWC) since the start of Rainfall Intensity 2 for the top and bottom layer of the sub-grade. The pavement responded to the rainfall event and there was no significant change in VWC level over the three week period. The increase in VWC was 0.89% and 0.24% for top and bottom layer, (respectively). If the results in Rainfall Intensity 1 and 2 are compared, a different response in the VWC level becomes obvious. Although the volume of Rainfall Intensity 2 is greater than Rainfall Intensity 1, the value of VWC for the top layer was less than Rainfall Intensity 1 by 5 times. It can be seen that the pre-event condition has a greater influence than rainfall intensity, if the duration of rainfall is the same. Furthermore, a general trend of increasing VWC over time is evident, indicating that the VWC level continued to increase slightly (0.89% and 0.24% for top and bottom layer, respectively) in the sub-grade over the full duration of the test.

Third Rainfall Intensity (21.7 mm/h)

Figure **4-12** shows the value of the volumetric water content (VWC) since the start of Rainfall Intensity 3 for the top and bottom layers of the sub-grade. It shows a slight increase in VWC level over the three weeks. Although the pavement underwent 6 consecutive weeks of simulation, it did not reach maximum saturation. The increase in VWC level was 1.28% and 0.83% for the top and bottom layer, respectively. The results show that Rainfall Intensity 3 had a different response from Rainfall Intensity 2. This can be explained by the fact that the rainfall in Rainfall Intensity 3 had a longer duration than that in Rainfall Intensity 2. However, the pre-event condition was noted to have a significant influence on the response of VWC to rainfall, even if the rain event was longer.

4.4.2 The influence of rainfall intensity on the response of the outflow

4.4.2.1 Overview

Rainfall simulations were performed using three rainfall intensities: 25.56, 31.12, and 21.7 mm/h (Rainfall Intensity 1, 2, and 3 respectively). A total of 43 rain events were applied with only 41 resulting in any outflow (the first two events had no outflow). This section presents and analyses the results of the rain events that were applied on the surface of the permeable pavement over three months. Full details of the analysis of all rain events can be found in (Table D - 1 to Table D - 3, in Appendix D).

Figure 4-14 illustrates the volume of rainfall and outflow during the course of the experiment. The graph includes data from the three simulated rainfall intensities. It includes all rainfall events, outflows, and retention. The base (low) values of the outflow line represent day 1 values. The remaining values represent the outflow from days 2 to 5 consecutively.

The result of the first simulation cycle was different to the following simulations due to the dry initial condition of pavement structure. During the first week of simulation, the first and second rain events produced no outflow, as the water was totally taken up by the sub-surface pavement material. In the third rain event, which was applied four days after the first rain event, the outflow began 10 minutes after the rainfall started. The outflow then continued for three hours after rainfall stopped. Only 0.99% of the rain

was discharged from the pavement during the rain event, and only 15.3 % discharged during this phase of the testing.

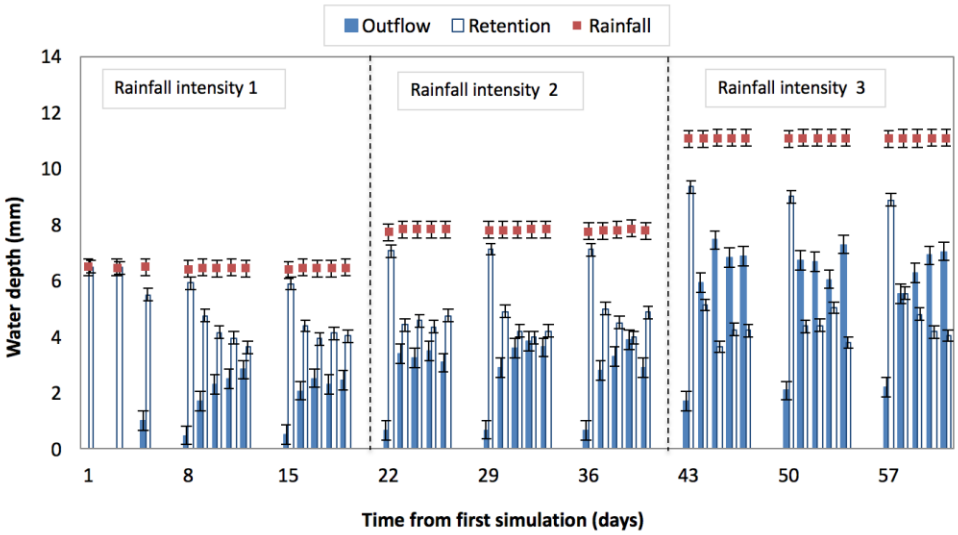

Figure 4-14: Analysis of rainfall, outflow and retention during the course of the experiment.

It can be seen from Figure 4-14 that the pavement on day 1 of each simulation cycle discharged the lowest volume. Thus, on day 1 of simulation, it is believed that the structure's materials had the highest absorption rate in comparison with other monitored days. After consecutive rain events during the week, the structure's materials became partially saturated by day 5. No rain events occurred during day 6 or 7, which decreased the retention volume within upper layers in the structure. The behaviour was repeated weekly during the simulation.

Figure 4-14 shows the retention volume during the experiment period. It can be seen that the pavement showed good performance for retaining rainfall within its structure. However, this is not the case for Rainfall Intensity 3. The pavement discharged more rainfall during Rainfall Intensity 3, than in Rainfall Intensity 1 and 2. The increase in outflow can be attributed to the increase in VWC level during earlier tests and the extended duration of rainfall. Overall, the available storage within pavement structure volume stayed at a constant level during the three rainfall intensities during the Day2-5 condition (days 2 to 5). It can be concluded that the pavement structure could

accommodate larger rainfall than the hydrologic requirements for Rainfall Intensity 1, 2, and 3.

Analysis was carried out to indicate the overall mass balance for the hydrological experiment. The change in water flux in the rig pavement can be calculated by Equation 9 (see Section 3.5.4). 43 rainfall events are used in mass balance equation (Eq. 9) to calculate the retention within structure over experimental period. The mass balance at time steps of rainfall input, evaporation, retention within the permeable pavement and outflow were calculated and it can be found in Table D-4 Appendix D. Figure 4.-15 shows the difference between measured and estimated retention volume in the system during experimental period. The difference between estimated and measured can be explained by the fact that the estimated retention was derived from two monitoring locations in the structure, probes located in the bottom layers of the structure. This results in a monitored saturation level throughout the structure which does not include consideration of the lower saturation level on the pavement surface. Considering the potential errors which were discussed in Section 3.6, the uncertainty level in retention volume is reasonably acceptable.

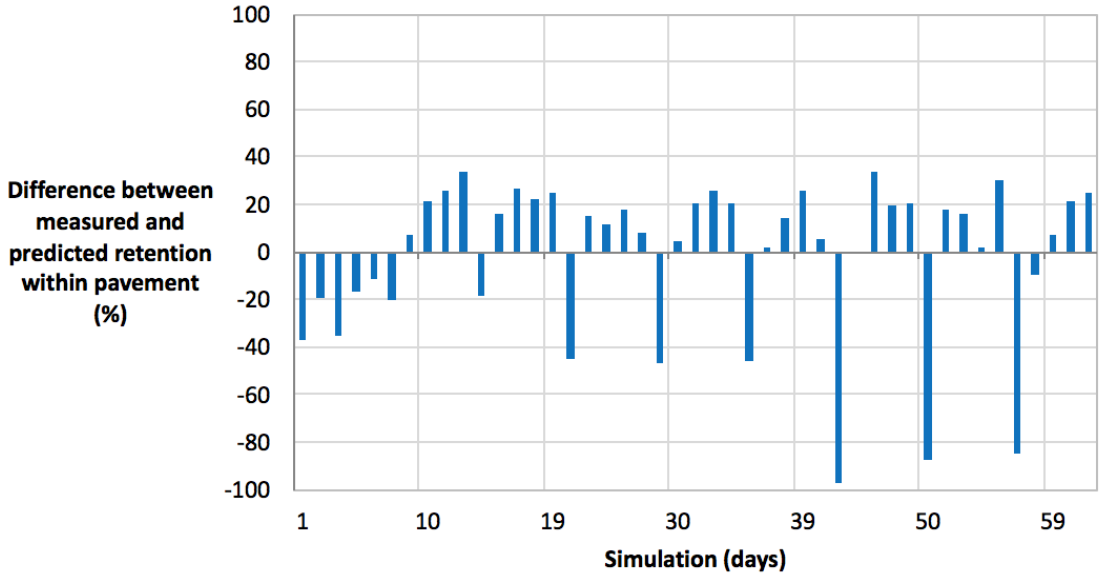

Figure 4-15: Difference between measured and predicted retention within the rig pavement.

4.4.2.2 Outflow response to rainfall intensity

The response of the pavement structure to rainfall was examined under three selected rainfall intensities. These were applied to the model over repeated simulations. Table 4-9 illustrates the average inflows and outflows for Rainfall Intensity 1, 2, and 3 (25.56, 31.12, and 21.7 mm/h, respectively). It also demonstrates the amount discharged over outflow duration, relative to the respective rainfall intensities and the condition of the pavement (Day-1 and Day2-5 condition).

Table 4-9: Outflow amount related to rainfall intensity and pavement condition

Rainfall intensity No.	Pavement condition	Average rainfall (L)	SD Dev.	Average outflow (L)	SD Dev.	Average amount (%)*
1	Day-1	6.45	0.08	0.50	0.02	7.7
	Day2-5	6.45	0.01	2.33	0.33	36.2
2	Day-1	7.78	0.05	0.67	0.02	8.6
	Day2-5	7.83	0.03	3.34	0.37	42.6
3	Day-1	11.07	0.01	1.99	0.25	18.0
	Day2-5	11.06	0.04	6.63	0.58	59.9
* Average amount discharged as a percentage of total rainfall volume (%)						

The results of the simulation cycles when the condition of the pavement was either Day-1 or Day2-5 are presented in Table 4-9. The response of the outflow was different from that in the initial simulation cycle. For example, while the pavement discharged 7.7% of rainfall during Day-1 condition (day 1) for Rainfall Intensity 1, the percentage increased to 8.6% and 18% for Rainfall Intensity 2 and 3, respectively. However, when the pavement was in Day2-5 condition, the observed outflow volume varied significantly from the Day1 condition. It is apparent from the data in Table 4-9 that the average volume discharged from the permeable pavement ranged between 7.7 and 60%.

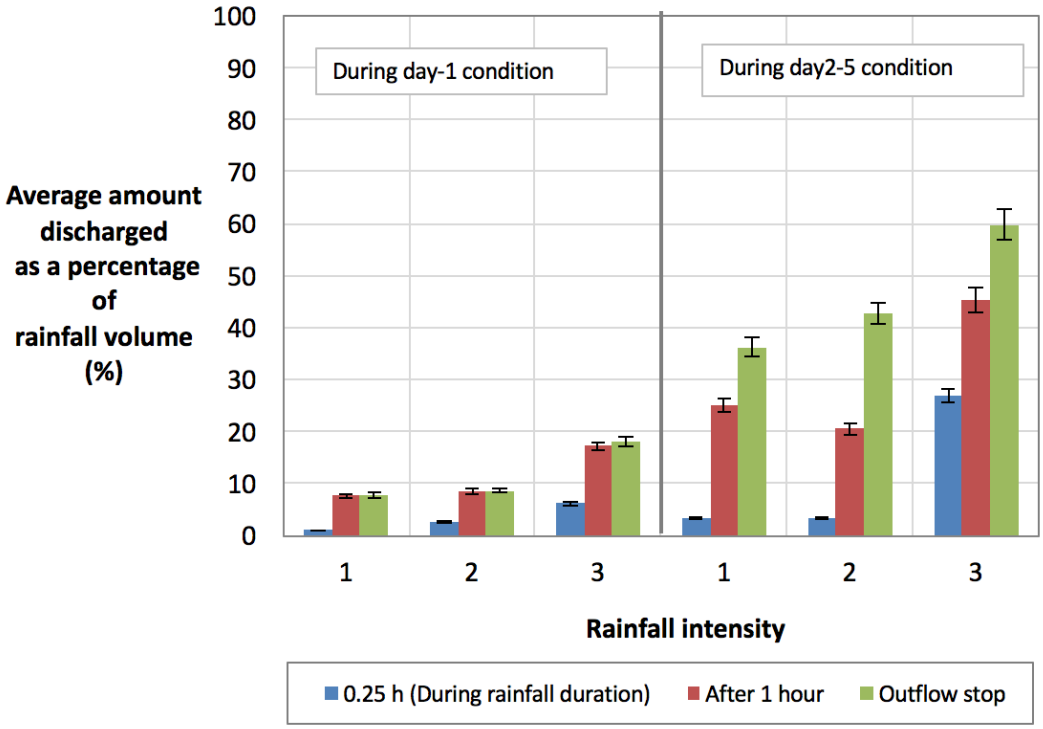

Figure 4-16: Average amount of outflow as a percentage of rainfall volume during Rainfall Intensity 1, 2, and 3.

Figure 4-16 shows the average amount discharged as a percentage of rainfall volume within different time and conditions (i.e. Day-1 and Day2-5 conditions) respectively. During Day-1 conditions, the results show that the pavement discharge rises up to 0.98%, 2.64%, and 6.18% of the rainfall during the rainfall duration for Rainfall Intensity 1,2, and 3 respectively, while the pavement discharged 7.64%, 8.5%, and 17.2% of the rainfall during one hour for Rainfall Intensity 1, 2, and 3, respectively. Within 24 hours the pavement was able to discharge only 7.68%, 8.6%, and 18% of rainfall. The pavement discharged most of the rainfall within the first hour of the start of the rainfall. There was no substantial change in outflow after one hour.

The pavement performed differently in the Day2-5 condition. During the rain event, the percentage of outflow ranged between 5% and 25% for all rainfall intensities. However, after one hour the percentage increased and ranged between 25% and 45%. Interestingly, the percentage of outflow increased, even after one hour, and thus after 24 hours it was found to range between 36% and 60%. Therefore, there is a significant difference between Day1 and Day2-5 condition. This is because whilst in a Day1

condition, the structure had a two day drying period before the commencement of the test, making the material more able to absorb the rainfall.

It can be confirmed that the performance of the permeable pavement effectively managed rain events and was able store more than 40 % of rainfall and release it slowly from the pavement structure. Comparisons were made between two wetness conditions. This comparison demonstrated that the outflow response varied depending on both rainfall intensity and pavement condition.

4.4.2.3 Hydrograph

The shape

Typical and cumulative hydrographs and hyetographs can also be drawn to visualize the discharge data from pavement structure with respect to rainfall intensity. Figure 4-17 (a), Figure 4-18 (a), and Figure 4-18 (a) illustrate the typical hydrographs for Rainfall Intensity 1, 2, and 3 (respectively). Figure 4-17 (b), Figure 4-18 (b), and Figure 4-19 (b) show the cumulative flow hydrographs for Rainfall Intensity 1, 2, and 3, respectively.

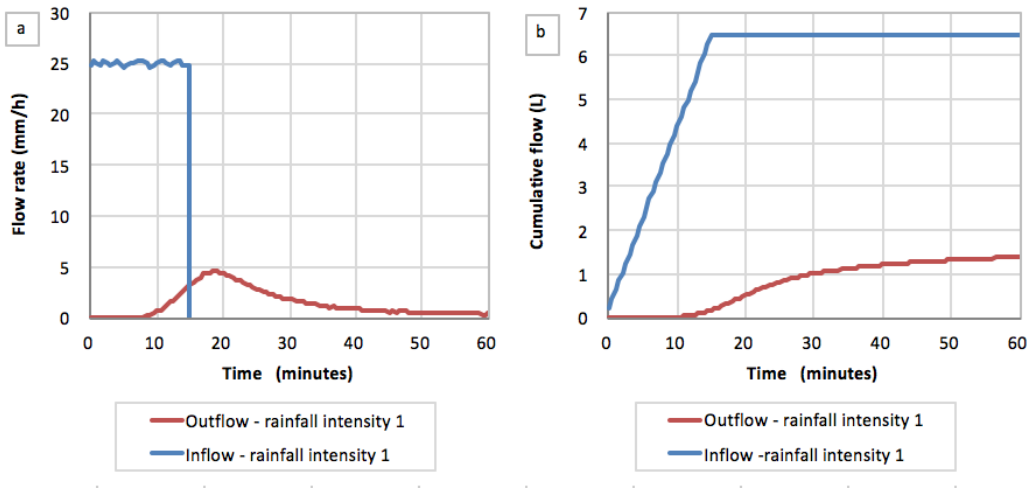

Figure 4-17: Average typical and cumulative hydrograph related to rainfall intensity, Rainfall Intensity 1.

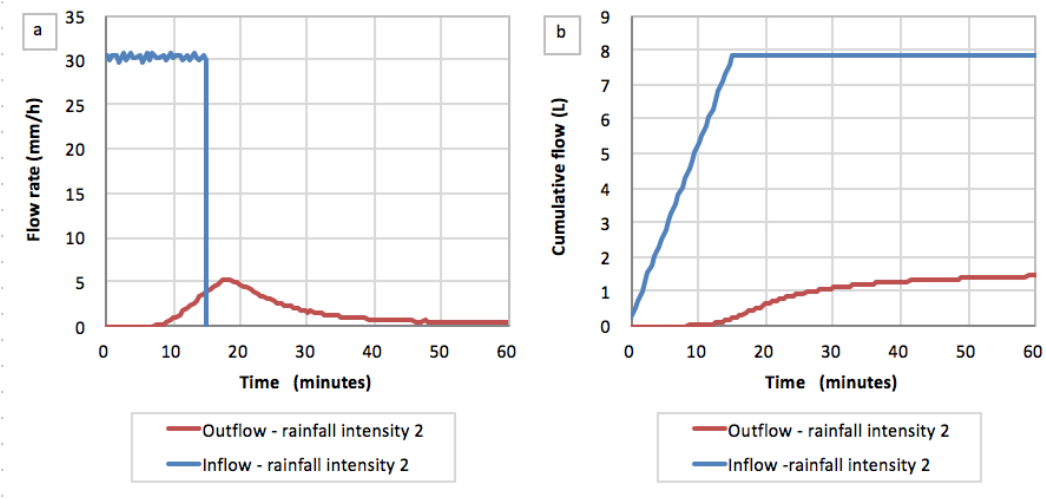

Figure 4-18: Average typical and cumulative hydrograph related to rainfall intensity, Rainfall Intensity 2.

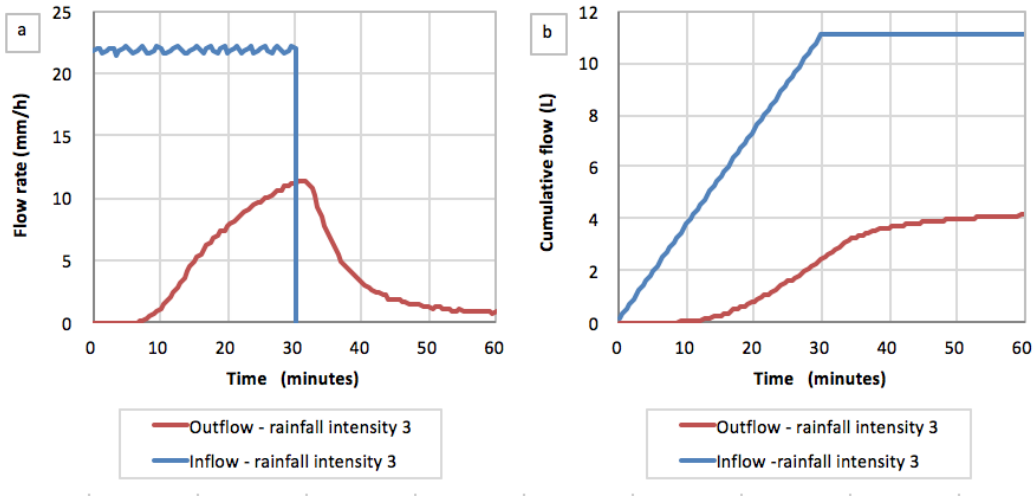

Figure 4-19: Average typical and cumulative hydrograph related to rainfall intensity, Rainfall Intensity 3.

It is apparent that the shape of the typical and cumulative outflow in Rainfall Intensity 1 and Rainfall Intensity 2 are similar, showing a comparable hydrologic performance. The gap between cumulative inflow and outflow in the hydrograph is large, confirming the ability of the pavement to attenuate the rainfall within its structure. Meanwhile, Rainfall Intensity 3 shows a different response from Rainfall Intensity 1 and 2 (see Figure 4-20). In Rainfall Intensity 3 the outflow lines increase, indicating that the longer the rain event duration the more rainfall will be discharged. Full details of all event hydrographs can be found in Figure E - 1 to Figure E - 41 in Appendix E.

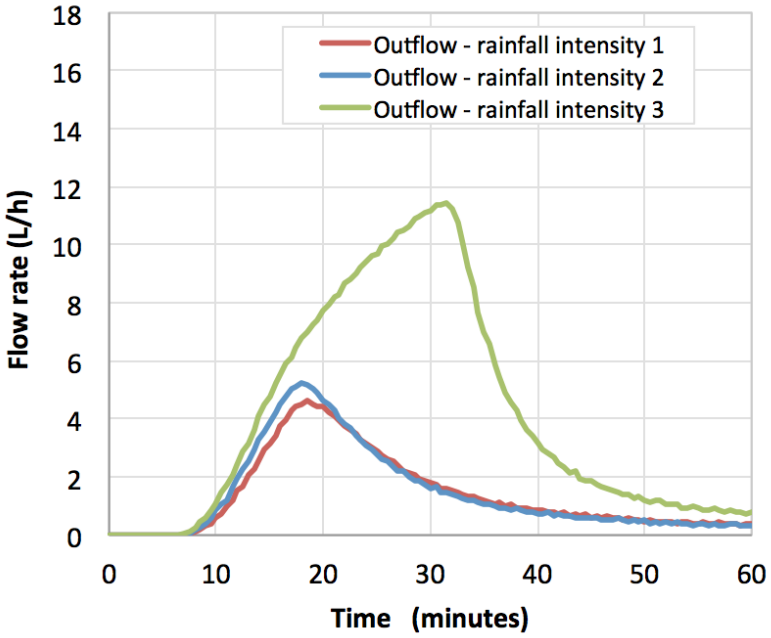

Figure 4-20: Showing average flow rate for each rainfall intensity.

Start delay to discharge & time delay to peak discharge

The hydrographs also illustrate the start delay to discharge and the time delay to peak discharge. There was a short delay (start delay) of outflow response to rainfall; this acted as a wetting phase in which the rainfall infiltrated the structure. In this case, the average start delay for Rainfall Intensity 1, 2, and 3 ranged between 7 and 10.6 minutes during Day2-5 and Day1 condition. The time (start delay) was longer if the sub-grade had less moisture content.

The first hydrology experiment was conducted in October 2012. The initial condition of VWC in sub-grade prior to starting the experiment was 0.1735 and 0.1867(m^3m^{-3}) for the top and bottom layers, respectively. The start delay to discharge was 85 hours since the initial rainfall event (see Figure 4-21). The second experiment was conducted after 10 months. The condition of the sub-grade was dryer than in the first experiment, where VWC was 0.087 m3/m3 and 0.131 m3/m3 for the top and bottom layers respectively. With this inflow the pavement took 334 hours to produce the first outflow; the difference in VWC between the two experiments was 100% and 42% for the top and bottom layer, respectively, so that it cab be seen that the start delay to discharge depends on the initial condition of the sub-grade.

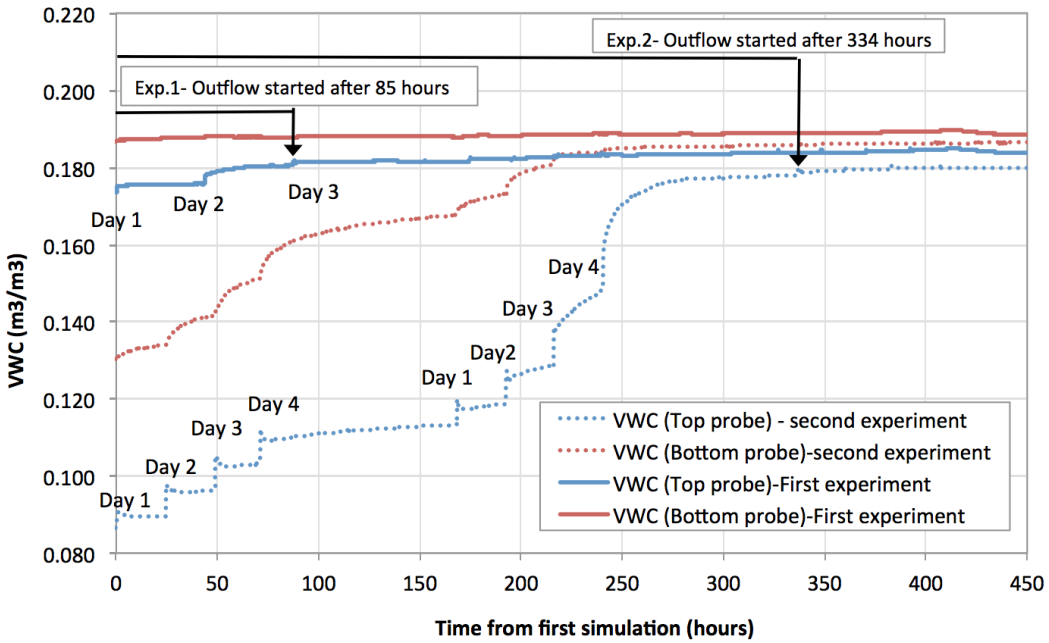

Figure 4-21: Showing start delay to discharge during two different experiments.

Peak discharge occurred after the cessation of the rainfall, with time delays in the range of 15 to 32.5 minutes for three rainfall intensities. In comparison with the rainfall duration, 15 and 30 minutes, this seems to be quick response from the structure. It can be supposed that the water head pressure governed the time delay to peak discharge.

Overall, it was obvious that there was different response in the hydrograph for the three rainfall intensities under different structure conditions. Rainfall Intensity 1 and 2, high rainfall intensity with same short rainfall duration, were able to produce identical shapes of outflow. On the other hand, the low rainfall intensity with longer duration produced a different shape.

4.4.2.4 Outflow duration

The outflow duration is defined as the period of time between the start of outflow and the end of the outflow during a single rain event. Over the monitoring period of the experiment, 41 separate outflows were recorded and analysed. Full details of the outflows can be found in Table D - 1 to Table D - 3, in Appendix D.

Figure 4-22 illustrates the average outflow duration during consecutive simulations for Rainfall Intensity 1, 2, and 3 tests. It shows the general trend of the outflow duration,

depending on the pavement condition. During Day-1 conditions, the average outflow time increased by up to two hours. The percentage change in outflow duration from Rainfall Intensity 1 was 6.26% and 126.6% for Rainfall Intensity 2 and 3 respectively. On the other hand, the average outflow duration was 5.64, 5.9, and 7.43 hours during Day2-5 conditions for Rainfall Intensity 1, 2, and 3 (respectively). The percentage change in outflow duration from Rainfall Intensity 1 ranges between 4.4% and 18.5% for Rainfall Intensity 2; and 54% and 17% for Rainfall Intensity 3. From the analysis, it is apparent that the duration of outflow was nearly comparable for Rainfall Intensity 1 and 2, due to identical rainfall duration, while Rainfall Intensity 3 shows an increase in time by up to seven hours. Thus the outflow duration of Rainfall Intensity 3 was longer than for Rainfall Intensity 1 and 2. This is significant evidence of the influence of rainfall duration on the discharge response.

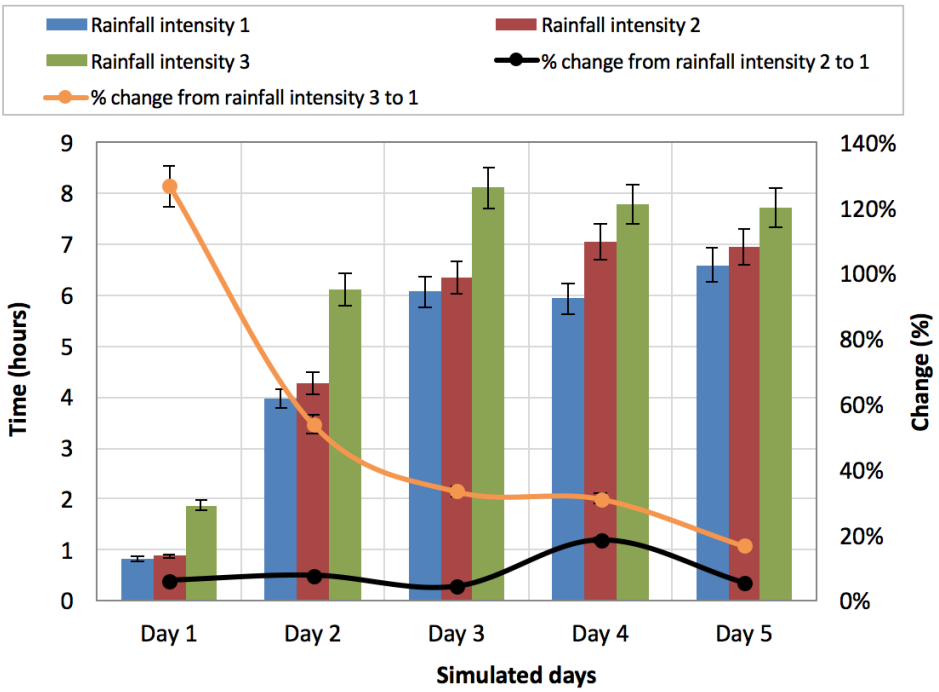

Figure 4-22: Showing the average outflow duration during consecutive simulation for Rainfall Intensity 1, 2, and 3; and showing also percentage change in outflow duration over three rainfall intensities.

4.4.2.5 Start delay to discharge

Overview

Start delay to discharge is defined as the time required for the rainfall to permeate through the pavement structure until it reaches the commencement of free drainage. This is related to antecedent conditions, infiltration rate, and pavement thickness. In this study, there were three phases of start delay, each dependent on the condition of the permeable pavement materials; during relatively dry conditions (1^{st} week of experiment), Day-1 conditions (day 1), and Day2-5 conditions. The relatively dry condition was when the structure materials were almost dry (before conducting the experiment). The condition of the structure materials before day 1, when it had two dry days (day 6 and 7) prior to day 1, was defined as 'Day1 conditions'. Days 2 to 5 were under Day2-5 conditions, due to the rainfall events during day 1 resulting in a wet starting condition on the following experiment days. Therefore, the conditions of the structure materials were subject to three different start delay times. Due to the lengthy process of drying out the rig in the laboratory, there was only one relatively dry condition period during the experiment period. Therefore, Day1 and Day2-5 conditions were the focus of the analysis and were compared and discussed. Full details of the start delay time during the three phases can be found in (Table D - 1 to Table D - 3, in Appendix D).

Relatively dry condition

It is expected that the start delay would be longer in the first day of simulation because it is dependent on the condition of the pavement and rain event characteristics. In this study, the pre-condition of the pavement was water retention greater than zero. The initial condition volumetric water content (VWC), found through monitoring over the three hours prior to the start of the experiment, was 0.1735 and 0.1867 (m^3m^{-3}) for the top and bottom layers respectively.

Figure 4-23 shows the average VWC during the initial week, clearly illustrating the increase in VWC after the three rain events. It can be seen that a large increase occurred during second rain event. In contrast, the third rain event had a lower increase due to the first discharge occurring during that rain event. The start delay was 85 hours, the time taken to start discharge during the initial (see Figure 4-21). It is possible to hypothesise

that this behaviour is less likely to occur in the following weeks or during different rainfall durations and volumes.

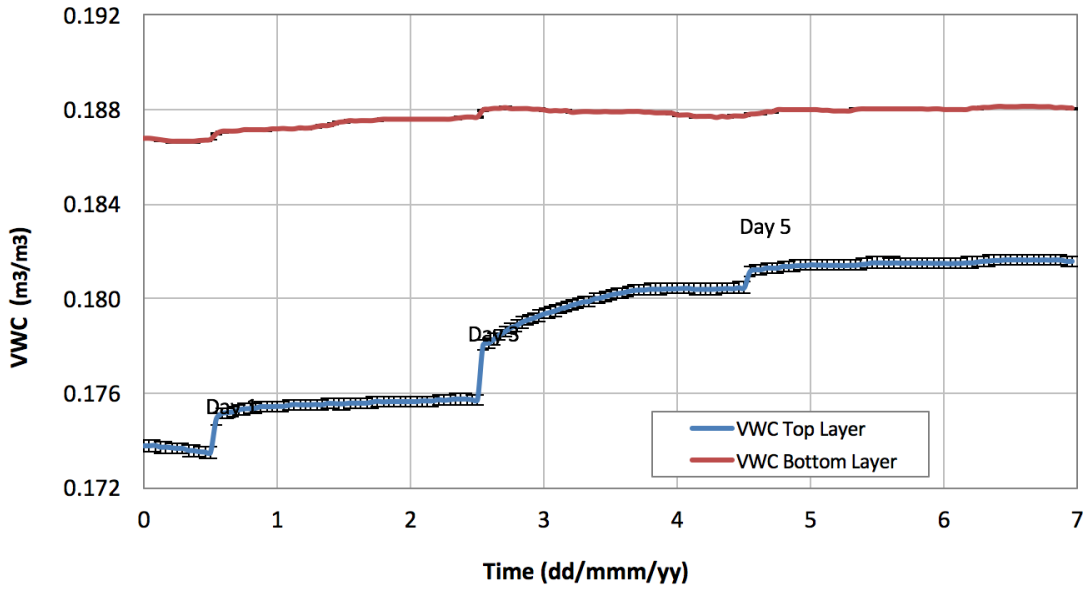

Figure 4-23: Average volumetric water content (VWC) within the initial week (8 – 12 October 2012).

Day-1 and Day2-5 condition

Figure 4-24 illustrates the general trend of the start delay, depending on rainfall intensity and the pavement condition (dry/wet). It can be seen that the start delay exceeded 10 minutes; this delay duration only occurred in Day1 condition. However, this duration was longer for the drier initial structure condition. Over the remaining experimental period (days 2 to 5) the start delay is shown to be shorter by two minutes. It is apparent that the start delay decreases over consecutive simulations, as the initial condition becomes wetter. The decrease in start delay may be explained by the fact that the water retention level in the pavement structure increases over consecutive rainfall events, causing the travel time through the thickness of the pavement to decrease.

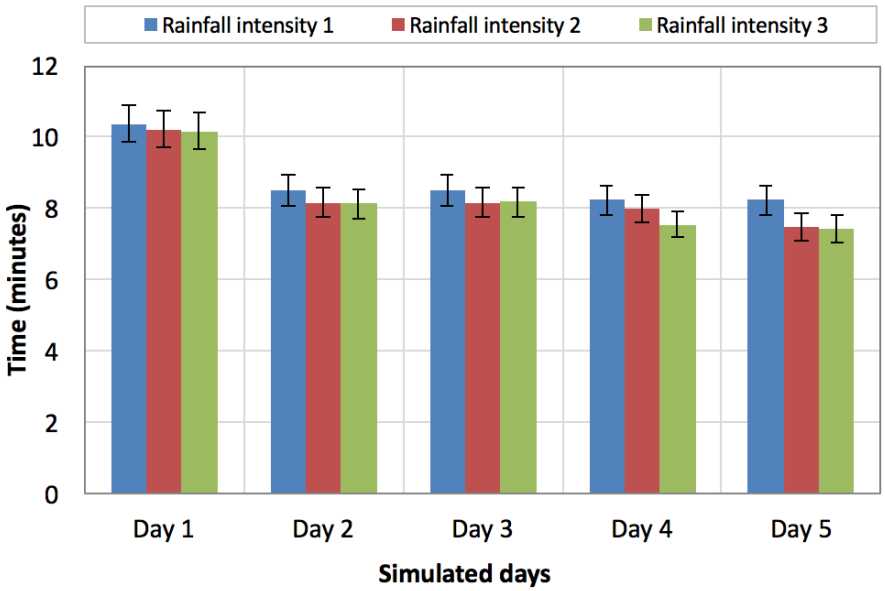

Figure 4-24: Average start delay to discharge for Rainfall Intensity 1, 2, and 3.

4.4.2.6 Water retention in the structure

To estimate the water retention, the process can be divided into three elements, input (simulated rainfall) output (outflow) and evaporation. The evaporation was estimated from the block paving in a small-scale experiment. The equivalent depth of rainfall was 0.72 mm per day as shown in Table 4-5. Therefore, the retention in the structure materials was defined as the difference between the volume of the rainfall and the volume of the outflow and water loss volume. The retention capacity was governed by factors including rainfall, outflow, pre-event retention (condition), and structure materials. This section focuses on the examination of the retention level for short and long-term condition. Full details of retention analysis can be found in Table F - 1, in Appendix F.

Figure 4-25 shows the retention volume for each single rain event over the whole period of the experiment. This figure demonstrates the general pattern over three different rainfall intensities 1, 2, and 3. Retention levels during Day1 conditions (days 1) were always higher than Day2-5 conditions, due to the condition of the pavement prior to the rainfall event. The increase in rainfall intensity caused an increase in retention volume, as it can be seen on Day1 condition days (day 1 of each simulation cycle). There is a

visible difference in retention volume between Rainfall Intensity 1 and 2, by 20.2%; and Rainfall Intensity 1 and Rainfall Intensity 3, by 53.67%.

The average retention volumes for Day2-5 conditions were 4.12 L, 4.48 L, and 4.45 L for Rainfall Intensity 1, 2, and 3 respectively. There is an increase in retention volume between Rainfall Intensity 1 and 2 by 9.08%; and Rainfall Intensity 1 to Rainfall Intensity 3 by 8%, and it can be noticed that the increase in retention in Rainfall Intensity 3 was less than that for Rainfall Intensity 2. The difference in contact time (Rainfall Intensity 2 = 15 min, Rainfall Intensity 3 = 30 min) allowed the pavement to discharge more water. This can be explained by the result in Table 4-9, where the average percentage discharge was 42.6% and 59.9% for Rainfall Intensity 2 and 3, respectively. It can be conclude that the rain event characteristics (volume and duration) show an influence on the pavement retention capacity.

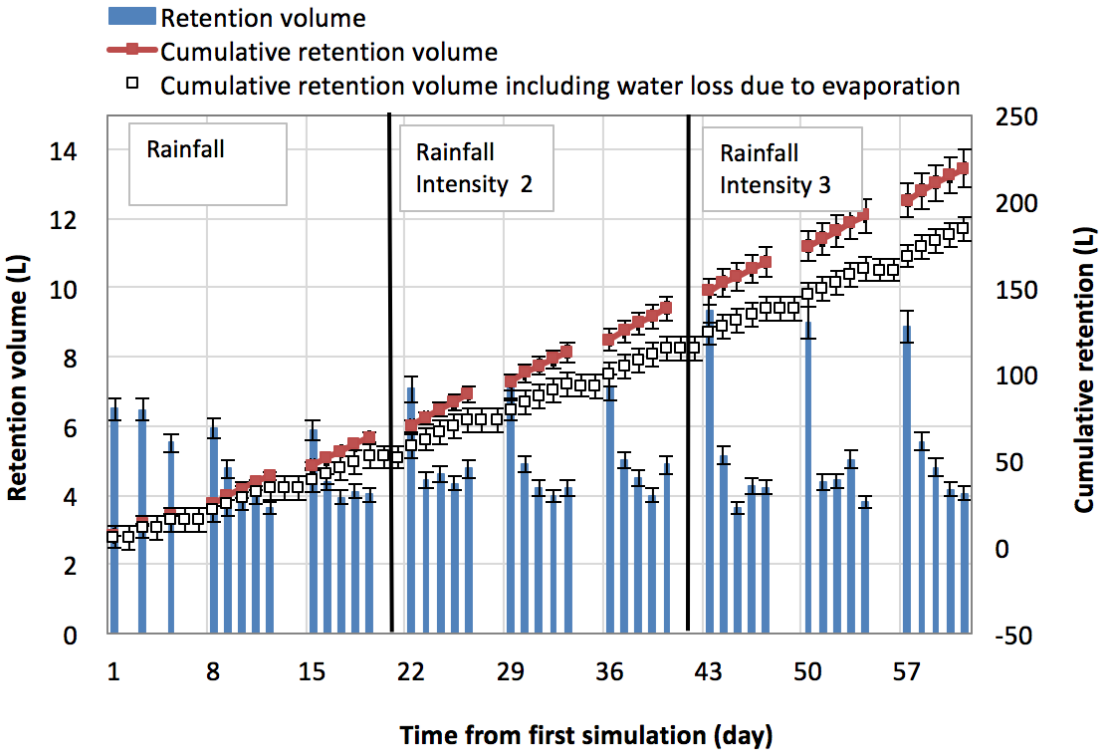

Figure 4-25: Retention volume and cumulative retention for single rain event over the experimental period.

4.5 Relationship between outflow and other variables

As described in section 4.4, the laboratory research was undertaken to illustrate the hydrological performance over three different rainfall intensities. Thus far it has shown the influence of rainfall intensity on the hydrological performance and answered the research question of whether pavement responds differently to different rainfall intensities. This section aims to present the findings of an analysis undertaken using SPSS software, in order to define the relationship between outflow and other independent variables such as inflow, antecedent rainfall, and moisture content (top and bottom layer) within different rainfall intensities (Rainfall Intensity 1, 2, and 3).

4.5.1 Regression (single variable) analysis

The change in outflow within consecutive rain events (from day 1 to 5) was described in Section 4.4.2. It was shown that there is a strong influence from rainfall intensity on the pavement response. Thus, linear regression was used to define the relationship between outflow and inflow for three rainfall intensities (Rainfall Intensity 1, 2, and 3). In this section, the relationship between outflow and a single independent variable is discussed. The following section will present the findings with regard to outflow and several selected independent variables.

In order to define the relationship between outflow and inflow, it was important to draw a scatterplot to visualize the linearity between the dependent variable (outflow) and the independent variable (inflow). Figure 4-26 to Figure 4-28 describe the linear relationship between outflow and inflow volume for Rainfall Intensity 1, 2, and 3 respectively. The plots show that there is a positive relationship between the outflow and inflow for all rainfall intensities. The results show that the correlation coefficient and the coefficient of determination were high, where R values of 0.85, 0.92, and 0.87; R^2 values of 0.72, 0.84, and 0.75 were obtained for Rainfall Intensity 1, 2, and 3 respectively. The relationships between the outflow and inflow showed strong correlation and were highly significant (p-value <0.001 for all rainfall intensities).

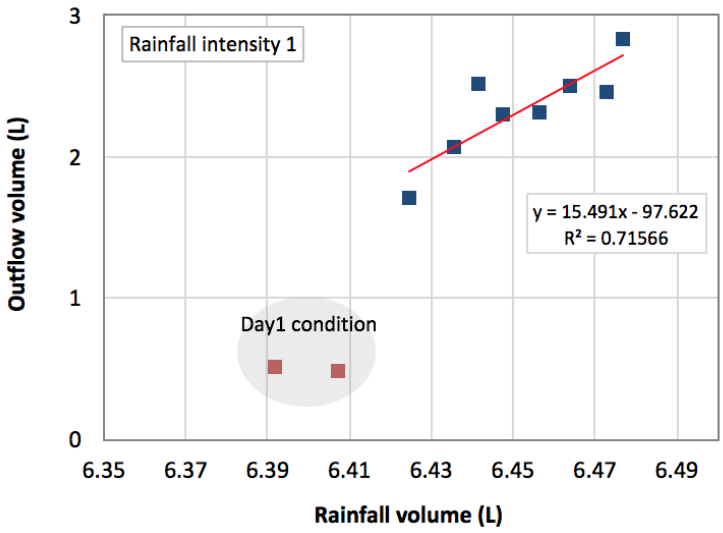

Figure 4-26: Scatterplot with fitted line between outflow and inflow volume for Rainfall Intensity 1.

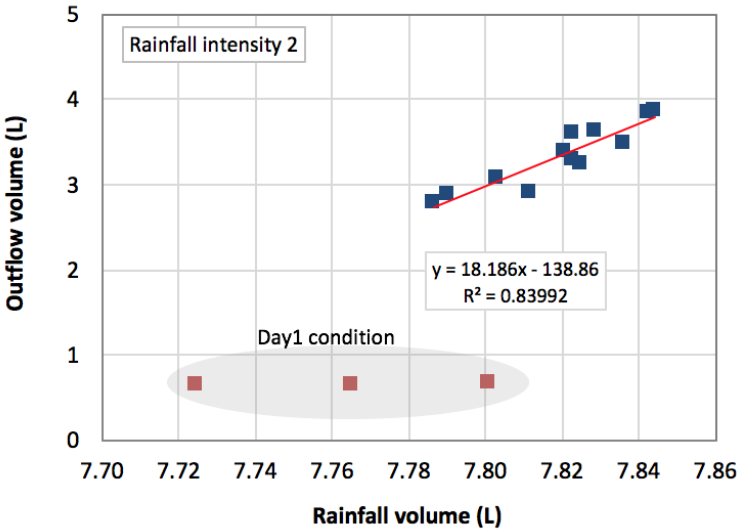

Figure 4-27: Scatterplot with fitted line between outflow and inflow volume for Rainfall Intensity 2.

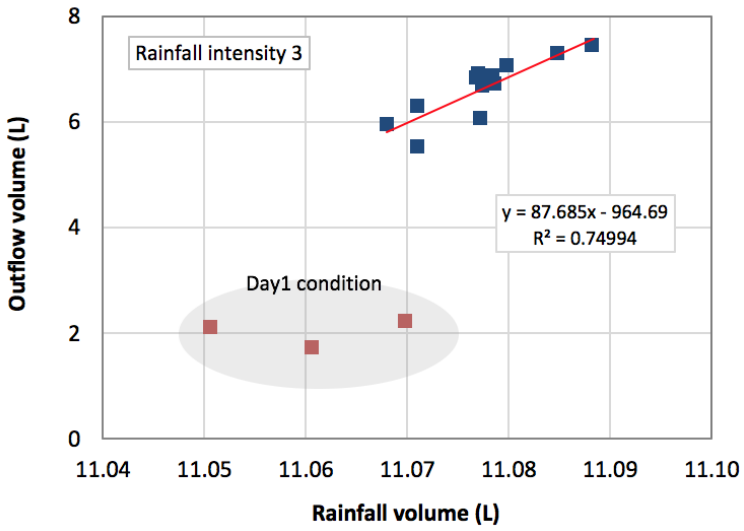

Figure 4-28: Scatterplot with fitted line between outflow and inflow volume for Rainfall Intensity 3.

From the analysis, it was observed that the gradients were lowest in Rainfall Intensity 1 and 2, but in Rainfall Intensity 3 were 6 times higher than in Rainfall Intensity 1 and 2, i.e., 15.49 for Rainfall Intensity 1, 18.19 for Rainfall Intensity 2, and 87.68 for Rainfall Intensity 3. This illustrates that if the gradient increases, this means there is less retention in the pavement. Although Rainfall Intensity 1 and 2 have same rainfall duration the gradient was higher in Rainfall Intensity 2 due to the difference in rainfall intensity (5 mm/h). The results indicate that the relationship between outflow and inflow was governed by the rainfall intensity and duration.

A paired t-test analysis was conducted to determine whether there was a statistically significant difference in the discharge of the rig for different rainfall intensities. The results are summarised in Table 4-10. The results indicate that there is a statistically significant difference between rainfall intensities. It was also observed that the relationship between outflows was governed by the rainfall intensity and duration.

Table 4-10: Paired t-test for comparison of outflow volume in Rainfall Intensity 1 to Rainfall Intensity 2 and 3. Critical t is 2.08 (p=0.05)

Rainfall Intensity	t-test	Significantly different
2	3.97	Yes
3	5.48	Yes

4.5.2 Multiple-regression analysis

In order to generate a predictive equation for the hydrological response from the permeable pavement resultant from the selected three rainfall intensities, multiple regression analysis was performed on the independent variables inflow, antecedent rainfall, duration, and moisture content with the dependent variable, outflow. The three rainfall intensities (Rainfall Intensity 1, 2, and 3) were analysed and multiple regression analysis results are shown in Table 4-11 to Table 4-13 for Rainfall Intensity 1, 2, and 3 respectively.

Table 4-11: Summary statistics, correlations and results from the multiple regression analysis for Rainfall Intensity 1

Variable	**Mean**	**Std. Error**	**Correlate with outflow**	**Multiple regression weights**		
				b	**Std. error**	**P-value**
Constant	-	-	-	57.76	81.91	0.40
Inflow (x_1)	6.44	0.00	0.88	18.97	4.76	0.00
Inflow (x_2) last 24hrs	5.14	0.85	0.94	0.09	0.04	0.07
VWC top (x_3)	0.183	0.03	0.49	2.49	1.88	0.22
VWC bottom (x_4)	0.188	0.01	0.45	-5.47	5.86	0.33
Duration (x_5)	0.25	0	0.43	-483.52	122.80	0.01
The correlation coefficient R						0.98
The coefficient of determination R^2						0.96
F- test						40.46
P-value for the generated model						<0.001

Table 4-12: Summary statistics, correlations and results from the multiple regression analysis for Rainfall Intensity 2

Variable	Mean	Std. Error	Correlate with outflow	Multiple regression weights		
				b	Std. error	P-value
Constant	-	-	-	-14.38	57.22	0.80
Inflow (x_1)	7.81	0.83	0.74	16.16	4.51	0.00
Inflow (x_2) last24hrs	6.25	0.02	0.96	0.13	0.04	0.01
VWC top (x_3)	18.49	0.01	0.42	3.78	1.99	0.11
VWC bottom (x_4)	18.88	0.01	0.20	-2.93	3.72	0.49
Duration (x_5)	0.25	0	0.21	-496.82	141.09	0.00
The correlation coefficient R						0.96
The coefficient of determination R^2						0.93
F- test						42.45
P-value for the generated model						<0.001

Table 4-13: Summary statistics, correlations and results from the multiple regression analysis for Rainfall Intensity 3

Variable	Mean	Std. Error	Correlate with outflow	Multiple regression weights		
				b	Std. error	P-value
Constant	-	-	-	-92.95	167.24	0.59
Inflow (x_1)	11.07	1.18	0.77	157.14	38.45	0.00
Inflow (x_2) last 24hrs	8.86	0.02	0.97	0.16	0.04	0.00
VWC top (x_3)	18.61	0.01	0.25	-15.32	18.83	0.43
VWC bottom (x_4)	18.94	0.00	0.29	20.11	26.80	0.46
Duration (x_5)	0.25	0	0.22	-3477.51	853.12	0.00
The correlation coefficient R						0.97
The coefficient of determination R^2						0.94
F- test						53.37
P-value for the generated model						<0.001

The correlation coefficient and the coefficient of determination were high for all three rainfall intensities, with R value of range 0.98 and 0.96; and R^2 value of range 0.96 and 0.93 respectively. From Table 4-11 to Table 4-13, the multiple regression Equations were formalised:

$$y = 18.97x_1 + 0.09x_2 + 2.49x_3 - 5.47x_4 - 483.52x_5 + 57.76 \quad (10)$$

$$y = 16.16x_1 + 0.13x_2 + 3.78x_3 - 2.93x_4 - 496.82x_5 - 14.38 \quad (11)$$

$$y = 157.14x_1 - 0.16x_2 - 15.32x_3 + 20.11x_4 - 3477.51x_5 - 92.95 \quad (12)$$

The multiple regression Equations (10, 11, and 12) represent rainfall intensities 1, 2, and 3 respectively, where, y is outflow volume (L), x_1 is rainfall volume (L), x_2 is antecedent rainfall within 24 h (L), x_3 is volumetric water content for top layer (%), x_4 is volumetric water content for bottom layer (%), and x_5 is rainfall duration (hours).

All three rainfall intensities were highly significant (p-value <0.001). Thus, the multiple regression analysis showed there is a good correlation between the four independent variables (inflow, antecedent rainfall, duration and moisture content) and the dependent variable (outflow).

Figure 4-29 to Figure 4-31 show measured and predicted outflow. The trend lines were plotted to show the degree of prediction efficiency. The three equations have a tendency to under-estimate the outflow volume, due to the dry period that existed before the start of the simulation in day 1. Analysis of the plots produced suggests more accurate equations may have been produced if the day 1 data was excluded from the multiple regression analysis. It was noted that the gradient of the outflow in Rainfall Intensity 3 was 6 times higher than outflow in Rainfall Intensity 1 and 2. This was due to the longer storm durations (Rainfall Intensity 1< Rainfall Intensity 2< Rainfall Intensity 3).

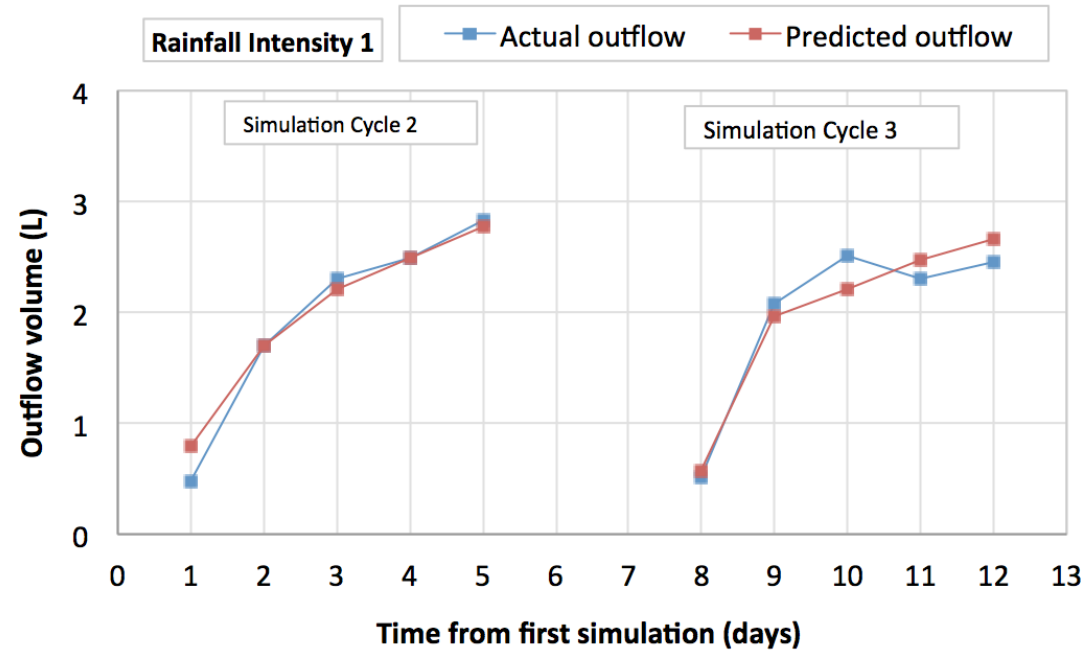

Figure 4-29: Showing predicted and actual outflow during two simulation cycles for Rainfall Intensity 1; simulation cycle 1 was excluded, because it represented dry conditions.

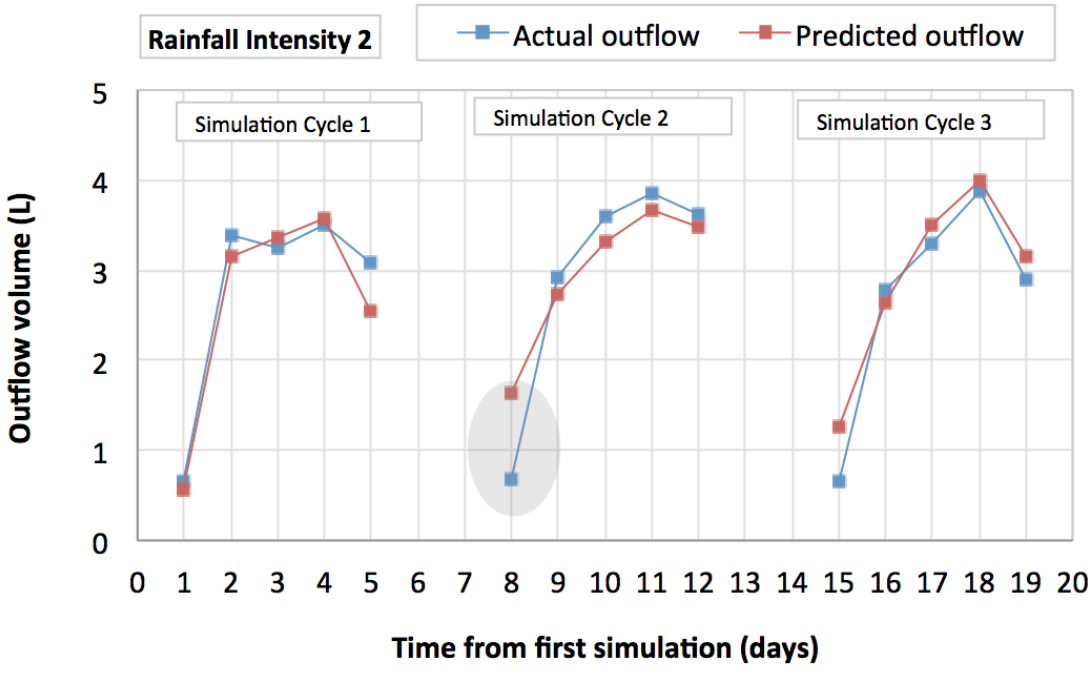

Figure 4-30: Predicted and actual outflow during three simulation cycles for Rainfall Intensity 2.

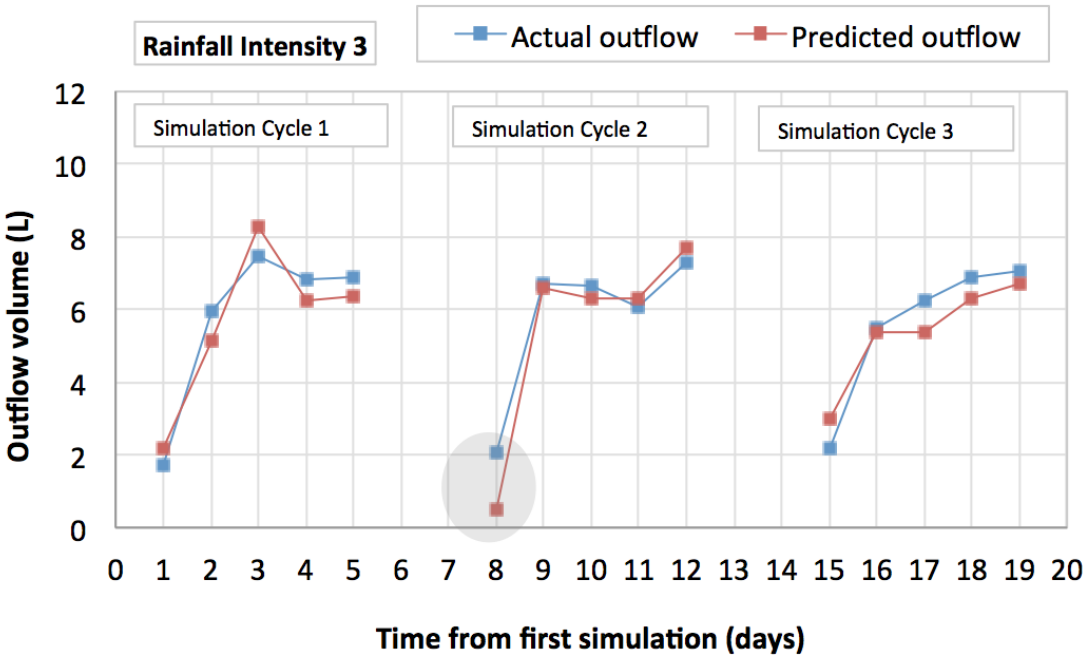

Figure 4-31: Predicted and actual outflow during three simulation cycles for Rainfall Intensity 3.

Equations 10, 11, and 12 were developed for each of the different rainfall intensity. To combine the three equations into a single equation in order to describe general discharge from the pavement, the rainfall (x_1 and x_2) must be expressed in terms of volume. The three equations can be combined into a single equation. Therefore, the general function can be formalised:

$$y = 0.24x_1 + 0.21x_2 + 1.72x_3 + 0.05x_4 + 3.67x_5 - 33.74 \quad (13)$$

The general equation (13) illustrates a statistically significant linear relationship ($p<0.001$). Thus, it shows very good regression performance with high coefficient of determination ($R^2=0.88$). The predicted outflow was plotted against the actual outflow (Figure 4-32). It is apparent that prediction is good at Rainfall Intensity 1 and 2, but there is a tendency by the equation to under-estimate outflow volume in Rainfall Intensity 3, by 7.52%.

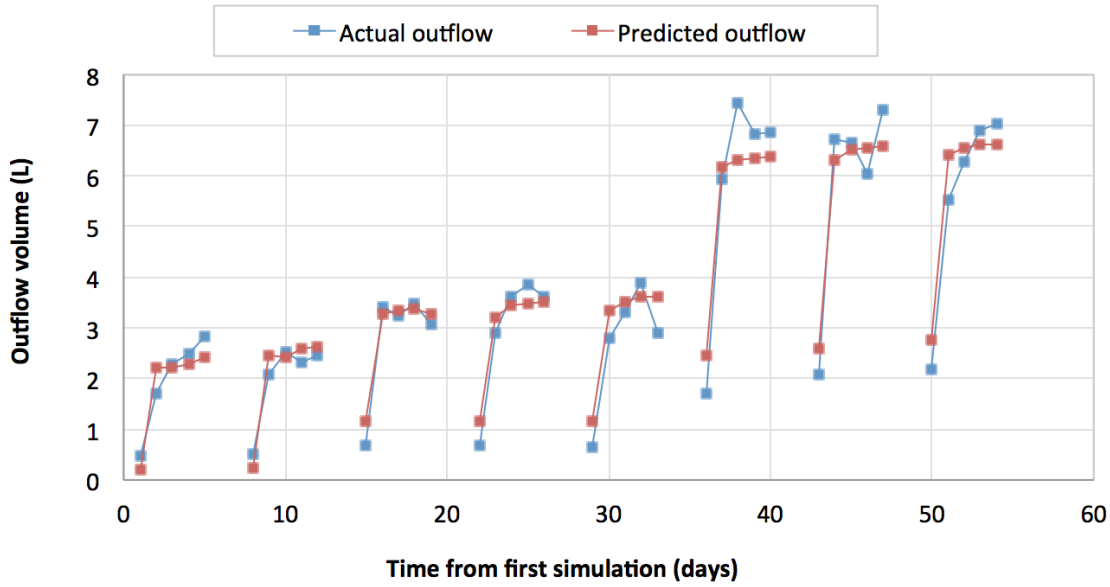

Figure 4-32: Predicted and actual outflow for combined three equations.

To estimate the degree of similarity between measured and predicted outflow, the percentage error was calculated by:

$$\boldsymbol{ercent\ error} = \frac{(\boldsymbol{predicted\ outflow} - \boldsymbol{actual\ outflow})}{\boldsymbol{actual\ outflow}} \times \mathbf{100} \qquad \textbf{(14)}$$

Figure 4-33 to Figure 4-35 show the percentage error for Rainfall Intensity 1, 2, and 3 respectively. The predictions show improvement during days 2 to 5 (during Day2-5 condition), but day 1 shows the biggest error in predicted outflow, due to the retention level prior to rainfall application, which was lower from days 2 to 5. During days 2 to 5, the figure shows that the accuracy in prediction was over 80%. Thus, the prediction equations provide a simple and effective approach to predict the hydrological response of the rig for different rainfall intensities. However, the limitations of the available data should be noted, with consideration given to the laboratory environment and time scale over which these experiments were conducted (9 weeks).

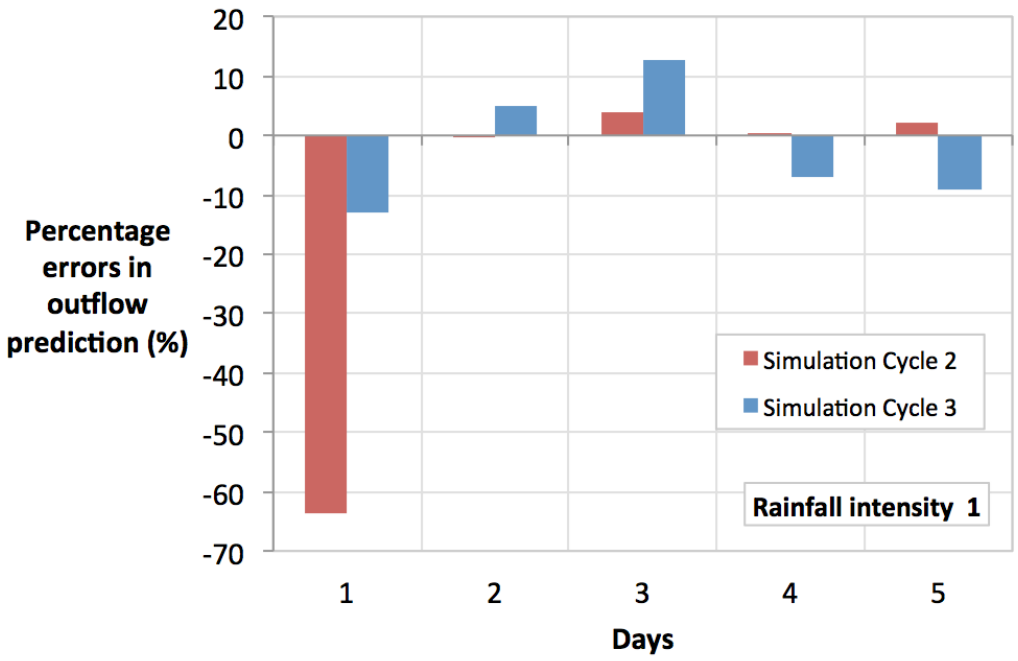

Figure 4-33: Showing percentage errors in outflow predictions during two simulation cycles for Rainfall Intensity 1.

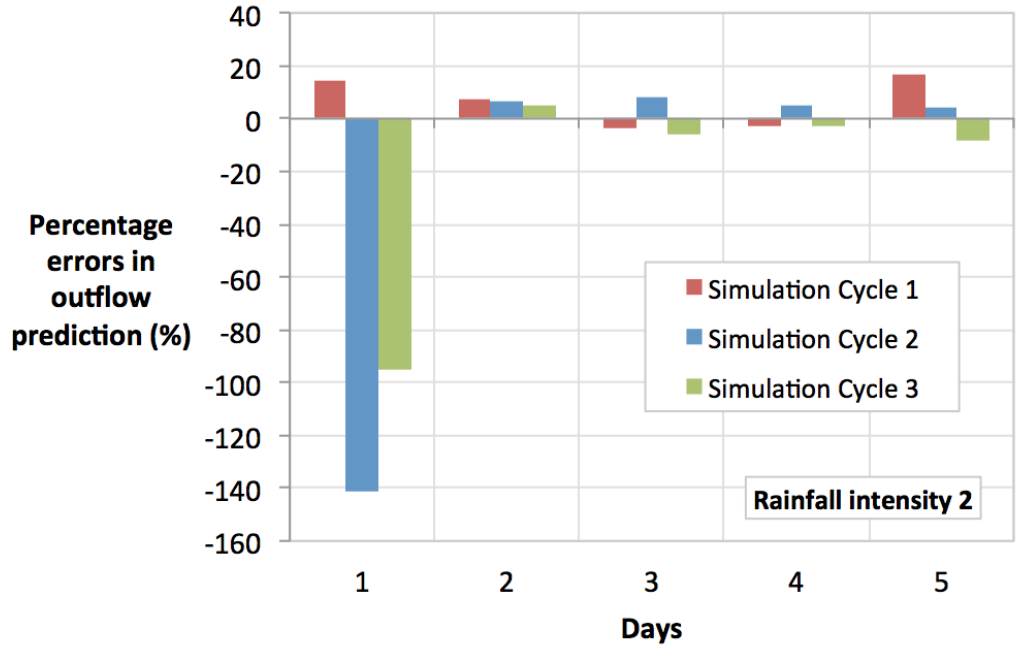

Figure 4-34: Showing percentage errors in outflow predictions during three simulation cycles for Rainfall Intensity 2.

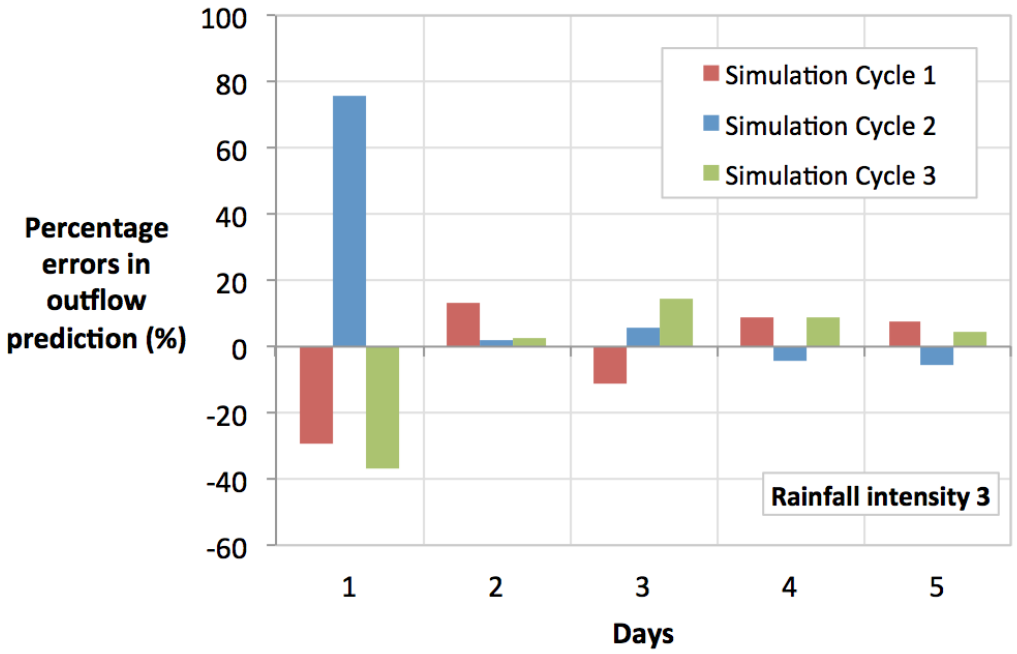

Figure 4-35: Showing percentage errors in outflow predictions during three simulation cycles for Rainfall Intensity 3.

Further testing would improve the accuracy of prediction in day 1 by further optimisation, but this was not the aim of the analysis and empirical model. This research has successfully designed a model car park that has been used to generate data to show the influence of rainfall duration and intensity on the hydrological performance of the pavement.

4.6 Chapter summary

This chapter has presented findings obtained from laboratory experiments that evaluated the performance of a $1m^2$ surface area of permeable pavement (and respective vertical infiltration structure) during different rainfall intensities and durations. Conclusions relevant to the performance of a permeable pavement can be drawn:

4.6.1 Hydrographs

The rainfall intensities (Rainfall Intensity 1, 2, and 3) influenced the shape of the hydrograph over long duration rain events. The outflow volume and the length of the wetting phase were affected by rainfall intensity.

4.6.2 Outflow response

The outflow analysis showed that the rainfall intensity influenced the drainage volume. This was not the only factor affected the outflow; the dry period condition during days 6 and 7 significantly affected the outflow volume.

4.6.3 Volumetric water content

The volumetric water content (VWC) was an indicator of the retention level of the structure before and after the rainfall events. It showed that the VWC response over consecutive rainfall events was governed by the pre-rainfall event retention within the pavement structure.

The experimental findings confirm that a permeable pavement designed in accordance with the SuDS manual (CIRIA C697) does provide rainfall runoff attenuation. Thus, appropriately designed permeable pavement offers an excellent source of control by dealing with a variety of storm water.

Source of potential error has been identified in Section (3.6). A number of steps were taken to minimise potential errors including calibration equipment and repeating the experiment. The uncertainty of the results was not found to have a significant impact on the results. Despite uncertainty in moisture content and inflow measurements, the results that were generated from calibrated instruments are consistent with performance results that has been revised in literature, For instance Pratt 1990, Abbott et al (2003), and Mullaney et al, 2011. Thus, the uncertainty of the results was not found to have a significant impact on the results.

CHAPTER 5 – SEDIMENT EXPERIMENT

5.1 Introduction

The aim of this chapter is to evaluate the process of sediment accumulation within the structure over a known time scale and to monitor the change in outflow after the addition of sediment to the pavement surface. The experiment was intended to simulate the long-term performance and the longevity of the structure, by subjecting it to consecutive rainfall events over a series of sediment input conditions.

In this study, the aim was to design and construct a 1:1 full scale model of a car park pavement surface, which brought substantial challenges to the operation of the rig in terms of delivering and collecting water over an extended time. The following work forms the main part of this study, which covers the equivalent of 12 years rainfall simulations, 10 years sedimentation application, outflow characteristics, monitoring of the level of suspended solids, and atmospheric conditions. The results begin to provide answers to life cycle efficiency and maintenance questions surrounding permeable pavements and make a significant contribution towards understanding the life span performance of these pavements.

5.2 Influence of sediment on Hydrological performance

5.2.1 The pre-experimental condition of the sub-grade

After the construction of the pavement, the volumetric water content (VWC) of the sub-grade was monitored continuously at two different depths. After six months, the VWC was higher, due to a series of rainfall events conducted from September to December 2012 (to study hydrology performance). The VWC increased significantly throughout this period. After the hydrology experiment, the sub-grade was fully saturated and the VWC was 0.184 m^3m^{-3} and 0.189 m^3m^{-3} for the top and bottom sub-grade layers respectively. Figure 5-1 shows the volumetric water content (VWC) for the top and the bottom layers of the sub-grade for the period between the hydrology and sediment experiments, (a ten-month period).

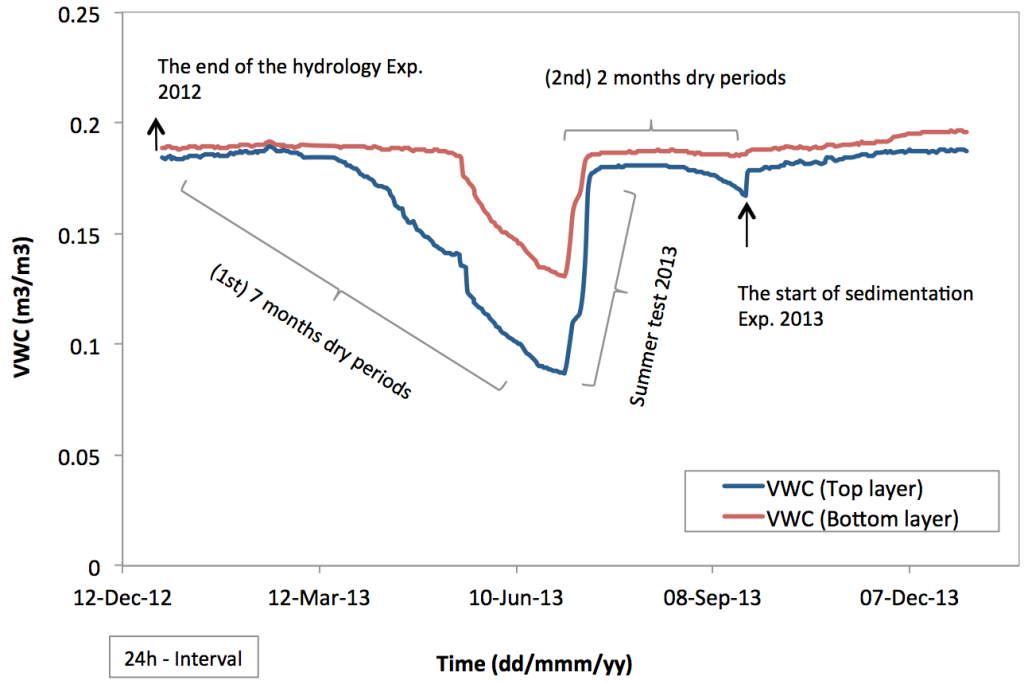

Figure 5-1: The condition of the volumetric water content (VWC) at the top and the bottom levels of the sub-grade throughout 2013.

The pavement did not receive any precipitation for a continuous period of 7 months (initial conditions). This was considered to be the 1st dry period for the pavement and, as a result, the VWC decreased significantly. A rainfall simulation was carried out in July 2013 (for four weeks) which caused a sharp increase in the VWC. Following this simulation experiment a further two month dry period occurred (the 2nd dry period). Prior to the sediment experiment, after the 2nd dry period, the VWC decreased by 6.6% and 0.3% for top and bottom sub-grade respectively. This occurred due to gravitational water movements downward. The VWC decreased less with increased depth below the pavement surface. Figure 5-1 illustrates the fact that the drying process was very slow and dependent on multiple factors. A key sub-grade drying factor was the atmospheric conditions surrounding the rig. In the laboratory, the temperature and relative humidity were monitored from 1 January to 31 December 2013 (summarised in Table 5-1).

Table 5-1: Statistical data for atmospheric conditions surrounding the rig during 2013

	Air Temperature (°C)	Surface Rig Temperature (°C)	Relative humidity (%)
Max	26.84	24.46	76.22
Min	19.12	16.87	17.42
Average	23.74	21.97	36.20
SD	1.54	1.49	10.93

The variation in temperature during 2013 was 7.7°C. It is evident from the data that the temperature changed over time but the fluctuations were not significant. The obvious difference occurs in the relative humidity (RH) level, which rises by 50%, during the summer period (see Figure 5-2), but was less variation for the rest of the year. RH was noted to be constant during the period in which the sediment experiment was carried out. These results indicate that in a stable environment the pavement could take months, potentially years, to become fully dry under laboratory conditions.

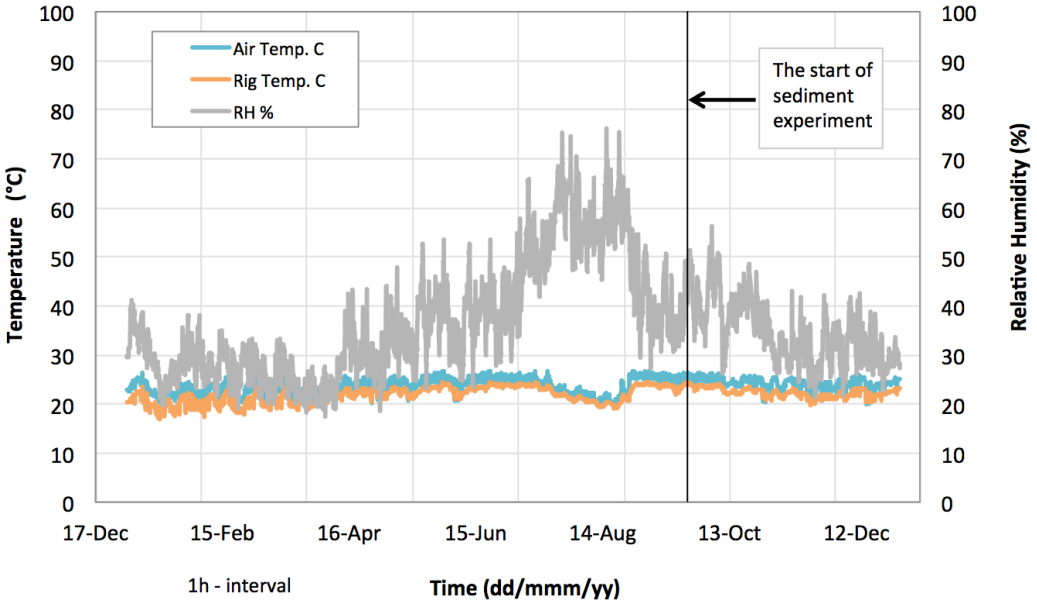

Figure 5-2: Temperatures and Relative humidity between the period 31/12/2012 - 01/01/2014, (sampled hourly).

It can be seen that the pavement was relatively saturated and some water was held in the sub-surface pavement material. Therefore, the amount of retained water needs to be taken into account when considering the initial conditions under which the sediment experiment took place.

5.2.2 The experimental condition

5.2.2.1 Volumetric Water Content and Temperatures & Relative Humidity

The analysis of the moisture content data demonstrates that the drying out period of the 300 mm sub-grade could be months, to become fully dry under laboratory conditions, as described in section 5.2.1. This may have a correlation with the climatic conditions surrounding the pavement. The influence of evaporation from the pavement structure on sub-grade drying time was also considered. However, it was difficult to measure this directly from the rig, due to the rig weight being in excess of 2 tons. Instead, the evaporation from the pavement materials was estimated by small small-scale experiment (see Section 4.2).

Table 5-2: Statistical data for atmospheric conditions surrounding the rig from September 2013 to April 2014

	Air Temperature (°C)	**Relative humidity (%)**	**Surface Rig Temperature (°C)**
Max	26.2	53.9	24.4
Min	19.7	22.0	19.5
Average	23.4	32.7	21.7
SD	1.3	5.4	1.0

Table 5-2 presents the analysed data relating to temperature and relative humidity from September 2013 to April 2014. The variation in temperature was 7.2 °C (+/-10.2%) throughout the period of the experiment, as shown in Figure 5-3, indicating that the temperature remained relatively constant. Relative humidity notably varied at the beginning of the experiment (see Figure 5-4) but was less variation for the rest of the experimental period. Therefore, it was assumed that the evaporation rate also remained

constant. The atmospheric conditions during the experiment could be said to have prolonged the drying period for the sub-grade.

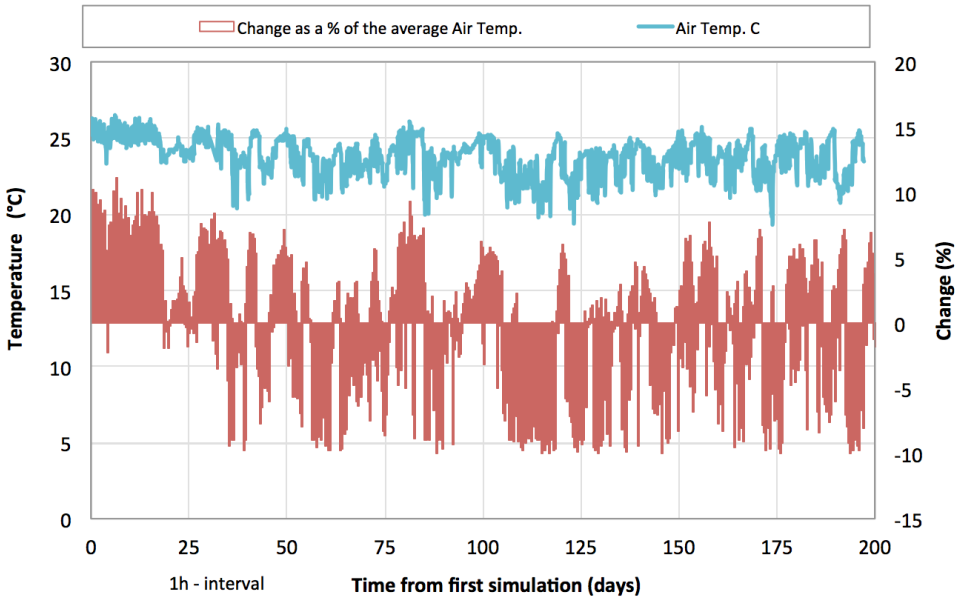

Figure 5-3: Air temperature and change as percentage of the average temperature during the experimental period.

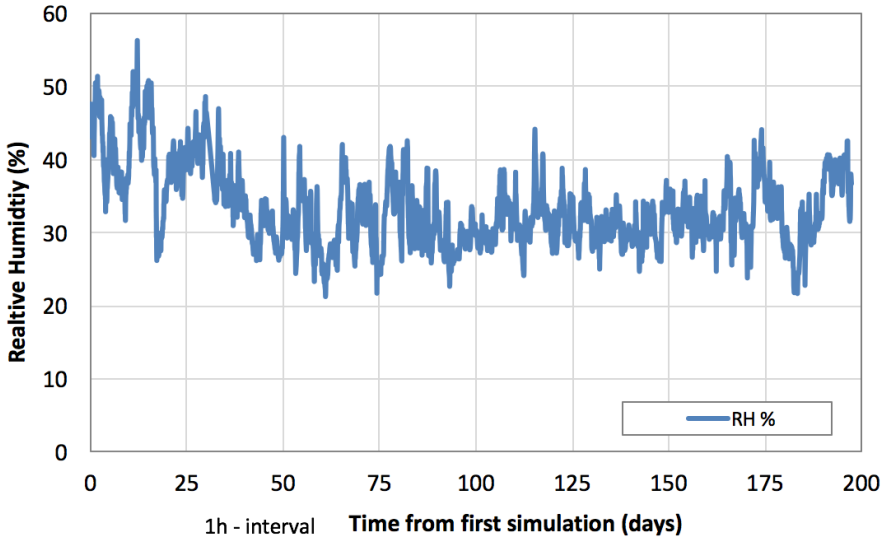

Figure 5-4: Temperature and relative humidity during the course of the experiment.

The data (see Figure 5-4

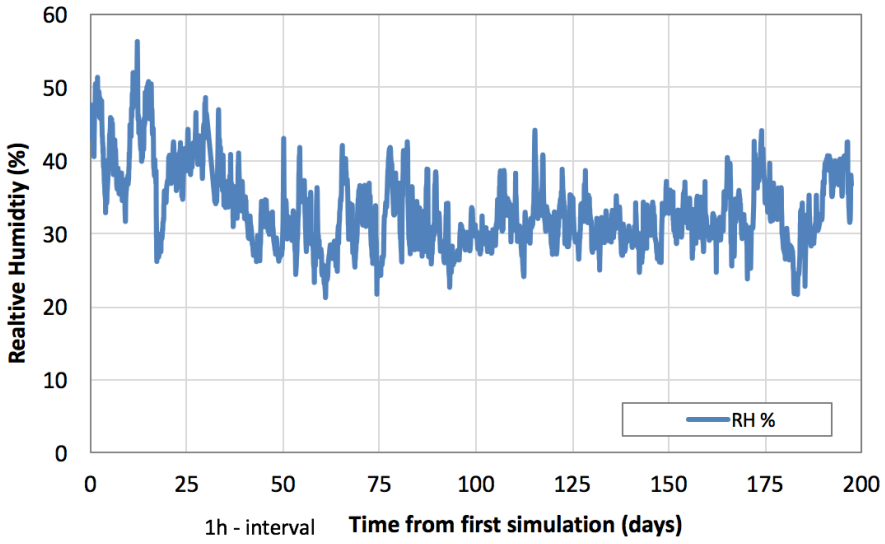

Figure 5-4) shows that the average temperature and relative humidity during the 24-week sediment experiment period are almost constant. Therefore, it can be assumed that the evaporation rate is also relatively constant. The top layer of the sub-grade was noted to have consistently lower volumetric water content than the bottom layer as shown in Figure 5-5. Overall, the volumetric water content increased dramatically during the first week and continued to increase slightly during the following weeks of the experiment.

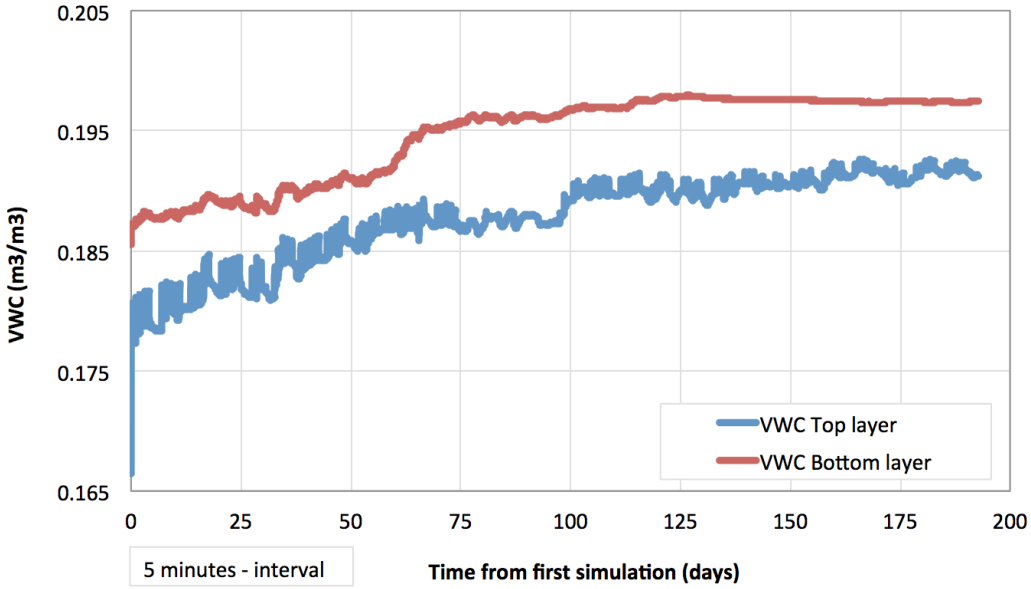

Figure 5-5: Volumetric water content for the whole of experiment.

5.2.2.2 The condition of the sub-grade during Christmas breaks

The sediment experiment was initiated at the beginning of September 2013 and continued up until April 2014, with a three week break over Christmas due to laboratory safety policies which prohibited access to the laboratory during that time. This three week Christmas period provided a three week dry period for the rig. The VWC, temperature and relative humidity were monitored during this time. Figure 5-6 shows the volumetric water content during the 24 week period, including the Christmas break. It can be seen that the VWC varied, especially in the top layer of the sub-grade. It remained virtually constant until the experiment was resumed after the break.

The precipitation caused the VWC to fluctuate during the 24-week period. A significant variation in moisture content was especially evident in the top layer. It appears that the precipitation had a noticeable effect on the VWC within this layer.

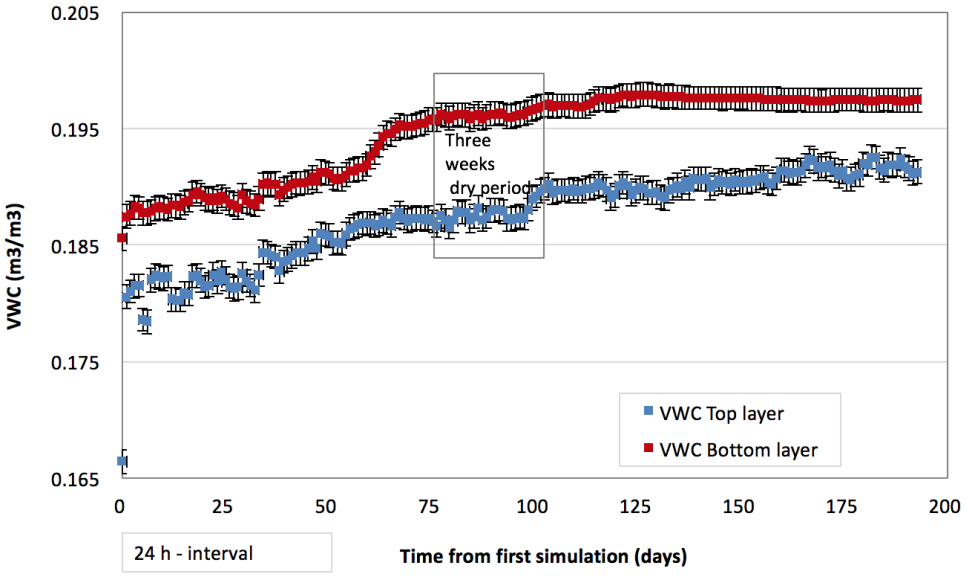

Figure 5-6: Volumetric water content (VWC) during Christmas 2013.

5.2.3 Outflow volume

A total of 120 rainfall events were applied over a 24-week period. Full details of daily outflow data can be found in (Table G - 1 to Table G - 24, in Appendix G). The outflow was monitored at 30 second intervals during the experimental period. The rig responded to the full series of the rain events. The total outflow was more than 80 % of the rainfall. It was important to divide the course of the experiment into three phases, the

initial day (first day in the experiment), the pre-sediment addition phase (days 2 to 25), and the post-sediment addition phase (days 26 to 120). Figure 5-7 illustrates the outflow volume over the period of the experiment. It also shows the general description of the outflow volume within the three phases.

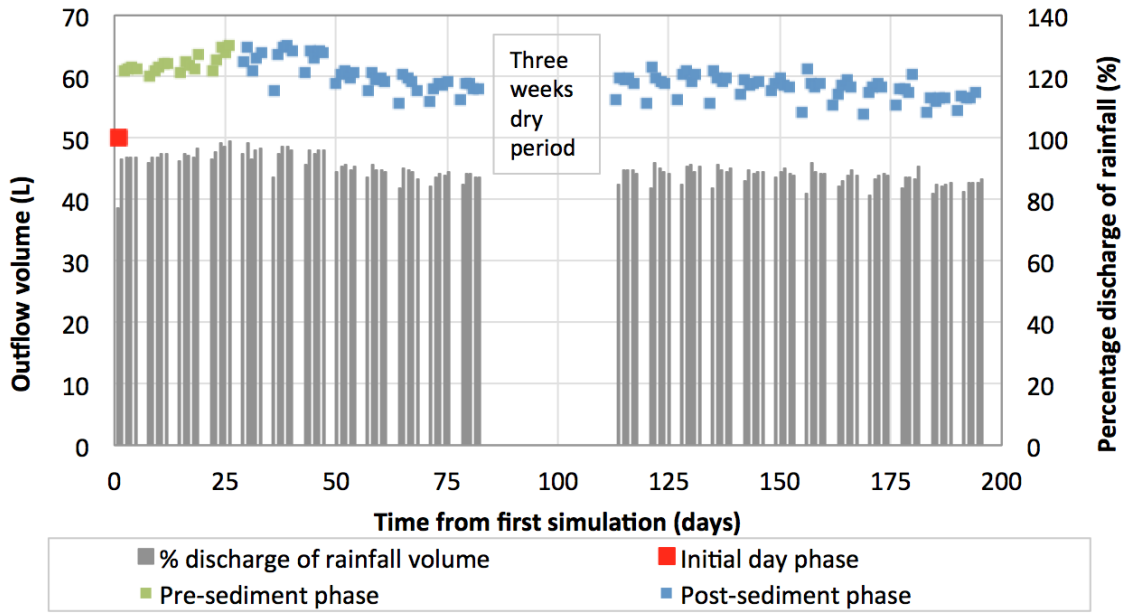

Figure 5-7: Showing outflow volume over 120 rain events and percentage discharge of rainfall, including days 6 and 7 (no rainfall).

The mass balance approach was applied to calculate the change in water volume in the rig pavement. The change in water flux in the rig pavement can be described by Equation 9 (Section 3.5.4). 120 rainfall events are used in Equation 9 to calculate the retention volume over the experimental period. Figure 5-8 shows the difference between measured and estimated retention volume within permeable pavement during the experimental period. The mass balance approach indicated significant difference in the estimated retention in the early simulations but reasonable agreement was found in the remaining simulations. In addition, the difference between estimated and measured can be also explained by the fact that the estimated retention was derived from two monitoring locations in the structure, probes located in the bottom layers of the structure. This results in a monitored saturation level throughout the structure which does not include consideration of the lower saturation level on the pavement surface. Considering the potential errors which were discussed in Section 3.6, the uncertainty level in retention volume is reasonably acceptable.

Full details of all events can be found in Table G-25 at Appendix G.

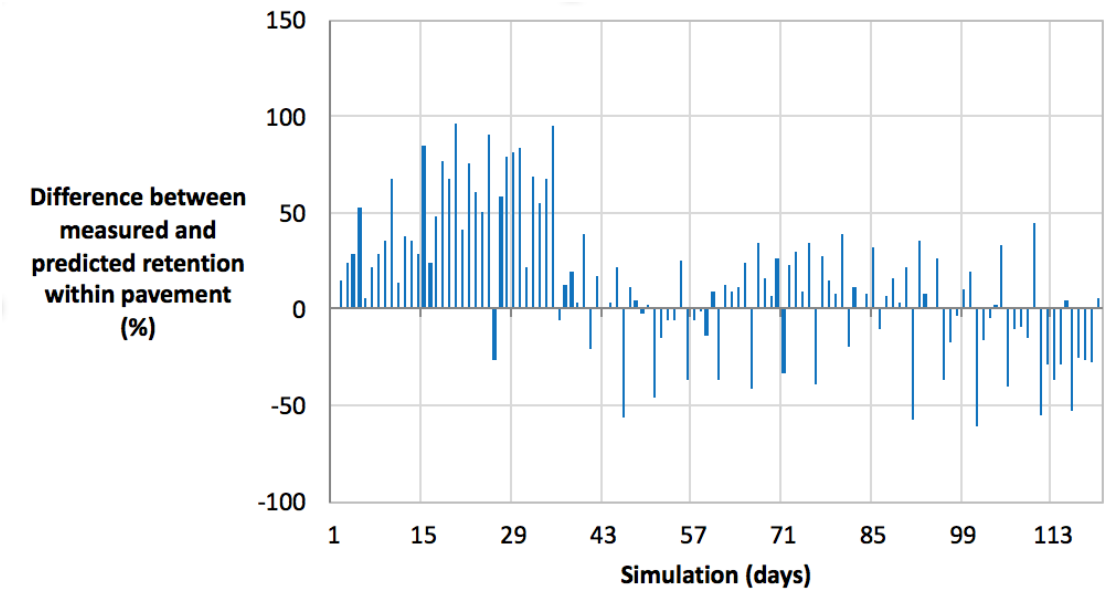

Figure 5-8: Difference between measured and predicted retention within the rig pavement.

5.2.3.1 The initial phase

The initial condition of the permeable pavement was tested during day 1. Permeable pavement initial moisture conditions have been shown to influence the attenuation capacity of the pavement during a rainfall event (Chapter 4). Therefore, on the first day of the experiment, it was important to consider the condition of the pavement and measure the pavement response to a rain event. A 71.06 L rainfall event was applied over the pavement, resulting in a pavement discharge volume of 53.90 L. The difference between inflow and outflow can be attributed to retention by the pavement material. Initial pavement moisture retention was assumed to be greater than zero; the moisture content in the subgrade was 0.166 and 0.186 (m^3m^{-3}) for top and bottom layers respectively. Therefore, the initial condition of the sub-grade was not 100% dry. Figure 5-9 shows the VWC during the first week of simulation. It is apparent that since the start of the rainfall on the first day there was a significant increase of 6.6 % in VWC in the top layers of the sub-grade. Conversely, the bottom layer showed a lower increase of 0.80 %. The results show that the bottom layer of the sub-grade was much more

saturated than the top layer. This is due to water accumulating in the bottom layer due to gravity. 0.80 % is not a significant change prior to the rain event on the first day.

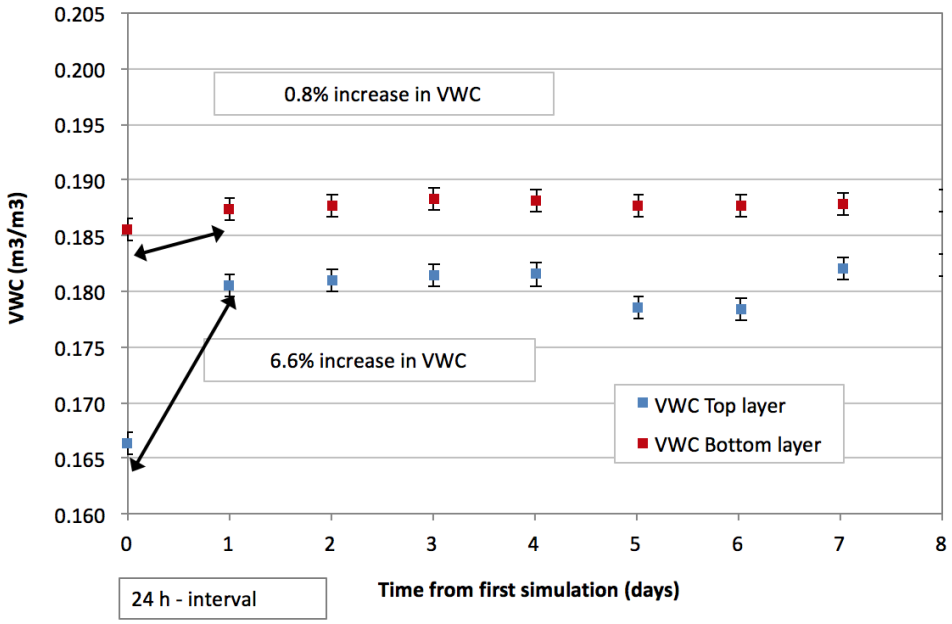

Figure 5-9: The volumetric water content at the first day (during the initial phase).

5.2.3.2 Pre-sediment Phase

This experimental phase covers the pavement performance from days 2 to 26. Figure 5-10 shows the 24 outflow volumes during this experimental period. A general trend of increasing outflow over increasing time is observed. This may be due to the fact that the pavement became more saturated. The percentage increase in outflow was 6.87 % (4.18 L) during pre-sediment phase.

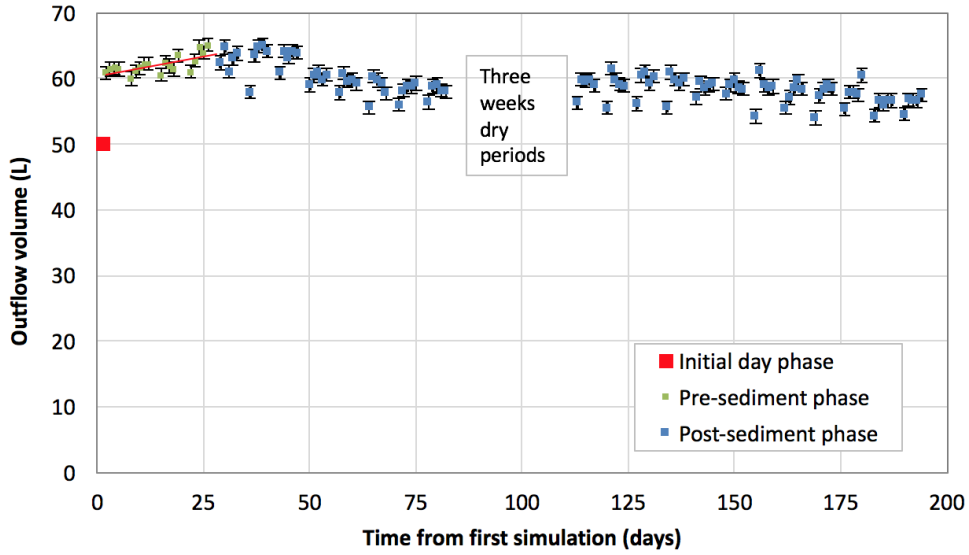

Figure 5-10: Showing outflow volume during the pre-sediment phase, including days 6 and 7 (no rainfall).

Figure 5-11 shows the VWC during the pre-sediment phase. The increase in VWC was 2.12% and 0.76% for the top and bottom layers respectively. It can be seen from the figure that the bottom layer has less variation during a rain event, because it is nearer to fully saturated conditions. The top layer has visible variation during the rain event, which is explained by continued infiltration until the pavement sub-layers reach the equilibrium point (saturation) during 24 h.

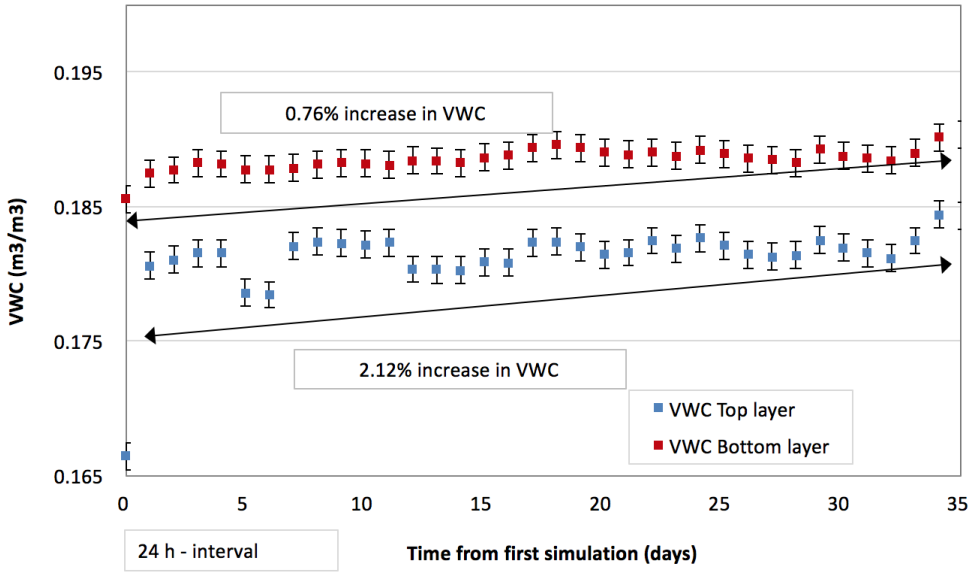

Figure 5-11: The volumetric water content of sub-grade during the pre-sediment phase.

It is possible to compare the results from the pre-sediment phase with the result from the initial phase. The bottom pavement layer had almost the same percentage change in VWC value within the two phases, i.e. 0.76% and 0.80 % for the initial phase and the pre-sediment addition phase respectively. This indicates that the change in VWC was very gradual during the pre-sediment addition. Therefore, the bottom layer of the sub-grade reached saturation earlier in the pre-sediment addition phase. The top layer VWC increased by 2.12 % within the pre-sediment addition phase, compared with 6.6 % during the initial phase (first day simulation). This indicates that the change in VWC was very slow. It can be seen that the pavement reached the partially saturated condition during the pre-sediment addition phase.

5.2.3.3 Post-sediment Phase

The pavement reaction to all 95 rainfall events, occurring post sediment addition, were recorded and analysed. Figure 5-12 illustrates the outflow volume during the post-sediment addition phase.

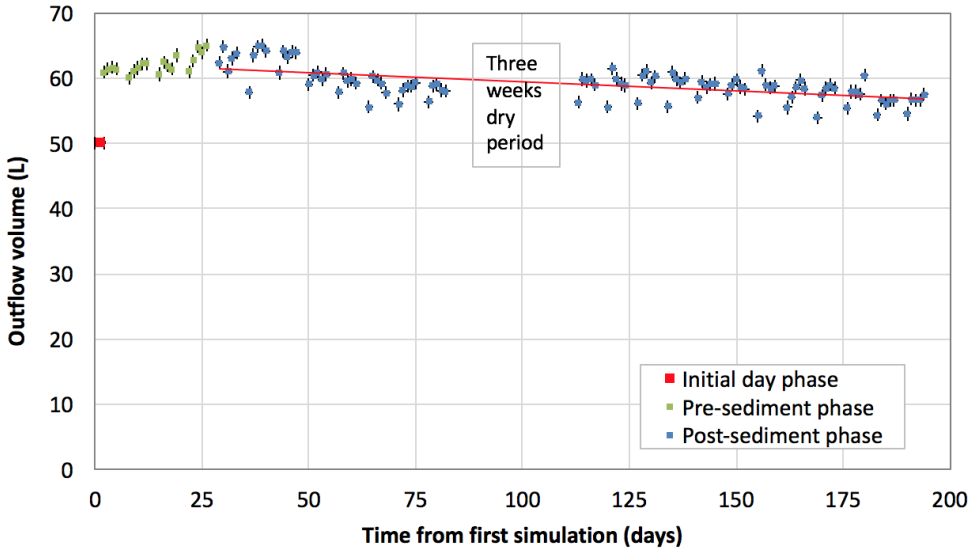

Figure 5-12: Showing outflow volume during the post-sediment phase, including days 6 and 7 (no rainfall).

Table 5-3 details the annual average outflow volume during the simulation of a year of rainfall events. To compare the outflow reduction before and after the application of sediment, the average percentage difference in outflows were calculated for each year of

simulation. Table 5-3 also gives the percentage reduction over a ten year simulation. In this case, it can be seen that the reduction in internal rainfall retention started after year 4 (equal to the second year of sediment simulation). The percentage reduction was based on the first outflow volume of year 1 simulation (65.17 L).

Table 5-3: Analysis of the results for outflow volume over the 12 years of the simulation

Year simulation	Average outflow per year simulation (litres)	Standard error	Percentage reduction (%)
1	65.17	1.30	0.00
2	67.80	0.59	-4.04*
3**	68.35	0.77	-4.88*
4	66.74	0.71	-2.41*
5	63.75	0.51	2.18
6	62.89	0.48	3.50
7	63.76	0.64	2.16
8	64.03	0.69	1.76
9	63.47	0.37	2.61
10	62.91	0.76	3.47
11	62.46	0.80	4.16
12	61.01	0.56	6.38
* The negative values mean that the outflow was more than the initial outflow (65.17 L) during the first stage of the experiment. ** The addition of sediment started from year 3.			

In general, the outflow volumes show a declining trend over time. The reduction of outflow volume was attributed to depleted infiltration capacity within the pavement voids. In other words, the volume reduction observed was comparable to the increase in VWC. The results given in Table 5-4 show that the percentage increases in VWC monitored by the top and bottom probe were 6.91 % and 5.36% (respectively), which have the same magnitude of value when compared with the results from the average outflow reduction (Table 5-3). Figure 5-13 and Figure 5-14 show the relationship between the outflow reduction and the VWC for the top and bottom layer, respectively. They shows highly significant ($p>0.01$) moderate correlation. It can be seen that there is a positive correlation between outflow and VWC before the addition of sediment ($r = 0.641$ and 0.637 for the top and bottom layer, respectively). Conversely, the relation

became negative after the addition of sediment (r = -0.609 and -0.559 for the top and bottom layer respectively). It can be explained that the change in relationship type was attributed to the addition of sediment.

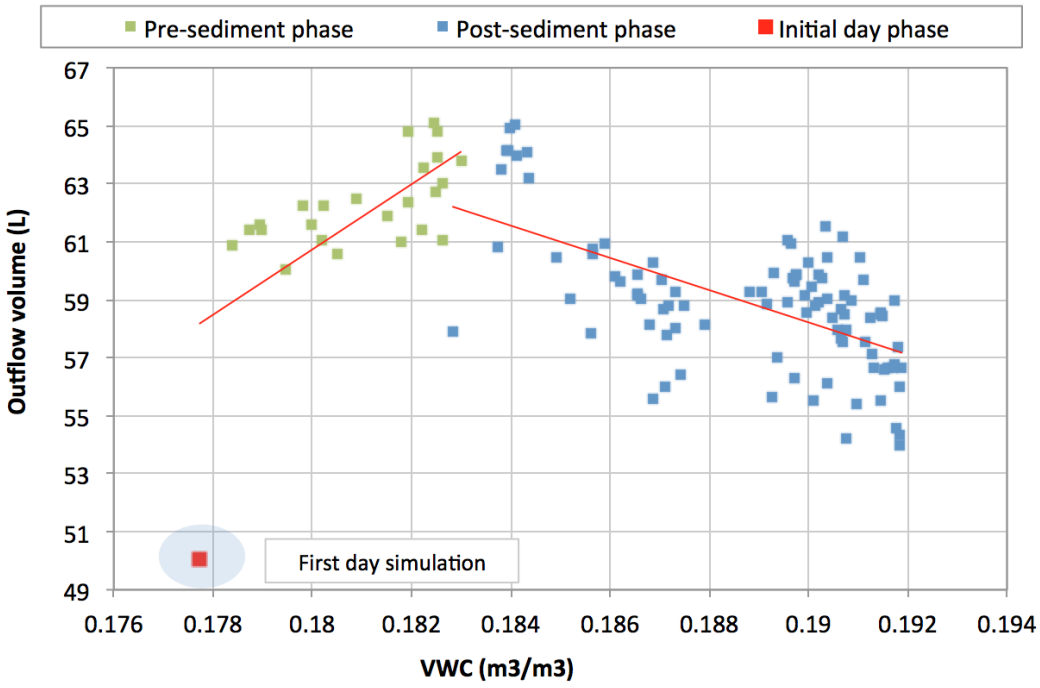

Figure 5-13: Showing correlation relationship between outflow volume and VWC top layer.

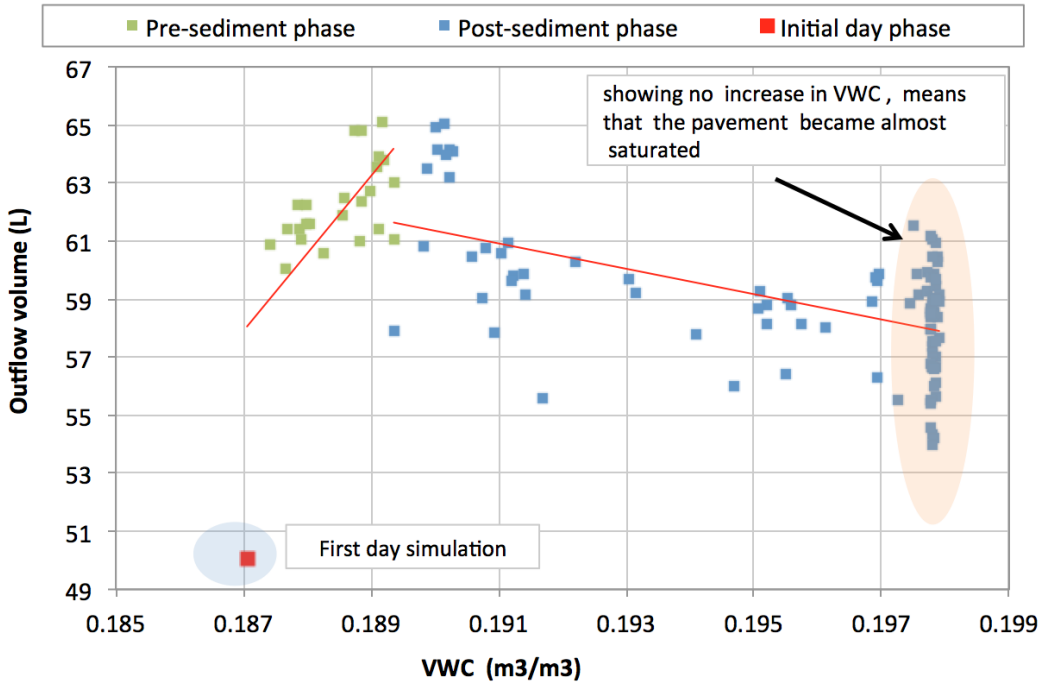

Figure 5-14: Showing correlation relationship between outflow volume and VWC bottom layer.

Table 5-4: VWC results over the 12 years of the simulation

Year simulation	Increase in VWC Top layer (%) since initial condition of VWC	Increase in VWC Bottom layer (%) since initial condition of VWC	Standard error VWC Top layer	Standard error VWC bottom layer
1	0.00	0.00	2.64×10^{-04}	9.68×10^{-05}
2	1.49	0.59	2.28×10^{-04}	9.82×10^{-05}
3	2.14	0.95	2.62×10^{-04}	1.60×10^{-04}
4	3.12	1.48	2.70×10^{-04}	1.56×10^{-04}
5	4.06	2.26	1.67×10^{-04}	3.47×10^{-04}
6	4.46	4.07	1.15×10^{-04}	1.29×10^{-04}
7	5.90	5.03	1.07×10^{-04}	9.58×10^{-05}
8	5.79	5.36	1.65×10^{-04}	2.15×10^{-05}
9	6.16	5.38	1.29×10^{-04}	1.56×10^{-05}
10	6.55	5.36	1.32×10^{-04}	8.91×10^{-06}
11	6.69	5.35	1.52×10^{-04}	7.86×10^{-06}
12	6.91	5.36	7.57×10^{-05}	7.93×10^{-06}

Figure 5-15 shows the VWC during the post-sediment addition. The increase in VWC was 5.25 % and 4.86 % for the top and bottom layers respectively, for the period of post-sediment monitoring. The top layer consistently showed a greater increase, due to its dryer initial condition. However, during the period of the experiment, the percentage increase was equal for both layers. This means that both layers reached the same partially saturated condition relative to their starting conditions. The equal percentage increase indicates that the top layer of the sub-grade became partially saturated to the same degree of saturation as the bottom layer. This is important because the both layers became surrounded by the same amount of water over time, which means the retention volume in the pavement was increasing.

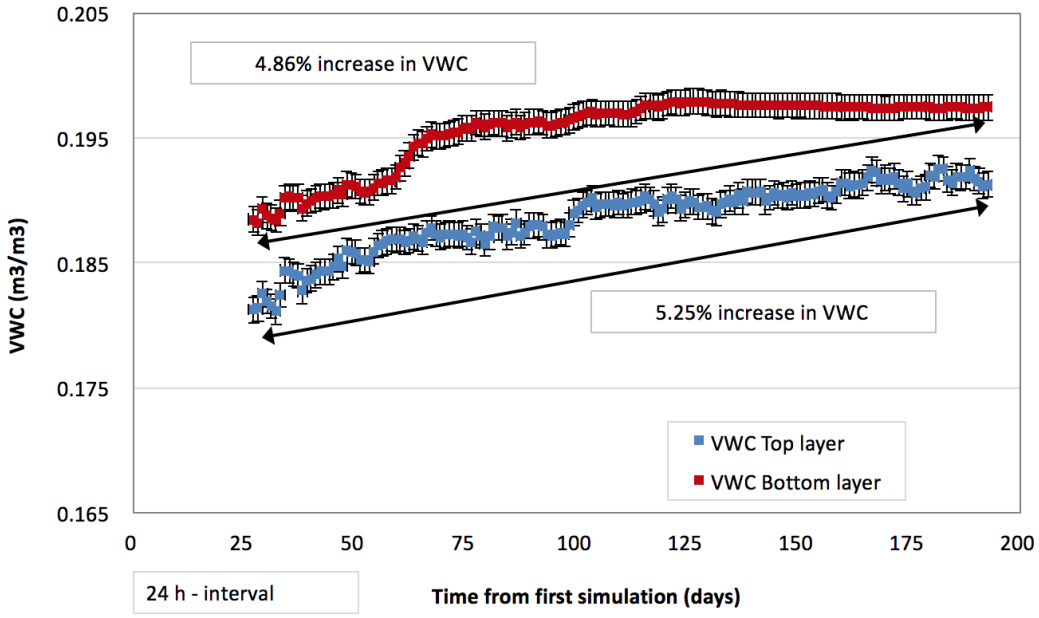

Figure 5-15: The volumetric water content of the sub-grade from day 27 to 120 (during the post-sediment phase).

In general, the outflow has a tendency to decline over time as a result of sediment addition to the pavement surface. A significant reduction can be seen following the addition of sediments. The average reduction in outflow over the 12-year simulation was 6.4 %. The impact of adding sediment was most evident in the fifth year of the simulation (equivalent to the third year of sediment simulation). The reduction of outflow volume was a result of the build-up of water content (VWC) over time. The volume reduction observed was comparable to the increase in VWC. The results show that the percentage VWC increase in the bottom layer was 5.36 %. Table 5-4 presents the statistical analysis of the outflow volume and VWC, top and bottom. It illustrates that there is a significant positive relationship between outflow volume and VWC. The correlation between the outflow and VWC suggests a relationship between the addition of sediment and the hydrologic performance of the pavement.

5.2.4 Outflow duration

The outflow duration was defined as the period of time the pavement takes to discharge a single rain event. In this study, the outflow duration was monitored from the start of the experiment. For a single rain event, the outflow duration was measured from the start of the outflow and continued until the outflow cessation. Over the monitoring period of the experiment, 120 outflows were generated during the experimental period.

Full details of the outflow durations can be found in (Table H - 1 and Table H - 2, in Appendix H).

5.2.4.1 Short term outflow duration

Figure 5-16 illustrates the average outflow duration for days 1 to 5 of the experimental period. The results show that the outflow duration increased for all rainfall events, after adding sediment. During the pre-sediment phase, days 2 to 5 shows a gradual increase gradually in outflow duration from the first day, up to 10%. Therefore, the observed increase is associated with the retention volume (water retained in the structure) increasing over days. This would also explain the increase in volumetric water content (VWC), as discussed in Section 5.4.2. It is interesting to note that a similar observation was observed in the hydrology experiment – Chapter 4.

On the other hand, the outflow duration also increased gradually from days 2 to 5 during the post-sediment phase. But the observed increase in outflow duration during this phase was less than in the pre-sediment phase. This is related to the structure becoming more saturated during the post-sediment phase.

Figure 5-16 shows the percentage change between the two phases. The results show that the percentage increases in outflow duration were 25.9%, 25.2%, 24.9%, 24.2 and 24.0% for days 1 to 5 respectively. It can be concluded that the increase in outflow duration by 2.2 hours can be associated within the addition of sediment to the pavement surface.

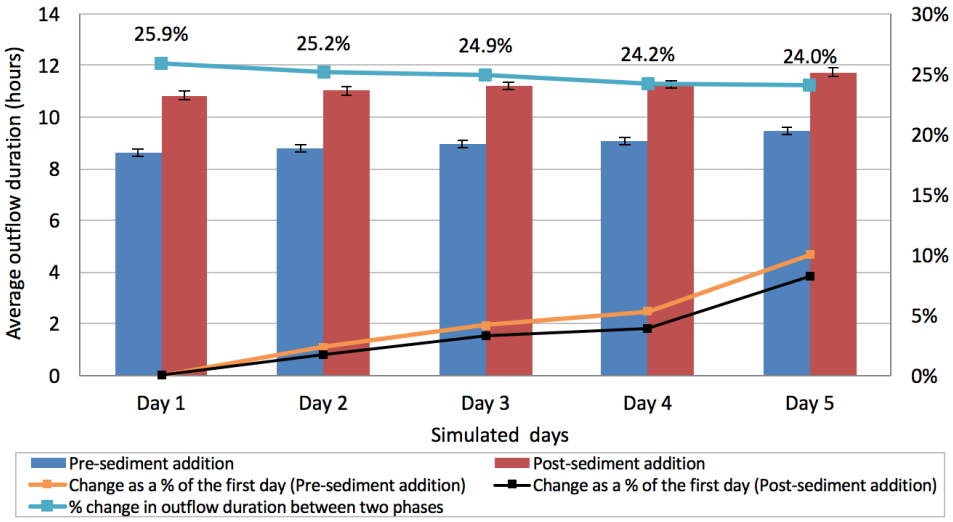

Figure 5-16: Showing average outflow duration from days 1 to 5 during two phases (pre/post-sediment addition).

5.2.4.2 Long term outflow duration

Figure 5-17 illustrates in detail the daily outflow duration over the period of the experiment of period. The results show an increase in the outflow duration after the addition of sediment. They show that the change in outflow duration started from day 65 (equivalent to the third year of sediment simulation). It is interesting that there is only a very small drop in outflow duration due to the Christmas break.

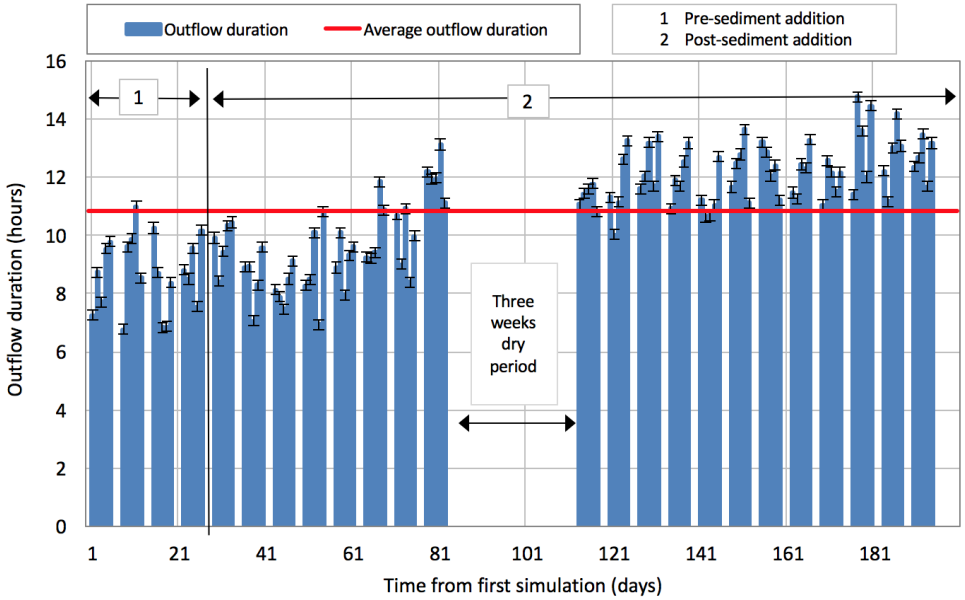

Figure 5-17: Showing daily outflow duration over the experimental period and the average outflow duration.

Figure 5-18 demonstrates the change as a percentage of the total average outflow duration. It can be seen that the total outflow percentage increased during the period of the experiment, as the outflow duration became prolonged over time. This agrees with the the results in Figure 5-17 where the change in outflow duration was observed from day 65. This indicates a general increase in outflow duration, which shows the influence of the sediment on the outflow duration. After the addition of sediment, the outflow duration ranged between 6.94 and 14.76 hours with an average of 10.73 hours (Std Dev. 1.76h).

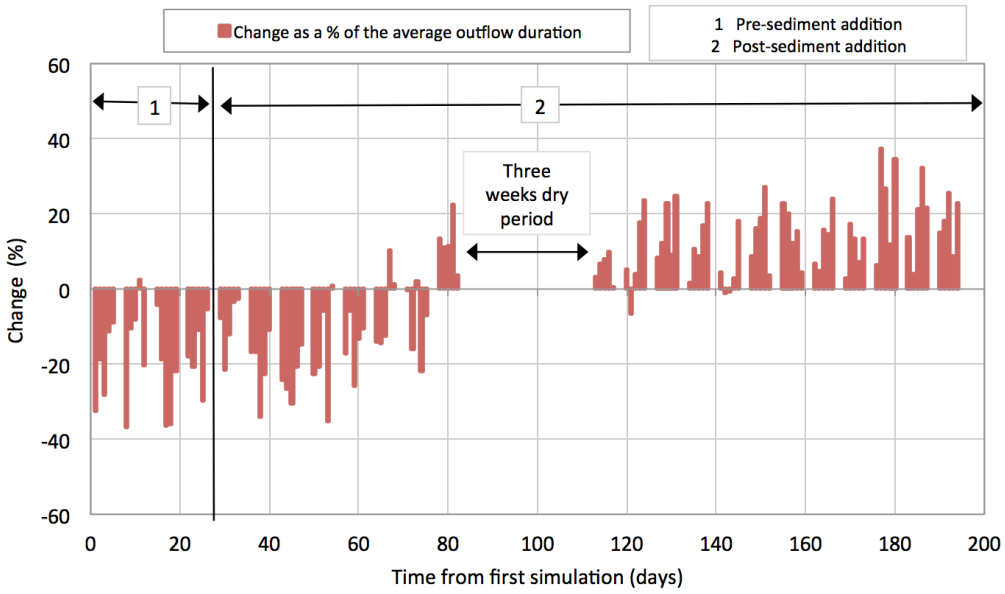

Figure 5-18: Showing the change as a percentage of the average outflow duration.

Over the total monitoring period, the pavement became partially saturated and the wet condition minimised the travel time through the structure. Axiomatically, during wet conditions the duration of outflow would be also minimised, unless an obstruction developed within the structure voids. However, for all events, the duration of outflow was positively correlated to volumetric water content. Figure 5-19 illustrates that the increase in the outflow duration is associated with the increase in volumetric water content. This means that the outflow duration and VWC increased simultaneously over time, from which it can be inferred that the sediment affected the void space in the structure.

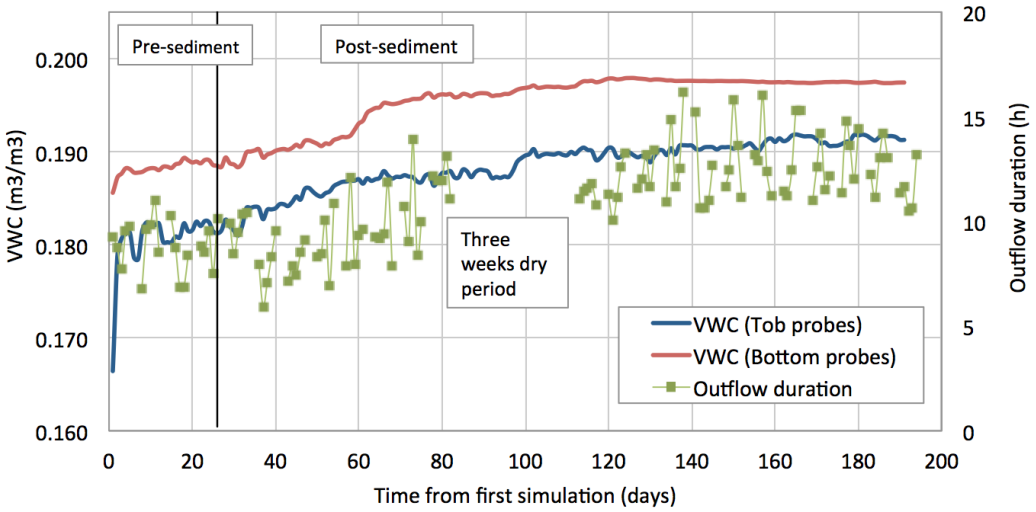

Figure 5-19: 120 Outflow duration events and the top and bottom VWC of the sub-grade over 120 days.

The above analysis provides evidence of increasing outflow duration over the experimental period. This fact shows that the hydrological performance of the permeable pavement was significantly affected by the sediment.

5.2.5 Start delay to discharge

The start delay is defined as the time required for the rainfall to permeate through the pavement structure until it reaches the free drainage point. In this study, there are three phases of start delay, each dependent on the condition of the permeable pavement material. The conditions were; (1) the initial condition is when the rig is almost dry; (2) the condition of the rig before day 1 simulation, when the rig is relatively dry; (3) the condition of the rig between days 2 to 5 inclusive (when it is wet). Therefore, the conditions of the rig are subject to three different start delay times. Due to the lengthy process of drying out the rig in the laboratory, it was difficult to study the initial conditions when measuring start delay. Therefore, day-1 and wet conditions are analysed and discussed. Full details of the start delay time during the three phases can be found in (Table I - 1 and Table I - 2, in Appendix I).

5.2.5.1 Short-term start delay time

The rig was exposed to dry periods extending over two consecutive days per week (the weekend) over the 24 week simulation. The dry two days decreased the moisture content within the pavement. However, although the reduction in the volumetric water content cannot be seen as a significant value during the weekly observation, it had a significant impact on the start delay in comparison with wet conditions.

Figure 5-20 illustrates average start delay from days 1 to 5 over the 24 week simulation. The figure also shows the two phases before and after adding sediment, including the percentage change in start delay between the two phases. During pre/post-sediment addition, all phases show that the change in start delay from day 1 to day 5 decreases over consecutive rainfall events. Therefore, the observed decrease is associated with the detention volume (water detained in the structure), the start delay time decreased when the pavement got wet.

Figure 5-20 also shows the percentage change between two phases. The results show that the percentage decreases were 17.7%, 6.0%, 5.6%, 6.4 and 7.3% for days 1 to 5 respectively. The start delay was larger during the post-sediment phase. It can be shown that the sediment influences the start delay time by affecting the void space in the structure.

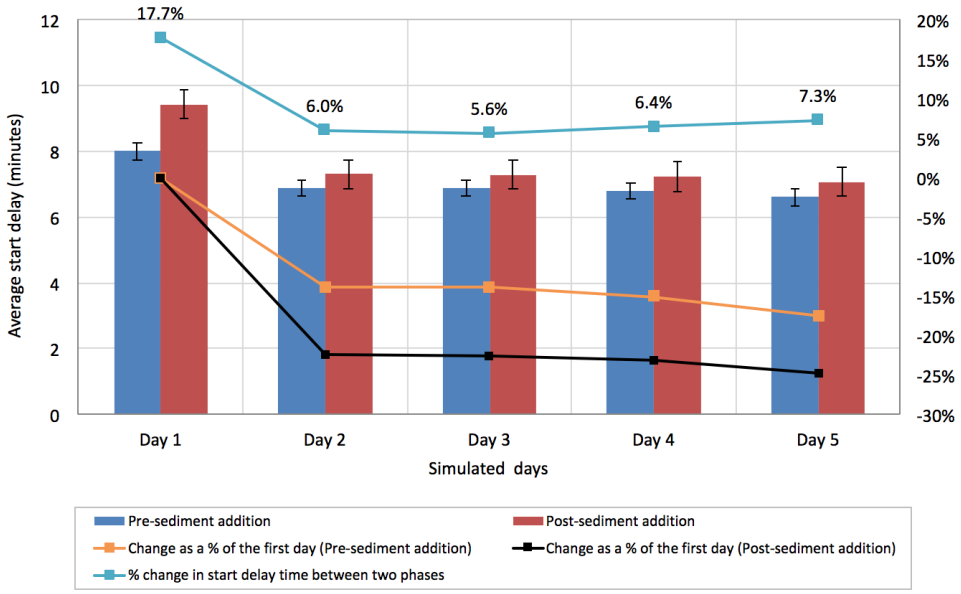

Figure 5-20: Average start delay from day 1 to 5 during two phases (pre/post-sediment addition).

5.2.5.2 Long-term start delay time

It was expected that the start delay would be longer for day 1 simulations, because they would have been dependent on the initial condition of the pavement and the rain event characteristics. The initial condition of the volumetric water content was found through monitoring over the three hours prior to starting the experiment; 0.168 and 0.188 (m^3m^{-3}) for the top and bottom layers respectively. On the same day, the rain event lasted 165 minutes and the pavement was able to discharge 75.85 % of the rainfall. Figure 5-21 shows the start delay at three phases (initial day phase, pre-sediment addition, and post-sediment addition). The longest start delay time over the period of the experiment was found to be 23 minutes (day 1).

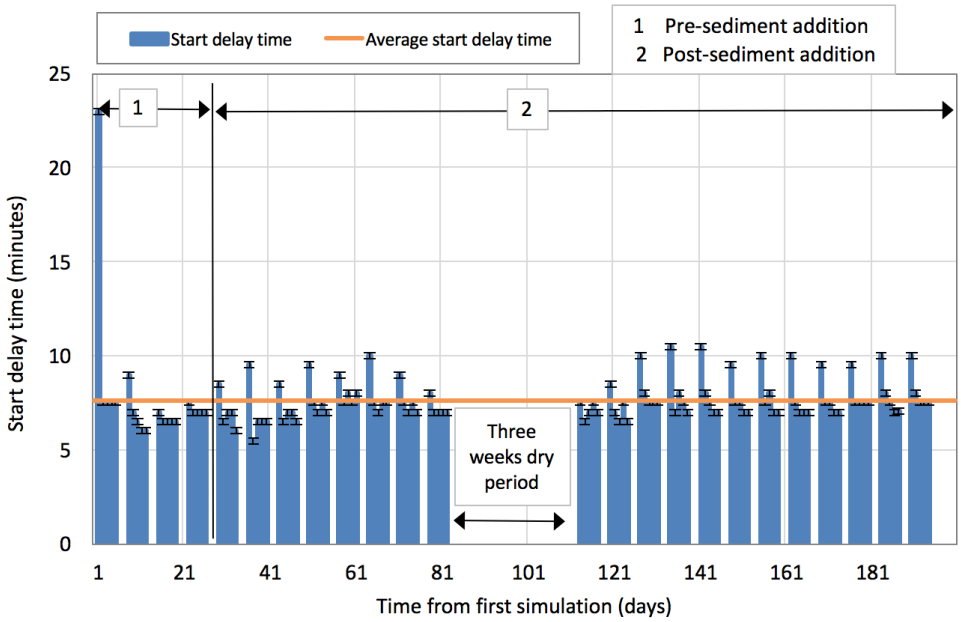

Figure 5-21: Showing daily start delay over experimental period, including longest start delay.

Figure 5-21 indicates a general increase in start delay time, which shows the influence of the sediment on the start delay results. The start delay time ranged between 5.5 and 10.5 minutes, with an average time of 7.66 minutes (SD dev. 1.05mins). It is clear that the addition of sediment affected the discharge start delay time. Figure 5-22 shows the change in start delay as a percentage of the average start delay within 120 events. As in Figure 5-21, it is obvious that the positive change occurred more noticeably after adding

sediment. This analysis provides evidence of the increase of the start delay due to the influence of sediment on the pavement over the experimental period.

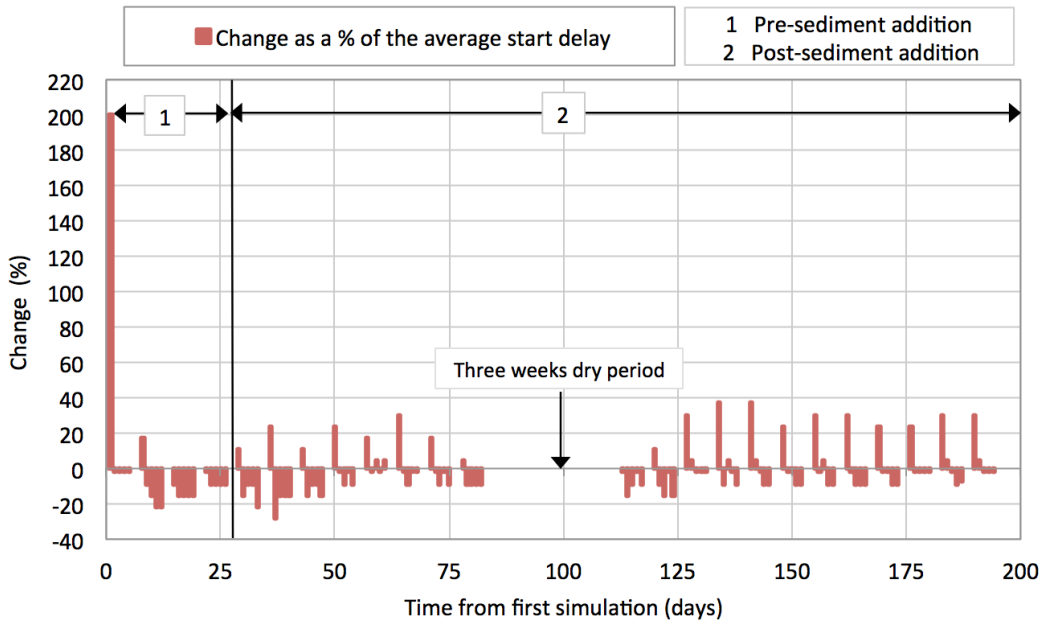

Figure 5-22: Showing the change as percentage of the average start delay.

5.2.6 Outflow rate

The outflow rates were monitored continuously at 30 second intervals. It was difficult to present all 120 outflow curves in a single graph so outflow curves have been separated into categories according to simulation year. Thus, Figure 5-23 to Figure 5-34 provide the entire range of outflows within the 12 year simulation. Each figure presents one year of simulation, including two cycles of rainfall. These figures represent outflow rates within the first 30 minutes of each rainfall event.

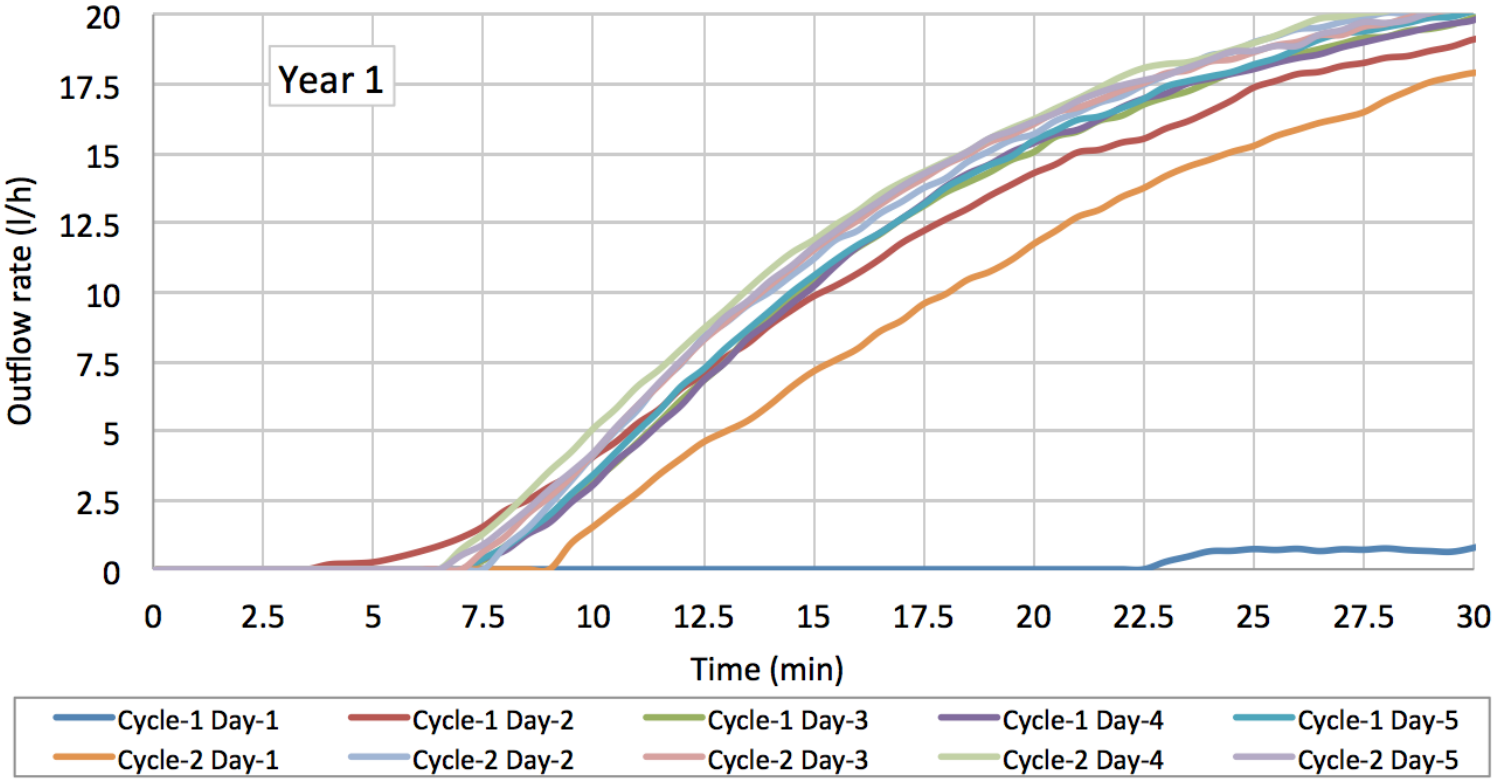

Figure 5-23 : Outflow rates during the first 30 minutes, showing the outflow for each 5-day cycle per year of simulation – Year 1.

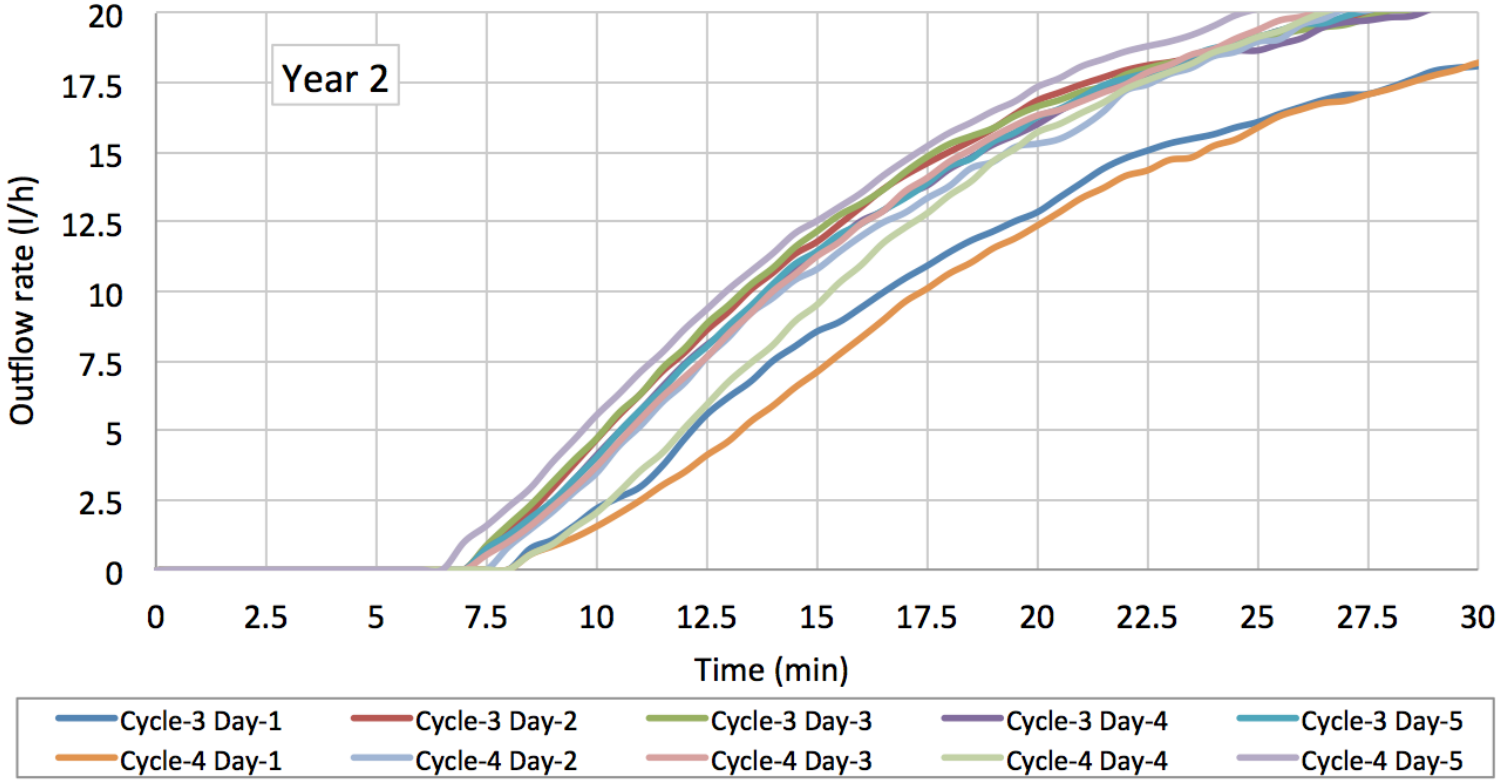

Figure 5-24: Outflow rates during the first 30 minutes, showing the outflow for each 5-day cycle per year of simulation – Year 2.

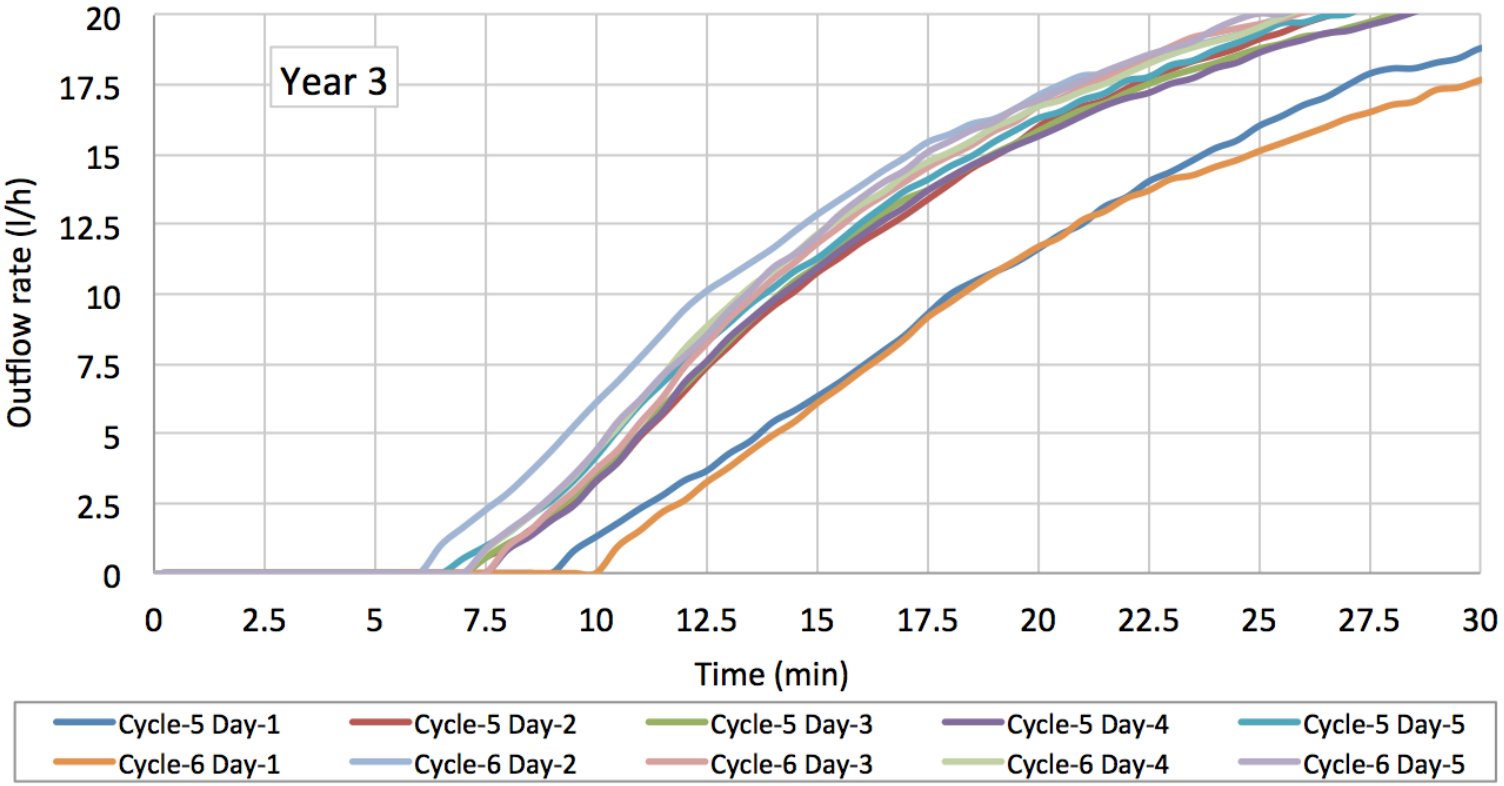

Figure 5-25: Outflow rates during the first 30 minutes, showing the outflow for each 5-day cycle per year of simulation – Year 3.

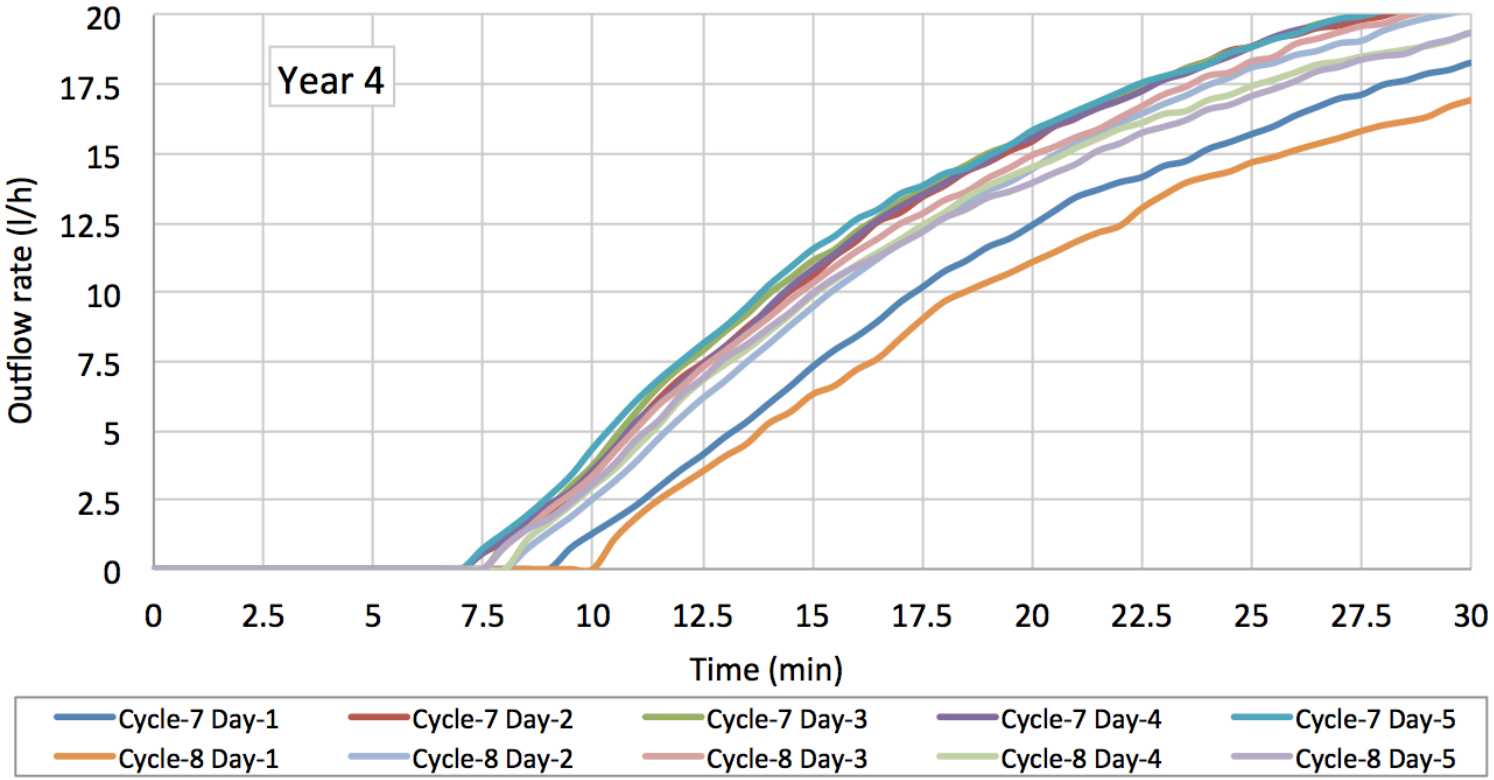

Figure 5-26: Outflow rates during the first 30 minutes, showing the outflow for each 5-day cycle per year of simulation – Year 4.

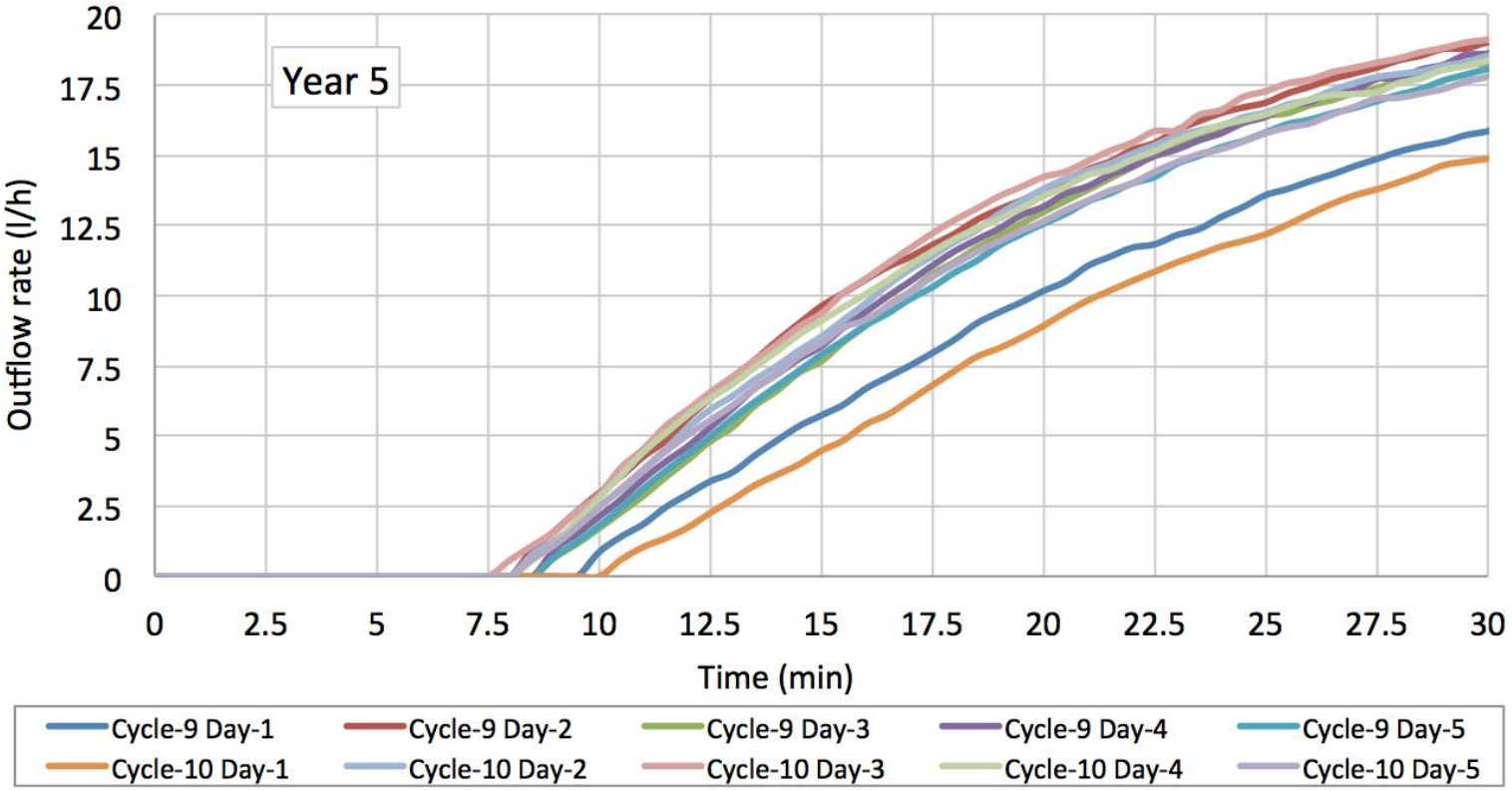

Figure 5-27: Outflow rates during the first 30 minutes, showing the outflow for each 5-day cycle per year of simulation – Year 5.

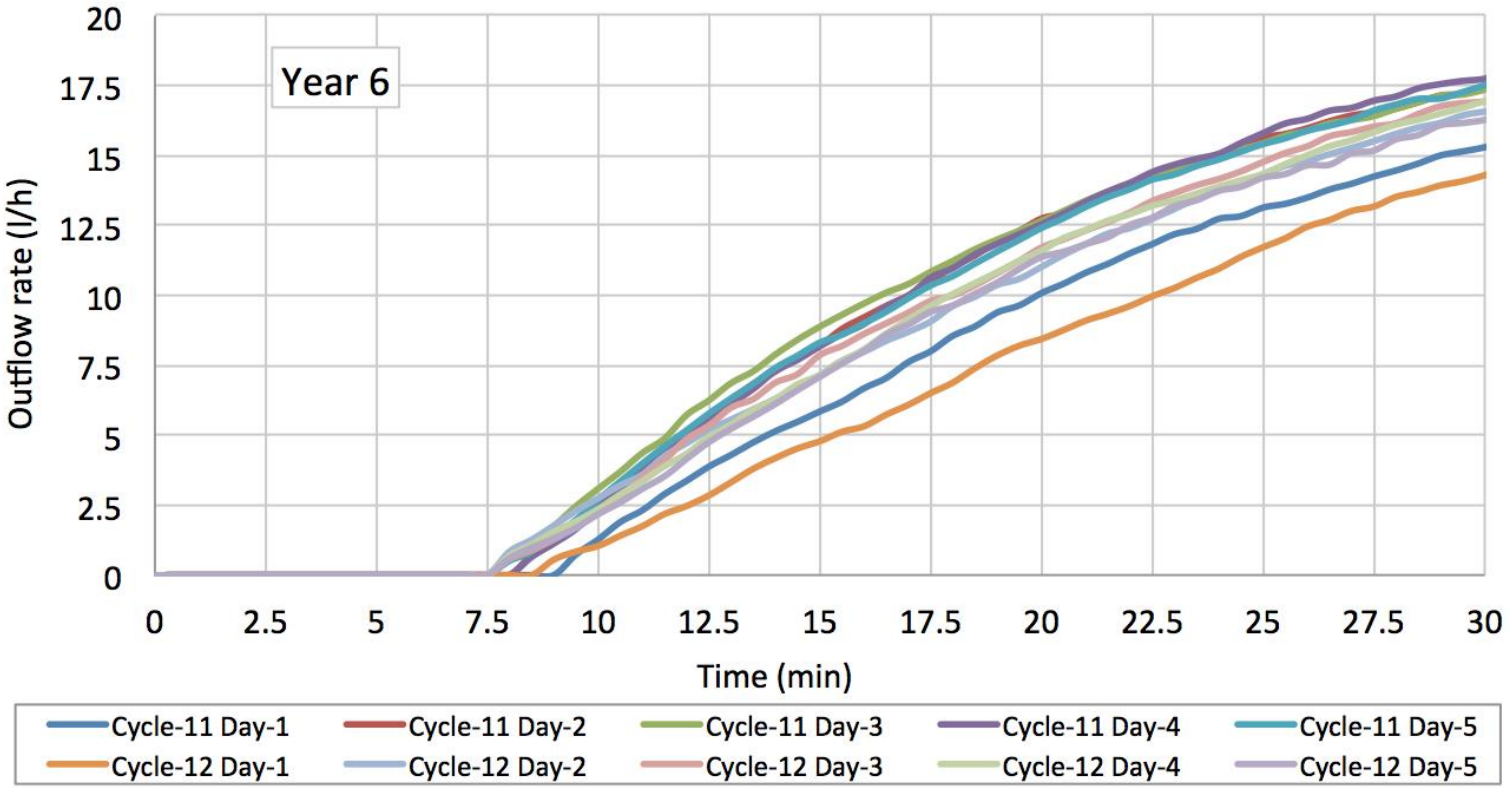

Figure 5-28: Outflow rates during the first 30 minutes, showing the outflow for each 5-day cycle per year of simulation – Year 6.

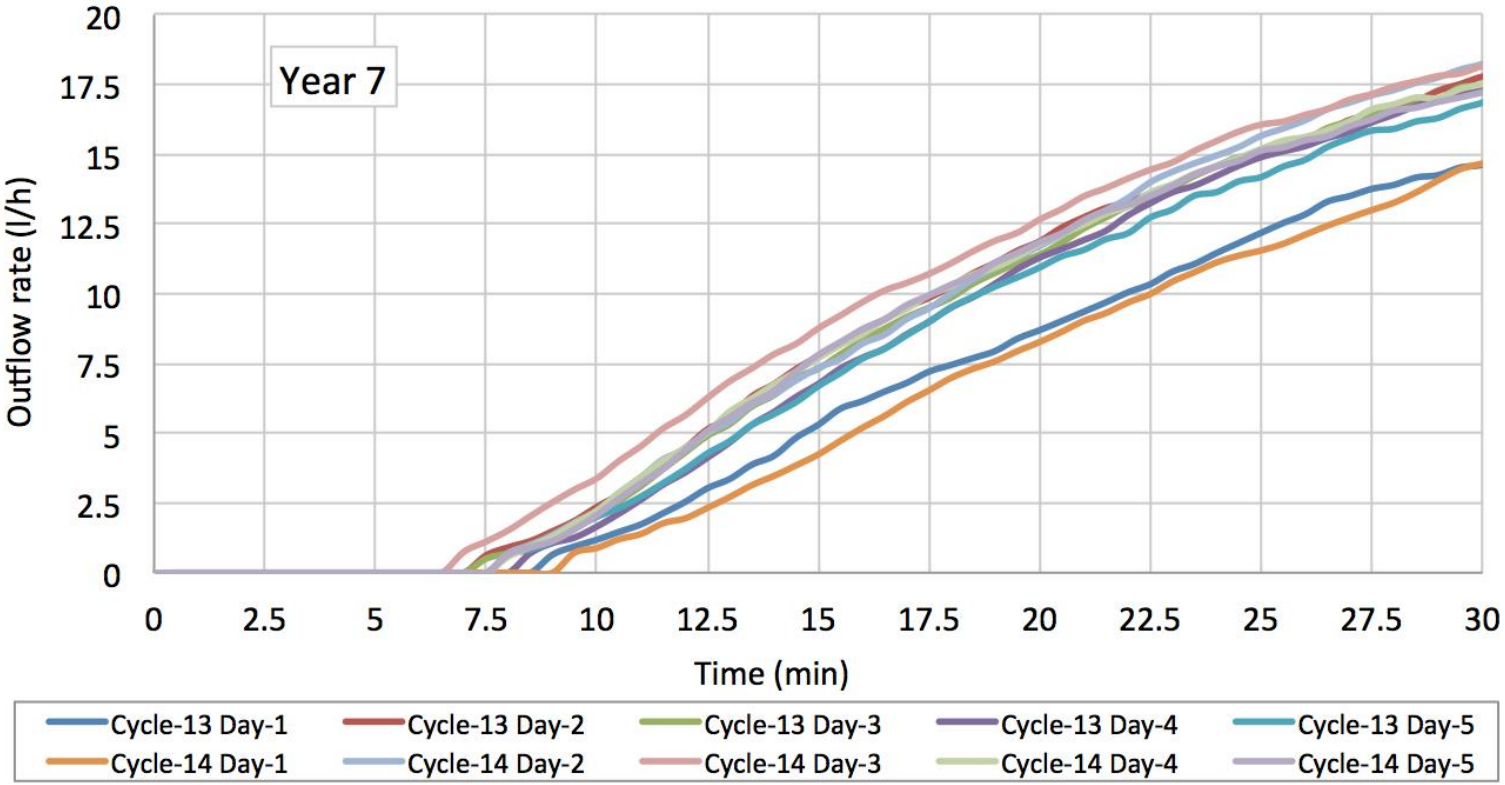

Figure 5-29: Outflow rates during the first 30 minutes, showing the outflow for each 5-day cycle per year of simulation – Year 7.

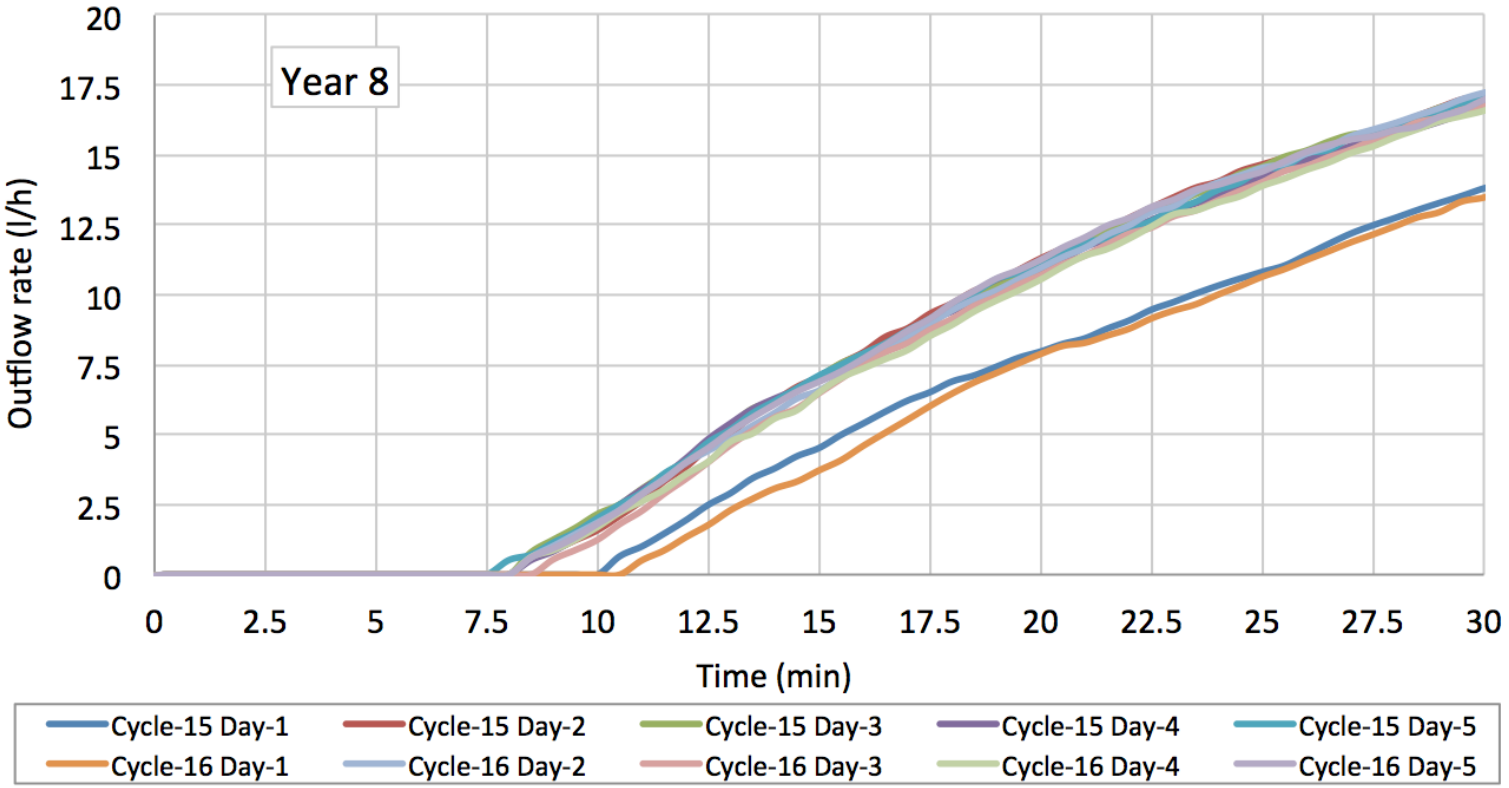

Figure 5-30: Outflow rates during the first 30 minutes, showing the outflow for each 5-day cycle per year of simulation – Year 8.

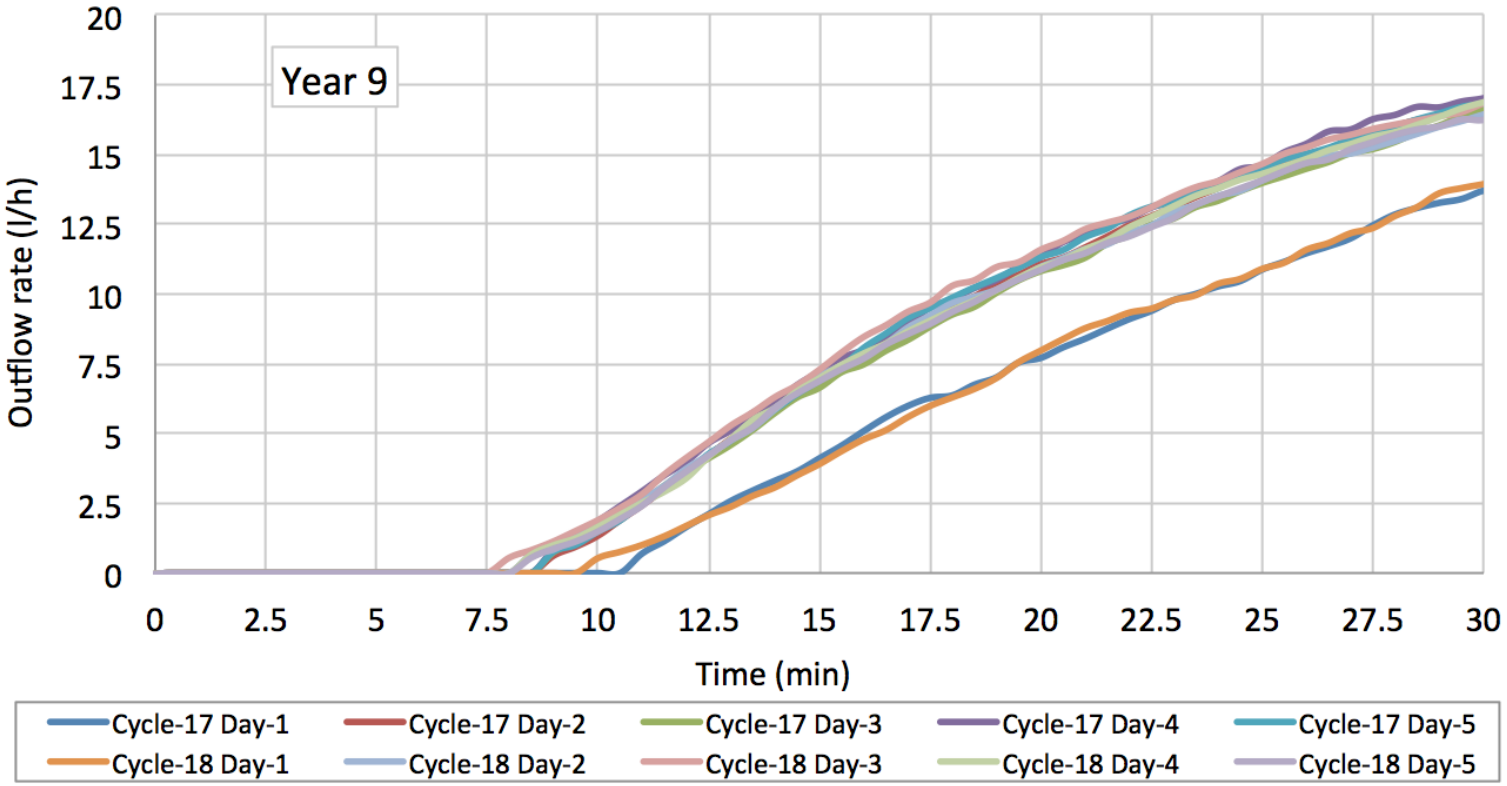

Figure 5-31: Outflow rates during the first 30 minutes, showing the outflow for each 5-day cycle per year of simulation – Year 9.

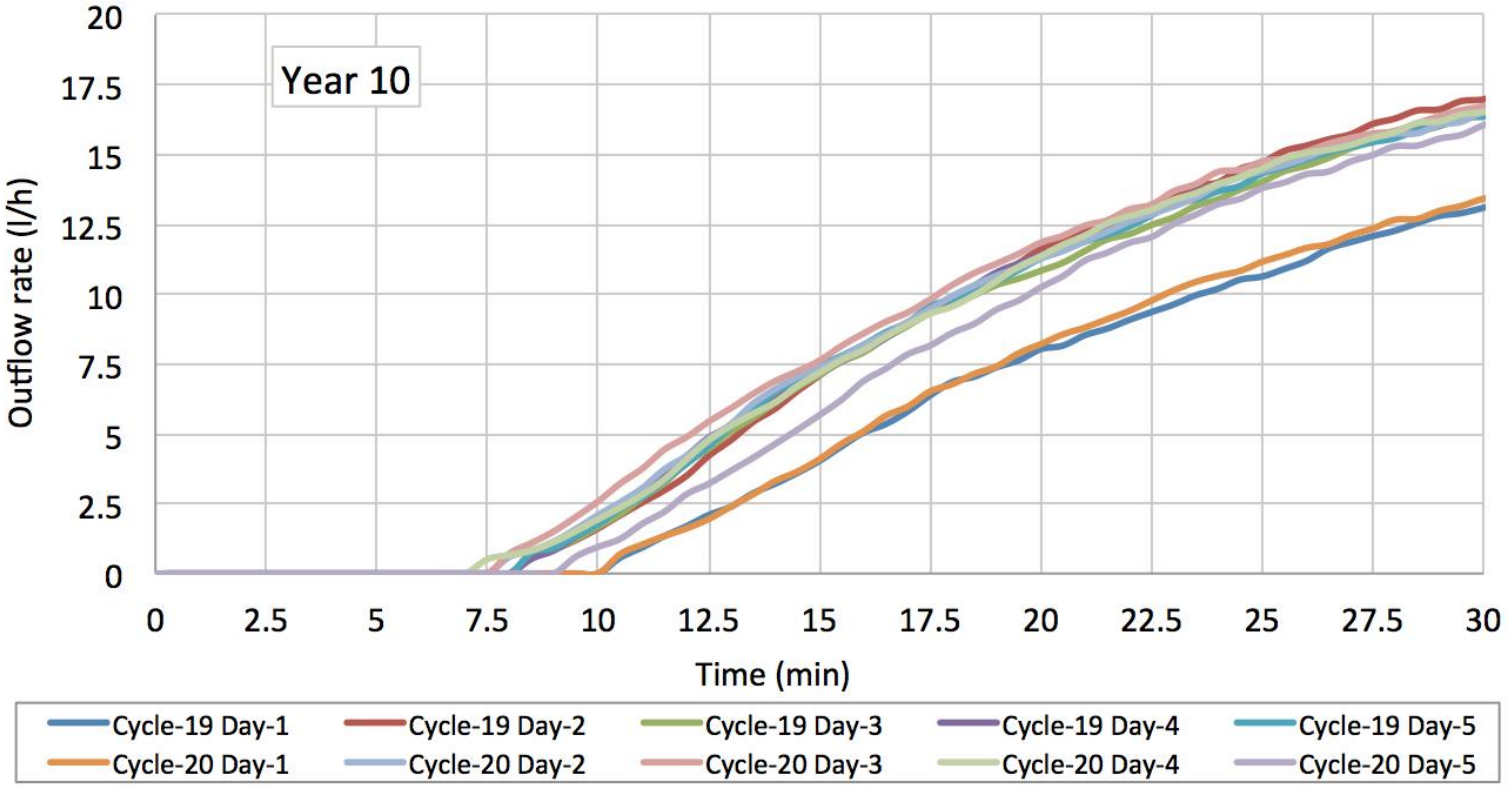

Figure 5-32: Outflow rates during the first 30 minutes, showing the outflow for each 5-day cycle per year of simulation – Year 10.

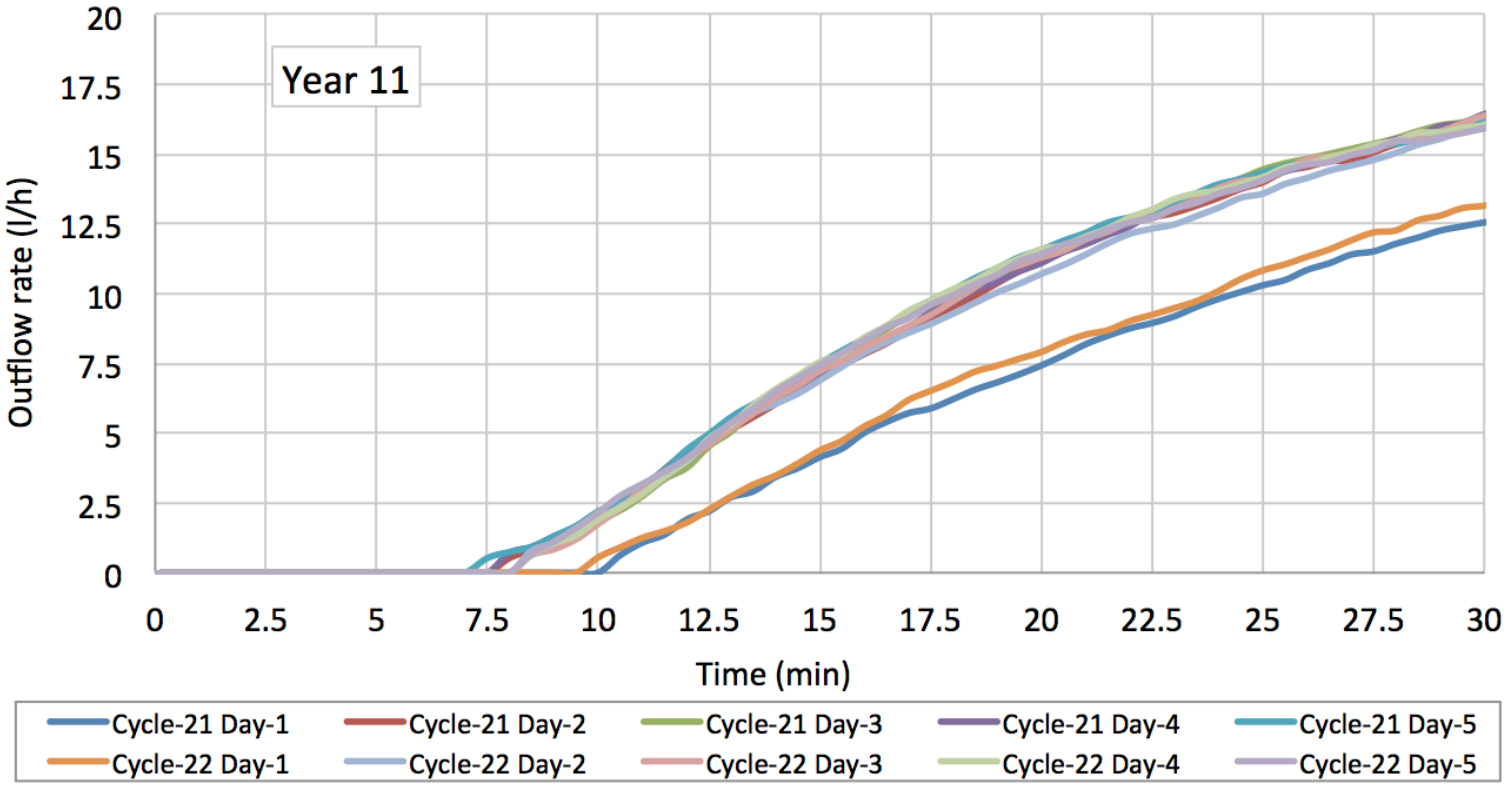

Figure 5-33: Outflow rates during the first 30 minutes, showing the outflow for each 5-day cycle per year of simulation – Year 11.

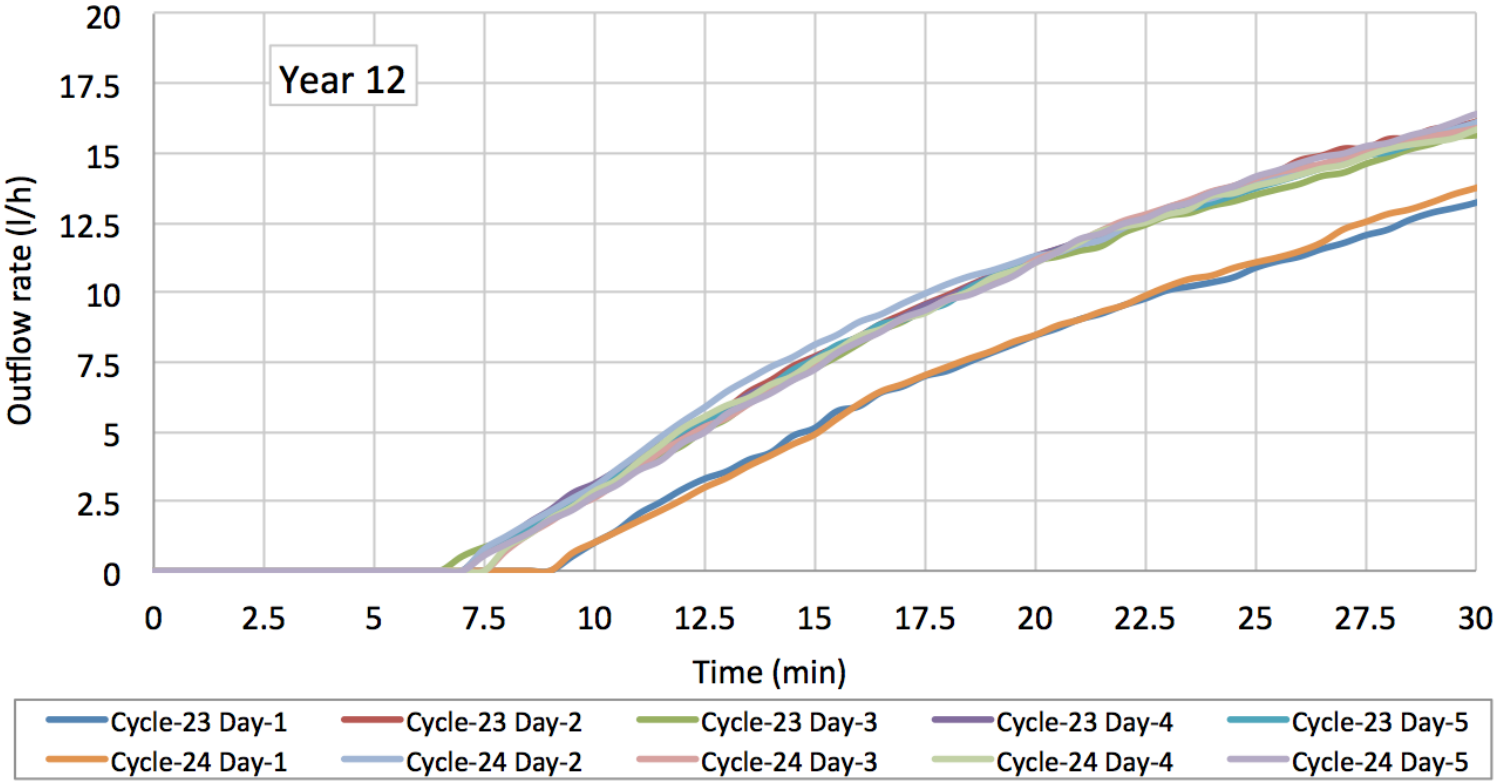

Figure 5-34: Outflow rates during the first 30 minutes, showing the outflow for each 5-day cycle per year of simulation – Year 12

Year 1 data shows a shallow delayed curve (Week1, day1), which represents the outflow rate on the first day of the experiment (see Figure 5-23). Presented in the same graph, the outflow curve represents the outflow from the first rain event of the second rain cycle (Week2, day1). The remaining graphs illustrate that there are consistently two shallower curves, which represent the outflow rate on the first day of the rain event cycle. Day 1 of the rain cycle shows the lowest outflow rates because the rig was exposed to two dry days prior to the day 1 simulations. Thus, the two dry days influenced water movement through the pavement structure. In contrast, the other days show higher outflow rates. This is due to the wet structure initial condition prior to rain events commencing, and therefore a lower void capacity to attenuate runoff.

Sediment was added to the rig during year 3. Following the addition of sediment there was a change in the outflow rate in year 5 (equivalent to the third year of sediment simulation). The results show that the outflow rates started to decrease as a result of the sediment's impact on the movement of the water through the structure. There was a 6.4% reduction in outflow over a 12 year period. The attenuation reduction commenced in year 5 and continued to increase until year 12.

5.2.7 Sediment/infiltration monitoring

5.2.7.1 Concentration of Suspended Solids

The pavement was constructed 15 months prior to the start of the sediment experiments. During this period, the pavement was subjected to a number of rain events that allowed the internal sediments to be washed out from the structure. Therefore, the early discharge volume had a relatively high level of sediments, which were particles derived from the pavement layers (that is, from the internal structure of the pavement rather than from sediment addition to the pavement surface). Unfortunately, there were no records of the sediment level in the period directly after structure completion, due to the unavailability of the equipment at that time. However, even after the initial washout phase, it may be that the pavement still discharged a small volume of internal sediment.

Table 5-5 shows the statistical data for monitoring SS during the experimental period. It is obvious that during early sampling runs, the average suspended solid concentrations

were strongly present in the outflow (21.4 mg/l) in comparison with the runs. It is possible that these high concentrations were caused by internal sources. After the Christmas break, there was a slight increase in suspended solids. The 3 week dry period is thought to have had an effect on the settling of the pavement structure, thus releasing a higher initial SS concentration in the events directly following the dry period.

Table 5-5: Statistical data of suspended solid: average SS per year of simulation within the course of the experiment

Year simulation	**Average (mg/L)**	**Std. Dev.**
1	21.41	19.21
2	5.00	2.79
The start of sediment addition		
3	5.24	2.68
4	4.07	2.31
5	4.93	2.28
6	5.50	2.20
Three weeks dry period*		
7	7.42	3.23
8	8.22	3.19
9	8.23	3.08
10	6.93	3.03
11	10.19	4.92
12	7.76	3.09
*During Christmas break		

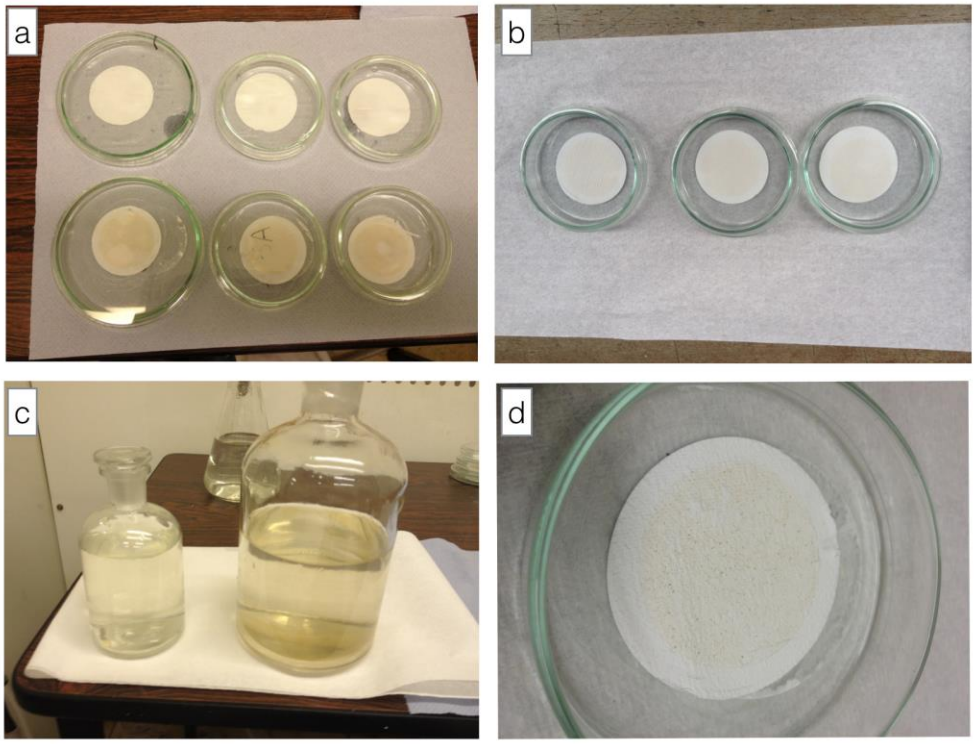

Figure 5-35: An example of outflow; (a) shows paper filter before and after SS test;(b) shows filtered paper after oven;(c) a sample compared to fresh water;(d) shows low SS.

The suspended solid concentration was monitored from the start of the experiment. 215 samples (Figure 5-35) were collected and analysed for sediment concentration. Full details can be found in (Table K - 1 and Table K - 12, in Appendix K). Table 5-5 details the average suspended solids concentration over the 12-year simulations. During the 1-year and 2-year simulations, the results show that the suspended solids concentration before the addition of sediment ranged between 2.0 and 59.0 mg/L, with a mean value of 21.4 and 5.16 mg/L (SD 19.21, 2.77) respectively. Elevated concentrations were expected within the first few simulations, as a result of pavement structure flushing (the release of any residual fine material entering the pavement structure during construction). The addition of sediment began in the 3-year simulation. The results show that SS concentration ranged between 2 and 23 mg/L, for the sediment phase of the experiment, with a mean value range between 4.07 and 10.19 mg/L (Table 5-5).

Figure 5-36 illustrates the pattern of sediment discharge throughout the experiment period, including suspended solid concentration before and after the addition of sediment. The trend of the suspended solid concentration decreased over the initial experimental period; however, before adding sediment, the SS concentration was

elevated during the first few simulations and then decreased. It indicates that the wash out phase reduced the internal SS concentration over time, but it is likely that the internal discharge continued over the experimental period.

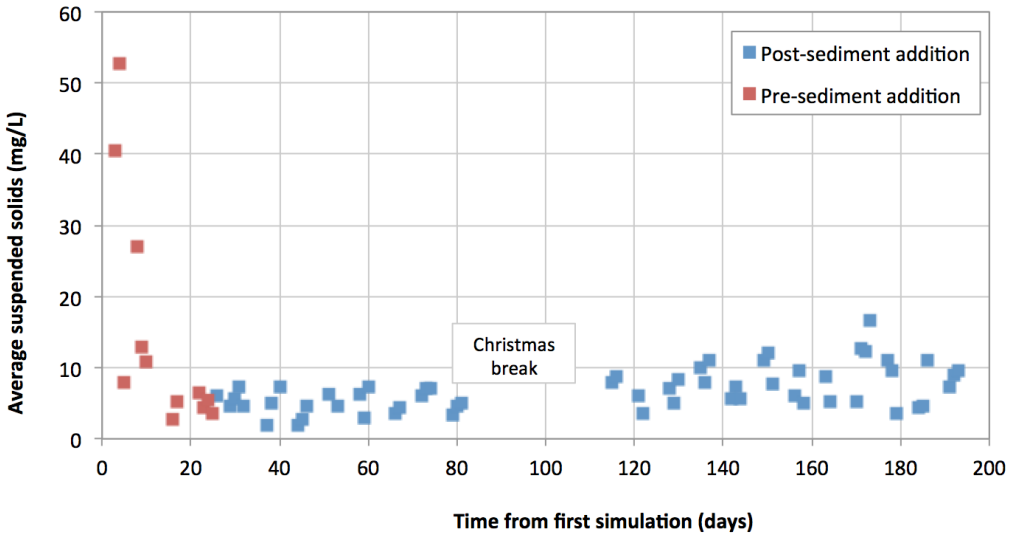

Figure 5-36: Suspended solid concentration levels during the course of the experiment.

After the three week dry period (Christmas break), the concentration of SS had a larger variability. It is difficult to ascertain whether the variability in the SS is due to the addition of sediment or the occurrence of the dry period. However, before the three week dry period, there was no obvious variation in comparison to after the break. Therefore, it can be inferred that the applied sediment was trapped within the pavement structure and had limited influence on the concentration of suspended solids in the outflow. The variation that occurred after the break was therefore attributed to the dry period.

Further analysis was carried out to verify whether there was a difference in SS concentration between each year of rainfall simulation. A paired t-test was carried out for comparison between the second year and all other simulated rainfall years, in order to identify the change in SS level over the experimental period. The results from the 2nd year of simulation were used as a baseline and all sediment results above this level (5mg/L) were considered to result from the additional sediment load on the pavement surface. The results from the paired t-test (Table 5-6) indicate that there is a t-test value difference after the seventh year of simulation. This confirmed the previous finiding that

the slight change in SS concentration level occurred due to the three weeks dry period between simulated rainfall years six and seven.

Table 5-6: Paired t-test for comparison of different SS concentrations. Critical t is 1.79(p=0.05)

Year simulation	**Average SS concentration (mg/L)**	**t-test**	**Significantly* different from Year 2**
1	21.41	4.13	Yes
2	5.00	-	-
The start of sediment addition (Christmas break)			
3	5.24	0.70	No
4	4.07	0.74	No
5	4.93	0.34	No
6	5.50	0.96	No
Three weeks dry period			
7	7.42	1.84	Yes
8	8.22	2.33	Yes
9	8.23	1.95	Yes
10	6.93	1.80	Yes
11	10.19	3.70	Yes
12	7.76	2.00	Yes
*Significant when it is greater than 10% change from the year 2 value			

Generally speaking, the trend of the SS concentration over the 12-year simulation decreased at the beginning of simulation, and then became relatively stable until the break. However, the level of suspended solids showed a greater variability after the break. It can be concluded that the level of suspended solids was low over the experimental period which indicates that the permeable pavement acted as a sediment filter or trap. In addition, the suspended solid concentration showed little variation over the long-term hydrological performance of the pavement.

5.2.7.2 Surface infiltration test

The infiltration test was performed by using a radial flow falling head permeameter over the course of the study, in order to assess any deterioration in infiltration rate. The first set of tests was taken before sediment application. The test was taken over two days,

with ten measurements taken each day. The infiltration rate ranged between 4450.3 and 5835.3 $L.m^{-2}.h^{-1}$, with a mean value of 5140 $L.m^{-2}.h^{-1}$. The second set of tests were taken at the end of the experiment, and the infiltration rate ranged between 2614.3 and 2955 $L.m^{-2}.h^{-1}$, with a mean value of 2813.5 $L.m^{-2}.h^{-1}$. Full details of the measurements can be found in (Table J - 1 to Table J - 4, in Appendix J).

This is a significant decrease in infiltration rate (45.3%). The change in infiltration rate can be attributed to the detention of added sediment within the pavement structure. However, the permeability of the pavement is still functional, even when the upper structure (80 mm of the surface) had a reduction in infiltration rate. Two key observations that show the pavement maintained a good condition of permeability are: (1) no ponding was observed during the experimental period, and (2) the reduction in outflow volume was low (6.4% of the initial outflow). Complete clogging of the pavement is unlikely to have occurred during the experimental period. To reach the point of failure, the pavement may require further simulation of +10 years of sediment load and/or further rainfall event simulations.

5.2.8 Relationship between outflow and other variables

The analysis undertaken and presented in this section was undertaken using SPSS. The results described in this chapter confirm the influence of sediment on the hydrological performance. An empirical equation was created to predict the hydrological response of the permeable pavement. The hypothesis is that the outflow can be predicted from rainfall volume and moisture content. It is also expected that an empirical relationship can be constructed to predict the influence of sediment on the outflow.

The dataset was separated into two phases: before and after addition of sediment to the pavement surface, in order to generate two equations that describe the hydrological response before and after the addition of sediment. The two equations were derived using multiple regression analysis.

A plot was drawn to visualize the type of relationship between inflow and outflow before and after adding sediment (see Figure 5-37). As can be seen from the figure, a straight line regression relationship was computed for both phases. The correlation between outflow and rainfall was moderate and highly significant for both phases (see

Table 5-7). The linear relationship between inflow and outflow also varied (see Figure 5-37), showing a strong, definable linear relationship between rainfall and outflow volume before and after adding sediment.

Table 5-7: Summary correlations and results from the linear regression analysis for two phases.

Phase	The correlation coefficient (R) (%)	The coefficient of determination (R^2) (%)	Correlation with outflow (%)	Significance level (p-value)
Pre-sediment addition	50.13	25.13	50.13	<0.05
Post-sediment addition	54.52	29.72	54.52	<0.01

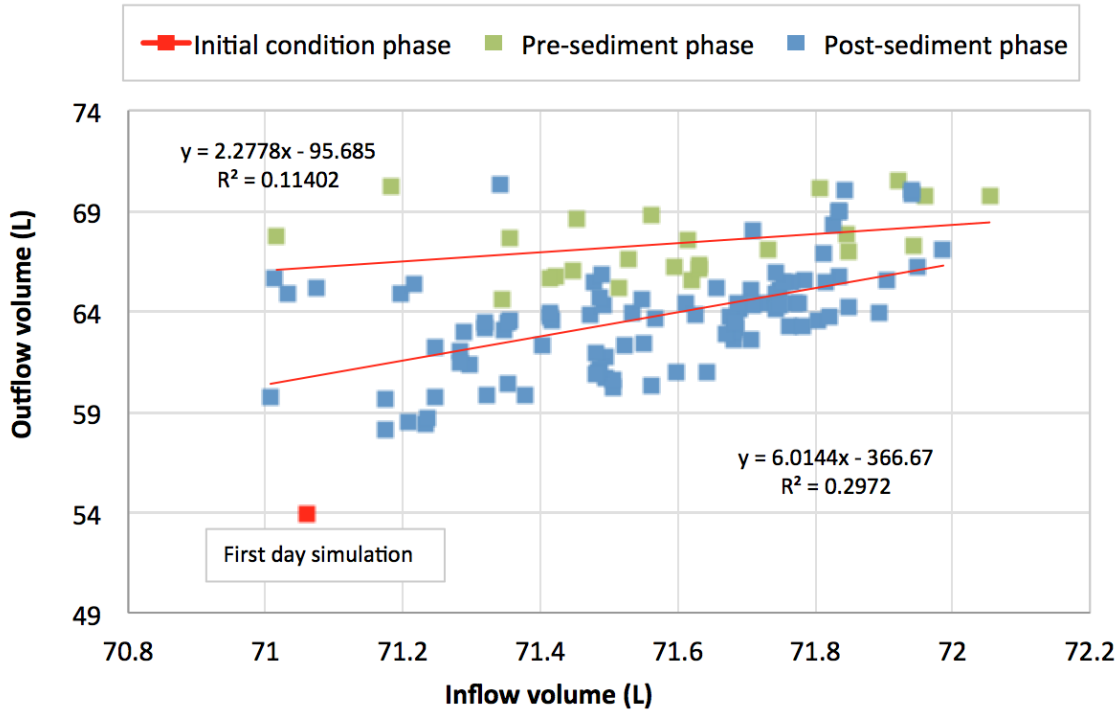

Figure 5-37: A plot of rainfall and outflow volume for two phases ; (i) before adding sediment,(ii) after adding sediment.

Figure 5-38 and Figure 5-39 show the relationship between the outflow volume and the VWC for the top and bottom layer, respectively. They shows highly significant (p>0.01) moderate correlation. It can be seen that there is a positive correlation between outflow and VWC before addition of sediment (r = 0.651 and 0.656 for the top and bottom layer, respectively). Conversely, the relation becomes negative after the addition of sediment (r = -0.561 and -0.512 for the top and bottom layer, respectively). The

change in the type of relationship can be explained as being attributed to the addition of sediment.

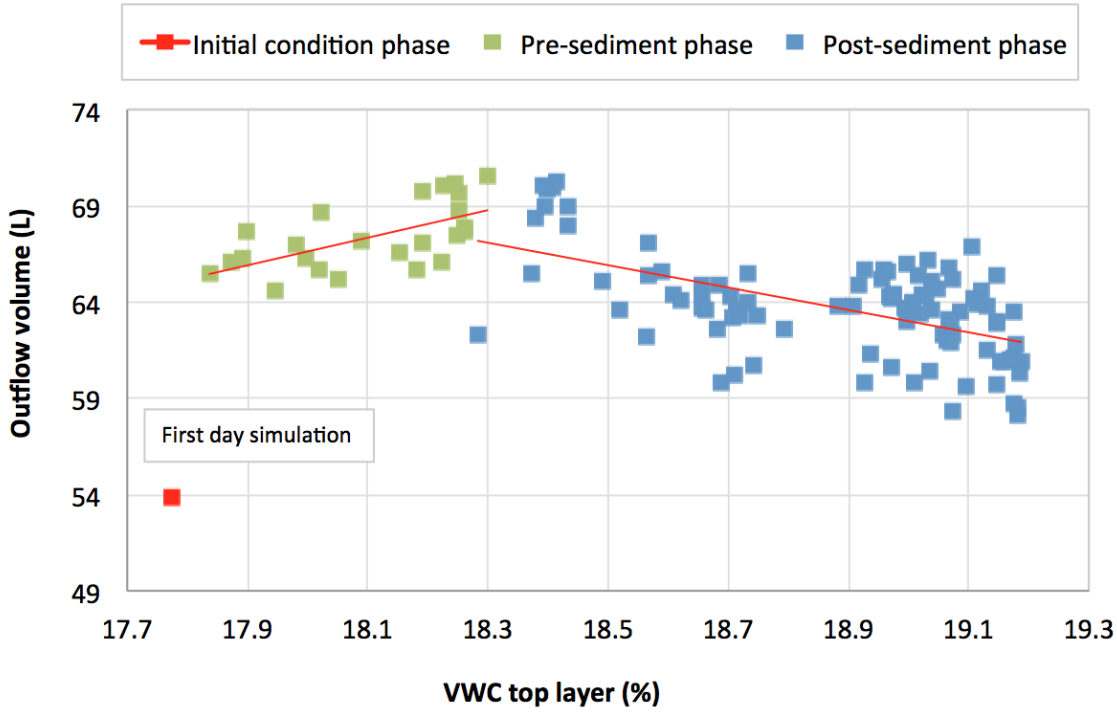

Figure 5-38: Showing correlation relationship between outflow volume and VWC top layer.

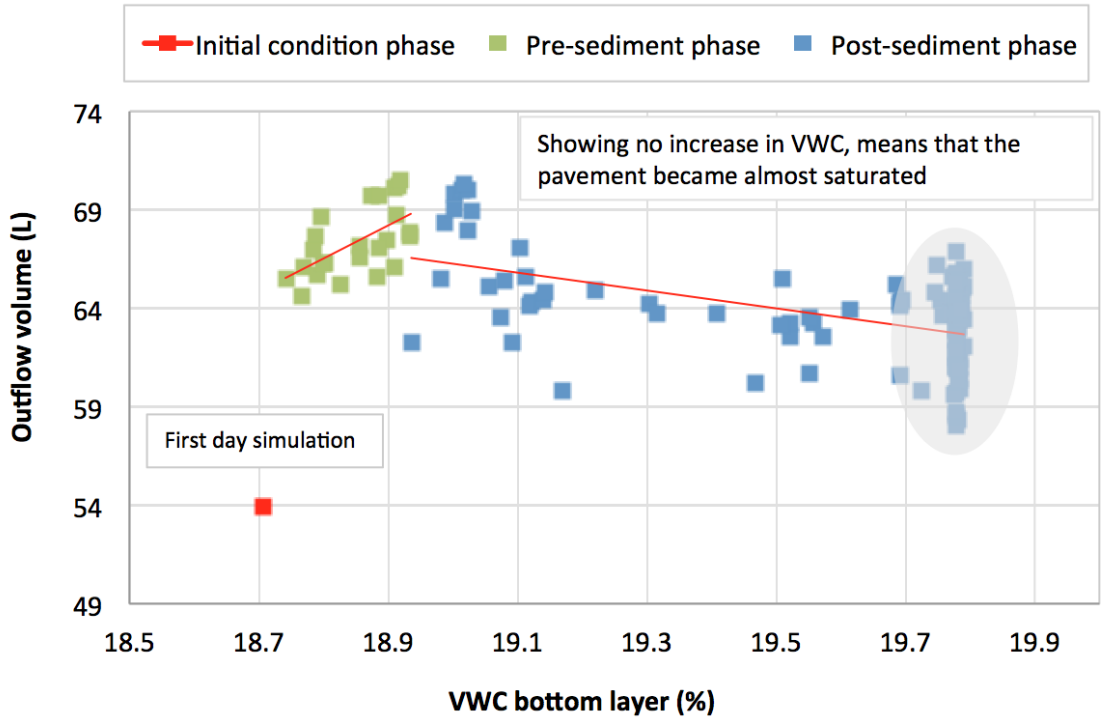

Figure 5-39: Showing correlation relationship between outflow volume and VWC bottom layer.

5.2.8.1 Multiple regression analysis

As described above, the relationship between outflow and one independent variable (rainfall volume) was moderate and highly significant. To provide a comprehensive review of the relationship and influence of all the pavement variables on outflow, other variables were considered when establishing the empirical relationship between outflow and the independent variables. Therefore, multiple regression analysis was used to define the best relationship between the dependent variable and other variables (independent, predictor). The relationship can be formalised by:

$$\boldsymbol{y = b_0 + b_1 x_2 + b_2 x_2 + \ldots + \varepsilon} \qquad \textbf{(15)}$$

Where, y is the predicant variable, x_1 and x_4 are independent variables, b is constant and ε is the error.

A multiple regression analysis was performed to develop a predictive equation to estimate the permeable pavement behaviour when rainfall infiltrated through it, specifically under the above described laboratory conditions. The outflow volume was found to be dictated primarily by rainfall, duration, moisture content and pavement permeability (associated with infiltration rate). It is important to highlight that the pavement permeability did not change during Phase 1, as no sediment was applied during this phase. However, the pavement permeability did change during Phase 2, due to the addition of sediment to the pavement surface. The sediment addition during Phase 2 was expected to influence the pavement permeability. Therefore, a new independent variable (sediment weight) was added in the multiple regression analysis.
The multiple regression analysis was performed before and after adding sediment, using a probability significance limit.

Some potentially large errors can be expected if the regression conditions are used without both calibration and validation of the model. In order to overcome this issue, model validation was carried out to evaluate the model. Therefore, the model needs to be validated with other data, thus, to complete the validation the data needs to be split into two datasets, one for the calibration (70%) and the second for validation (30%).

Pre/Post Sediment Model

The results from multiple regressions are shown in Table 5-8 and Table 5-9 for the pre/post-sediment phases, respectively. Full details of the analysis can be found in Table L - 1 to Table L - 6, in Appendix L.

Table 5-8: Summary results from the multiple regression analysis for Phase 1 (pre-sediment addition)

Variable	**Correlate with outflow**	**Multiple regression weights**		
		b	**Std. error**	**P-value**
Constant		-1040.69	543.04	0.0794
Inflow (x_1)	0.501	8.75	3.32	0.0217
VWC top layer (x_2)	0.651	14.14	28.0	0.6228
VWC bottom layer (x_3)	0.656	12.14	38.68	0.0217
Duration (x_4)	0.612	-0.12	0.22	0.6162
The correlation coefficient R				0.76
The coefficient of determination R^2				0.58
F- test				4.15
P-value for the generated model				<0.001

Table 5-9: Summary statistics, correlations and results from the multiple regression analysis for Phase 2 (post-sediment addition)

Variable	**Correlate with outflow**	**Multiple regression weights**		
		b	**Std. error**	**P-value**
Constant		-73.78	97.0	0.4499
Inflow (x_1)	0.545	4.64	1.23	0.0004
VWC top layer (x_2)	-0.561	-6.57	4.00	0.1060
VWC bottom layer (x_3)	-0.512	-3.79	3.10	0.2271
Duration (x_4)	-0.530	6.44	3.91	0.1043
Sediment weight (x_5)	-0.530	-3806.11	2319.88	0.1061
The correlation coefficient R				0.66
The coefficient of determination R^2				0.44
F- test				9.26

P-value for the generated model	<0.001

As it can be seen from the above tables, the outflow correlates well with all variables, with a range of -0.561 and 0.656 for both phases. The relationships were moderate and highly significant (p-value<0.001). However, it was noted that the correlation became negative after the application of sediment. This can be explained by the sediment modifying the internal structure of the permeable pavement material, increasing/decreasing the void connectivity and volume and therefore changing the VWC within the substrate. The empirical equations can be formalised:

$$y = 8.75\,x_1 - 14.14x_2 + 12.14\,x_3 - 0.12x_5 - 1040.7 \quad \textbf{(16)}$$

$$y = 4.64\,x_1 - 6.57x_2 - 3.79x_3 + 6.44x_4 - 3806.11x_5 - 73.78 \quad \textbf{(17)}$$

Equation (16) represents outflow volume during pre-sediment phase, while Equation (17) represents outflow volume during post-sediment phase, y is outflow volume (L), x_1 is rainfall volume (L), x_2 is moisture content for top layer (%), x_3 is moisture content for bottom layer (%), x_4 is duration (hours) , and x_5 is cumulative sediment weight per day (kg).

The regression analysis was found in both phases to illustrate a statistically significant linear relationship (p<0.001) between outflow and independent variables. The two Equations (16 and 17) were used to calculate the predicted outflow. The performance of the two equations during calibration and validation is shown in Figure 5-41. These Figures illustrate the measured and predicted outflow within two phases (pre/post-sediment addition). The multiple regression analysis explained 58% and 44% the variance with a best fit regression curve being described by Equations 16 and 17.

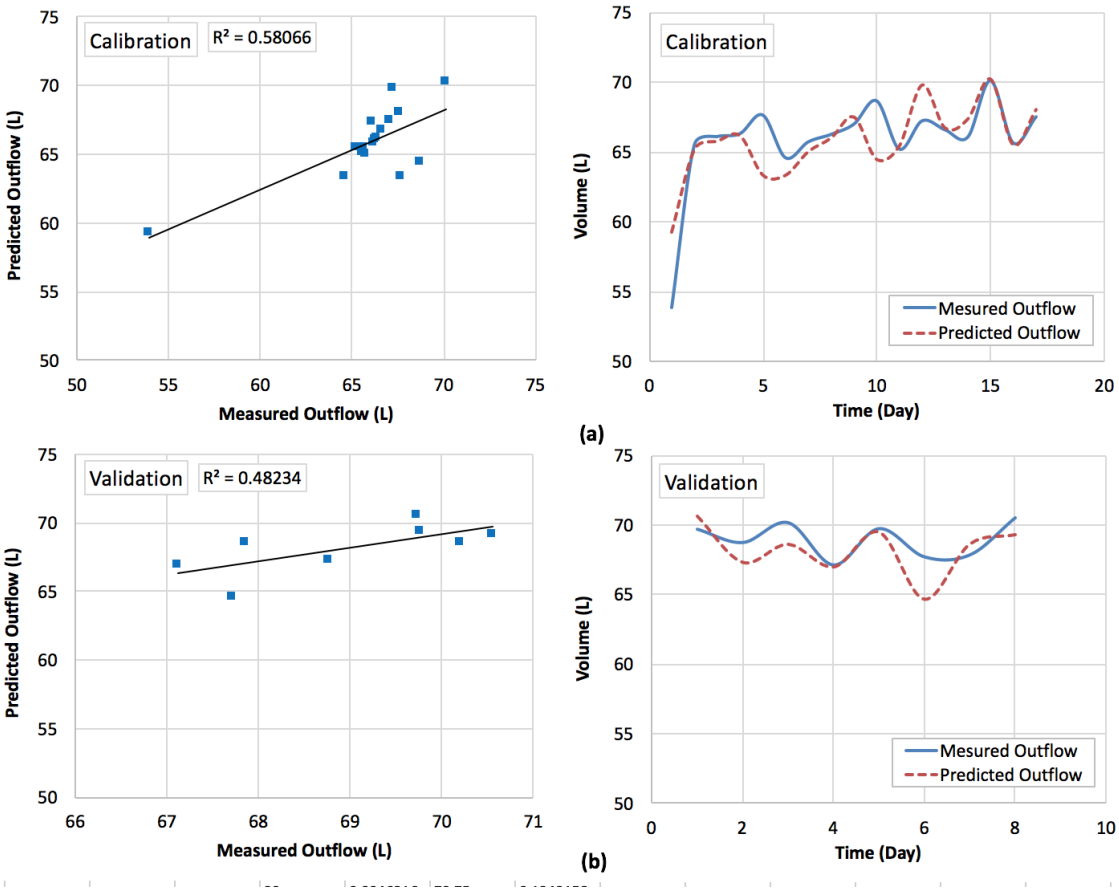

Figure 5-40: Comparison of measured and predicted outflow during pre-sediment phase: a calibration; and b validation.

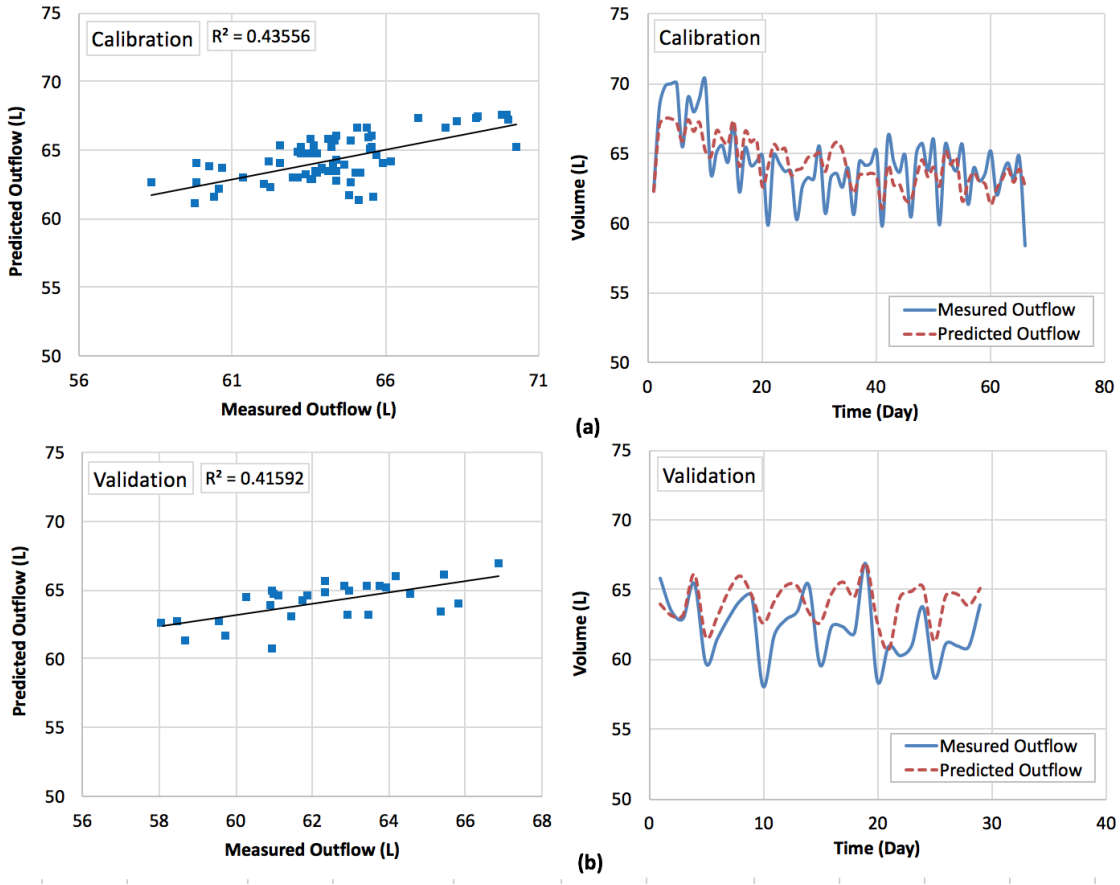

Figure 5-41: Comparison of measured and predicted outflow during post-sediment phase: a calibration; and b validation.

General Model

The equations for the outflow before and after adding sediment have been developed separately, but need to be combined so that the general function of how outflow performs with or without sediment can be obtained. The Equations 16 and 17 for pre/post sediment can be combined into a single equation. Therefore, Equation 18 shows the formula after combing the two equations.

$$y = 4.85\,x_1 - 2.18x_2 - 4.96x_3 - 14.82x_4 + 0.04x_5 - 149 \qquad (18)$$

Where x_1, x_2, x_3, x_4, and x_5 are the respective regression weights, as can be seen in Table 5-10.

From multiple regression analysis, the results are shown in Table 5-10. The general equation (18) represents a statistically significant linear relationship ($p<0.001$). Thus,

the combined phases showed good regression performance with low coefficient of determination. The performance of the model during calibration and validation is shown in Figure 5-42. The results show that the performance of the model has performed reasonably well in estimating the outflow from the pavement during calibration and validation.

Table 5-10: Summary statistics, correlations and results from the multiple regression analysis for combined phases (pre/post-sediment addition)

Variable	**Correlate with outflow**	**Multiple regression weights**		
		b	**Std. error**	**P-value**
Constant		-149	101.97	0.1480
Inflow (x_1)	0.442	4.85	1.14	0.0001
VWC top layer (x_2)	-0.398	-2.18	4.27	0.6106
VWC bottom layer (x_3)	-0.467	-4.96	4.22	0.2431
Duration (x_4)	-0.487	-14.82	19.69	0.4541
Sediment weight (x_5)	-0.431	0.04	0.03	0.2297
The correlation coefficient R				0.64
The coefficient of determination R^2				0.41
F- test				10.68
P-value for the generated model				<0.0001

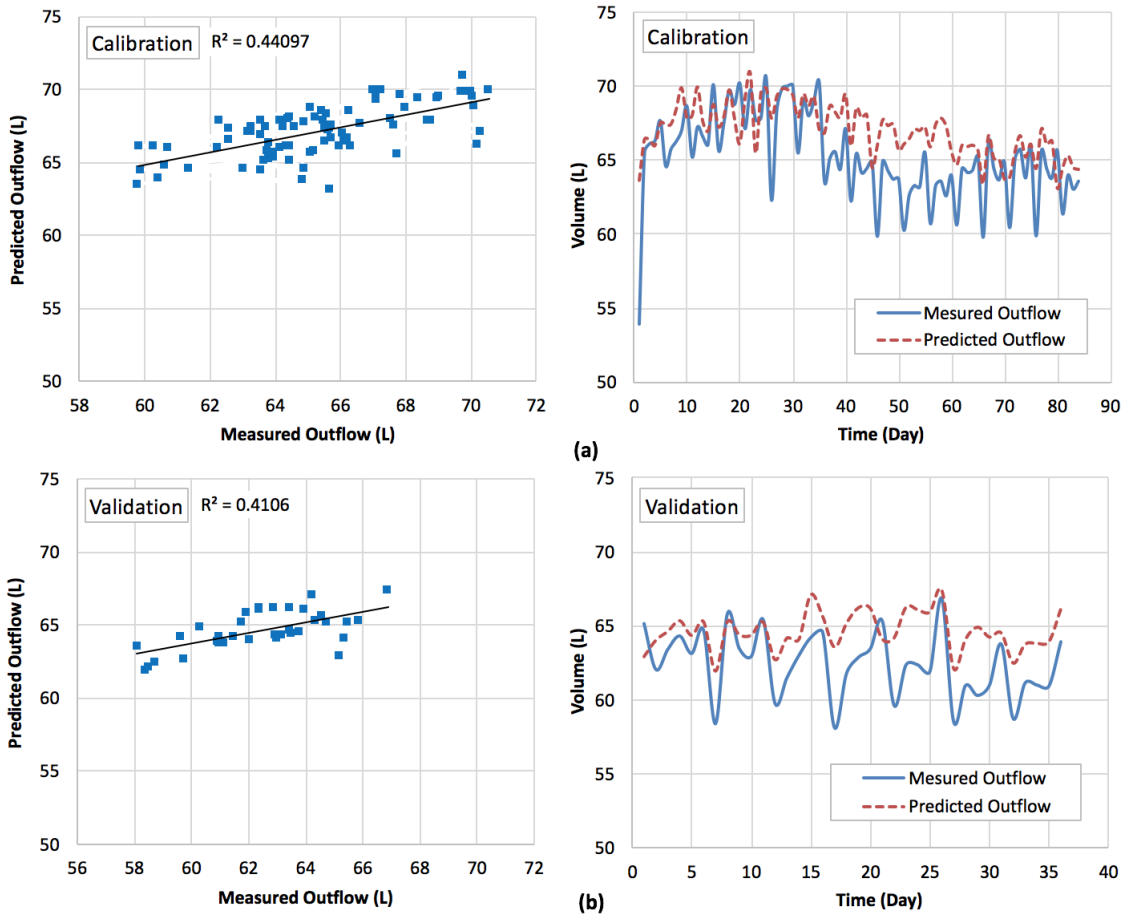

Figure 5-42: Comparison of measured and predicted outflow for general model: a calibration; b validation.

5.2.8.2 Analysis of variance

Analysis of variance (ANOVA) is a statistical approach for examining variables by comparing the variability within a group versus variability among different groups (Brown and Mac Berthouex, 2002). This can be verified if the *F*-statistic is larger that means the null hypothesis (H_0) of no difference among the group means is false. In other words, if the variables are similar, the variation within each phase (pre/post sediment) will be the same as the variation between the phases.

One way ANOVA was used to examine whether there is a significant difference existing in outflow and moisture content between the pre-sediment and post-sediment phases. A confidence level of 95% ($p<0.05$) was used for the analysis. Table 5-11 shows the analysis results. It can be seen that the difference between groups is bigger than the difference within a group; therefore, it is not random chance, and it is a real effect that the addition of sediment has an impact on the hydrological performance.

Table 5-11: One-Way ANOVA between pre-sediment phase (outflow and moisture content) and post-sediment phase (outflow and moisture content), significance values <0.0001

Variables	Source of Variation	SS	df	MS	F	P-value	F_{crit}
Outflow volume	Between Groups	199.54	1	199.54	26.163	0.000	3.921
	Within Groups	899.96	118	7.63			
VWC top	Between Groups	12.33	1	12.33	216.694	0.000	3.921
	Within Groups	6.71	118	0.06			
VWC bottom	Between Groups	10.36	1	10.36	144.795	0.000	3.921
	Within Groups	8.44	118	0.07			

5.3 Chapter Summary

The experiment evaluated the performance of the permeable pavement during a twelve-year life-cycle period. The study showed that the outflow underwent a significant reduction after the addition of the sediment to the pavement surface. The duration of outflow increased over time, as a result of a decreased infiltration rate, which was reduced due to clogging by sediment. It was also shown that the concentration of SS had a limited (low) variability during the ten-year period, but that there was no significant difference in SS outflow concentration. After the addition of sediment to the pavement surface, no temporary ponding occurred on the surface. This confirms that permeable pavement continues to infiltrate rainfall easily, despite receiving no maintenance after construction. In other words, this finding suggests that the lifespan of a permeable pavement could easily exceed ten years of simulated sediment loading without maintenance. The experimental findings are summarised in the following section.

5.3.1 Outflow

- The 6.4 % reduction in outflow volume throughout this study shows the impact of sediment on hydrological performance over ten year simulations.
- The shape of the outflow rate flattened out after the addition of sediment, indicating that the infiltration rate has been restricted by the addition of the sediment on the pavement surface.

- The average increase in drainage time by 2.36 hours indicates that the movement of water through the structure materials became slow, due to the restriction in infiltration rate.
- The start delay time ranged between 5.5 and 10.5 minutes, with an average time of 7.66 minutes.

5.3.2 Infiltration rate

- The average initial infiltration rate was 5140 L/m^2.h. However, after the addition of 440 g of sediments to simulate ten years of deposition, the surface infiltration rate was reduced to 2813.5 L/m^2.h. The percentage reduction in infiltration rate was 45.3 % over 15 months (equivalent to 10 years of rainfall).

5.3.3 Suspended solids concentration

- The average concentration of suspended solids was 6.87 mg/l. There was no significant change in the suspended solids outflow concentration, meaning that the structure managed to trap the additional sediment.

5.3.4 Sediments

- Sediment was detained within pavement structure. However, it is not certain whether sediment became trapped within the upper layer or on the geotextile layer within the pavement structure.
- There is no doubt that the accumulation of sediment diminishes the surface infiltration rate over time. This has a detrimental influence on the other hydrological characteristics of permeable pavement.

5.3.5 Relationship between outflow and other variables

- The relationship between outflow and inflow was strong for both phases, but the relation became negative after the addition of sediment. The results of multiple regressions show that there is a good correlation between the four independent variables (inflow, duration, moisture content, and sediment) and the dependent variable (outflow). The multiple regression analysis explained 71.24% and 46.72% of the variance with a best fit regression curve. The percentage errors range between +7.86% and -6.76%, indicating the prediction can provide 93.24% accuracy.

5.3.6 Potential error and uncertainty

As discussed early in this research (Section 3.6) the potential errors and uncertainty were identified. The error bar was added into each single figure that measured and derived quantities from associated equipment. The uncertainty of the results would not be found to have a significant impact on the results.

These findings are valid for the laboratory conditions under which these experiments were undertaken. While they are not valid under field conditions they provide a valid representation of permeable pavement structure processes in controlled conditions and an indicative understanding of the permeable pavement processes and functionality in other locations. In addition, the study included a ten-year sediment simulation, an indicative rather than full lifespan simulation of the permeable pavement. Overall, these findings confirm that permeable pavement designed according to the SuDS Manual specifications (CIRIA C697) offers excellent source control by dealing with surface run-off and pollutants.

CHAPTER 6 – CONCLUSIONS AND FUTURE WORK

6.1 Overview

This research has studied the hydrological performance of a permeable pavement from two aspects; (i) to examine the hydrological response to different rainfall events, (ii) to assess the influence of sediment on the hydrological performance of the permeable pavement. This involved designing a physical structure in the laboratory, which represented a car park surface with full scale build-up and designing and developing monitoring equipment.

A critical review of literature was undertaken to cover the background of pervious pavements, types of pervious pavement (porous and permeable), the hydraulic function of each type, the best practice design, the current accepted use, the water quality improvement function, the water quantity improvement function, hydrological performance, pollutant characteristics, operational life: clogging, the effect of frost, cost and maintenance. This review was important in order to understand the hydrological performance of permeable pavements. The review presented the current knowledge on the approach to design and construction of permeable pavements and identified the research gap which has been addressed in this research study.

The objectives of this research were:

- Design and construction of a permeable pavement that represent a car park surface with full scale build-up.
- Design and development of monitoring equipment
- To quantify the ability of the designed structure to reduce surface runoff in response to different rainfall conditions.
- To assess the influence of sediment on the hydrological performance of the designed structure.

To meet the first and second research objectives, a physical structure was constructed to provide enough space for all (3-dimensional) constituents of a permeable pavement. The manufacturer's guidelines, the SuDS manual CIRIA C697, British Standard BS 7533-13-2009 were used to design and construct the depth of the permeable pavement.

A rainfall simulator and collection system were designed for delivering and collecting water to and from the rig, plus to provide accurate flow rate readings. The third objective was met by conducting a series of rainfall simulations in order to understand the hydrological response of the rig under the three different rainfall intensities. This hydrological experiment was important in order to provide information about the ability of the rig to infiltrate rainfall when there was no sediment application. The fourth objective was met by conducting a series tests in order to simulate 10 years of sediment load. Outflow was recorded for each rainfall event, and VWC was monitored over the experimental period. In addition, water quality testing was undertaken within the experimental period, in order to monitor the suspended solids' concentration change.

6.2 Main findings

The results presented in Chapter 4 and Chapter 5 were discussed in terms of the two main aspects of the research:

1. The hydrological performance of a permeable pavement; and
2. The influence of sediments on the hydrological performance of a permeable pavement.

This chapter presents the important findings obtained from the laboratory research in relation to the performance of permeable pavements in controlling and managing urban storm water.

Hydrological performance of a permeable pavement

The analysis of the pavement hydrological performance (Chapter 4) revealed that the permeable pavement performed differently in the context of three rain events (25.56, 31.12, and 21.7 $mm.h^{-1}$). During day-1 conditions (i.e. the condition of sub-grade during day 1) the pavement discharged 7.7%, 8.6%, and 18.0 % of rainfall for rainfall intensities 1, 2, and 3, and the response of the pavement was influenced by the characteristics of the rain event. There was a slight difference in response in Rainfall Intensity 1 and 2, which was due to the fact that both storms were of the same duration but different return periods (therefore different intensities), resulting in a relatively similar volume of rainfall. However, Rainfall Intensity 3 demonstrated a marked increase of 10% in relation to previous rain events, which can be explained by a

difference in duration of the rainfall. It was therefore demonstrated that the response in outflow volume was significantly influenced by contact time (rainfall duration).

The same scenario occurred in response to the initial moisture content. When the permeable pavement was wet (i.e. the condition of sub-grade during days 2 to 5) it discharged 36.2, 42.6, and 59.9% of the rainfall. A significant difference was observed between the response of the pavement during Day1 and that for Day2-5 conditions. This was a result of the condition of the pavement during Day1 and before the simulation, i.e. the structure created an additional retention capacity by the absence of water during days 6 and 7. Thus after the simulation, it could be seen that the upper materials tended to detain the majority of the rainfall.

The hydrological performance for rainfall intensity 1 and 2 were comparable. The difference in inflow rates between rainfall intensity 1 and 2 was up to 5mm h^{-1}. This illustrates the fact that an increase in the intensity of rainfall above 25 mm h^{-1}, without an increase in its duration, results in an increase in rainfall storage within the pavement structure. The outflow rates from the third rainfall intensity reveal a different response to that seen in rainfall intensity 1 and 2. Outflow during and after rainfall event 3 was higher than for either rainfall intensity 1 or 2. It can therefore be concluded that increasing the duration of the rainfall results in an increase in outflow, and therefore a decrease in the rainfall storage within the pavement structure.

A further characteristics of the pavement condition concerns the duration of the outflow. As the results demonstrate (Chapter 4), the outflow duration was 0.86, 0.85, and 1.87 hours for rainfall intensities 1, 2, and 3, respectively, during a 1-day period (i.e. Day 1). However, during Day2-5 conditions, the outflow duration increased to 5.64, 5.9, and 7.43 hours for rainfall intensities 1, 2, and 3, respectively. A comparison of Day-1 and Day2-5 conditions reveals an increase of outflow duration of 4.78 – 5.56 hours, a 300-600% increase between Day-1 and Day2-5 conditions. The outflow duration was influenced by both the condition of the pavement and the characteristics of the rain event. On the other hand, the start delay, during Day1 conditions exceeded 10 minutes, but the start delay decreased by 3 minutes during Day2-5 conditions. In response, little difference was observed between rainfall intensities, with the start delay being more influenced by the condition of the subgrade rather than rain event characteristics.

Multiple regression analysis was carried for three rainfall intensities (section 4.5). The results showed the gradient (drawn relationship between inflow and outflow) increases, meaning there is greater outflow from the pavement. Although the accuracy in prediction was over 80%, the model has a tendency to under-estimate the outflow volume during Day-1 conditions.

The changing of rain event characteristics influenced the outflow volume, outflow duration, start delay, and VWC. The hydrological performance revealed that the permeable pavement detained between 40-60% of the rainfall within its structure. Thus, the permeable pavement offers an excellent source of control in dealing with a variety of storm water flows.

Influence of sediment on the hydrological performance of a permeable pavement

The impact of sediment on the hydrological performance of a permeable pavement was examined in Chapter 5, with results revealing the change in outflow and VWC behaviour over time. However, the clogging stage was difficult to reach in this research, including the use of a 10-year sediment load. The application of sediment and rainfall simulated natural conditions which generally occur on the surface of a permeable pavement. The design of the permeable pavement (provided by The SuDS manual) is able to cope with a heavy rain event, but there is a lack of information on sediment performance. The research undertaken during this study is the first to assess hydrological performance on full scale permeable pavement, therefore it has been difficult to draw comparisons with other work.

The results reveal that the outflow volume responded to the addition of sediment, leading to a 6.4% reduction in outflow. In addition, the volumetric water content (VWC) was increased by a similar percentage of outflow (5.36%). This can be explained by the fact that the amount of outflow was reduced over time, but was detained in the structure, leading to the presence of this water raising the VWC level. The results also showed that the relationship between the outflow volume and the VWC showed highly significant ($p>0.01$) moderate correlation. It can be seen that there is a positive correlation between outflow and VWC before addition of sediment ($r = 0.651$ and 0.656 for top and bottom layer, respectively. Conversely, the relation became

negative after addition of sediment (r = -0.561 and -0.512 for top and bottom layer respectively). The change in relationship type can be explained by the addition of sediment.

The addition of sediment has had an impact on other aspects of the hydrological performance of the permeable pavement, such as outflow duration and start delay, and outflow rate. It is clear from the results that the outflow duration became prolonged over time: it ranged between 6.94 and 14.76 with an average of 10.73(Std Dev. 1.76h). On the other hand, the start delay showed a range from 5.5 to 10.5 minutes, with an average time of 7.66 minutes (Std Dev. 1.05 min).

The monitoring of suspended solids since the completion of the pavement structure has not been addressed due to limitations of equipment. However, the level of suspended solids was monitored at the beginning of the experiment. The initial SS concentration was high, 59 mg/l, but the concentration of suspended solids reduced through the experimental period, with average value between 4.07 – 10.19 mg/L. The concentration of SS varied slightly after the three week dry period (Christmas break). It is difficult to ascertain whether the variability in the SS is due to sediment implementation or the occurrence of the dry period. There is no doubt that the removal of suspended solids was very high, between 90 - 100%.

Multiple regression analysis was performed before and after adding sediment. The results showed that the correlation coefficient became negative after the application of sediment. The percentage errors of the model ranged between +7.86% and -6.76%, indicating that the prediction equation can provide 93.24% accuracy. The results in Chapter 5 indicate that permeable pavements have the ability to manage stormwater and pollutants easily.

This research demonstrated that the current design and installations by the SuDS Manual and BS 7533-13 proved their workability, both by reducing surface runoff and trapping pollutants. The contribution to SuDS offered by permeable pavements seems to be small, but the greatest benefit can be seen as component parts of SuDS. In order to fully understand whether the current design of permeable pavement requires any further improvements, long simulation on the designed permeable pavement is needed.

6.3 Recommendation for future work

Although the current design has helped to strengthen the knowledge of hydrological performance and how this type of design can reduce surface runoff, there still remains a number of areas that have not been addressed through this research. These areas are:

- The monitoring of upper layers of pavement,
- Further consideration of sediment load,
- Testing of additional factors such as maintenance,
- Testing the hydrological performance for extreme events,
- Testing the impact of dry periods on clogging, and
- Testing the removal efficiency of the permeable pavement for heavy metals and oil
-

6.3.1 The monitoring of upper layers of pavement

The total depth of 780 mm of permeable pavement was constructed in four different layers. Monitoring the moisture content of the structure materials was useful for this research. However, only the sub-grade layer was monitored. It would be very useful to monitor moisture content of each layer.

6.3.2 Further consideration of sediment load

The permeable pavement has been shown to maintain a good condition of permeability after 10 years of sediment load. The next stage of research should examine the permeable pavement for further 20 years' sediment load. This would provide data that can be useful to indicate the blockage point, or how long it would take to reach blockage point? It would be informative to see the results after 20 years of sediment simulation. In addition, it would be useful to examine the hydrology performance in terms of the ponding point when it occurs in relation to years of service.

6.3.3 Testing of additional factors such as maintenance

The surface infiltration rate has significantly reduced during the sediment experiment. The permeable pavement did not received maintenance during the experimental period of this research. It would be worthwhile to estimate the relief in the infiltration rate after maintenance. The question then becomes "to what extent could maintenance improve the infiltration rate, especially for current designs?

6.3.4 Testing the hydrological performance for extreme events

The relationship between rainfall and outflow has been investigated in this research for Edinburgh conditions. The study only carried out rainfall intensity of between 20-30 mm per hour. Thus, it is a good idea to subject the rig into high rainfall intensity. Hence, more detailed studies into different conditions are needed.

6.3.5 Testing the impact of dry periods on clogging

The antecedent dry period has been seen as a crucial factor in clogging, but it has not been examined deeply in this research. However, practically, the permeable pavement requires significant time to dry. Thus, in this case, additional equipment is required to speed up the rig drying.

6.3.6 Testing the removal efficiency of the permeable pavement for heavy metals and oil

Permeable pavement systems degrade the hydrocarbons with their structure; therefore the degradation of organic matter and the microbial activity of suspended solids increase the bioavailability of metals and PAHs. Additionally, testing for the removal efficiency of heavy metals has not been addressed in this research, hence more detailed studies on this area are needed.

It would certainly appear that permeable pavement showed the ability to reduce surface runoff; thus, eventually the impacts of urbanisation would be minimised. It also demonstrated (chapter 5) the functionality of hydrological performance, even after 10 years' sediment loading. The structure has acted as a sediment filter, although there was no maintenance carried out. It seems that the maintenance requirements are low.

References

ABBOTT, C. & COMINO-MATEOS, L. 2003. In-Situ Hydraulic Performance Of A Permeable Pavement Sustainable Urban Drainage System. *Water and Environment Journal,* 17**,** 187-190.

AL-RUBAEI, A. M., STENGLEIN, A. L., VIKLANDER, M. & BLECKEN, G.-T. 2013. Long-Term Hydraulic Performance of Porous Asphalt Pavements in Northern Sweden. *Journal of Irrigation and Drainage Engineering,* 139**,** 499-505.

ANDERSEN, C. T., FOSTER, I. D. L. & PRATT, C. J. 1999. The role of urban surfaces (permeable pavements) in regulating drainage and evaporation: development of a laboratory simulation experiment. *Hydrological Processes,* 13**,** 597-609.

ANDRAL, M., ROGER, S., MONTREJAUD-VIGNOLES, M. & HERREMANS, L. 1999. Particle size distribution and hydrodynamic characteristics of solid matter carried by runoff from motorways. *Water Environment Research***,** 398-407.

BACKSTORM, M. 2000. Ground Temperature in Porous Pavement During Freezing and Thawing. *Journal of Transportation Engineering***,** 375-381.

BÄCKSTRÖM, M. & BERGSTRÖM, A. 2000. Draining function of porous asphalt during snowmelt and temporary freezing. *Canadian Journal of Civil Engineering,* 27**,** 594-598.

BALL, J. E. & RANKIN, K. 2010. The hydrological performance of a permeable pavement. *Urban Water Journal,* 7**,** 79-90.

BALMFORTH, D., DIGMAN, C., KELLAGHER, R. & BUTLER, D. 2006. *Designing for exceedance in urban drainage: good practice - C635 CIRIA* London, CIRIA.

BARBOSA, A., FERNANDES, J. & DAVID, L. 2012. Key issues for sustainable urban stormwater management. *Water research,* 46**,** 6787-6798.

BEAN, E. Z., HUNT, W. F. & BIDELSPACH, D. A. 2007. Field Survey of Permeable Pavement Surface Infiltration Rates. *Journal of Irrigation and Drainage Engineering,* 133**,** 249-255.

BEDDOW, J. 2010. Stormwater discharge quality test resultson porous asphalt pavement systems. Coventry: SUDS applied Research Group

BEECHAM, S., PEZZANITI, D. & KANDASAMY, J. 2012. Stormwater treatment using permeable pavements. *Proceedings of the ICE - Water Management,* 165**,** 161-170.

BOND, P. C., PRATT, C. J. & NEWMAN, A. P. 1999. A review of stormwater quantity and quality performance of permeable pavements in the UK. *Proc. 8th International Conference on Urban Storm Drainage.* Sydney, Australia.

BOOGAARD, F., LUCKE, T., VAN DE GIESEN, N. & VAN DE VEN, F. 2014. Evaluating the Infiltration Performance of Eight Dutch Permeable Pavements Using a New Full-Scale Infiltration Testing Method. *Water,* 6**,** 2070-2083.

BOOTH, D. B. & LEAVITT, J. 1999. Field Evaluation of Permeable Pavement Systems for Improved Stormwater Management. *Journal of the American Planning Association,* 65**,** 314-325.

BORGWARDT, S. 2006. Long-term in-situ infiltration performance of permeable concrete block pavement. *8th International Conference on Concrete Block Paving.* Citeseer.

BOWYER-BOWER, T. A. S. & BURT, T. P. 1989. Rainfall simulators for investigating soil response to rainfall. *Soil technology,* 2**,** 1-16.

BRATTEBO, B. O. & BOOTH, D. B. 2003. Long-term stormwater quantity and quality performance of permeable pavement systems. *Water Research,* 37**,** 4369-4376.

BROWN, L. C. & MAC BERTHOUEX, P. 2002. *Statistics for environmental engineers,* CRC press.

BSI 1981. Code of practice for site investigations. ***BS*** *5930:1981*. British Standards Institution

BSI 1990a. Methods of test for Soils for civil Engineering purposes — Part 1: General requirements and sample preparation. ***BS*** *1377-1*. British Standards Institution

BSI 1990b. Methods of test for Soils for civil engineering purposes — Part 4: Compaction-related tests. . ***BS*** *1377-4*. British Standards Institution

BSI 1990c. Methods of test for Soils for civil engineering purposes — Part 5: Compressibility, permeability and durability tests. ***BS*** *1377-5*. British Standards Institution

BSI 1996. Method for Determination of the Relative Hydraulic Conductivity of Permeable Surfacing. ***BS*** *DD 229:1996*. British Standards Institution

BSI 2002. Aggregates for unbound and hydraulically bound materials for use in civil engineering work and road construction. ***BS*** *EN 13242:2002*. British Standards Institution

BSI 2009. Pavements constructed with clay, natural stone or concrete pavers Part 13: Guide for the design of permeable pavements constructed with concrete paving blocks and flags, natural stone slabs and setts and clay pavers
BS *7533-13:2009*. British Standards Institution.

BUTLER, D. & DAVIES, J. 2004. *Urban drainage*, CRC Press.

CAHILL, T. 1994. A second look at porous pavement/underground recharge. *Watershed Protection Techniques* [Online]. Available: https://www7011.ssldomain.com/ncufc/uploads/porouspavement.pdf.

CAMPBELL-SCIENTIFIC 2012. *Instruction manual: CS650 and CS655 water content reflectometers* Logan, Utah, Campbell-Scientific, Inc.

CAMPBELL, N. S. 2004. *Diffuse pollution: an introduction to the problems and solutions*, IWA Publishing.

CEH 2009. Flood Estimation Handbook Software. *The FED CD-ROM 3.* Wallingford, UK: Wallingford HydroSolutions Ltd (WHS).

COLLINS, K. A., HUNT, W. F. & HATHAWAY, J. M. 2006. Evaluation of various types of permeable pavements with respect to water quality improvement and flood control. *8th International conference on concrete block paving.*

COLLINS, K. A., HUNT, W. F. & HATHAWAY, J. M. 2008. Hydrologic Comparison of Four Types of Permeable Pavement and Standard Asphalt in Eastern North Carolina. *Journal of Hydrologic Engineering,* 13**,** 1146-1157.

COOLEY, L. A., PROWELL, B. D. & BROWN, E. R. 2002. Issues pertaining to the permeability characteristics of coarse-graded Superpave mixes. *ASPHALT PAVING TECHNOLOGY,* 71**,** 1-29.

DAVIES, J., PRATT, C. & SCOTT, M. Laboratory study of permeable pavement systems to support hydraulic modelling. Proc. 9th Int. Conf. on Urban Drainage, 2002.

DAWSON, A. R. 2008. *Water in road structures: movement, drainage & effects*, Springer Science & Business Media.

DELETIC, A. & ORR, D. W. 2005. Pollution buildup on road surfaces. *Journal of Environmental Engineering.*

DICKIE, S., MCKAY, G., IONS, L. & SHAFFER, P. 2010. *Planning for SuDS - making it happen- C687 CIRIA,* London, CIRIA.

DIERKES, C., BENZE, W. & WELLS, J. 2002. Sustainable urban drainage and pollutant source control by infiltration. *Proc. Stormwater Industry Assn Regional Conf. Orange.*

DREELIN, E. A., FOWLER, L. & RONALD CARROLL, C. 2006. A test of porous pavement effectiveness on clay soils during natural storm events. *Water Research,* 40**,** 799-805.

DUIN, B. V., BROWN, C., CHU, A., MARSALEK, J. & VALEO, C. 2008. Characterization of Long-Term Solids Removal and Clogging Processes in Two Types of Permeable Pavement under Cold Climate Conditions. *Water Research***,** 1-10.

DZURIK, A. A. 2003. *Water resources planning,* Rowman & Littlefield.

ELLIS, J., D'ARCY, B. & CHATFIELD, P. 2002. Sustainable Urban-Drainage Systems and Catchment Planning. *Water and Environment Journal,* 16**,** 286-291.

ELLIS, J. B. & REVITT, D. M. 1982. Incidence of heavy metals in street surface sediments: solubility and grain size studies. *Water, Air, and Soil Pollution,* 17**,** 87-100.

FASSMAN, E. A., PH, D., ASCE, A. M. & BLACKBOURN, S. 2010. Urban Runoff Mitigation by a Permeable Pavement System over Impermeable Soils. *Journal of Hydrologic Engineering,* 15**,** 475-485.

FERGUSON, B. K. 2005. *Porous pavements*, CRC Press.

FERGUSON, B. K. 2006. Porous pavements: the making of progress in technology and design. *8th International Conference on Concrete Block Paving.*

FLETCHER, T., ANDRIEU, H. & HAMEL, P. 2013. Understanding, management and modelling of urban hydrology and its consequences for receiving waters: A state of the art. *Advances in Water Resources,* 51**,** 261-279.

FLETCHER, T. D., SHUSTER, W., HUNT, W. F., ASHLEY, R., BUTLER, D., ARTHUR, S., TROWSDALE, S., BARRAUD, S., SEMADENI-DAVIES, A., BERTRAND-KRAJEWSKI, J.-L., MIKKELSEN, P. S., RIVARD, G., UHL, M., DAGENAIS, D. & VIKLANDER, M. 2014. SUDS, LID, BMPs, WSUD

and more – The evolution and application of terminology surrounding urban drainage. *Urban Water Journal***,** 1-18.

FRANCEY, M. 2005. *WSUD Engineering Procedures: Stormwater*.

FUJITA, S. 1997. Measures to promote stormwater infiltration. *Water Science and Technology,* 36**,** 289-293.

FUJITA, Y., DING, W.-H. & REINHARD, M. 1996. Identification of wastewater dissolved organic carbon characteristics in reclaimed wastewater and recharged groundwater. *Water Environment Research,* 68**,** 867-876.

GILBERT, J. K. & CLAUSEN, J. C. 2006. Stormwater runoff quality and quantity from asphalt, paver, and crushed stone driveways in Connecticut. *Water Research,* 40**,** 826-832.

GOMEZ-ULLATE, E., BAYON, J. R., COUPE, S. & CASTRO-FRESNO, D. 2010. Performance of pervious pavement parking bays storing rainwater in the north of Spain. *Water Science and Technology,* 62**,** 615-621.

GOMEZ-ULLATE, E., CASTILLO-LOPEZ, E., CASTRO-FRESNO, D. & BAYON, J. R. 2011. Analysis and Contrast of Different Pervious Pavements for Management of Storm-Water in a Parking Area in Northern Spain. *Water Resources Management,* 25**,** 1525-1535.

GOPALAKRISHNAN, K. 2011. *Sustainable Highways, Pavements and Materials: An Introduction*, Transdependenz LLC.

HAWLEY, R. J. & BLEDSOE, B. P. 2011. How do flow peaks and durations change in suburbanizing semi-arid watersheds? A southern California case study. *Journal of Hydrology,* 405**,** 69-82.

HEAL, K., MCLEAN, N. & D'ARCY, B. 2004. SUDS and Sustainability. *26th Meeting of the Standing Conf. on Stormwater Source Control, Dunfermline.*

HERNGREN, L., GOONETILLEKE, A. & AYOKO, G. A. 2005. Understanding heavy metal and suspended solids relationships in urban stormwater using simulated rainfall. *Journal of environmental management,* 76**,** 149-158.

HOGLAND, W. & NIEMCZYNOWICZ, J. 1986. The unit Superstructure-A New Construction to prevent groundwater depletion. *BUDAPEST SYMPOSIUM.*

HUANG, H. J., CHENG, S. J., WEN, J. C. & LEE, J. H. 2008. Effect of growing watershed imperviousness on hydrograph parameters and peak discharge. *Hydrological processes,* 22**,** 2075-2085.

HUNT, W. F. & COLLINS, K. A. 2008. Permeable pavement: Research update and design implications. *North Carolina Cooperative Extension Service. Raleigh, NC* [Online].

INTEPAVE 2010. Permeable Pavements - Guide To The Design Construction and Maintenance of Concrete Block Permeable Pavements Interpave. Edition 6 ed. Leicester, UK: Interpave.

INTERPAVE 2010. Understanding Permeable Paving: Guidance for Designers, Developers, Planners and Local Authorities. Edition 3 ed. Leicester, UK: Interpave.

JACOBSON, C. R. 2011. Identification and quantification of the hydrological impacts of imperviousness in urban catchments: A review. *Journal of environmental management,* 92**,** 1438-1448.

KAYHANIAN, M., ANDERSON, D., HARVEY, J. T., JONES, D. & MUHUNTHAN, B. 2012. Permeability measurement and scan imaging to assess clogging of pervious concrete pavements in parking lots. *Journal of Environmental Management,* 95**,** 114-123.

KAYHANIAN, M., STRANSKY, C., BAY, S., LAU, S.-L. & STENSTROM, M. K. 2008. Toxicity of urban highway runoff with respect to storm duration. *Science of the total environment,* 389**,** 386-406.

LAMPE, L., BARRETT, M. & WOODS-BALLARD, B. 2004. *Post-project monitoring of BMPs/SUDS to determine performance and whole-life costs*, IWA Publishing.

LUCKE, T. & BEECHAM, S. 2011. Field investigation of clogging in a permeable pavement system. *Building Research & Information,* 39**,** 603-615.

MARSALEK, J. & SCHREIER, H. 2009. Innovation in Stormwater Management in Canada : The Way Forward. *Water Quality Research Journal of Canada*.

MARSHALLS 2013. Permeable Paving Design Guide. Elland, UK: Marshalls.

MARTIN, P. 2001. Sustainable urban drainage systems Best practice manual for England, Scotland, Wales and Northern Ireland - CIRIA report C523. London: Construction Industry Research Information Association

MET-OFFICE. 2013. *Royal Botanic Gardens Edinburgh climate - Met Office* [Online]. Met Office. Available: http://www.metoffice.gov.uk/public/weather/climate/gcvwqum6h [Accessed 02/06/2013.

MILLER, J. D., KIM, H., KJELDSEN, T. R., PACKMAN, J., GREBBY, S. & DEARDEN, R. 2014. Assessing the impact of urbanization on storm runoff in a peri-urban catchment using historical change in impervious cover. *Journal of Hydrology,* 515**,** 59-70.

MOULTON, L. K. 1980. Highway subdrainage design.

MULLANEY, J. & LUCKE, T. 2014. Practical review of pervious pavement designs. *CLEAN - Soil, Air, Water,* 42**,** 111-124.

NAPIER, F., D'ARCY, B. & JEFFERIES, C. 2008. A review of vehicle related metals and polycyclic aromatic hydrocarbons in the UK environment. *Desalination,* 226**,** 143-150.

NEWMAN, A. P., AITKEN, D. & ANTIZAR-LADISLAO, B. 2013. Stormwater quality performance of a macro-pervious pavement car park installation

equipped with channel drain based oil and silt retention devices. *Water research,* 47**,** 7327-36.

NNADI, E. O., NEWMAN, A. P. & PUEHMEIER, T. 2008. An Evaluation of the Use Of Stored Water Derived From Permeable Paving Systems for Irrigation Purposes. *International Conference on Urban Drainage.*

NOVOTNY, V. 2003. *Water quality: diffuse pollution and watershed management*, John Wiley & Sons.

OPHER, T. & FRIEDLER, E. 2010. Factors affecting highway runoff quality. *Urban Water Journal*.

PAGOTTO, C., LEGRET, M. & CLOIREC, P. L. E. 2000. Comparison Of The Hydraulic Behaviour And The Quality Of Highway Runoff Water. *Water research,* 34**,** 4446-4454.

PALLA, A., GNECCO, I., CARBONE, M., GAROFALO, G., LANZA, L. G. & PIRO, P. 2015. Influence of stratigraphy and slope on the drainage capacity of permeable pavements: laboratory results. *Urban Water Journal,* 12**,** 394-403.

PEZZANITI, D., BEECHAM, S. & KANDASAMY, J. 2009. Influence of clogging on the effective life of permeable pavements. *Proceedings of the ICE - Water Management,* 162**,** 211-220.

POLETO, C. & TASSI, R. 2012. *Sustainable Urban Drainage Systems*, INTECH Open Access Publisher.

PONCE, V. M. & HAWKINS, R. H. 1996. Runoff curve number: Has it reached maturity? *Journal of hydrologic engineering,* 1**,** 11-19.

PRATT, C. 1999. Use of permeable, reservoir pavement constructions for stormwater treatment and storage for re-use. *Water Science and Technology,* 39**,** 145-151.

PRATT, C., WILSON, S. & COOPER, P. 2002. *Source control using constructed pervious surfaces - CIRIA C582* London, Costruction Industry Research and Information Association.

PRATT, C. J. 1990. Permeable pavements for stormwater quality enhancement. *Urban Stormwater Quality Enhancement@ sSource Control, Retrofitting, and Combined Sewer Technology*. ASCE.

PRATT, C. J. 1997. Design guidelines for porous/permeable pavements. *Sustaining urban water resources in the 21st century* [Online]. Available: http://cedb.asce.org/cgi/WWWdisplay.cgi?9901963.

PRATT, C. J., MANTLE, J. & SCHOFIELD, P. 1995. UK research into the performance of permeable pavement, reservoir structures in controlling stormwater discharge quantity and quality. *Water Science and Technology,* 32**,** 63-69.

PRATT, C. J., MANTLE, J. D. G. & SCHOFIELD, P. A. 1989. Urban stormwater reduction and quality improvement through the use of permeable pavements. *Water Science & Technology,* 21**,** 769–778.

ROGER, S. & MONTREJAUD-VIGNOLES, M. 1998. Mineral, physical and chemical analysis of the solid matter carried by motorway runoff water. *Water Research*.

ROSEEN, R. M., BALLESTERO, T. P., HOULE, J. J., AVELLANEDA, P., BRIGGS, J., FOWLER, G. & WILDEY, R. 2009. Seasonal Performance Variations for Storm-Water Management Systems in Cold Climate Conditions. *Journal of Environmental Engineering,* 135**,** 128-137.

ROSEEN, R. M., BALLESTERO, T. P., HOULE, J. J., BRIGGS, J. F. & HOULE, K. M. 2012. Water Quality and Hydrologic Performance of a Porous Asphalt Pavement as a Storm-Water Treatment Strategy in a Cold Climate. *Journal of Environmental Engineering,* 138**,** 81-89.

RUSHTON, B. T. 2001. Low-impact parking lot design reduces runoff and pollutant loads. *Journal of Water Resources Planning and Management,* 127**,** 172-179.

SANSALONE, J. J. & BUCHBERGER, S. G. 1997. Partitioning and first flush of metals in urban roadway storm water. *Journal of Environmental engineering,* 123**,** 134-143.

SANSALONE, J. J. & CRISTINA, C. M. 2004. First flush concepts for suspended and dissolved solids in small impervious watersheds. *Journal of Environmental Engineering,* 130**,** 1301-1314.

SARTOR, J. D., BOYD, G. B. & AGARDY, F. J. 1974. Water pollution aspects of street surface contaminants. *Journal (Water Pollution Control Federation)*.

SCHLUTER, W. & JEFFERIES, C. 2002. Modelling the outflow from a porous pavement. *Urban Water,* 4**,** 245-253.

SCHLÜTER, W. & JEFFERIES, C. 2005. The real issues with in-ground SUDS in Scotland. *10th International Conference on Urban Drainage, Copenhagen, Denmark, August 21-26, 2005.* Institute of Environment & Resources, Technical University of Denmark/IAHR/IWA.

SCHOLZ, M. 2013. Water Quality Improvement Performance of Geotextiles Within Permeable Pavement Systems: A Critical Review. *Water,* 5**,** 462-479.

SCHOLZ, M. & GRABOWIECKI, P. 2007. Review of permeable pavement systems. *Building and Environment,* 42**,** 3830-3836.

SCHUELER, T. R. 1987. *Controlling urban runoff: A practical manual for planning and designing urban BMPs*, Department of Environmental Programs, Metropolitan Washington Council of Governments.

SELBIG, W. R. & BANNERMAN, R. T. 2011. Characterizing the size distribution of particles in urban stormwater by use of fixed-point sample-collection methods. US Geological Survey.

SHACKEL, B., BEECHAM, S., PEZZANITI, D. & MYERS, B. 2008. Design of permeable pavements for Australian conditions. *23rd ARRB Conference - Research Partnering with Practitioners, Adelaide Australia, 2008.*

SHAFFER, P., WILSON, S., BRINDLE, F., BAFFOE-BONNIE, B., PRESCOTT, C. & TARBET, N. 2009. Understanding permeable and impermeable surfaces: technical report on surfacing options and cost benefit analysis. London.

SIEKER, F. & ZIMMERMAN, U. 2001. Source Control Measures for Stormwater Runoff in Urban Areas. *Advances in Urban Stormwater and Agricultural ….*

SIPES, J. L. 2010. *Sustainable solutions for water resources: policies, planning, design, and implementation*, John Wiley & Sons.

SMITH, D. R. 2006. *Permeable Interlocking Concrete Pavements: Selection, Design, Construction, Maintenance*, Interlocking Concrete Pavement Institute.

STARKE, P., GÖBEL, P. & COLDEWEY, W. G. 2011. Effects on evaporation rates from different water-permeable pavement designs. *Water science and technology : a journal of the International Association on Water Pollution Research,* 63**,** 2619-27.

STONE, M. & MARSALEK, J. 1996. Trace metal composition and speciation in street sediment: Sault Ste. Marie, Canada. *Water, Air, and Soil Pollution*.

SUTHERLAND, R. A. 2003. Lead in grain size fractions of road-deposited sediment. *Environmental Pollution*.

TRERRAM. 2012. TERRAM Fiberweb Geosynthetics Ltd. Available: file:///C:/Users/ma773/Downloads/Standard_BC_geotextiles_product_data_sheet%20(2).pdf [Accessed 20/01/2012 2012].

TYNER, J. S., WRIGHT, W. C. & DOBBS, P. A. 2009. Increasing exfiltration from pervious concrete and temperature monitoring. *Journal of Environmental Management,* 90**,** 2636-2641.

USEPA 1999. Storm Water Technology Fact Sheet: Porous Pavement. United States Environmental Protection Agency. Washington: EPA.

USEPA 2003. Protecting Water Quality from Urban Runoff. United States Environmental Protection Agency. EPA.

VAZE, J. & CHIEW, F. H. S. 2002. Experimental study of pollutant accumulation on an urban road surface. *Urban Water,* 4**,** 379-389.

VIGNOLES, M. & HERREMANS, L. 1995. Metal contamination in motorway surface runoff water. *Proc., Water Environmental Federation 68th Annual Conf. Exposition.*

WILD, T., JEFFERIES, C. & D'ARCY, B. 2002. SUDS in Scotland: the Scottish SUDS database - Final Report SR(02)51. Edinburgh, Scotland: SNIFFER.

WILSON, C., CLARKE, R., D'ARCY, B., HEAL, K. & WRIGHT, P. 2005. Persistent pollutants urban rivers sediment survey: implications for pollution control. *Water Science & Technology,* 51**,** 217-224.

WILSON, S., BRAY, R. & COOPER, P. 2004. *Sustainable drainage systems - CIRIA C609,* London, Construction Industry Research Information Association

WOODS-BALLARD, B., KELLAGHER, R., MARTIN, P., JEFFERIES, C., BRAY, R. & SHAFFER, P. 2007. *The SUDS manual - CIRIA C697* London, Construction Industry Research Information Association

WRIGHT, G., ARTHUR, S., BASTIEN, N., BOWLES, G. & UNWIN, D. 2010. Extent and cost of designing and constructing small areas of hardstanding around new and existing, domestic and non-domestic buildings. *The Scottish Government. Directorate for the Built Environment, Building Standards Division.*

YONG, C. F., MCCARTHY, D. T. & DELETIC, A. 2013. Predicting physical clogging of porous and permeable pavements. *Journal of Hydrology,* 481**,** 48-55.

ZANDERS, J. 2005. Road sediment: characterization and implications for the performance of vegetated strips for treating road run-off. *Science of the Total Environment,* 339**,** 41-47.

ZHAO, H. & LI, X. 2013. Understanding the relationship between heavy metals in road-deposited sediments and washoff particles in urban stormwater using simulated rainfall. *Journal of hazardous materials,* 246**,** 267-276.

Appendix A Sub-grade Test

Determination of dry density/ moisture content relationship (Proctor Test)

The test was carried out in accordance with clause 4 of BS 1377-5:1990. Using method 2.5 kg rammer for soils with particle up to medium gravel size. The test producers are described in the standard.

Table A - 1: Data dry density (kg/m3) and water content (%)

Density						
	Mass of mould & soil (g)	**Mass of mould (g)**	**Mass of soil (g)**	**Density (kg/m3)**	**Dry density (kg/m3)**	
1	3656	2926	730	778.45	777.28	
2	3720	2926	794	846.70	846.08	
3	3767	2926	841	896.81	896.15	
4	3806	2926	880	938.40	937.69	
5	3875	2926	949	1011.98	1011.21	
6	3791	2926	865	922.41	921.69	
7	3767	2926	841	896.81	896.13	
Water content						
Container number	**Mass of sample & container (g)**	**Mass of dry sample & container (g)**	**Mass of water (g)**	**Mass of container (g)**	**Mass of dry soil (g)**	**Water content (%)**
1	60.1	58.1	150	9.8	48.3	4.14
2	60.5	57.2	72.6	9.6	47.6	6.93
3	46.4	43.4	74.4	9.6	33.8	8.88
4	51.4	47.2	75.6	9.7	37.5	11.20
5	63.3	57.2	76.5	9.8	47.4	12.87
6	76.1	66.9	77.8	9.9	57	16.14
7	74.4	64	76	9.7	54.3	19.15

Determination of permeability of sand by the constant-head method

The test was carried out in accordance with clause 5 of BS 1377-5:1990. The test producers are described in the standard. The coefficient of permeability *k* (m/s) was obtained from the Equation:

$K = (q/i) / (R_t/A)$

$$\boldsymbol{k = (\frac{q}{i})/(\frac{R_t}{A})} \quad \textbf{(19)}$$

Where

q= flow rate (mL/s)

i= hydraulic gradient (i=h/y) where, h is the difference between the two manometer kevels (mm), y is the difference between the corresponding gland points (mm).

A = the area of cross section of the sample (mm^2)

R_t = Temperature correction factor for the viscosity of water to standardize the permeability to 20 °C.

Analysis

The area of cross section is 4359.3 mm^2. The hydraulic gradient is 3.80 and 4.14 for Test 1 and 2 (respectively). R_T is 1.1 and 1 for test 1 and 2, respectively (accordance with Figure 4 in the standard). Thus, by applying pervious equation the test results are shown in Table 8.2 and 8.3:

Table A - 2: Data Test No. 1 - Date 19/11/2011 and water temperature was 17 °C

Test No.	Time (sec)	Outflow volume (ml)	q (mL/sec)	Water Temperature °C	K_T (m/s)	*K*20 (m/s)	*K*20 (mm/h)
1	120	130	1.08	17	6.54E-05	7.20E-05	259.11
2	120	130	1.08	17	6.54E-05	7.20E-05	259.11
3	180	190	1.06	17	6.38E-05	7.01E-05	252.46
4	240	200	0.83	17	5.03E-05	5.54E-05	199.31
Average					6.12E-05	6.74E-05	242.50

Table A - 3: Data Test No. 1 - Date 20/11/2011 and water temperature was 20 °C

Test No.	Time (sec)	Outflow volume (ml)	q (mL/sec)	Water Temperature °C	K_T (m/s)	*K*20 (m/s)	*K*20 (mm/h)
1	120	130	1.08	17	5.54E-05	5.54E-05	199.27
2	120	130	1.08	17	5.54E-05	5.54E-05	199.27
3	180	190	1.06	17	5.54E-05	5.54E-05	199.27
4	240	200	0.83	17	5.27E-05	5.27E-05	189.75
5	240	200	0.83	18	5.32E-05	5.32E-05	191.41
Average					5.44E-05	5.44E-05	195.79

Therefore the average coefficient of permeability k, which obtained from both test is 219.15 (mm/h).

Appendix B Rainfall simulator calibration

Table B - 1: Measured flow rate from 9 nozzles for 14 times

Test No.	**Nozzles number**								
	1	**2**	**3**	**4**	**5**	**6**	**7**	**8**	**9**
	Flow rate (L/h)								
1	2.91	3.01	2.68	3.13	2.69	2.91	2.96	2.13	2.62
2	2.99	3.10	2.78	3.23	2.78	3.00	3.04	2.53	2.71
3	3.01	3.12	2.79	3.24	2.80	3.02	3.06	2.55	2.73
4	3.00	3.12	2.79	3.29	2.89	3.02	3.05	2.55	2.73
5	2.95	3.09	2.75	3.24	2.88	2.99	3.00	2.47	2.70
6	2.94	3.06	2.73	3.22	2.87	2.96	3.00	3.86	2.68
7	2.97	3.10	2.76	3.26	2.97	2.99	3.03	3.46	2.70
8	3.00	3.12	2.78	3.31	2.99	3.02	3.05	2.54	2.72
9	2.98	3.10	2.76	3.29	2.98	3.00	3.03	2.53	2.71
10	2.96	3.09	2.76	3.27	2.96	2.99	3.01	2.50	2.68
11	2.93	3.06	2.73	3.25	2.94	2.96	2.98	2.48	2.65
12	2.99	3.11	2.79	3.31	2.98	3.01	3.04	2.53	2.72
13	2.96	3.14	2.84	3.34	3.12	3.14	3.02	2.50	2.69
14	2.93	3.05	2.74	3.24	2.92	2.95	2.98	2.52	2.64
Avera	2.97	3.09	2.76	3.26	2.91	3.00	3.02	2.65	2.69
SD	0.03	0.04	0.04	0.05	0.11	0.05	0.03	0.45	0.03

Table B- 2: Average water volume for 81 cups at duration 15 minutes

Cup No.	Water volume (ml)								
	1	2	3	4	5	6	7	8	9
A	17.27	15.5	19.05	23.53	19.84	18.58	24.82	37.63	17.78
B	122.66	18.93	19.37	45.86	66.02	26.17	28.28	52.26	30.54
C	28.45	14.92	15.85	19.79	22.89	19.29	21.12	23.34	18.31
D	15.99	12.97	13.12	15.96	18.4	21.54	62.51	42.3	14.49
E	72.55	17.26	13.41	15.51	38.84	51.07	43.32	25.17	13.61
F	83.66	33.39	14.92	14.14	32.43	54.42	24.51	17.68	13.18
G	20.9	18.19	15.64	20.35	32.21	19.59	15.73	14.82	13.82
H	19.9	21.35	19.42	42.64	70.49	21.84	13.59	22.97	43.91
L	75.92	69.68	20.15	19.31	16	14.79	13.96	32.75	62.21

Table B- 3: Average water volume for 81 cups at duration 30 minutes

Cup No.	Water volume (ml)								
	1	2	3	4	5	6	7	8	9
A	34.92	31.05	41.32	51.68	41.78	39.88	55.56	76.92	37.63
B	137.06	54.01	42.22	101.93	132.86	56.01	44.51	108.06	69.34
C	59.97	31.88	34.11	38.34	39	39.03	41.16	45.72	28.56
D	32.44	27.01	27.31	33.22	39.75	46.26	131.8	84.35	31.11
E	131.22	35.3	27.53	30.93	102.58	122.88	90.58	63.07	29.35
F	139.78	69.16	31.42	27.79	60.46	108.73	53.16	39.85	26.97
G	40.8	36.28	31.21	42.77	68.8	45.34	33.58	32.99	29.57
H	33.76	47.59	42.17	84.46	119.15	56.4	30.37	55.54	94.34
L	115.64	138.54	46.22	38.9	31.83	29.86	28.41	57.94	126.94

Table B- 4: Average water volume for 81 cups at duration 45 minutes

Cup No.	Water volume (ml)								
	1	2	3	4	5	6	7	8	9
A	58.38	51.24	59.59	72.52	60.54	57.73	75.33	124.88	57.43
B	162.51	73.17	64.47	119.75	157.37	67.49	70.92	122.19	82
C	77.83	50.5	55.07	61.65	59.69	57.88	62.5	66.86	49.05
D	50.46	46.49	47.01	51.65	58.54	62.76	146.95	91.15	50.9
E	138.3	55.5	47.39	52.67	98.73	136.87	109.34	71.01	48.51
F	158.85	89.71	51.44	48.24	80.78	140.43	69.18	56.43	48.06
G	60.41	58.58	51.21	62.84	80.03	70.91	53.38	52.86	48.8
H	55.33	72.72	60.77	99.73	135.29	85.31	50.47	77.39	89.85
L	157.75	53.74	61.53	58.85	52.18	50.82	49.41	89.11	148.68

Table B- 5: Average water volume for 81 cups at duration 60 minutes

Cup No.	Water volume (ml)								
	1	2	3	4	5	6	7	8	9
A	146.87	95.11	144.82	153.18	146.1	133.87	152.84	145.99	132.44
B	149.5	152.81	145.48	153.97	153.41	149.75	153.07	152.75	148.85
C	156.71	103.42	109.21	144.8	134.66	125.85	147.02	149.86	73.91
D	100.25	65.95	68.93	88.78	120.95	135.12	150.65	155.51	109.06
E	147.88	90.66	70.06	94.14	152.02	153.23	154.84	149.63	85.01
F	150.95	149.3	93.01	78.58	157.25	151.63	153.04	140.38	76.27
G	161.62	139.89	93.41	140.09	156.45	155.58	109.91	103.04	80.67
H	123.33	149.84	132.78	148.98	151.79	152.71	79.4	151.88	149.21
L	149.2	151.14	149.85	117.81	81.85	66.89	67.27	148.91	153.47

Table B- 6: Calibration data for flow meter – Test No. 1

Test No.	Glass Weight (g)	Total Weight (g)	Net Weight (g)	Duration (min)	Flow Rate (L/min)	Output Voltage (v)
1	251.97	653.75	401.78	1	0.40178	1.909869272
2	251.97	650.38	398.41	1	0.39841	1.791187555
3	251.97	647.71	395.74	1	0.39574	1.66825108
4	251.97	645.03	393.06	1	0.39306	1.515489366
5	251.97	642.38	390.41	1	0.39041	1.359277755
6	251.97	638.33	386.36	1	0.38636	1.185167101
7	251.97	631.73	379.76	1	0.37976	1.021590583

Table B- 7: Calibration data for flow meter – Test No. 2

Test No.	Glass Weight (g)	Total Weight (g)	Net Weight (g)	Duration (min)	Flow Rate (L/min)	Output Voltage (v)
1	251.97	658.09	406.12	1	0.40612	1.897868704
2	251.97	649.7	397.73	1	0.39773	1.582134118
3	251.97	639.92	387.95	1	0.38795	1.113059933
4	251.97	644	392.03	1	0.39203	1.389277755
5	251.97	640	388.03	1	0.38803	1.209711217

Table B- 8: Calibration data for flow meter – Test No. 3

Test No.	Glass Weight (g)	Total Weight (g)	Net Weight (g)	Duration (min)	Flow Rate (L/min)	Output Voltage (v)
1	251.97	652.69	400.72	1	0.40072	1.86826016
2	251.97	650.01	398.04	1	0.39804	1.815147722
3	251.97	647.99	396.02	1	0.39602	1.754808224
4	251.97	644.53	392.56	1	0.39256	1.641246574
5	251.97	642.72	390.75	1	0.39075	1.487071783
6	251.97	643.41	391.44	1	0.39144	1.586107846
7	251.97	637.19	385.22	1	0.38522	1.246857727
8	251.97	630.5	378.53	1	0.37853	0.998559058
9	251.97	639.06	387.09	1	0.38709	1.365713703

Table B- 9: Calibration data for flow meter – Test No. 4

Test No.	Glass Weight (g)	Total Weight (g)	Net Weight (g)	Duration (min)	Flow Rate (L/min)	Output Voltage (v)
1	251.97	653.77	401.8	1	0.4018	1.874428752
2	251.97	651.43	399.46	1	0.39946	1.809997136
3	251.97	650.43	398.46	1	0.39846	1.705214605
4	251.97	637.86	385.89	1	0.38589	1.241830419
5	251.97	631.06	379.09	1	0.37909	0.998633354
6	251.97	643.13	391.16	1	0.39116	1.381455105
7	251.97	646.81	394.84	1	0.39484	1.624757562
8	251.97	643.7	391.73	1	0.39173	1.518513884
9	251.97	635.87	383.9	1	0.3839	1.101156283

Appendix C CS650 TDR probes calibration data

Table C - 1: Test No. 1 - Output data during calibration CS650 TDR probe (interval 60 minutes)

Time (min)	**Moisture content (%)**							
	5%	7%	10%	12%	15%	18%	20%	23%
	The bulk dielectric permittivity of the sand (Ka)							
60	3.94	5.28	7.21	8.94	11.39	12.30	13.64	14.49
120	3.95	5.28	7.20	8.94	11.40	12.30	13.63	14.48
180	3.95	5.28	7.20	8.94	11.41	12.30	13.63	14.48
240	3.96	5.28	7.20	8.93	11.42	12.30	13.63	14.48
300	3.95	5.28	7.20	8.93	11.43	12.30	13.63	14.48
360	3.95	5.29	7.21	8.95	11.43	12.31	13.64	14.49
420	3.95	5.29	7.21	8.95	11.45	12.31	13.64	14.49
480	3.96	5.29	7.21	8.94	11.46	12.31	13.64	14.49
540	3.96	5.29	7.21	8.95	11.46	12.31	13.64	14.49
600	3.97	5.30	7.22	8.96	11.47	12.32	13.65	14.50
660	3.97	5.30	7.22	8.96	11.47	12.32	13.66	14.51
720	3.97	5.30	7.22	8.95	11.47	12.32	13.65	14.50
780	3.98	5.30	7.22	8.95	11.48	12.32	13.65	14.50
840	3.98	5.30	7.22	8.95	11.48	12.32	13.65	14.50
900	3.98	5.30	7.22	8.95	11.48	12.32	13.65	14.50
960	3.99	5.30	7.22	8.95	11.50	12.32	13.65	14.50
1020	3.99	5.29	7.22	8.95	11.49	12.31	13.65	14.50
1080	3.99	5.30	7.22	8.95	11.51	12.32	13.65	14.50
1140	3.99	5.30	7.22	8.95	11.51	12.32	13.65	14.50
1200	3.99	5.30	7.22	8.96	11.52	12.32	13.65	14.50
1260	3.99	5.28	7.20	8.93	11.53	12.30	13.63	14.48
1320	3.98	5.29	7.22	8.95	11.53	12.31	13.65	14.50
1380	4.00	5.30	7.22	8.95	11.53	12.32	13.65	14.50
1440	4.00	5.29	7.21	8.94	11.53	12.31	13.64	14.49
1500	4.00	5.30	7.22	8.96	11.55	12.32	13.65	14.50
1560	4.00	5.30	7.22	8.96	11.55	12.32	13.66	14.51

1620	4.00	5.30	7.22	8.96	11.55	12.32	13.66	14.51
1680	4.00	5.30	7.22	8.96	11.54	12.32	13.66	14.51
1740	4.00	5.30	7.22	8.96	11.54	12.32	13.65	14.50
1800	4.00	5.30	7.22	8.96	11.54	12.32	13.66	14.51
1860	4.00	5.30	7.22	8.96	11.56	12.32	13.65	14.50
1920	4.00	5.30	7.22	8.96	11.56	12.32	13.65	14.50
1980	4.00	5.30	7.22	8.96	11.56	12.32	13.65	14.50
2040	4.00	5.30	7.22	8.96	11.55	12.32	13.65	14.50
2100	4.01	5.30	7.22	8.96	11.55	12.32	13.65	14.50
2160	4.01	5.30	7.22	8.95	11.55	12.32	13.65	14.50
2220	4.01	5.30	7.22	8.96	11.55	12.32	13.65	14.50
2280	4.01	5.30	7.22	8.95	11.55	12.32	13.65	14.50
2340	4.01	5.30	7.22	8.96	11.55	12.32	13.65	14.50
2400	4.01	5.30	7.22	8.95	11.55	12.32	13.65	14.50
2460	4.01	5.30	7.22	8.96	11.55	12.32	13.65	14.50
2520	4.01	5.30	7.22	8.96	11.57	12.32	13.66	14.51
2580	4.01	5.30	7.22	8.95	11.58	12.32	13.65	14.50
2640	4.00	5.29	7.21	8.95	11.57	12.31	13.64	14.49
2700	4.00	5.30	7.23	8.96	11.57	12.32	13.66	14.51
2760	4.00	5.29	7.21	8.95	11.57	12.31	13.65	14.50
2820	4.01	5.30	7.23	8.96	11.59	12.32	13.66	14.51
Average	3.99	5.29	7.22	8.95	11.51	12.31	13.65	14.50

Table C - 2: Test No. 2 - Output data during calibration CS650 TDR probe (interval 60 minutes)

Time (min)	Moisture content (%)							
	5%	7%	10%	12%	15%	18%	20%	23%
	The bulk dielectric permittivity of the sand (Ka)							
60.00	4.13	5.24	6.94	8.87	11.42	12.41	13.56	14.33
120.00	4.13	5.23	6.98	8.86	11.45	12.40	13.56	14.32
180.00	4.14	5.23	6.99	8.86	11.47	12.40	13.56	14.32
240.00	4.14	5.23	7.00	8.86	11.49	12.40	13.56	14.32
300.00	4.14	5.23	7.01	8.86	11.49	12.40	13.56	14.32
360.00	4.14	5.24	7.02	8.87	11.50	12.41	13.57	14.33
420.00	4.14	5.24	7.04	8.87	11.51	12.41	13.57	14.33
480.00	4.14	5.24	7.05	8.87	11.51	12.41	13.57	14.33
540.00	4.14	5.24	7.03	8.87	11.51	12.41	13.57	14.33
600.00	4.14	5.25	7.05	8.88	11.51	12.42	13.58	14.34
660.00	4.14	5.25	7.05	8.88	11.52	12.43	13.58	14.35
720.00	4.14	5.25	7.06	8.88	11.52	12.42	13.58	14.34
780.00	4.14	5.25	7.06	8.88	11.52	12.42	13.58	14.34
840.00	4.14	5.25	7.07	8.88	11.52	12.42	13.58	14.34
900.00	4.14	5.25	7.08	8.88	11.54	12.42	13.58	14.34
960.00	4.14	5.25	7.08	8.88	11.54	12.42	13.57	14.34
1020.00	4.14	5.25	7.08	8.88	11.54	12.42	13.57	14.34
1080.00	4.14	5.25	7.09	8.88	11.53	12.42	13.57	14.34
1140.00	4.14	5.25	7.09	8.88	11.53	12.42	13.57	14.34
1200.00	4.14	5.25	7.10	8.88	11.53	12.42	13.58	14.34
1260.00	4.14	5.23	7.11	8.86	11.53	12.40	13.56	14.32
1320.00	4.15	5.25	7.11	8.88	11.53	12.42	13.57	14.34
1380.00	4.15	5.25	7.13	8.88	11.53	12.42	13.57	14.34
1440.00	4.15	5.24	7.12	8.87	11.53	12.41	13.56	14.33
1500.00	4.15	5.25	7.12	8.88	11.52	12.42	13.58	14.34
1560.00	4.15	5.25	7.14	8.88	11.52	12.43	13.58	14.35
1620.00	4.15	5.25	7.14	8.88	11.52	12.43	13.58	14.35

1680.00	4.15	5.25	7.13	8.88	11.54	12.43	13.58	14.35
1740.00	4.15	5.25	7.14	8.88	11.54	12.42	13.58	14.34
1800.00	4.15	5.25	7.13	8.88	11.54	12.43	13.58	14.35
1860.00	4.15	5.25	7.13	8.88	11.54	12.42	13.58	14.34
1920.00	4.15	5.25	7.13	8.88	11.53	12.42	13.58	14.34
1980.00	4.16	5.25	7.14	8.88	11.53	12.42	13.58	14.34
2040.00	4.16	5.25	7.14	8.88	11.53	12.42	13.58	14.34
2100.00	4.16	5.25	7.14	8.88	11.53	12.42	13.58	14.34
2160.00	4.16	5.25	7.14	8.88	11.53	12.42	13.57	14.34
2220.00	4.16	5.25	7.14	8.88	11.53	12.42	13.58	14.34
2280.00	4.16	5.25	7.16	8.88	11.53	12.42	13.57	14.34
2340.00	4.16	5.25	7.15	8.88	11.53	12.42	13.58	14.34
2400.00	4.16	5.25	7.15	8.88	11.53	12.42	13.58	14.34
2460.00	4.16	5.25	7.15	8.88	11.54	12.42	13.58	14.34
2520.00	4.16	5.25	7.15	8.88	11.55	12.43	13.58	14.35
2580.00	4.15	5.25	7.15	8.88	11.54	12.42	13.57	14.34
2640.00	4.15	5.24	7.16	8.87	11.54	12.41	13.57	14.33
2700.00	4.16	5.26	7.16	8.89	11.54	12.43	13.58	14.35
2760.00	4.16	5.24	7.16	8.87	11.54	12.42	13.57	14.34
2820.00	4.16	5.26	7.16	8.89	11.54	12.43	13.58	14.35
Average	4.15	5.25	7.10	8.88	11.52	12.42	13.57	14.34

Appendix D Rain event analysis

Table D - 1: Individual Rainfall event analysis for Rainfall intensity - 1

Event no.	Start of rainfall event	Rainfall	Outflow	Ratio of outflow to inflow	During storm outflow	Duration	Start Delay to discharge	Value of outflow peak	Time delay to peak discharge	Time delay to discharge	Rainfall intensity	Outflow rate	Ratio of outflow peak to rainfall intensity	Retention	Cumulative retention
	(dd/mm/yy)	(mm)	(mm)	(%)	(mm)	(h)	(min)	(L h^{-1})	(min)	(min)	(mm h^{-1})	(%)	(%)	(mm)	(mm)
R1	08/10/12	6.49		0.00							25.12		0.00	6.49	6.49
R2	10/10/12	6.46		0.00							25.01		0.00	6.46	12.95
R3	12/10/12	6.49	0.99	15.27	0.06	2.70	10.00	2.64	21.13	10.00	25.14	10.50	10.50	5.50	18.45
R4	15/10/12	6.41	0.48	7.43	0.02	0.93	10.63	1.656	16.13	10.63	24.40	6.79	6.79	6.02	24.48
R5	16/10/12	6.45	1.70	26.39	0.15	9.54	8.00	3.864	19.13	8.00	24.21	15.96	15.96	4.75	29.23
R6	17/10/12	6.45	2.30	35.67	0.16	10.59	8.00	4.752	19.13	8.00	24.18	19.65	19.65	4.15	33.38
R7	18/10/12	6.46	2.50	38.69	0.21	10.88	7.00	5.448	18.13	7.00	24.24	22.48	22.48	3.96	37.34
R8	19/10/12	6.45	2.83	43.82	0.23	10.89	7.00	5.976	19.13	7.00	24.18	24.72	24.72	3.62	40.96
R9	22/10/12	6.39	0.51	7.95	0.10	0.80	10.13	2.184	17.13	10.13	23.97	9.11	9.11	5.88	46.85
R10	23/10/12	6.46	2.07	32.05	0.24	8.94	8.00	5.424	18.63	8.00	24.21	22.40	22.40	4.39	51.23
R11	24/10/12	6.44	2.52	39.06	0.19	10.52	8.00	5.904	19.13	8.00	24.16	24.44	24.44	3.93	55.16
R12	25/10/12	6.43	2.31	35.94	0.29	10.47	7.00	6.336	18.63	7.00	24.10	26.29	26.29	4.12	59.27
R13	26/10/12	6.47	2.45	37.81	0.23	9.55	8.00	6.288	18.63	8.00	24.27	25.91	25.91	4.03	63.30

Table D - 2: Individual Rainfall event analysis for Rainfall intensity - 2

Event no.	Start of rainfall event	Rainfall	Outflow	Ratio of outflow to inflow	During storm outflow	Duration	Start Delay to discharge	Value of outflow peak	Time delay to peak discharge	Time delay to discharge	Rainfall intensity	Outflow rate	Ratio of outflow peak to rainfall intensity	Retention	Cumulative retention
	(dd/mm/yy)	(mm)	(mm)	(%)	(mm)	(h)	(min)	(L h^{-1})	(min)	(min)	(mm h^{-1})	(%)	(%)	(mm)	(mm)
R14	29/10/12	7.72	0.67	8.62	0.21	1.91	10.00	3	15.00	10.00	28.97	10.36	10.36	7.06	70.36
R15	30/10/12	7.82	3.40	43.35	0.39	11.05	8.00	5.376	18.50	8.00	29.39	18.29	18.29	4.44	74.80
R16	31/10/12	7.82	3.25	41.47	0.26	10.78	8.00	5.76	18.47	8.00	29.34	19.63	19.63	4.58	79.38
R17	01/11/12	7.84	3.49	44.68	0.26	10.66	8.00	6.096	18.55	8.00	29.33	20.79	20.79	4.33	83.70
R18	02/11/12	7.83	3.07	39.16	0.23	9.99	8.87	6.384	18.37	8.87	29.44	21.69	21.69	4.78	88.48
R19	05/11/12	7.80	0.68	8.72	0.17	2.77	10.33	3.096	16.33	10.33	29.33	10.55	10.55	7.14	95.62
R20	06/11/12	7.81	2.91	37.24	0.25	9.07	8.00	5.712	18.40	8.00	29.30	19.50	19.50	4.90	100.52
R21	07/11/12	7.81	3.60	46.13	0.31	10.48	7.00	6.24	17.97	7.00	29.29	21.30	21.30	4.21	104.73
R22	08/11/12	7.82	3.85	49.13	0.26	10.58	8.00	6.408	18.03	8.00	29.36	21.83	21.83	3.98	108.71
R23	09/11/12	7.83	3.62	46.41	0.29	10.10	8.00	6.888	18.62	8.00	29.29	23.52	23.52	4.19	112.90
R24	12/11/12	7.76	0.65	8.35	0.24	1.05	10.32	2.904	17.32	10.32	29.19	9.95	9.95	7.13	120.03
R25	13/11/12	7.79	2.78	35.71	0.24	10.36	8.50	5.76	17.38	8.50	29.22	19.71	19.71	5.01	125.04
R26	14/11/12	7.79	3.29	42.29	0.20	10.13	8.50	6.312	18.45	8.50	29.20	21.62	21.62	4.49	129.54
R27	15/11/12	7.86	3.88	49.36	0.28	10.11	8.00	6.744	19.52	8.00	29.49	22.87	22.87	3.98	133.52
R28	16/11/12	7.77	2.90	36.84	0.28	11.14	8.50	6.624	17.08	8.50	29.51	22.44	22.44	4.97	138.49

Table D - 3: Individual Rainfall event analysis for Rainfall intensity - 3

Event no.	Start of rainfall event	Rainfall	Outflow	Ratio of outflow to inflow	During storm outflow	Duration	Start Delay to discharge	Value of outflow peak	Time delay to peak discharge	Time delay to discharge	Rainfall intensity	Outflow rate	Ratio of outflow peak to rainfall intensity	Retention	Cumulative retention
	(dd/mm/yy)	(mm)	(mm)	(%)	(mm)	(h)	(min)	(L h^{-1})	(min)	(min)	(mm h^{-1})	(%)	(%)	(mm)	(mm)
R29	19/11/12	11.06	1.71	15.46	0.67	1.68	10.23	3.6	18.22	10.23	21.26	16.93	16.93	9.36	147.85
R30	20/11/12	11.07	5.94	53.39	2.57	9.01	8.00	13.56	31.78	8.00	21.82	62.14	62.14	5.18	153.03
R31	21/11/12	11.09	7.45	67.17	3.36	10.61	8.33	14.712	31.83	8.33	21.86	67.31	67.31	3.64	156.67
R32	22/11/12	11.08	6.83	61.63	3.01	11.28	7.90	14.352	30.90	7.90	21.21	67.66	67.66	4.25	160.92
R33	23/11/12	11.08	6.86	62.04	3.28	9.74	7.47	15.312	30.97	7.47	21.78	70.30	70.30	4.20	165.12
R34	26/11/12	11.07	2.08	17.53	0.49	0.94	10.50	2.952	18.00	10.50	22.93	12.87	12.87	9.77	174.89
R35	27/11/12	11.08	6.72	56.90	3.35	9.08	8.50	13.344	32.50	8.50	22.84	58.41	58.41	5.09	179.98
R36	28/11/12	11.08	6.67	56.52	2.58	10.53	8.00	14.16	32.00	8.00	22.83	62.03	62.03	5.13	185.10
R37	29/11/12	11.08	6.05	51.29	2.23	11.20	7.50	14.232	31.00	7.50	22.81	62.39	62.39	5.74	190.84
R38	30/11/12	11.08	7.29	61.87	4.06	9.57	7.00	14.928	30.00	7.00	22.82	65.42	65.42	4.49	195.34
R39	03/12/12	11.07	2.20	19.85	0.89	0.67	9.80	3.216	17.30	9.80	21.00	15.32	15.32	8.86	204.20
R40	04/12/12	11.07	5.52	50.12	2.56	8.17	7.88	13.224	31.88	7.88	21.81	60.62	60.62	5.49	209.70
R41	05/12/12	11.07	6.27	57.00	2.87	10.38	8.20	14.28	31.70	8.20	21.64	65.99	65.99	4.73	214.43
R42	06/12/12	11.08	6.90	62.76	2.96	10.33	7.28	14.304	31.78	7.28	20.99	68.13	68.13	4.10	218.52
R43	07/12/12	11.08	7.04	64.03	3.03	11.35	7.85	14.28	30.85	7.85	21.64	65.99	65.99	3.95	222.47
Total		370.69	148.21												222.47

Table D – 4: Analysis of the mass balance of the measured water fluxes in the hydrology experiment.

Days	Rainfall volume (L)	evaporation (L)	Outflow (L)	Measured Retention (L)	Estimated Retention(L)	Unaccountable Water (%)
1	6.49	0.72	0.00	5.77	4.21	-36.89
3	6.46	0.72	0.00	5.74	4.25	-35.14
5	6.49	0.72	0.99	4.78	4.31	-11.02
8	6.41	0.72	0.48	5.20	4.33	-20.29
9	6.45	0.72	1.70	4.03	4.33	6.91
10	6.45	0.72	2.30	3.43	4.34	21.10
11	6.46	0.72	2.50	3.24	4.35	25.47
12	6.45	0.72	2.83	2.90	4.35	33.36
15	6.39	0.72	0.51	5.16	4.36	-18.54
16	6.46	0.72	2.07	3.67	4.36	15.92
17	6.44	0.72	2.52	3.21	4.37	26.58
18	6.43	0.72	2.31	3.40	4.37	22.27
19	6.47	0.72	2.45	3.31	4.37	24.38
22	7.72	0.72	0.67	6.34	4.36	-45.47
23	7.82	0.72	3.40	3.70	4.38	15.44
24	7.82	0.72	3.25	3.86	4.38	11.95
25	7.84	0.72	3.49	3.62	4.38	17.39
26	7.83	0.72	3.07	4.04	4.39	7.95
29	7.80	0.72	0.68	6.40	4.37	-46.47
30	7.81	0.72	2.91	4.18	4.38	4.58
31	7.81	0.72	3.60	3.49	4.39	20.49
32	7.82	0.72	3.85	3.26	4.39	25.86
33	7.83	0.72	3.62	3.48	4.39	20.63
36	7.76	0.72	0.65	6.39	4.37	-46.20
37	7.79	0.72	2.78	4.28	4.37	2.07
38	7.79	0.72	3.29	3.78	4.38	13.76
39	7.86	0.72	3.88	3.26	4.39	25.61
40	7.77	0.72	2.90	4.15	4.39	5.41
43	11.06	0.72	1.71	8.63	4.38	-97.09
44	11.07	0.72	5.94	4.41	4.38	-0.69
45	11.09	0.72	7.45	2.92	4.39	33.42
46	11.08	0.72	6.83	3.53	4.39	19.62
47	11.08	0.72	6.86	3.50	4.37	20.05
50	11.07	0.72	2.08	8.27	4.40	-87.97
51	11.08	0.72	6.72	3.64	4.41	17.35

Days	Rainfall volume (L)	evaporation (L)	Outflow (L)	Measured Retention (L)	Estimated Retention(L)	Unaccountable Water (%)
52	11.08	0.72	6.67	3.69	4.41	16.31
53	11.08	0.72	6.05	4.31	4.41	2.24
54	11.08	0.72	7.29	3.07	4.41	30.28
57	11.07	0.72	2.20	8.15	4.41	-85.00
58	11.07	0.72	5.52	4.83	4.42	-9.45
59	11.07	0.72	6.27	4.08	4.41	7.54
60	11.08	0.72	6.90	3.45	4.41	21.70
61	11.08	0.72	7.04	3.32	4.41	24.75

Appendix E Hydrograph Data

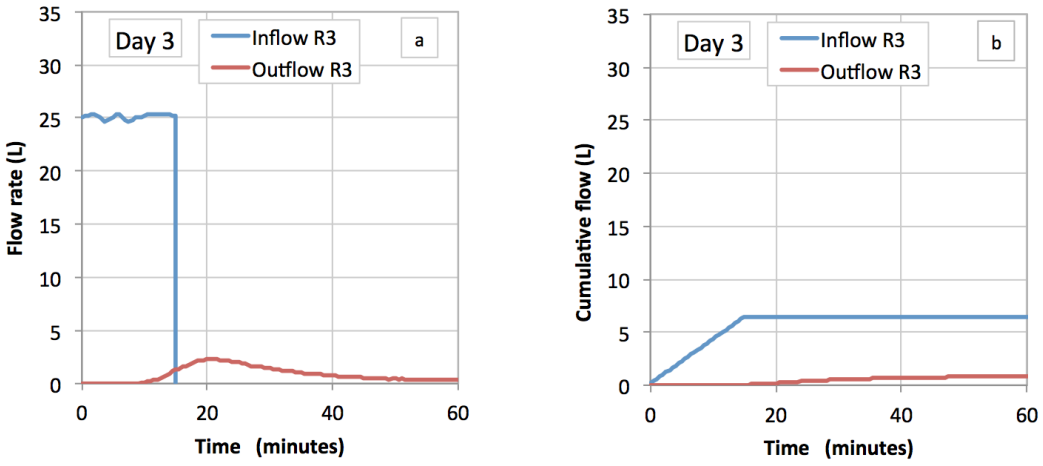

Figure E - 1: Rainfall intensity 1 – week 1, one rain event on day 3, illustrate the flow rate and cumulative of rainfall and outflow.

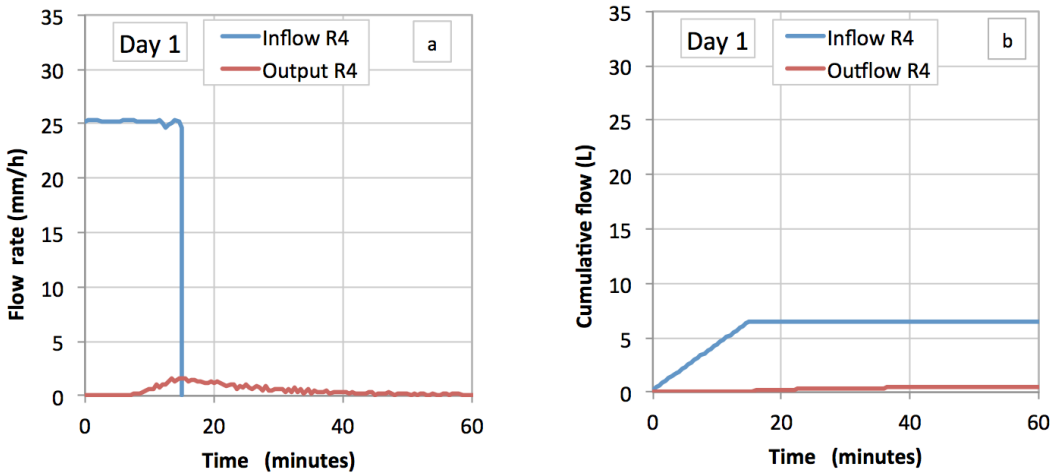

Figure E - 2: Rainfall intensity 1 – week 2, one rain event on day 1, illustrate the flow rate and cumulative of rainfall and outflow.

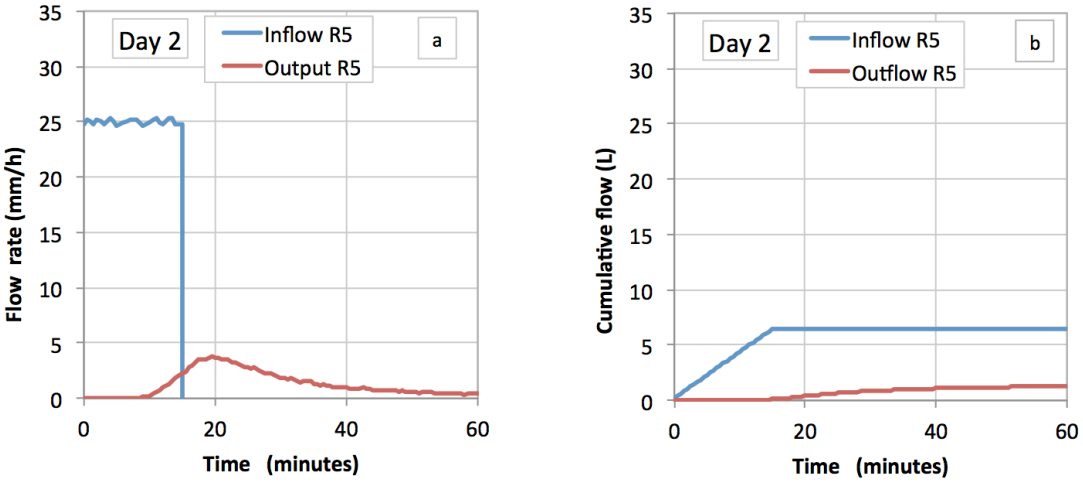

Figure E - 3: Rainfall intensity 1 – week 2, one rain event on day 2, illustrate the flow rate and cumulative of rainfall and outflow.

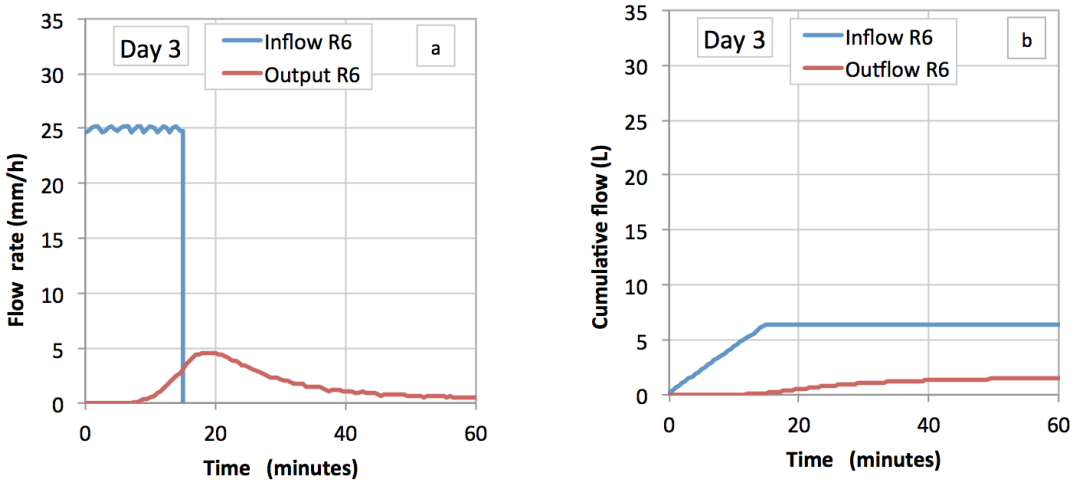

Figure E - 4: Rainfall intensity 1 – week 2, one rain event on day 3, illustrate the flow rate and cumulative of rainfall and outflow.

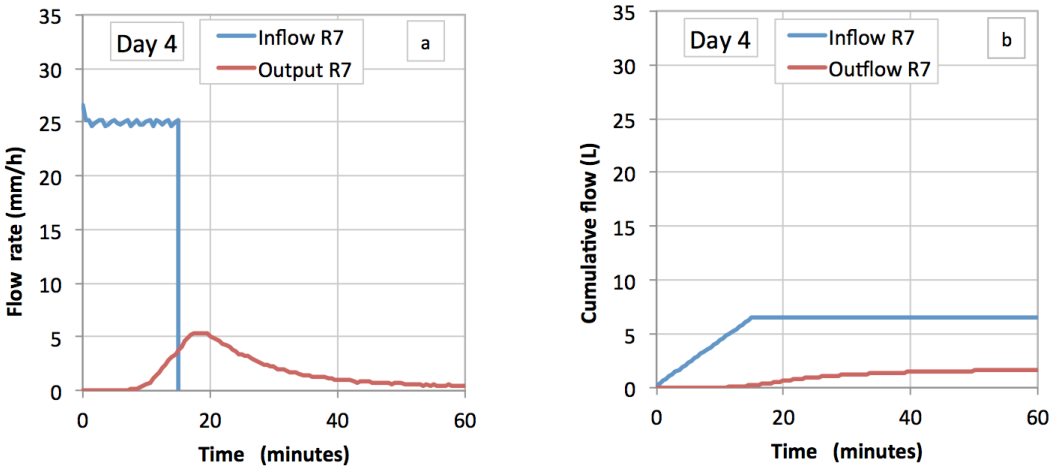

Figure E - 5: Rainfall intensity 1 – week 2, one rain event on day 4, illustrate the flow rate and cumulative of rainfall and outflow.

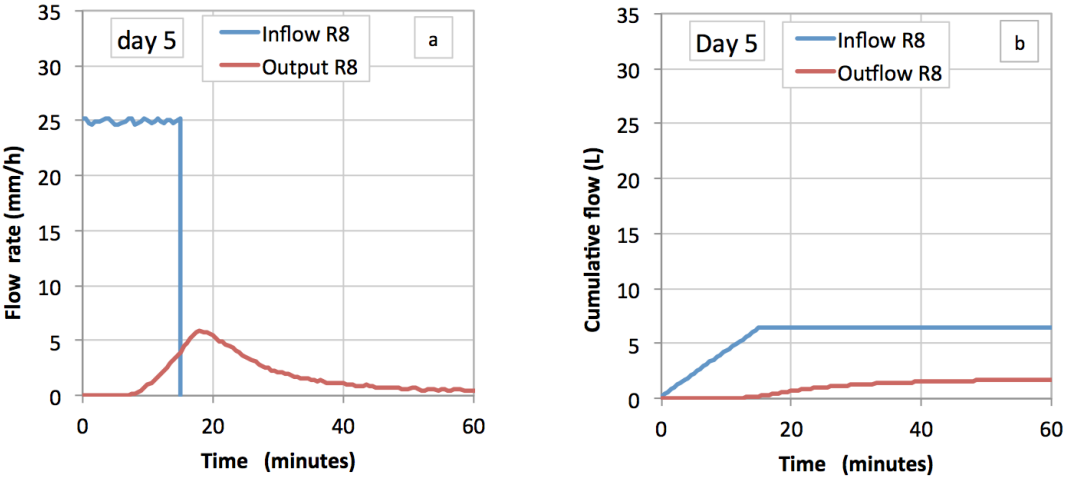

Figure E - 6: Rainfall intensity 1 – week 2, one rain event on day 5, illustrate the flow rate and cumulative of rainfall and outflow.

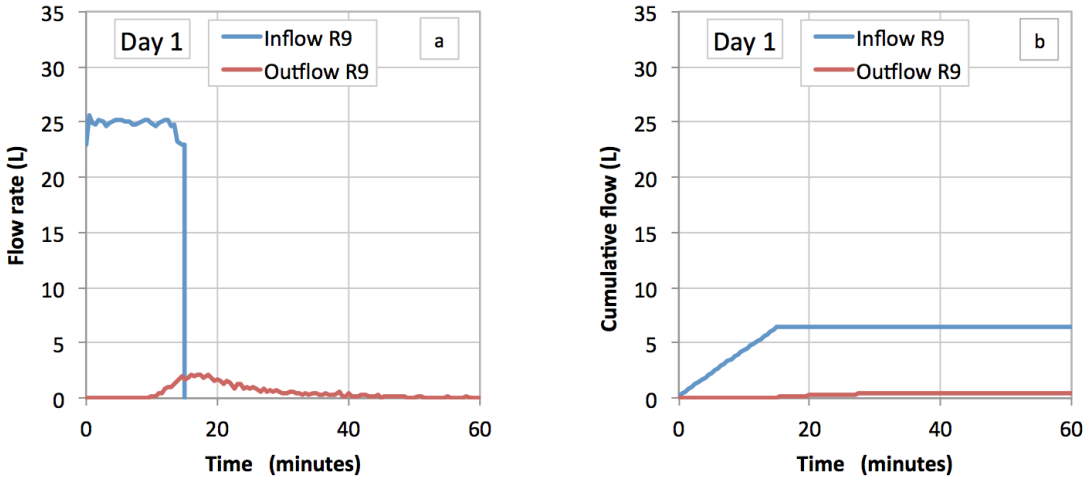

Figure E - 7: Rainfall intensity 1 – week 3, one rain event on day 1, illustrate the flow rate and cumulative of rainfall and outflow.

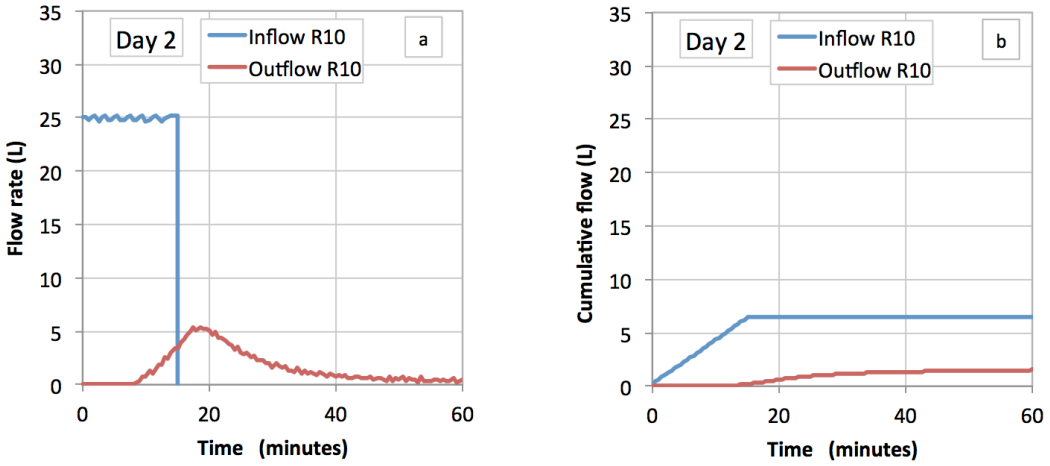

Figure E - 8: Rainfall intensity 1 – week 3, one rain event on day 2, illustrate the flow rate and cumulative of rainfall and outflow.

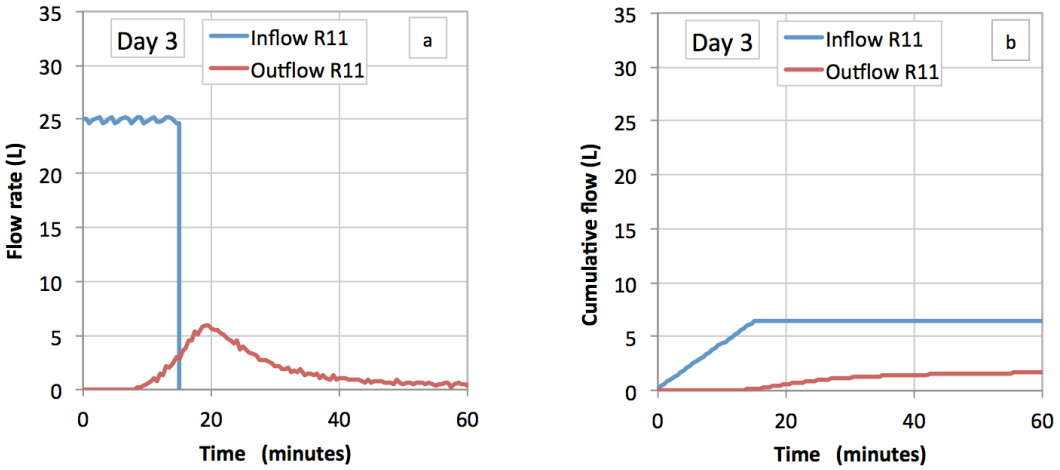

Figure E - 9: Rainfall intensity 1 – week 3, one rain event on day 3, illustrate the flow rate and cumulative of rainfall and outflow.

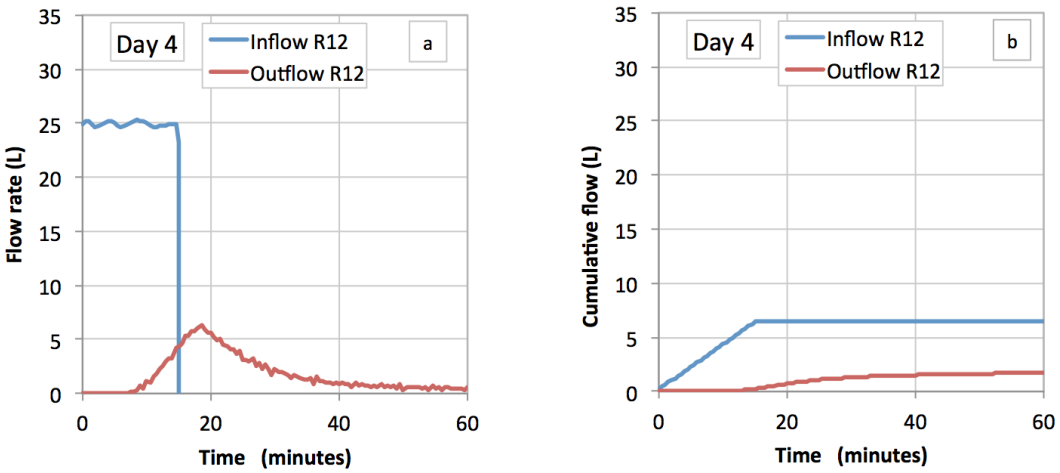

Figure E - 10: Rainfall intensity 1 – week 3, one rain event on day 4, illustrate the flow rate and cumulative of rainfall and outflow.

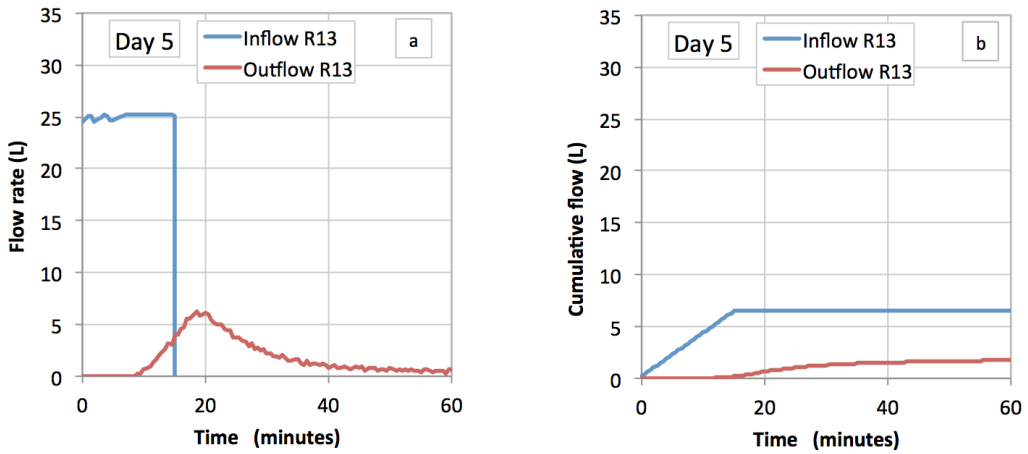

Figure E - 11: Rainfall intensity 1 – week 3, one rain event on day 5, illustrate the flow rate and cumulative of rainfall and outflow.

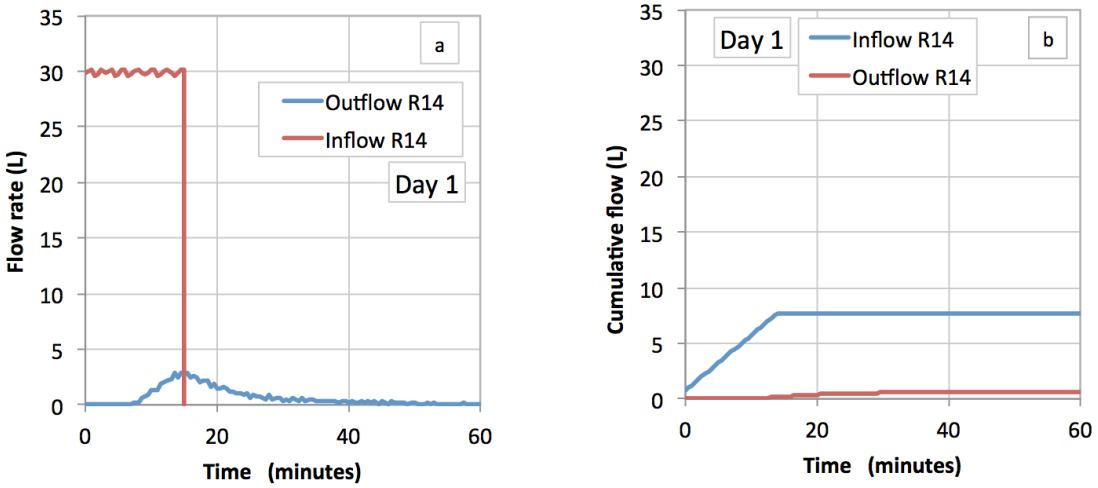

Figure E - 12: Rainfall intensity 2 – week 1, one rain event on day 1, illustrate the flow rate and cumulative of rainfall and outflow.

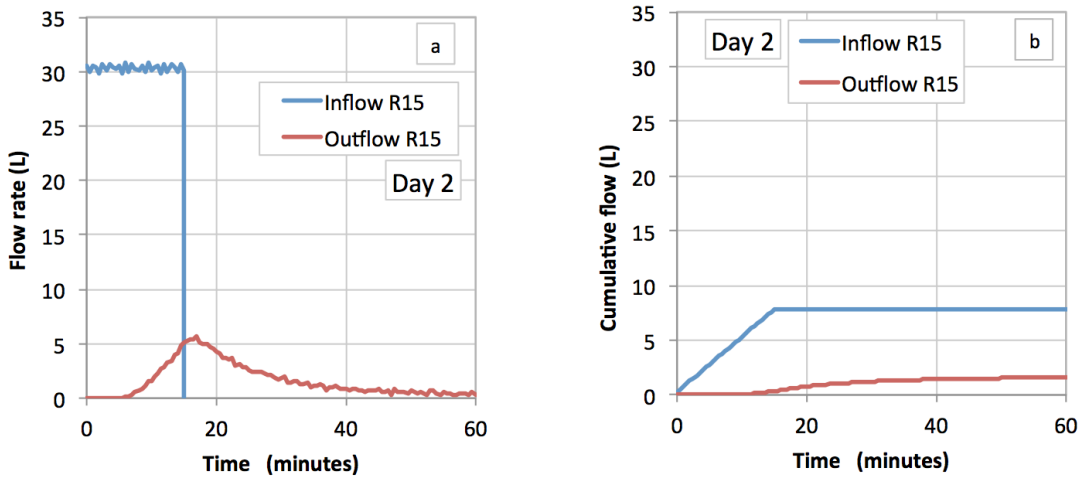

Figure E - 13: Rainfall intensity 2 – week 1, one rain event on day 2, illustrate the flow rate and cumulative of rainfall and outflow.

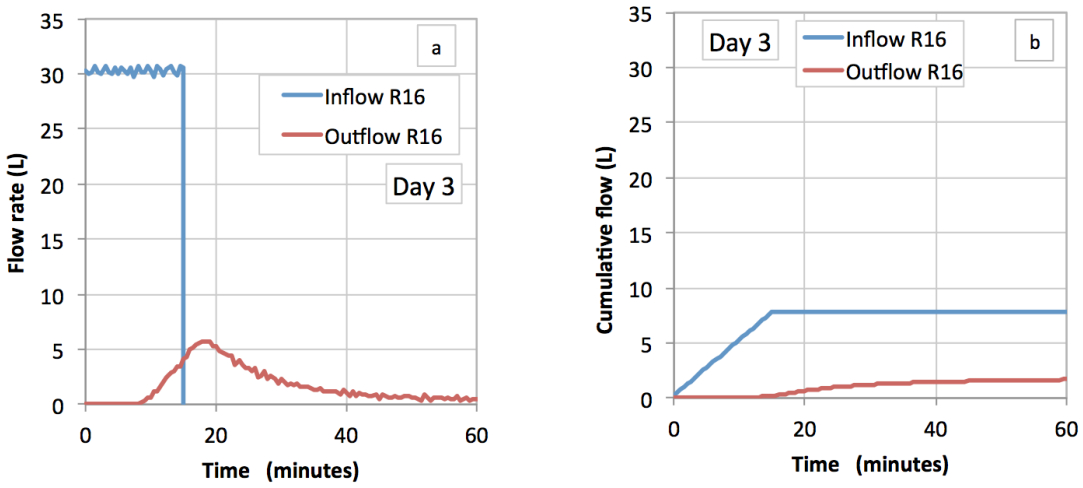

Figure E - 14: Rainfall intensity 2 – week 1, one rain event on day 3, illustrate the flow rate and cumulative of rainfall and outflow.

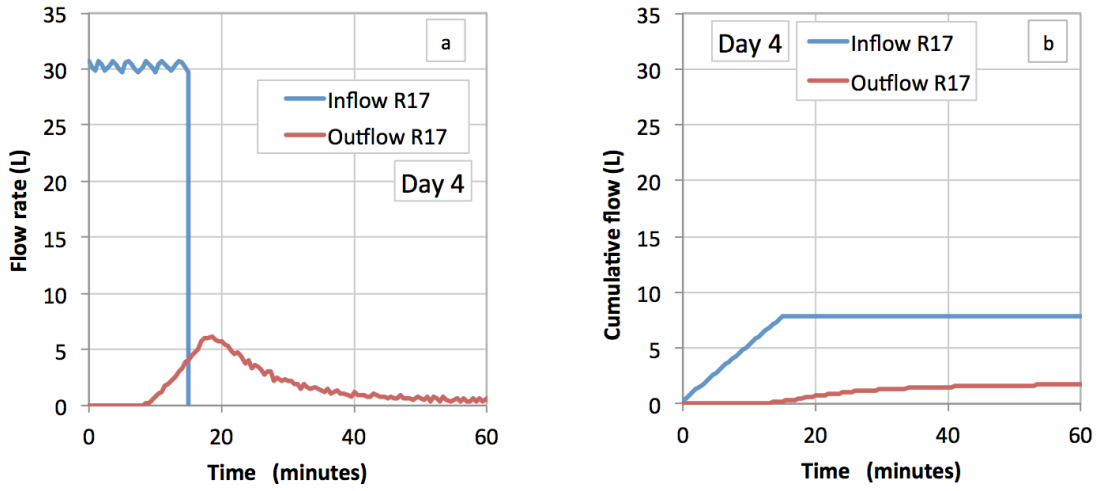

Figure E - 15: Rainfall intensity 2 – week 1, one rain event on day 4, illustrate the flow rate and cumulative of rainfall and outflow.

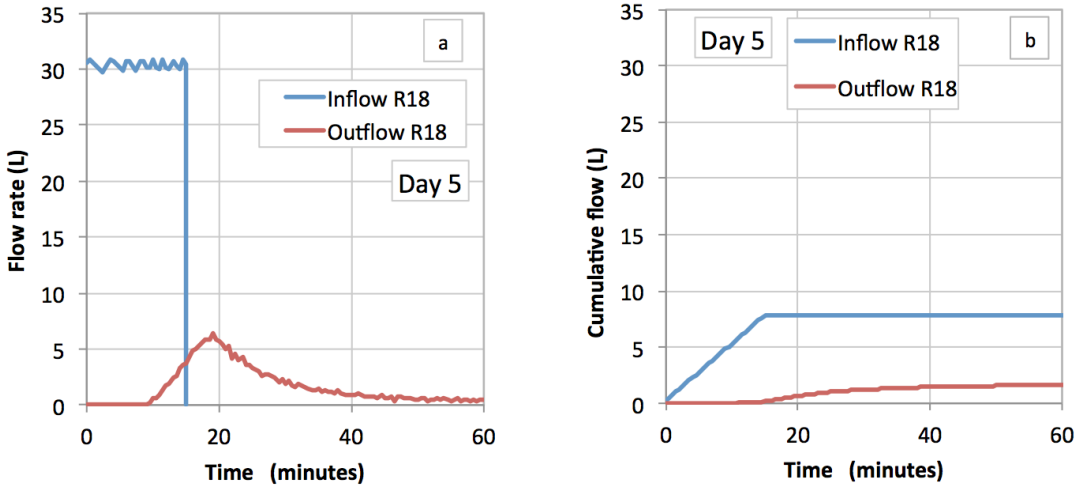

Figure E - 16: Rainfall intensity 2 – week 1, one rain event on day 5, illustrate the flow rate and cumulative of rainfall and outflow.

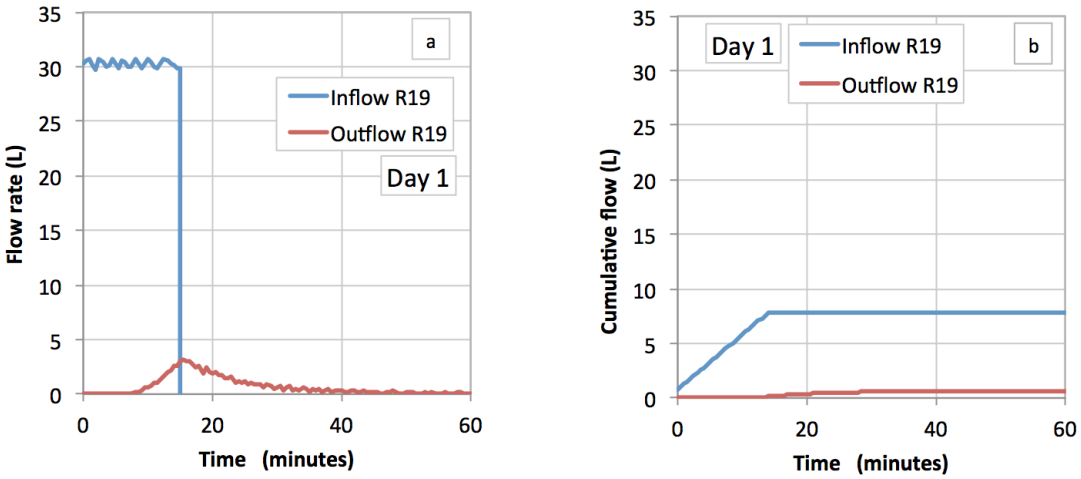

Figure E - 17: Rainfall intensity 2 – week 2, one rain event on day 1, illustrate the flow rate and cumulative of rainfall and outflow.

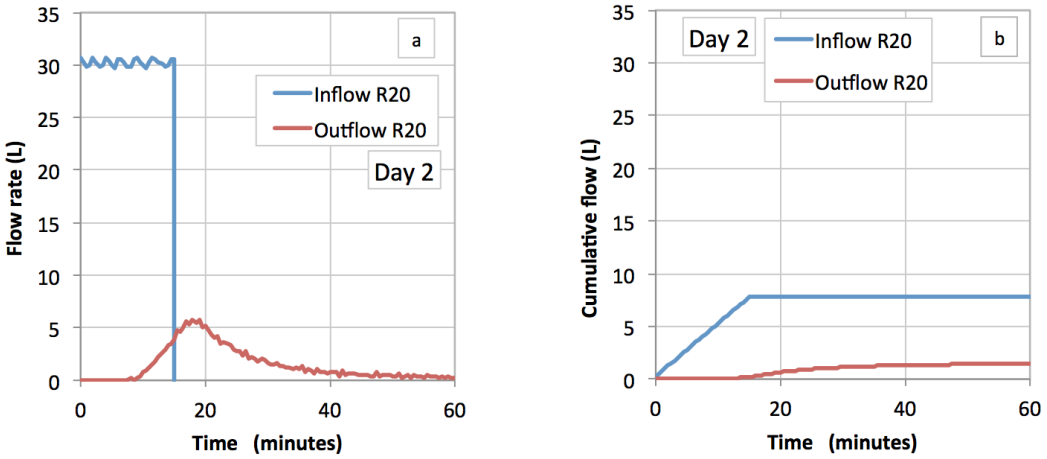

Figure E - 18: Rainfall intensity 2 – week 2, one rain event on day 2, illustrate the flow rate and cumulative of rainfall and outflow.

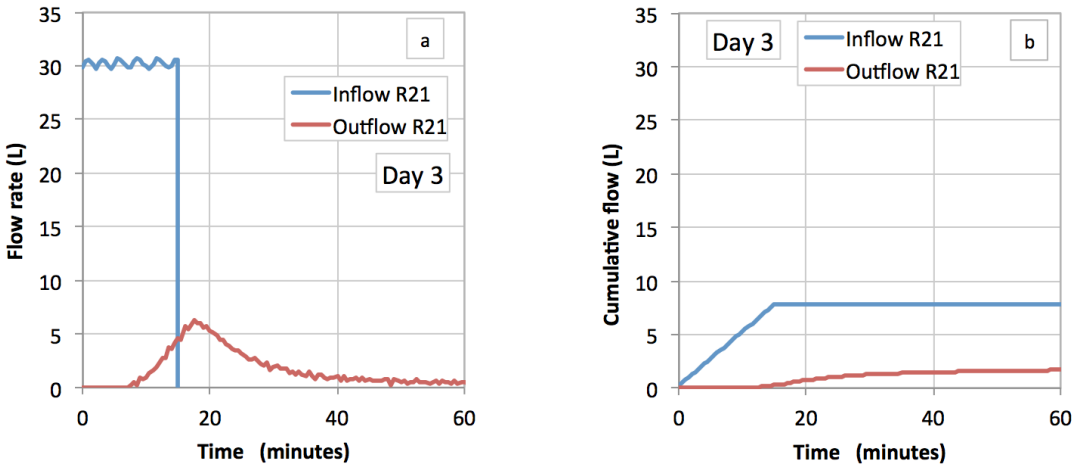

Figure E - 19: Rainfall intensity 2 – week 2, one rain event on day 3, illustrate the flow rate and cumulative of rainfall and outflow.

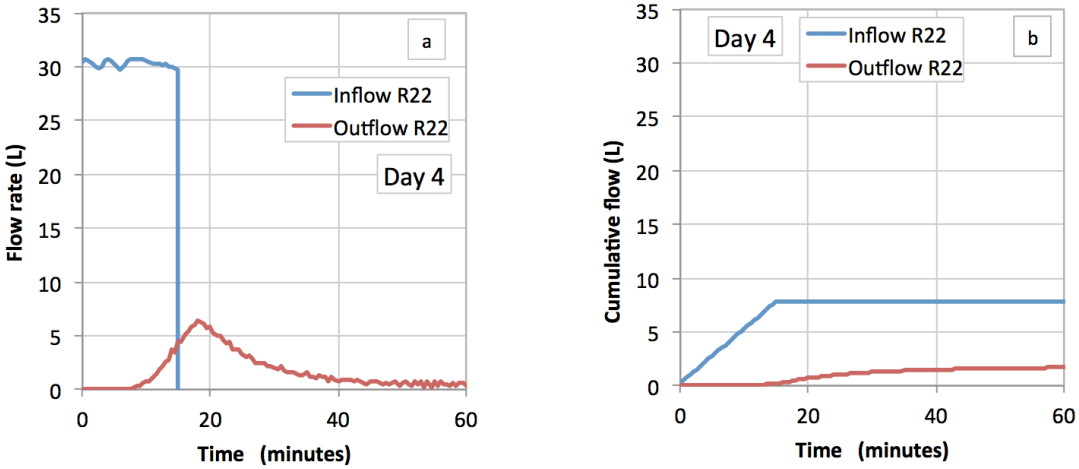

Figure E - 20: Rainfall intensity 2 – week 2, one rain event on day 4, illustrate the flow rate and cumulative of rainfall and outflow.

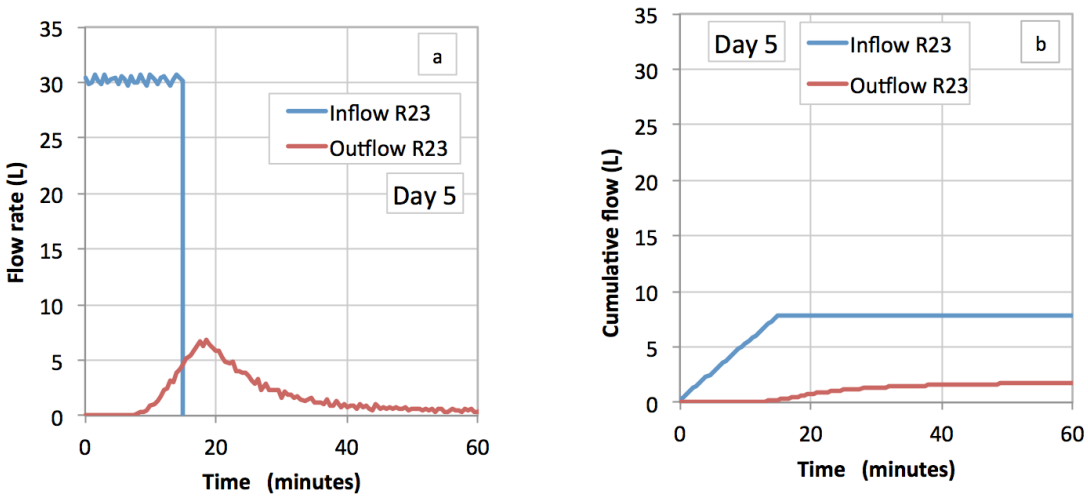

Figure E - 21: Rainfall intensity 2 – week 2, one rain event on day 5, illustrate the flow rate and cumulative of rainfall and outflow.

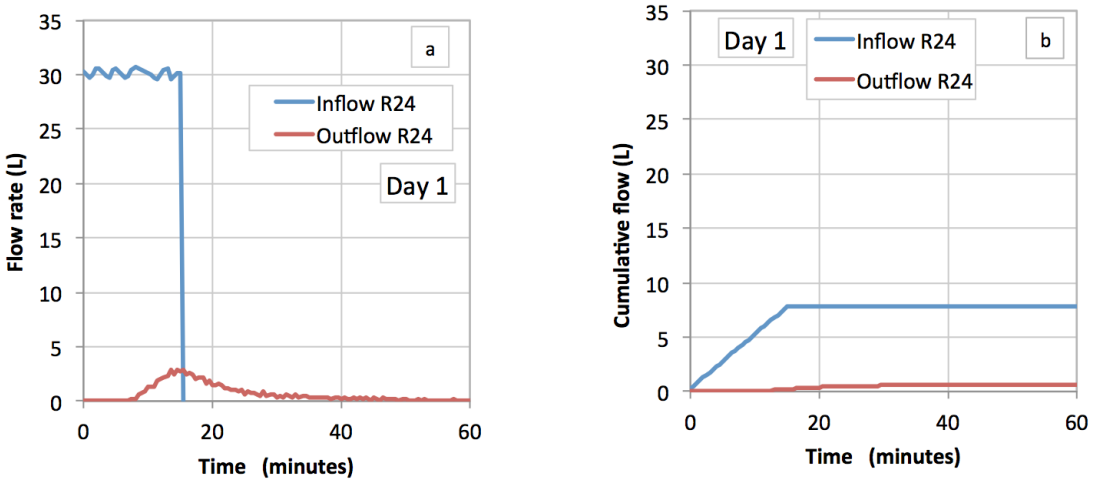

Figure E - 22: Rainfall intensity 2 – week 3, one rain event on day 1, illustrate the flow rate and cumulative of rainfall and outflow.

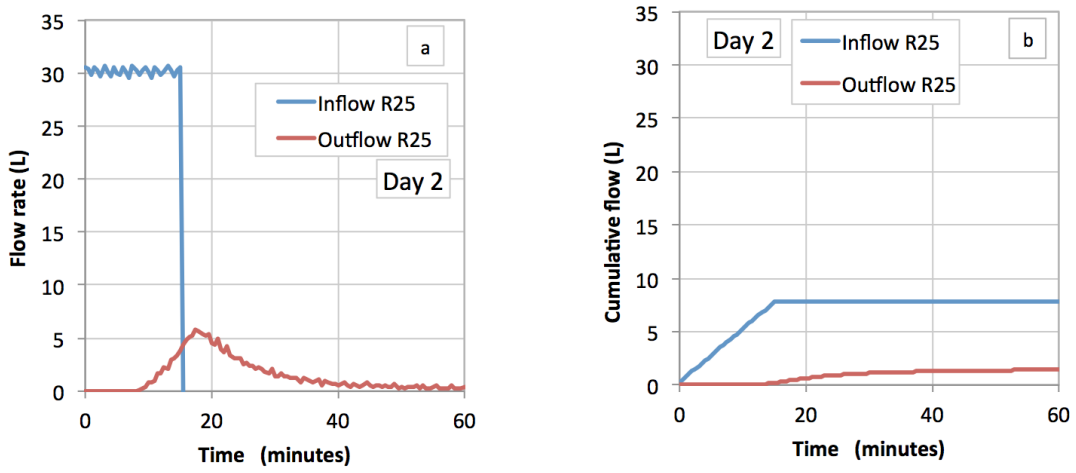

Figure E - 23: Rainfall intensity 2 – week 3, one rain event on day 2, illustrate the flow rate and cumulative of rainfall and outflow.

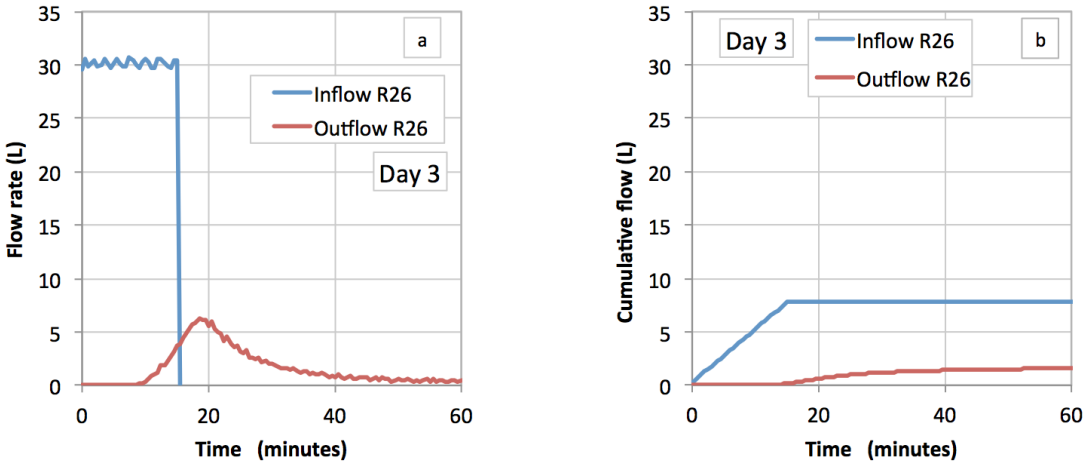

Figure E - 24: Rainfall intensity 2 – week 3, one rain event on day 3, illustrate the flow rate and cumulative of rainfall and outflow.

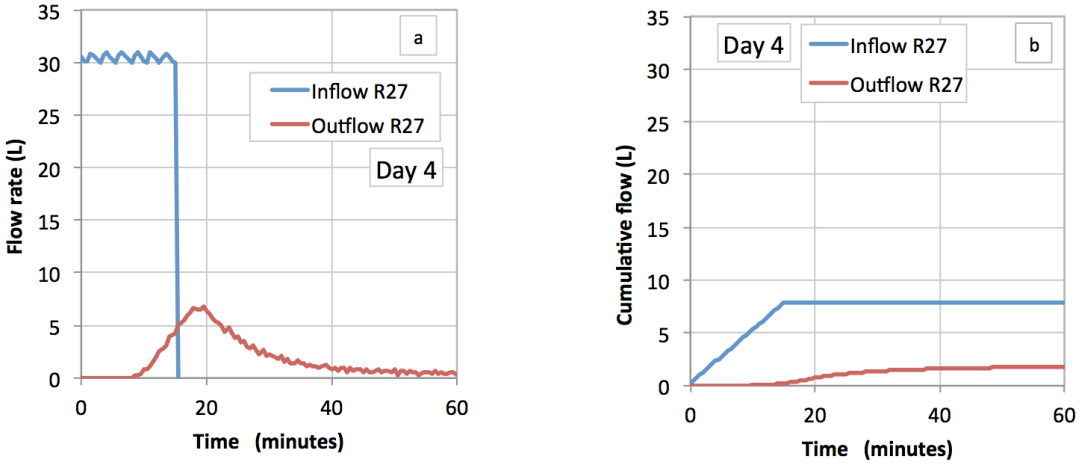

Figure E - 25: Rainfall intensity 2 – week 3, one rain event on day 4, illustrate the flow rate and cumulative of rainfall and outflow.

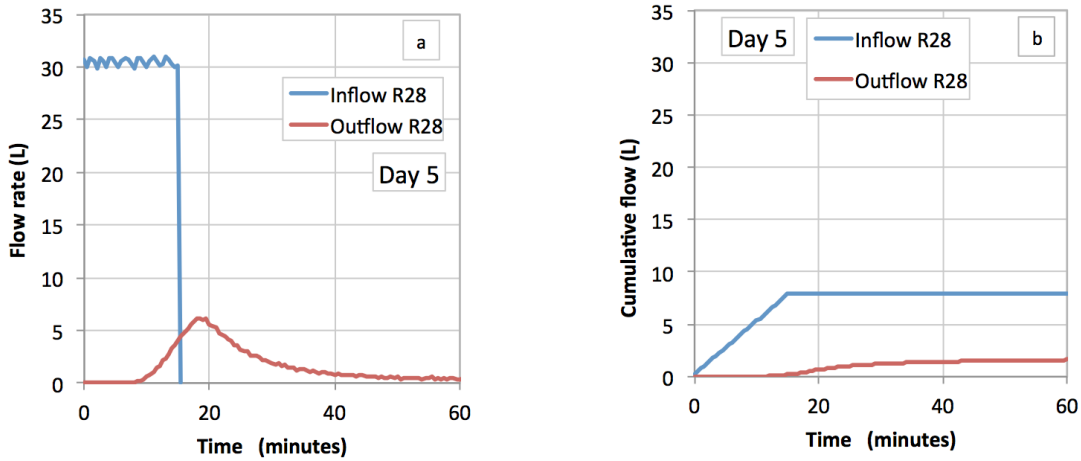

Figure E - 26: Rainfall intensity 2 – week 3, one rain event on day 5, illustrate the flow rate and cumulative of rainfall and outflow.

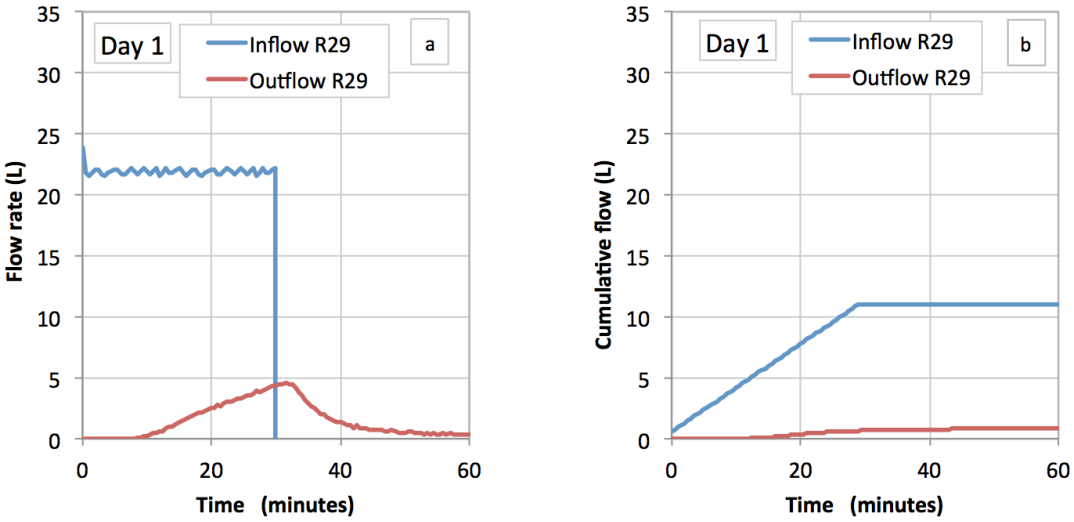

Figure E - 27: Rainfall intensity 3 – week 1, one rain event on day 1, illustrate the flow rate and cumulative of rainfall and outflow.

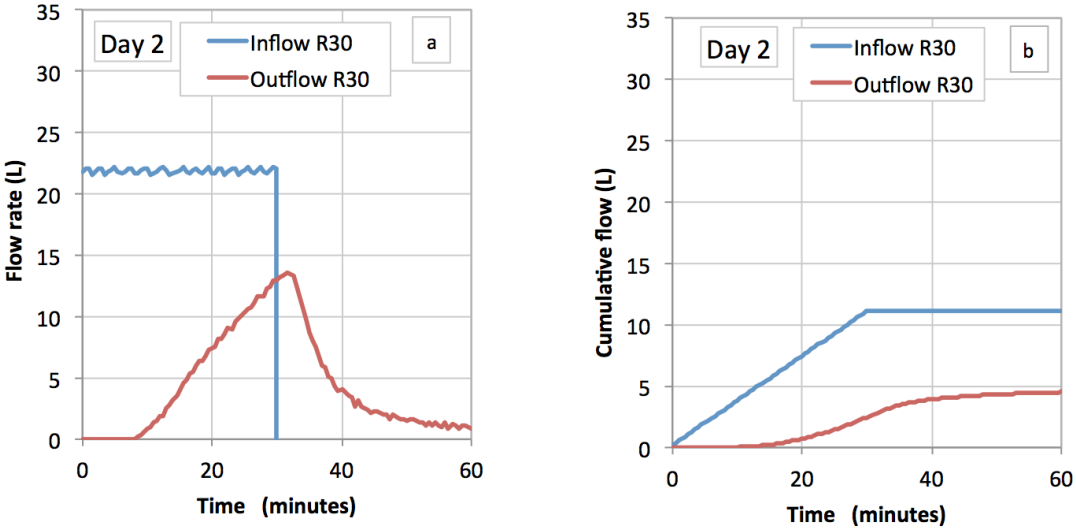

Figure E - 28: Rainfall intensity 3 – week 1, one rain event on day 2, illustrate the flow rate and cumulative of rainfall and outflow.

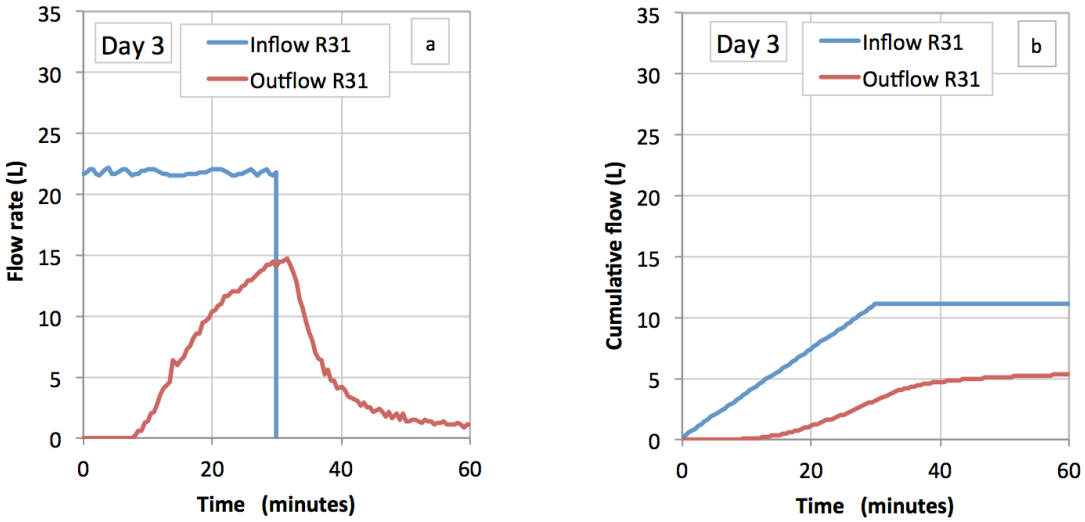

Figure E - 29: Rainfall intensity 3 – week 1, one rain event on day 3, illustrate the flow rate and cumulative of rainfall and outflow.

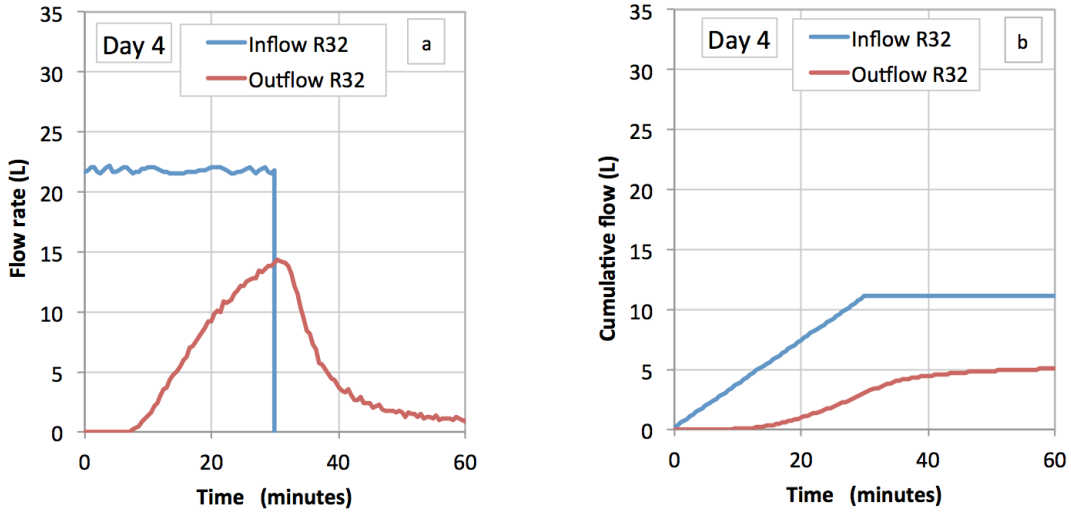

Figure E - 30: Rainfall intensity 3 – week 1, one rain event on day 4, illustrate the flow rate and cumulative of rainfall and outflow.

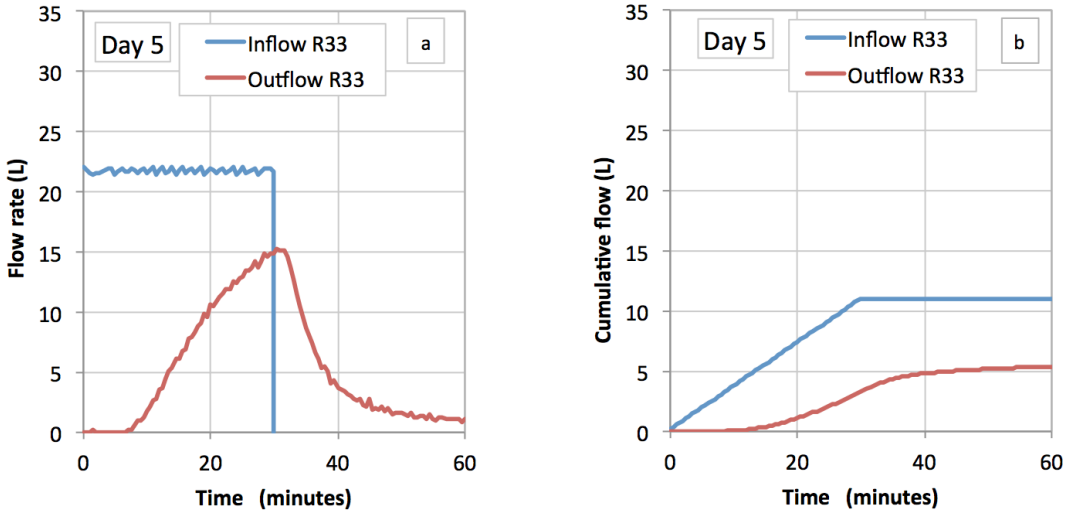

Figure E - 31: Rainfall intensity 3 – week 1, one rain event on day 5, illustrate the flow rate and cumulative of rainfall and outflow.

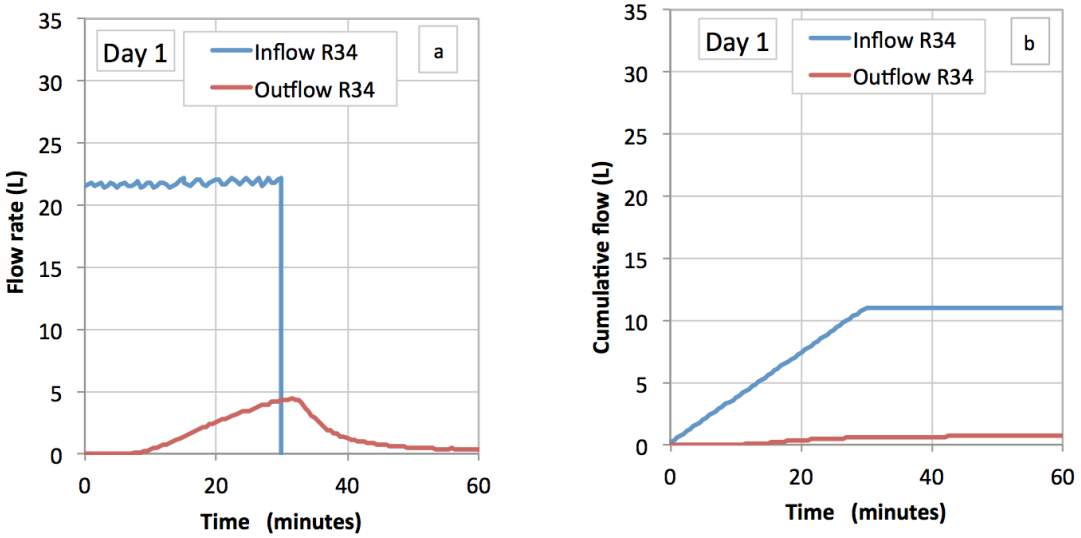

Figure E - 32: Rainfall intensity 3 – week 2, one rain event on day 1, illustrate the flow rate and cumulative of rainfall and outflow.

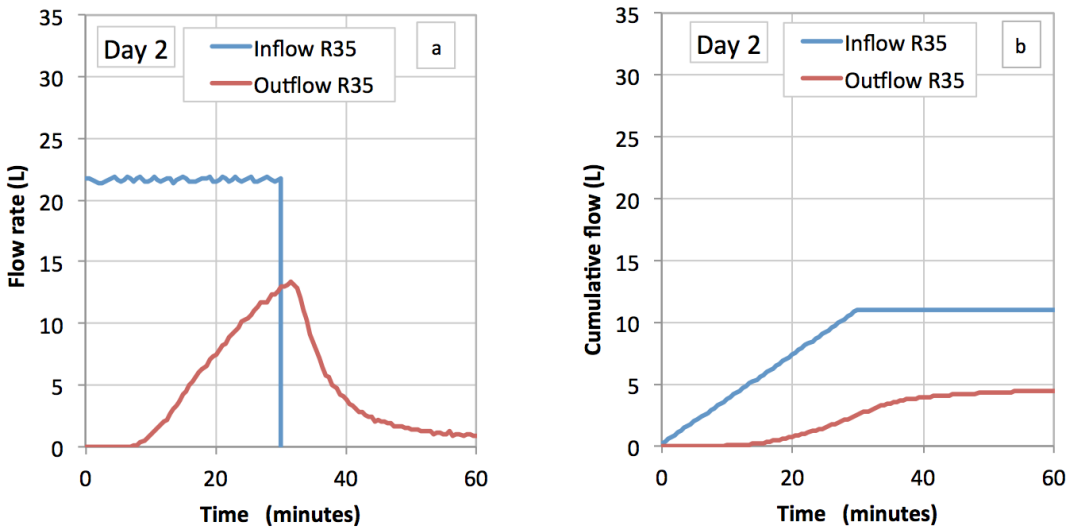

Figure E - 33: Rainfall intensity 3 – week 2, one rain event on day 2, illustrate the flow rate and cumulative of rainfall and outflow.

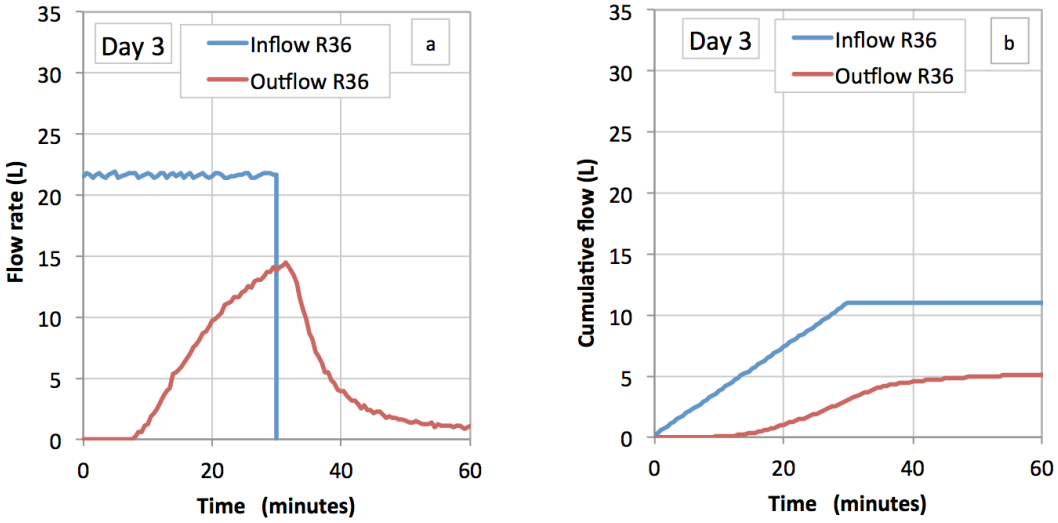

Figure E - 34: Rainfall intensity 3 – week 2, one rain event on day 3, illustrate the flow rate and cumulative of rainfall and outflow.

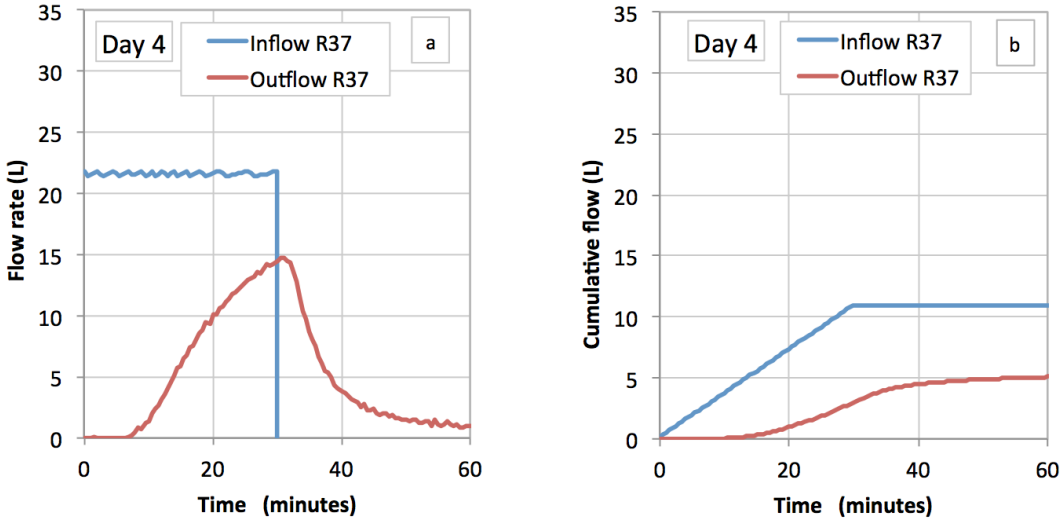

Figure E - 35: Rainfall intensity 3 – week 2, one rain event on day 4, illustrate the flow rate and cumulative of rainfall and outflow.

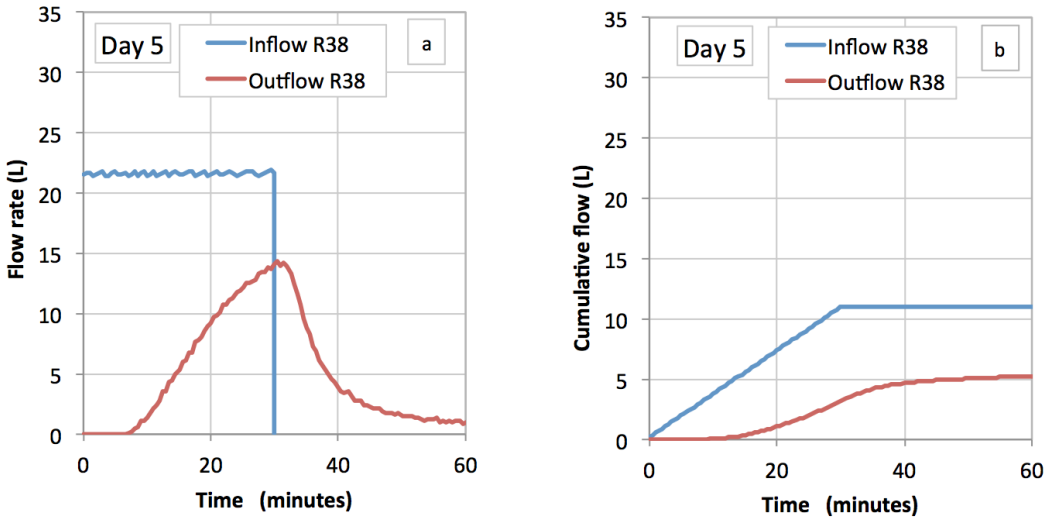

Figure E - 36: Rainfall intensity 3 – week 2, one rain event on day 5, illustrate the flow rate and cumulative of rainfall and outflow.

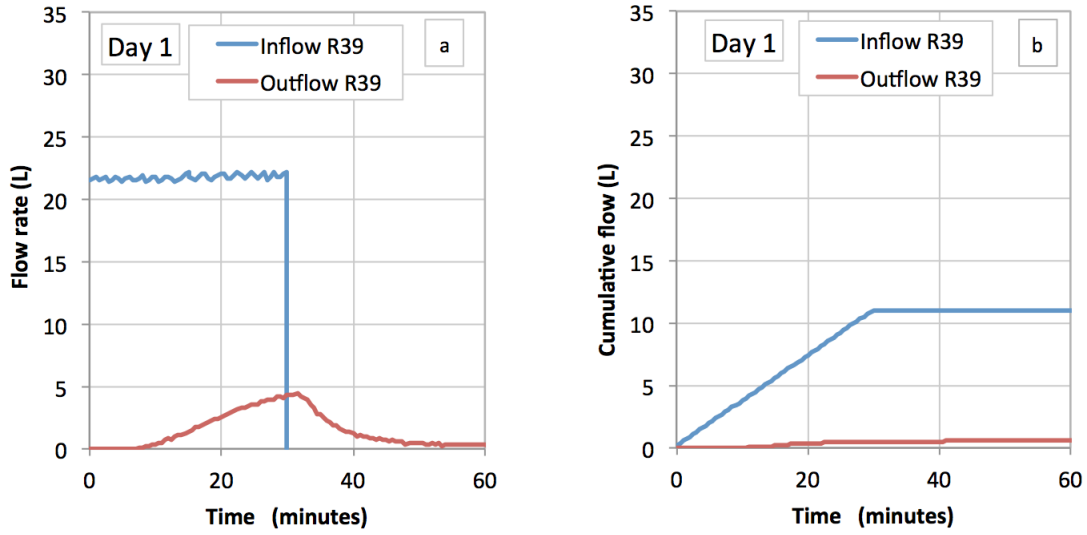

Figure E - 37: Rainfall intensity 3 – week 3, one rain event on day 1, illustrate the flow rate and cumulative of rainfall and outflow.

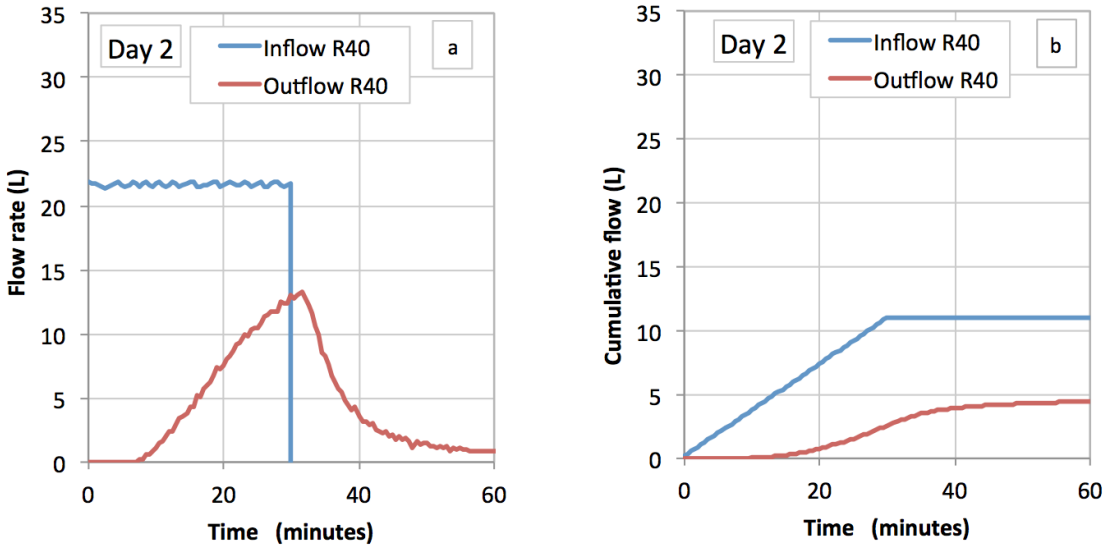

Figure E - 38: Rainfall intensity 3 – week 3, one rain event on day 2, illustrate the flow rate and cumulative of rainfall and outflow.

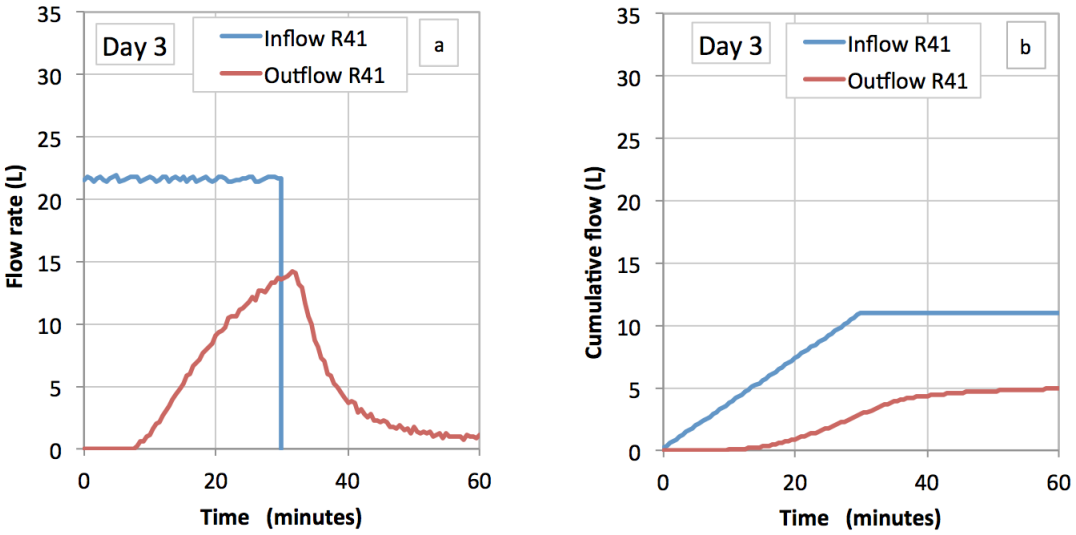

Figure E - 39: Rainfall intensity 3 – week 3, one rain event on day 3, illustrate the flow rate and cumulative of rainfall and outflow.

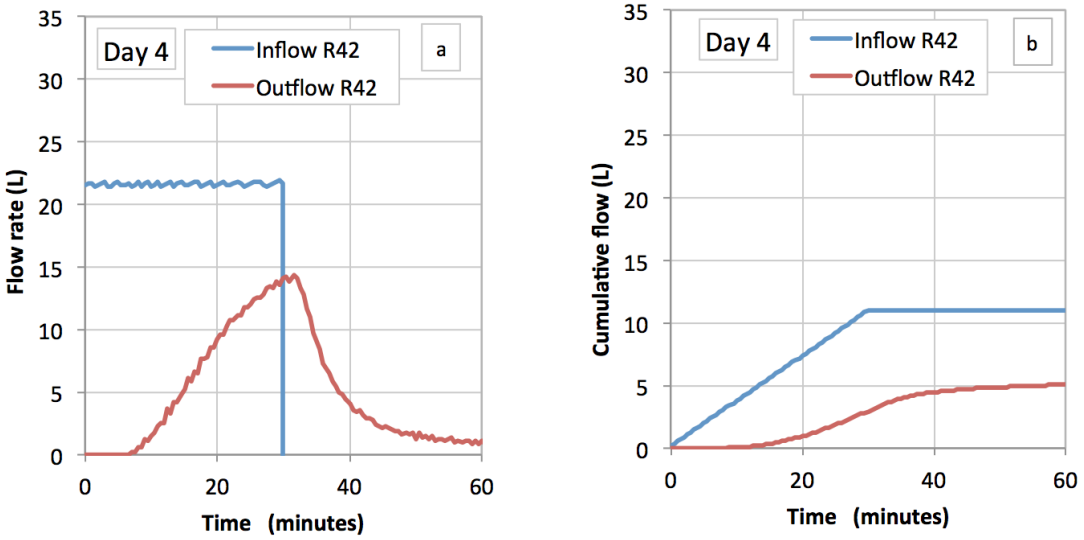

Figure E - 40: Rainfall intensity 3 – week 3, one rain event on day 4, illustrate the flow rate and cumulative of rainfall and outflow.

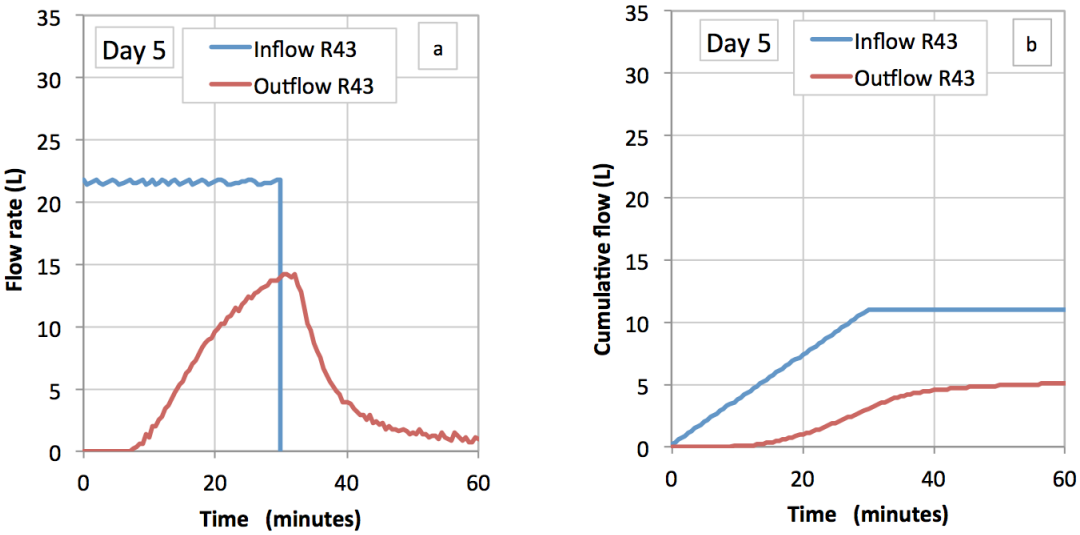

Figure E - 41: Rainfall intensity 3 – week 3, one rain event on day 5, illustrate the flow rate and cumulative of rainfall and outflow.

Appendix F Retention and cumulative retention

Table F - 1: daily and cumulative retention for all rain events

Week	Run	Day simulation (No.)	Total Rain volume (mm)	Total discharge volume (mm)	Retention volume during individual rain event (mm)	Cumulative Retention held with the rig (mm)
1	1	1	6.49	0.00	6.49	6.49
		3	6.46	0.00	6.46	12.95
		5	6.49	0.99	5.50	18.45
2		1	6.51	0.48	6.02	24.48
		2	6.45	1.70	4.75	29.23
		3	6.45	2.30	4.15	33.38
		4	6.46	2.50	3.96	37.34
		5	6.45	2.83	3.62	40.96
3		1	6.39	0.51	5.88	46.85
		2	6.46	2.07	4.39	51.23
		3	6.44	2.52	3.93	55.16
		4	6.43	2.31	4.12	59.27
		5	6.47	2.45	4.03	63.30
4	2	1	7.72	0.67	7.06	70.36
		2	7.84	3.40	4.44	74.80
		3	7.82	3.25	4.58	79.38
		4	7.82	3.49	4.33	83.70
		5	7.85	3.07	4.78	88.48
5		1	7.82	0.68	7.14	95.62
		2	7.81	2.91	4.90	100.52
		3	7.81	3.60	4.21	104.73
		4	7.83	3.85	3.98	108.71
		5	7.81	3.62	4.19	112.90
6		1	7.78	0.65	7.13	120.03
		2	7.79	2.78	5.01	125.04
		3	7.79	3.29	4.49	129.54
		4	7.86	3.88	3.98	133.52

Week	Run	Day simulation (No.)	Total Rain volume (mm)	Total discharge volume (mm)	Retention volume during individual rain event (mm)	Cumulative Retention held with the rig (mm)
		5	7.87	2.90	4.97	138.49
7	3	1	11.07	1.71	9.36	147.85
		2	11.12	5.94	5.18	153.03
		3	11.09	7.45	3.64	156.67
		4	11.08	6.83	4.25	160.92
		5	11.06	6.86	4.20	165.12
8		1	11.08	2.08	9.01	174.13
		2	11.08	6.72	4.36	178.49
		3	11.08	6.67	4.41	182.90
		4	11.08	6.05	5.03	187.94
		5	11.08	7.29	3.79	191.72
9		1	11.06	2.20	8.86	200.59
		2	11.01	5.52	5.49	206.08
		3	11.00	6.27	4.73	210.81
		4	11.00	6.90	4.10	214.90
		5	10.99	7.04	3.95	218.86

Appendix G Daily Rainfall and Outflow data – Sediment Experiment

Table G - 1: Daily rainfall and outflow data – week 1

Day	Rainfall start	Rainfall end	Outflow Start	Outflow End	Rainfall duration (hh:mm:ss)	Time delay to discharge (mm:ss)	Time to outflow stop (hh:mm)	Rainfall volume (L)	Water draining during 24 h (L)
1	11:22:15	14:07:15	11:45:15	18:48:46	02:45:00	23:00	07:03	71.06	53.90
2	10:22:19	13:07:19	10:27:49	17:51:50	02:45:00	05:30	07:24	71.62	65.53
3	10:07:53	12:52:53	10:15:23	16:38:24	02:45:00	07:30	06:23	71.63	66.11
4	10:11:27	12:56:27	10:18:57	17:26:59	02:45:00	07:30	07:08	71.63	66.32
5	10:17:31	13:02:31	10:25:02	19:32:03	02:45:00	07:31	09:07	71.36	67.63

Table G - 2: Daily rainfall and outflow data – week 2

Day	Rainfall start	Rainfall end	Outflow Start	Outflow End	Rainfall duration (hh:mm:ss)	Time delay to discharge (mm:ss)	Time to outflow stop (hh:mm)	Rainfall volume (L)	Water draining during 24 h (L)
1	10:26:14	13:11:14	10:35:14	16:36:45	02:45:00	09:00	06:01	71.34	64.59
2	10:04:48	12:49:48	10:11:48	16:44:49	02:45:00	07:00	06:33	71.42	65.72
3	10:24:23	13:09:23	10:30:53	16:44:49	02:45:00	06:30	06:13	71.59	66.26
4	10:17:57	13:02:57	10:23:57	16:45:58	02:45:00	06:00	06:22	71.85	66.99
5	10:33:01	13:18:01	10:39:01	16:41:02	02:45:00	06:00	06:02	71.45	68.65

Table G - 3: Daily rainfall and outflow data – week 3

Day	Rainfall start	Rainfall end	Outflow Start	Outflow End	Rainfall duration (hh:mm:ss)	Time delay to discharge (mm:ss)	Time to outflow stop (hh:mm)	Rainfall volume (L)	Water draining during 24 h (L)
1	10:32:13	13:17:13	10:39:13	16:47:45	02:45:00	07:00	06:08	71.51	65.21
2	10:28:18	13:13:18	10:34:48	15:50:19	02:45:00	06:30	05:15	71.94	67.23
3	09:41:22	12:26:22	09:47:52	15:55:23	02:45:00	06:30	06:07	71.53	66.59
4	10:27:26	13:12:26	10:33:56	15:41:27	02:45:00	06:30	05:07	71.45	66.07
5	10:21:00	13:06:00	10:27:30	16:46:02	02:45:00	06:30	06:18	71.81	70.10

Table G - 4: Daily rainfall and outflow data – week 4

Day	Rainfall start	Rainfall end	Outflow Start	Outflow End	Rainfall duration (hh:mm:ss)	Time delay to discharge (mm:ss)	Time to outflow stop (hh:mm)	Rainfall volume (L)	Water draining during 24 h (L)
1	10:30:01	13:15:01	10:37:31	17:36:02	02:45:00	07:30	06:58	71.41	65.65
2	11:01:05	13:46:05	11:08:05	17:52:06	02:45:00	07:00	06:44	71.61	67.51
3	09:45:39	12:30:39	09:52:39	17:23:11	02:45:00	07:00	07:30	71.96	69.72
4	09:24:13	12:09:13	09:31:13	15:50:15	02:45:00	07:00	06:19	71.56	68.75
5	10:18:48	13:03:48	10:25:48	17:18:49	02:45:00	07:00	06:53	71.18	70.19

Table G - 5: Daily rainfall and outflow data – week 5

Day	Rainfall start	Rainfall end	Outflow Start	Outflow End	Rainfall duration (hh:mm:ss)	Time delay to discharge (mm:ss)	Time to outflow stop (hh:mm)	Rainfall volume (L)	Water draining during 24 h (L)
1	09:41:00	12:26:00	09:49:31	16:21:02	02:45:00	08:31	06:31	71.73	67.11
2	10:21:35	13:06:35	10:28:05	17:22:36	02:45:00	06:30	06:54	72.05	69.76
3	10:16:39	13:01:39	10:23:39	15:50:40	02:45:00	07:00	05:27	71.02	67.71
4	12:03:35	14:48:35	12:10:35	19:24:06	02:45:00	07:00	07:13	71.85	67.85
5	10:38:09	13:23:09	10:44:09	17:25:10	02:45:00	06:00	06:41	71.92	70.55

Table G - 6: Daily rainfall and outflow data – week 6

Day	Rainfall start	Rainfall end	Outflow Start	Outflow End	Rainfall duration (hh:mm:ss)	Time delay to discharge (mm:ss)	Time to outflow stop (hh:mm)	Rainfall volume (L)	Water draining during 24 h (L)
1	10:53:50	13:38:50	11:03:20	16:42:50	02:45:00	09:30	05:39	71.40	62.29
2	09:57:53	12:42:53	10:03:23	15:26:24	02:45:00	05:30	05:23	71.82	68.36
3	10:18:57	13:03:57	10:25:27	16:42:58	02:45:00	06:30	06:17	71.94	69.84
4	10:25:31	13:10:31	10:32:01	17:07:02	02:45:00	06:30	06:35	71.94	70.00
5	09:53:04	12:38:04	09:59:34	15:56:35	02:45:00	06:30	05:57	71.84	70.06

Table G - 7: Daily rainfall and outflow data – week 7

Day	Rainfall start	Rainfall end	Outflow Start	Outflow End	Rainfall duration (hh:mm:ss)	Time delay to discharge (mm:ss)	Time to outflow stop (hh:mm)	Rainfall volume (L)	Water draining during 24 h (L)
1	10:21:54	13:06:54	10:30:24	16:43:55	02:45:00	08:30	06:13	71.48	65.48
2	10:40:27	13:25:27	10:46:57	17:07:28	02:45:00	06:30	06:20	71.84	69.02
3	10:14:01	12:59:01	10:21:01	16:47:32	02:45:00	07:00	06:26	71.71	67.99
4	12:06:35	14:51:35	12:13:35	18:25:06	02:45:00	07:00	06:11	71.84	68.97
5	10:15:38	13:00:38	10:22:08	16:54:09	02:45:00	06:30	06:32	71.34	70.28

Table G - 8: Daily rainfall and outflow data – week 8

Day	Rainfall start	Rainfall end	Outflow Start	Outflow End	Rainfall duration (hh:mm:ss)	Time delay to discharge (mm:ss)	Time to outflow stop (hh:mm)	Rainfall volume (L)	Water draining during 24 h (L)
1	10:27:01	13:12:01	10:36:31	16:50:02	02:45:00	09:30	06:13	71.42	63.55
2	09:50:35	12:35:35	09:58:05	15:48:05	02:45:00	07:30	05:50	71.75	65.08
3	09:59:38	12:44:38	10:06:38	17:58:10	02:45:00	07:00	07:51	71.78	65.56
4	09:43:42	12:28:42	09:51:12	15:52:43	02:45:00	07:30	06:01	71.72	64.38
5	10:01:16	12:46:16	10:08:16	16:52:17	02:45:00	07:00	06:44	71.99	67.10

Table G - 9: Daily rainfall and outflow data – week 9

Day	Rainfall start	Rainfall end	Outflow Start	Outflow End	Rainfall duration (hh:mm:ss)	Time delay to discharge (mm:ss)	Time to outflow stop (hh:mm)	Rainfall volume (L)	Water draining during 24 h (L)
1	13:52:46	16:37:46	14:01:46	20:18:17	02:45:00	09:00	06:16	71.25	62.23
2	09:59:19	12:44:19	10:06:49	17:22:20	02:45:00	07:30	07:15	71.76	65.41
3	10:14:23	12:59:23	10:22:23	17:04:54	02:45:00	08:00	06:42	71.69	64.15
4	09:46:26	12:31:26	09:53:56	16:11:57	02:45:00	07:30	06:18	71.77	64.42
5	12:50:31	15:35:31	12:58:31	19:59:32	02:45:00	08:00	07:01	71.03	64.87

Table G - 10: Daily rainfall and outflow data – week 10

Day	Rainfall start	Rainfall end	Outflow Start	Outflow End	Rainfall duration (hh:mm:ss)	Time delay to discharge (mm:ss)	Time to outflow stop (hh:mm)	Rainfall volume (L)	Water draining during 24 h (L)
1	10:42:23	13:27:23	10:52:23	18:13:24	02:45:00	10:00	07:21	71.38	59.84
2	12:35:27	15:20:27	12:42:57	19:47:58	02:45:00	07:30	07:05	71.74	64.89
3	10:50:00	13:35:00	10:57:00	19:26:32	02:45:00	07:00	08:29	71.71	64.27
4	09:47:04	12:32:04	09:54:34	18:17:06	02:45:00	07:30	08:22	71.68	63.70
5	12:17:38	15:02:38	12:25:08	19:15:40	02:45:00	07:30	06:50	71.41	63.74

Table G - 11: Daily rainfall and outflow data – week 11

Day	Rainfall start	Rainfall end	Outflow Start	Outflow End	Rainfall duration (hh:mm:ss)	Time delay to discharge (mm:ss)	Time to outflow stop (hh:mm)	Rainfall volume (L)	Water draining during 24 h (L)
1	10:18:34	13:03:34	10:27:34	17:41:35	02:45:00	09:00	07:14	71.51	60.25
2	10:51:38	13:36:38	10:59:08	18:58:39	02:45:00	07:30	07:59	71.68	62.59
3	09:43:11	12:28:11	09:50:11	18:10:43	02:45:00	07:00	08:20	71.76	63.27
4	10:14:45	12:59:45	10:22:15	17:55:16	02:45:00	07:30	07:33	71.69	63.17
5	10:23:49	13:08:49	10:30:48	18:53:20	02:45:00	06:59	08:22	71.75	65.50

Table G - 12: Daily rainfall and outflow data – week 12

Day	Rainfall start	Rainfall end	Outflow Start	Outflow End	Rainfall duration (hh:mm:ss)	Time delay to discharge (mm:ss)	Time to outflow stop (hh:mm)	Rainfall volume (L)	Water draining during 24 h (L)
1	10:42:02	13:27:02	10:50:02	19:58:34	02:45:00	08:00	09:08	71.50	60.72
2	11:17:36	14:02:36	11:24:36	20:22:38	02:45:00	07:00	08:58	71.78	63.27
3	11:16:40	14:01:40	11:23:40	21:58:42	02:45:00	07:00	10:35	71.80	63.56
4	10:43:44	13:28:44	10:50:44	20:56:15	02:45:00	07:00	10:05	71.71	62.57
5	11:18:45	14:03:45	11:25:45	21:45:16	02:45:00	07:00	10:19	71.41	63.95

Table G - 13: Daily rainfall and outflow data – week 13

Day	Rainfall start	Rainfall end	Outflow Start	Outflow End	Rainfall duration (hh:mm:ss)	Time delay to discharge (mm:ss)	Time to outflow stop (hh:mm)	Rainfall volume (L)	Water draining during 24 h (L)
1	11:17:23	14:02:23	11:24:53	18:59:24	02:45:00	07:30	07:34	71.50	60.60
2	09:47:56	12:32:56	09:54:26	19:43:58	02:45:00	06:30	09:49	71.77	64.42
3	11:40:31	14:25:31	11:47:31	20:10:32	02:45:00	07:00	08:23	71.74	64.15
4	09:42:04	12:27:04	09:49:34	18:06:05	02:45:00	07:30	08:16	71.75	64.32
5	12:00:08	14:45:08	12:07:08	20:07:09	02:45:00	07:00	08:00	71.66	65.20

Table G - 14: Daily rainfall and outflow data – week 14

Day	Rainfall start	Rainfall end	Outflow Start	Outflow End	Rainfall duration (hh:mm:ss)	Time delay to discharge (mm:ss)	Time to outflow stop (hh:mm)	Rainfall volume (L)	Water draining during 24 h (L)
1	09:45:42	12:30:42	09:54:12	18:20:13	02:45:00	08:30	08:26	71.25	59.78
2	09:48:16	12:33:16	09:55:16	18:06:47	02:45:00	07:00	08:11	71.95	66.21
3	09:37:49	12:22:49	09:44:19	19:23:21	02:45:00	06:30	09:39	71.61	64.43
4	09:47:53	12:32:53	09:55:23	19:08:24	02:45:00	07:30	09:13	71.57	63.66
5	10:08:57	12:53:57	10:15:27	19:22:28	02:45:00	06:30	09:07	71.20	64.85

Table G - 15: Daily rainfall and outflow data – week 15

Day	Rainfall start	Rainfall end	Outflow Start	Outflow End	Rainfall duration (hh:mm:ss)	Time delay to discharge (mm:ss)	Time to outflow stop (hh:mm)	Rainfall volume (L)	Water draining during 24 h (L)
1	10:26:44	13:11:44	10:36:44	19:18:46	02:45:00	10:00	08:42	71.35	60.42
2	10:26:48	13:11:48	10:34:48	18:49:49	02:45:00	08:00	08:15	71.71	65.05
3	09:38:51	12:23:51	09:46:21	18:18:52	02:45:00	07:30	08:32	71.83	65.72
4	11:18:25	14:03:25	11:26:25	20:46:26	02:45:00	08:00	09:20	71.47	63.79
5	10:17:28	13:02:28	10:24:58	19:59:30	02:45:00	07:30	09:34	71.74	65.96

Table G - 16: Daily rainfall and outflow data – week 16

Day	Rainfall start	Rainfall end	Outflow Start	Outflow End	Rainfall duration (hh:mm:ss)	Time delay to discharge (mm:ss)	Time to outflow stop (hh:mm)	Rainfall volume (L)	Water draining during 24 h (L)
1	12:49:35	15:34:35	13:00:05	21:08:07	02:45:00	10:30	08:08	71.32	59.87
2	10:44:09	13:29:09	10:51:09	20:30:10	02:45:00	07:00	09:39	71.90	65.60
3	11:13:42	13:58:42	11:21:42	19:59:43	02:45:00	08:00	08:38	71.69	64.41
4	11:40:46	14:25:46	11:48:46	21:00:17	02:45:00	08:00	09:11	71.63	63.79
5	10:25:19	13:10:19	10:32:49	19:57:50	02:45:00	07:30	09:25	71.01	65.65

Table G - 17: Daily rainfall and outflow data – week 17

Day	Rainfall start	Rainfall end	Outflow Start	Outflow End	Rainfall duration (hh:mm:ss)	Time delay to discharge (mm:ss)	Time to outflow stop (hh:mm)	Rainfall volume (L)	Water draining during 24 h (L)
1	10:27:11	13:12:11	10:37:41	20:22:42	02:45:00	10:30	09:45	71.30	61.36
2	09:53:14	12:38:14	10:01:14	19:02:46	02:45:00	08:00	09:01	71.53	63.96
3	11:53:48	14:38:48	12:01:18	20:29:49	02:45:00	07:30	08:28	71.35	63.03
4	10:30:21	13:15:21	10:38:21	19:55:23	02:45:00	08:00	09:17	71.35	63.56
5	10:39:55	13:24:55	10:47:55	20:00:56	02:45:00	08:00	09:13	71.07	65.16

Table G - 18: Daily rainfall and outflow data – week 18

Day	Rainfall start	Rainfall end	Outflow Start	Outflow End	Rainfall duration (hh:mm:ss)	Time delay to discharge (mm:ss)	Time to outflow stop (hh:mm)	Rainfall volume (L)	Water draining during 24 h (L)
1	10:02:14	12:47:14	10:11:44	18:27:45	02:45:00	09:30	08:16	71.28	62.05
2	12:31:48	15:16:48	12:39:18	22:10:49	02:45:00	07:30	09:31	71.35	63.42
3	10:57:51	13:42:51	11:05:21	20:41:53	02:45:00	07:30	09:36	71.49	64.32
4	10:24:25	13:09:25	10:32:25	19:48:56	02:45:00	08:00	09:16	71.32	63.14
5	10:25:58	13:10:58	10:33:28	20:14:00	02:45:00	07:30	09:40	71.49	64.70

Table G - 19: Daily rainfall and outflow data – week 19

Day	Rainfall start	Rainfall end	Outflow Start	Outflow End	Rainfall duration (hh:mm:ss)	Time delay to discharge (mm:ss)	Time to outflow stop (hh:mm)	Rainfall volume (L)	Water draining during 24 h (L)
1	11:46:15	14:31:15	11:56:15	21:05:47	02:45:00	10:00	09:09	71.23	58.37
2	09:59:57	12:44:57	10:07:27	18:20:58	02:45:00	07:30	08:13	71.49	65.84
3	10:58:01	13:43:01	11:06:01	20:57:03	02:45:00	08:00	09:51	71.32	63.47
4	09:35:36	12:20:36	09:43:36	19:36:08	02:45:00	08:00	09:52	71.29	62.93
5	09:34:10	12:19:10	09:41:10	18:33:42	02:45:00	07:00	08:52	71.81	65.44

Table G - 20: Daily rainfall and outflow data – week 20

Day	Rainfall start	Rainfall end	Outflow Start	Outflow End	Rainfall duration (hh:mm:ss)	Time delay to discharge (mm:ss)	Time to outflow stop (hh:mm)	Rainfall volume (L)	Water draining during 24 h (L)
1	13:05:50	15:50:50	13:15:50	23:27:22	02:45:00	10:00	10:11	71.01	59.74
2	10:50:54	13:35:54	10:58:24	19:31:55	02:45:00	07:30	08:33	71.28	61.48
3	10:19:58	13:04:58	10:26:58	20:09:00	02:45:00	07:00	09:42	71.68	63.00
4	10:14:33	12:59:33	10:21:33	18:57:35	02:45:00	07:00	08:36	71.85	64.21
5	11:54:38	14:39:38	12:02:08	21:48:40	02:45:00	07:30	09:46	71.55	64.58

Table G - 21: Daily rainfall and outflow data – week 21

Day	Rainfall start	Rainfall end	Outflow Start	Outflow End	Rainfall duration (hh:mm:ss)	Time delay to discharge (mm:ss)	Time to outflow stop (hh:mm)	Rainfall volume (L)	Water draining during 24 h (L)
1	11:09:38	13:54:38	11:19:08	19:11:10	02:45:00	09:30	07:52	71.17	58.09
2	10:13:13	12:58:13	10:20:43	19:52:45	02:45:00	07:30	09:32	71.49	61.77
3	09:38:17	12:23:17	09:45:47	20:44:19	02:45:00	07:30	10:58	71.67	62.87
4	09:48:22	12:33:22	09:55:22	18:43:19	02:45:00	07:00	08:47	71.68	63.46
5	11:07:52	13:52:52	11:14:52	20:55:24	02:45:00	07:00	09:40	71.22	65.36

Table G - 22: Daily rainfall and outflow data – week 22

Day	Rainfall start	Rainfall end	Outflow Start	Outflow End	Rainfall duration (hh:mm:ss)	Time delay to discharge (mm:ss)	Time to outflow stop (hh:mm)	Rainfall volume (L)	Water draining during 24 h (L)
1	09:37:36	12:22:36	09:47:06	18:42:37	02:45:00	09:30	08:55	71.18	59.60
2	10:00:10	12:45:10	10:07:40	19:33:42	02:45:00	07:30	09:26	71.55	62.36
3	10:52:45	13:37:45	11:00:15	22:33:17	02:45:00	07:30	11:33	71.52	62.35
4	09:39:49	12:24:49	09:47:19	18:51:51	02:45:00	07:30	09:04	71.48	61.90
5	10:57:54	13:42:54	11:05:24	21:10:26	02:45:00	07:30	10:05	71.81	66.86

Table G - 23: Daily rainfall and outflow data – week 23

Day	Rainfall start	Rainfall end	Outflow Start	Outflow End	Rainfall duration (hh:mm:ss)	Time delay to discharge (mm:ss)	Time to outflow stop (hh:mm)	Rainfall volume (L)	Water draining during 24 h (L)
1	12:10:41	14:55:41	12:19:41	22:11:43	02:45:00	09:00	09:52	71.21	58.50
2	10:18:45	13:03:45	10:25:45	18:49:17	02:45:00	07:00	08:23	71.64	60.95
3	11:41:20	14:26:20	11:47:50	20:07:52	02:45:00	06:30	08:20	71.56	60.28
4	09:38:54	12:23:54	09:45:54	18:21:56	02:45:00	07:00	08:36	71.60	60.97
5	09:40:24	12:25:24	09:47:29	19:43:01	02:45:00	07:05	09:55	71.82	63.76

Table G - 24: Daily rainfall and outflow data – week 24

Day	Rainfall start	Rainfall end	Outflow Start	Outflow End	Rainfall duration (hh:mm:ss)	Time delay to discharge (mm:ss)	Time to outflow stop (hh:mm)	Rainfall volume (L)	Water draining during 24 h (L)
1	11:31:14	14:16:14	11:40:14	20:09:15	02:45:00	09:00	08:29	71.23	58.71
2	09:54:18	12:39:18	10:01:18	17:59:49	02:45:00	07:00	07:58	71.49	61.13
3	09:42:22	12:27:22	09:49:22	17:54:24	02:45:00	07:00	08:05	71.48	60.99
4	10:16:57	13:01:57	10:24:27	18:40:28	02:45:00	07:30	08:16	71.48	60.92
5	09:38:31	12:23:31	09:45:31	19:41:33	02:45:00	07:00	09:56	71.89	63.92

Table G – 25: Analysis of the mass balance of the measured water fluxes in the sediment experiment.

Days	Rainfall volume (L)	Evaporation (L)	Outflow (L)	Measured Retention (L)	Estimated Retention (L)	Unaccountable water (%)
1	71.06	0.72	53.9	16.44	0.00	0.00
2	71.62	0.72	65.53	5.37	6.30	14.74
3	71.63	0.72	66.11	4.80	6.35	24.38
4	71.63	0.72	66.32	4.59	6.38	28.09
5	71.36	0.72	67.63	3.01	6.43	53.16
6	71.34	0.72	64.59	6.03	6.41	5.92
7	71.42	0.72	65.72	4.98	6.39	22.05
8	71.59	0.72	66.26	4.61	6.43	28.25
9	71.85	0.72	66.99	4.14	6.43	35.65
10	71.45	0.72	68.65	2.08	6.41	67.57
11	71.51	0.72	65.21	5.58	6.43	13.29
12	71.94	0.72	67.23	3.99	6.47	38.33
13	71.53	0.72	66.59	4.22	6.51	35.20
14	71.45	0.72	66.07	4.66	6.52	28.50
15	71.81	0.72	70.1	0.99	6.59	84.98
16	71.41	0.72	65.65	5.04	6.59	23.53
17	71.61	0.72	67.51	3.38	6.55	48.43
18	71.96	0.72	69.72	1.52	6.58	76.89
19	71.56	0.72	68.75	2.09	6.55	68.10
20	71.18	0.72	70.19	0.27	6.60	95.91
21	71.73	0.72	67.11	3.90	6.60	40.91
22	72.05	0.72	69.76	1.57	6.56	76.06
23	71.02	0.72	67.71	2.59	6.56	60.50
24	71.85	0.72	67.85	3.28	6.62	50.48
25	71.92	0.72	70.55	0.65	6.62	90.19
26	71.4	0.72	62.29	8.39	6.61	-26.93
27	71.82	0.72	68.36	2.74	6.63	58.65
28	71.94	0.72	69.84	1.38	6.70	79.40
29	71.94	0.72	70	1.22	6.72	81.84
30	71.84	0.72	70.06	1.06	6.73	84.26
31	71.48	0.72	65.48	5.28	6.74	21.67
32	71.84	0.72	69.02	2.10	6.69	68.61
33	71.71	0.72	67.99	3.00	6.72	55.35
34	71.84	0.72	68.97	2.15	6.75	68.14
35	71.34	0.72	70.28	0.34	6.75	94.97

Days	Rainfall volume (L)	Evaporation (L)	Outflow (L)	Measured Retention (L)	Estimated Retention (L)	Unaccountable water (%)
36	71.42	0.72	63.55	7.15	6.74	-6.12
37	71.75	0.72	65.08	5.95	6.82	12.72
38	71.78	0.72	65.56	5.50	6.79	19.04
39	71.72	0.72	64.38	6.62	6.87	3.66
40	71.99	0.72	67.1	4.17	6.88	39.41
41	71.25	0.72	62.23	8.30	6.86	-21.03
42	71.76	0.72	65.41	5.63	6.84	17.73
43	71.69	0.72	64.15	6.82	6.83	0.14
44	71.77	0.72	64.42	6.63	6.88	3.66
45	71.03	0.72	64.87	5.44	6.91	21.26
46	71.38	0.72	59.84	10.82	6.91	-56.53
47	71.74	0.72	64.89	6.13	6.95	11.78
48	71.71	0.72	64.27	6.72	7.01	4.11
49	71.68	0.72	63.7	7.26	7.11	-2.16
50	71.41	0.72	63.74	6.95	7.11	2.32
51	71.51	0.72	60.25	10.54	7.23	-45.77
52	71.68	0.72	62.59	8.37	7.30	-14.67
53	71.76	0.72	63.27	7.77	7.37	-5.42
54	71.69	0.72	63.17	7.80	7.37	-5.89
55	71.75	0.72	65.5	5.53	7.35	24.72
56	71.5	0.72	60.72	10.06	7.35	-36.83
57	71.78	0.72	63.27	7.79	7.40	-5.28
58	71.8	0.72	63.56	7.52	7.41	-1.53
59	71.71	0.72	62.57	8.42	7.39	-13.89
60	71.41	0.72	63.95	6.74	7.42	9.17
61	71.5	0.72	60.6	10.18	7.47	-36.24
62	71.77	0.72	64.42	6.63	7.59	12.69
63	71.74	0.72	64.15	6.87	7.60	9.57
64	71.75	0.72	64.32	6.71	7.59	11.62
65	71.66	0.72	65.2	5.74	7.59	24.38
66	71.25	0.72	59.78	10.75	7.58	-41.76
67	71.95	0.72	66.21	5.02	7.64	34.27
68	71.61	0.72	64.43	6.46	7.67	15.74
69	71.57	0.72	63.66	7.19	7.67	6.29
70	71.2	0.72	64.85	5.63	7.67	26.60
71	71.35	0.72	60.42	10.21	7.65	-33.49
72	71.71	0.72	65.05	5.94	7.71	22.94

Days	Rainfall volume (L)	Evaporation (L)	Outflow (L)	Measured Retention (L)	Estimated Retention (L)	Unaccountable water (%)
73	71.83	0.72	65.72	5.39	7.71	30.10
74	71.47	0.72	63.79	6.96	7.69	9.52
75	71.74	0.72	65.96	5.06	7.68	34.10
76	71.32	0.72	59.87	10.73	7.71	-39.19
77	71.9	0.72	65.6	5.58	7.70	27.50
78	71.69	0.72	64.41	6.56	7.70	14.81
79	71.63	0.72	63.79	7.12	7.70	7.52
80	71.01	0.72	65.65	4.64	7.67	39.53
81	71.3	0.72	61.36	9.22	7.68	-20.03
82	71.53	0.72	63.96	6.85	7.70	10.99
83	71.35	0.72	63.03	7.60	7.71	1.39
84	71.35	0.72	63.56	7.07	7.70	8.18
85	71.07	0.72	65.16	5.19	7.70	32.63
86	71.28	0.72	62.05	8.51	7.72	-10.24
87	71.35	0.72	63.42	7.21	7.72	6.58
88	71.49	0.72	64.32	6.45	7.71	16.37
89	71.32	0.72	63.14	7.46	7.70	3.10
90	71.49	0.72	64.7	6.07	7.70	21.21
91	71.23	0.72	58.37	12.14	7.71	-57.40
92	71.49	0.72	65.84	4.93	7.71	36.05
93	71.32	0.72	63.47	7.13	7.70	7.44
94	71.29	0.72	62.93	7.64	7.71	0.91
95	71.81	0.72	65.44	5.65	7.71	26.72
96	71.01	0.72	59.74	10.55	7.70	-36.99
97	71.28	0.72	61.48	9.08	7.71	-17.73
98	71.68	0.72	63	7.96	7.71	-3.21
99	71.85	0.72	64.21	6.92	7.71	10.28
100	71.55	0.72	64.58	6.25	7.72	19.02
101	71.17	0.72	58.09	12.36	7.71	-60.31
102	71.49	0.72	61.77	9.00	7.72	-16.60
103	71.67	0.72	62.87	8.08	7.72	-4.68
104	71.68	0.72	63.46	7.50	7.71	2.78
105	71.22	0.72	65.36	5.14	7.73	33.47
106	71.18	0.72	59.6	10.86	7.71	-40.79
107	71.55	0.72	62.36	8.47	7.71	-9.91
108	71.52	0.72	62.35	8.45	7.70	-9.71
109	71.48	0.72	61.9	8.86	7.70	-15.00

Days	Rainfall volume (L)	Evaporation (L)	Outflow (L)	Measured Retention (L)	Estimated Retention (L)	Unaccountable water (%)
110	71.81	0.72	66.86	4.23	7.71	45.10
111	71.21	0.72	58.5	11.99	7.71	-55.50
112	71.64	0.72	60.95	9.97	7.72	-29.15
113	71.56	0.72	60.28	10.56	7.72	-36.81
114	71.6	0.72	60.97	9.91	7.72	-28.34
115	71.82	0.72	63.76	7.34	7.72	4.95
116	71.23	0.72	58.71	11.80	7.71	-53.00
117	71.49	0.72	61.13	9.64	7.72	-24.93
118	71.48	0.72	60.99	9.77	7.72	-26.62
119	71.48	0.72	60.92	9.84	7.72	-27.51
120	71.89	0.72	63.92	7.25	7.72	6.06

Appendix H Outflow duration

Table H - 1: Outflow duration during the whole period of the experiment

Simulated Week	Outflow duration (hours)				
	Day 1	**Day 2**	**Day 3**	**Day 4**	**Day 5**
1	7.27	8.73	7.72	9.54	9.79
2	6.77	9.62	9.88	10.99	8.53
3	10.26	8.73	6.83	6.88	8.37
4	8.81	8.51	9.56	7.54	10.17
5	9.92	8.43	9.45	10.35	10.45
6	8.92	8.93	7.06	8.30	9.58
7	8.13	7.88	7.47	8.51	9.13
8	8.28	8.49	10.09	6.94	10.83
9	8.90	10.09	7.95	9.33	9.62
10	9.24	9.20	9.41	11.85	10.88
11	10.71	9.02	10.93	8.39	9.98
12	12.18	11.93	11.98	13.13	11.11
13	11.08	11.44	11.58	11.78	10.80
14	11.31	10.03	11.15	12.62	13.25
15	11.61	12.03	13.19	11.69	13.40
16	10.93	11.89	11.68	12.54	13.18
17	11.23	10.61	10.68	11.03	12.70
18	11.67	12.48	12.78	13.64	11.13
19	13.20	12.88	12.05	12.40	11.21
20	11.48	11.24	12.44	12.32	13.29
21	11.03	12.58	12.18	11.52	12.18
22	11.40	14.76	13.60	12.01	14.46
23	12.21	11.16	13.02	14.18	13.08
24	12.36	12.68	13.48	11.68	13.18

Table H - 2: Statistic analysis of outflow duration based on weekdays, before and after sediment

	Pre-sediment addition				**Post-sediment addition**			
	Mean	**SD**	**Min**	**Max**	**Mean**	**SD**	**Min**	**Max**
Day 1	8.60	1.55	6.77	10.26	10.83	1.45	8.13	13.20
Day 2	8.80	0.47	8.43	9.62	11.02	1.79	7.88	14.76
Day 3	8.69	1.34	6.83	9.88	11.20	1.99	7.06	13.60
Day 4	9.06	1.78	6.88	10.99	11.26	2.00	6.94	14.18
Day 5	9.46	0.95	8.37	10.45	11.74	1.57	9.13	14.46

Appendix I Start delay

Table I - 1: Start delay during the whole period of the experiment

Simulated Week	Outflow duration (hours)				
	Day 1	Day 2	Day 3	Day 4	Day 5
1	23.00	7.50	7.50	7.50	7.52
2	9.00	7.00	6.50	6.00	6.00
3	7.00	6.50	6.50	6.50	6.50
4	7.50	7.00	7.00	7.00	7.00
5	8.52	6.50	7.00	7.00	6.00
6	9.50	5.50	6.50	6.50	6.50
7	8.50	6.50	7.00	7.00	6.50
8	9.50	7.50	7.00	7.50	7.00
9	9.00	7.50	8.00	7.50	8.00
10	10.00	7.50	7.00	7.50	7.50
11	9.00	7.50	7.00	7.50	6.98
12	8.00	7.00	7.00	7.00	7.00
13	7.50	6.50	7.00	7.50	7.00
14	8.50	7.00	6.50	7.50	6.50
15	10.00	8.00	7.50	7.50	7.50
16	10.50	7.00	8.00	7.50	7.00
17	10.50	8.00	7.50	7.00	7.00
18	9.50	7.50	7.50	7.00	7.00
19	10.00	7.50	8.00	7.00	7.00
20	10.00	7.50	7.00	7.00	7.00
21	9.50	7.50	7.50	7.00	7.00
22	9.50	7.50	7.50	7.50	7.50
23	10.00	8.00	7.50	7.00	7.08
24	10.00	8.00	7.50	7.50	7.50

Table I - 2: Statistic analysis of start delay based on weekdays, before and after sediment

	Pre-sediment addition				**Post-sediment addition**			
	Mean	**SD**	**Min**	**Max**	**Mean**	**SD**	**Min**	**Max**
Day 1	11.00	6.75	7.00	23.00	9.42	0.82	7.50	10.50
Day 2	6.90	0.42	6.50	7.50	7.32	0.63	5.50	8.00
Day 3	6.90	0.42	6.50	7.50	7.29	0.45	6.50	8.00
Day 4	6.80	0.57	6.00	7.50	7.24	0.31	6.50	7.50
Day 5	6.60	0.66	6.00	7.52	7.08	0.38	6.50	8.00

Appendix J Infiltration rate test

Table J - 1: Test 1 in August 2014, data for Resistance Outflow (r) Time and Outflow Time (t)

Water Temperature: 16 C°						
Test date: 14 / 08/ 2014						
Test no	**Resistance Outflow Time (r)**	**Resistance Outflow Time corrected to 20 °C (r)**	**Outflow Time (t)**	**Outflow Time corrected to 20 °C (t)**	**Infiltration rate**	**Infiltration rate**
	(Sec)	**(Sec)**	**(Sec)**	**(Sec)**	**(mm h^{-1})**	**L $sec^{-1}ha^{-1}$**
1	1.16	1.05	8.9	8.02	2947.55	8187.64
2	1.02	0.92	9.07	8.17	2885.04	8013.99
3	1.01	0.91	9.15	8.24	2856.53	7934.79
4	0.97	0.87	9.46	8.52	2751.17	7642.15
5	1.03	0.93	9.39	8.46	2774.28	7706.33
6	1.02	0.92	9.29	8.37	2807.97	7799.90
7	1.12	1.01	9.42	8.49	2764.33	7678.69
8	1.15	1.04	9.64	8.68	2693.49	7481.93
9	0.96	0.86	9.38	8.45	2777.61	7715.59
10	1.09	0.98	9.25	8.33	2821.67	7837.97

Table J - 2: Test 2 in August 2014, data for Resistance Outflow (r) Time and Outflow Time (t)

Water Temperature: 16 C°						
Test date: 15 / 08/ 2014						
Test no	**Resistance Outflow Time (r)**	**Resistance Outflow Time corrected to 20 °C (r)**	**Outflow Time (t)**	**Outflow Time corrected to 20 °C (t)**	**Infiltration rate**	**Infiltration rate**
	(sec)	**(sec)**	**(sec)**	**(sec)**	**(mm h^{-1})**	**L $sec^{-1}ha^{-1}$**
1	1.05	0.95	9.9	8.92	2614.32	7262.01
2	0.82	0.74	9.57	8.62	2715.64	7543.43
3	0.99	0.89	9.03	8.14	2899.50	8054.18
4	1.17	1.05	9.01	8.12	2906.79	8074.43
5	1.07	0.96	8.88	8.00	2955.08	8208.56
6	0.9	0.81	8.95	8.06	2928.88	8135.79
7	0.95	0.86	9.09	8.19	2877.85	7994.04
8	1.05	0.95	9.5	8.56	2738.14	7605.96
9	1.06	0.95	9.21	8.30	2835.51	7876.42
10	1.12	1.01	9.56	8.61	2718.83	7552.30

Table J - 3: Test 1 in May 2013, data for Resistance Outflow (r) Time and Outflow Time (t)

Water Temperature: 13 C°						
Test date: 13 / 05/ 2013						
Test no	**Resistance Outflow Time (r)**	**Resistance Outflow Time corrected to 20 °C (r)**	**Outflow Time (t)**	**Outflow Time corrected to 20 °C (t)**	**Infiltration rate**	**Infiltration rate**
	(sec)	**(sec)**	**(sec)**	**(sec)**	**(mm h^{-1})**	**L $sec^{-1}ha^{-1}$**
1	1.14	0.95	5.5	4.58	5733.94	15927.62
2	1.1	0.92	5.78	4.82	5387.93	14966.48
3	1.09	0.91	6.16	5.13	4980.08	13833.55
4	1.1	0.92	6.03	5.03	5112.47	14201.32
5	1.03	0.86	6.12	5.10	5020.08	13944.67
6	1.1	0.92	6.06	5.05	5081.30	14114.72
7	1.03	0.86	6.15	5.13	4990.02	13861.17
8	1.03	0.86	6.25	5.21	4892.37	13589.91
9	1.03	0.86	6.15	5.13	4990.02	13861.17
10	1.06	0.88	6.25	5.21	4892.37	13589.91

Table J - 4: Test 1 in May 2013, data for Resistance Outflow (r) Time and Outflow Time (t)

Water Temperature: 13 C°						
Test date: 20 / 05/ 2013						
Test no	**Resistance Outflow Time (r)**	**Resistance Outflow Time corrected to 20 °C (r)**	**Outflow Time (t)**	**Outflow Time corrected to 20 °C (t)**	**Infiltration rate**	**Infiltration rate**
	(sec)	**(sec)**	**(sec)**	**(sec)**	**(mm h^{-1})**	**L $sec^{-1}ha^{-1}$**
1	1.05	0.88	6.00	5.00	5144.03	14288.98
2	0.82	0.68	5.80	4.83	5364.81	14902.24
3	0.99	0.83	5.47	4.56	5770.04	16027.88
4	1.17	0.98	6.46	5.38	4698.71	13051.98
5	1.07	0.89	6.38	5.32	4769.34	13248.16
6	0.9	0.75	5.42	4.52	5835.34	16209.27
7	0.95	0.79	5.51	4.59	5722.01	15894.48
8	1.05	0.88	6.76	5.63	4450.32	12362
9	1.06	0.88	6.58	5.48	4594.05	12761.26
10	1.12	0.93	5.79	4.83	5371.79	14921.65

Appendix K Suspended solids concentration

Table K - 1: Analysis of outflow samples within a 1-year simulation

Sample no.	Simulated		Date	Sample container	Mass of filter after the filtration (b) mg	Mass of filter before the filtration (a) mg	The volume of the sample (v) mL	Suspended solids (ρ) mg/L
	Year	Week						
1	1	1	25-Sep-13	A3	30636.25	30633.1	100	31.50
2			25-Sep-13	A4	30711.89	30706.8	100	50.90
3			25-Sep-13	B2	31251.4	31247.5	100	39.00
4			26-Sep-13	A1	31146.4	31140.5	100	59.00
5			26-Sep-13	A2	31051.25	31046.8	100	44.50
6			26-Sep-13	B1	30638.8	30633.3	100	55.00
7			27-Sep-13	A3	31139.6	31139.1	100	5.00
8			27-Sep-13	A4	31048.5	31047.3	100	12.00
9			27-Sep-13	B2	30632.3	30631.6	100	7.00
10			30-Sep-13	A1	31271.4	31265.5	100	59.00
11			30-Sep-13	A2	30729.4	30728.2	100	12.00
12			30-Sep-13	B1	31142	31141	100	10.00
13		2	01-Oct-13	A3	31047.8	31046.5	100	13.00
14			01-Oct-13	A4	30634.4	30633.1	100	13.00
15			02-Oct-13	B2	30579.7	30576.8	100	29.00
16			02-Oct-13	A1	30647.1	30646.4	100	7.00
17			02-Oct-13	A2	31706.6	31706.1	100	5.00
18			02-Oct-13	B1	30713.1	30712.4	100	7.00
19			02-Oct-13	A3	30657	30655	100	20.00
20			02-Oct-13	A4	31703.3	31702.8	100	5.00
21			02-Oct-13	B2	30610	30609.2	100	8.00
22			02-Oct-13	A1	30645	30644.5	100	5.00
23			02-Oct-13	A2	31141.8	31141	100	8.00
24			02-Oct-13	B1	31047.4	31046.5	100	9.00

Table K - 2: Analysis of outflow samples within a 2-year simulation

Sample no.	Simulated		Date	Sample container	Mass of filter after the filtration (b) mg	Mass of filter before the filtration (a) mg	The volume of the sample (v) mL	Suspended solids (ρ) mg/L
	Year	Wee						
1	2	3	08-Oct-13	A3	30712.8	30712.6	100	2.00
2			08-Oct-13	A4	30541.4	30541	100	4.00
3			08-Oct-13	B2	30653.4	30653.2	100	2.00
4			09-Oct-13	A1	30799.7	30798.9	100	8.00
5			09-Oct-13	A2	30704.6	30704.4	100	2.00
6			09-Oct-13	B1	31711.4	31710.9	100	5.00
7			09-Oct-13	A3	30540.6	30539.7	100	9.00
8		4	14-Oct-13	A4	31136.6	31136.4	100	2.00
9			14-Oct-13	B2	31043.7	31042.6	100	11.00
10			15-Oct-13	A1	30629.9	30629.7	100	2.00
11			15-Oct-13	A2	30706.3	30705.6	100	7.00
12			16-Oct-13	B1	31136.7	31136.5	100	2.00
13			16-Oct-13	A3	31043.5	31042.6	100	9.00
14			17-Oct-13	A4	30630	30629.7	100	3.00
15			17-Oct-13	B2	30704.7	30704.3	100	4.00
16			17-Oct-13	A1	30480.6	30480.2	100	4.00
17			18-Oct-13	A2	31138.3	31137.8	100	5.00
18			18-Oct-13	B1	31043.5	31042.8	100	7.00
19			18-Oct-13	A3	46082.7	46082.1	100	6.00
20			18-Oct-13	A4	47238.6	47238	100	6.00

Table K - 3: Analysis of outflow samples within a 3-year simulation

Sample no.	Simulated		Date	Sample container	Mass of filter after the filtration (b) mg	Mass of filter before the filtration (a) mg	The volume of the sample (v) mL	Suspended solids (ρ) mg/L
	Year	Week						
1	3	5	21-Oct-13	B2	30630.8	30630.4	100	4.00
2			21-Oct-13	A1	30703	30702.5	100	5.00
3			21-Oct-13	A2	30480.8	30480.3	100	5.00
4			22-Oct-13	B1	31137.6	31137.2	100	4.00
5			22-Oct-13	A3	31043	31042.5	100	5.00
6			22-Oct-13	A4	46084.5	46083.7	100	8.00
7			23-Oct-13	B2	30631.8	30630.9	100	9.00
8			23-Oct-13	A1	30703.6	30702.5	100	11.00
9			23-Oct-13	A2	30479.1	30478.9	100	2.00
10			24-Oct-13	B1	31135.8	31135.6	100	2.00
11			24-Oct-13	A3	31043.6	31043.1	100	5.00
12			24-Oct-13	A4	46083.9	46083.2	100	7.00
13		6	29-Oct-13	B2	30630.4	30630.2	100	2.00
14			29-Oct-13	A1	30703.5	30703.3	100	2.00
15			29-Oct-13	A2	47236.8	47236.6	100	2.00
16			30-Oct-13	B1	31137.5	31137.1	100	4.00
17			30-Oct-13	A3	31043.7	31042.9	100	8.00
18			30-Oct-13	A4	46081.8	46081.5	100	3.00
19			01-Nov-13	B2	30630.5	30629.9	100	6.00
20			01-Nov-13	A1	30705.3	30704.5	100	8.00
21			01-Nov-13	A2	47239.3	47238.5	100	8.00

Table K - 4: Analysis of outflow samples within a 4-year simulation

Sample no.	Simulated		Date	Sample container	Mass of filter after the filtration (b) mg	Mass of filter before the filtration (a) mg	The volume of the sample (v) mL	Suspended solids (ρ) mg/L
	Year	Wee						
1	4	7	05-Nov-13	B1	31137.8	31137.6	100	2.00
2			05-Nov-13	A3	31043.9	31043.7	100	2.00
3			05-Nov-13	A4	46082.8	46082.6	100	2.00
4			06-Nov-13	B2	30630.8	30630.6	100	2.00
5			06-Nov-13	A1	30704	30703.6	100	4.00
6			06-Nov-13	A2	47236.8	47236.6	100	2.00
7			07-Nov-13	B1	31137.4	31136.8	100	6.00
8			07-Nov-13	A3	31043.4	31043	100	4.00
9			07-Nov-13	A4	46083.4	46083	100	4.00
10		8	12-Nov-13	B2	31139	31138.4	100	6.00
11			12-Nov-13	A1	31043.1	31042.3	100	8.00
12			12-Nov-13	A2	46085.1	46084.6	100	5.00
13			14-Nov-13	B1	30630.5	30630.3	100	2.00
14			14-Nov-13	A4	30704.7	30703.8	100	9.00
15			14-Nov-13	B2	47235.5	47235.2	100	3.00

Table K - 5: Analysis of outflow samples within a 5-year simulation

Sample no.	Simulated		Date	Sample container	Mass of filter after the filtration (b) mg	Mass of filter before the filtration (a) mg	The volume of the sample (v) mL	Suspended solids (ρ) mg/L
	Year	Wee						
1	5	9	19-Nov-13	A3	30631.3	30630.5	100	8.00
2			19-Nov-13	A4	30703	30702.3	100	7.00
3			19-Nov-13	B2	47238	47237.6	100	4.00
4			20-Nov-13	A1	31137.4	31137.2	100	2.00
5			20-Nov-13	A2	31043.7	31043.4	100	3.00
6			20-Nov-13	B1	46082.8	46082.4	100	4.00
7			21-Nov-13	A3	30632.4	30631.6	100	8.00
8			21-Nov-13	A4	30704.8	30703.9	100	9.00
9			21-Nov-13	B2	47237	47236.5	100	5.00
10		10	27-Nov-13	A1	31137.3	31136.7	100	6.00
11			27-Nov-13	A2	31042.1	31041.8	100	3.00
12			27-Nov-13	B1	46083.3	46083.1	100	2.00
13			28-Nov-13	A3	30630.3	30629.7	100	6.00
14			28-Nov-13	A4	30703.7	30703.3	100	4.00
15			28-Nov-13	B2	47235.6	47235.3	100	3.00

Table K - 6: Analysis of outflow samples within a 6-year simulation

Sample no.	Simulated		Date	Sample container	Mass of filter after the filtration (b) mg	Mass of filter before the filtration (a) mg	The volume of the sample (v) mL	Suspended solids (ρ) mg/L
	Year	Wee						
1	6	11	03-Dec-13	A3	30629.6	30628.6	100	10.00
2			03-Dec-13	A4	30704.8	30704.5	100	3.00
3			03-Dec-13	B2	47237.4	47236.9	100	5.00
4			04-Dec-13	A1	31137.5	31136.8	100	7.00
5			04-Dec-13	A2	31042.5	31041.6	100	9.00
6			04-Dec-13	B1	46081.5	46081	100	5.00
7			05-Dec-13	A3	30630.9	30630.3	100	6.00
8			05-Dec-13	A4	30702.3	30701.5	100	8.00
9			05-Dec-13	B2	47236.9	47236.2	100	7.00
10		12	10-Dec-13	A3	30630.1	30629.6	100	5.00
11			10-Dec-13	A4	30703	30702.7	100	3.00
12			10-Dec-13	B2	47236.2	47236	100	2.00
13			11-Dec-14	A1	31136.3	31135.8	100	5.00
14			11-Dec-14	A2	31043.3	31042.7	100	6.00
15			11-Dec-14	B1	46081.5	46081.2	100	3.00
16			12-Dec-14	A3	30630.2	30629.8	100	4.00
17			12-Dec-14	A4	30702.2	30701.8	100	4.00
18			12-Dec-14	B2	47236.5	47235.8	100	7.00

Table K - 7: Analysis of outflow samples within a 7-year simulation

Sample no.	Simulated		Date	Sample container	Mass of filter after the filtration (b) mg	Mass of filter before the filtration (a) mg	The volume of the sample (v) mL	Suspended solids (ρ) mg/L
	Year	Wee						
1	7	13	15-Jan-14	A1	30633.6	30632.2	100	14.00
2			15-Jan-14	A2	30704.7	30704.3	100	4.00
3			15-Jan-14	B1	47236.8	47236.2	100	6.00
4			16-Jan-14	A3	31137.6	31136.6	100	10.00
5			16-Jan-14	A4	31042.6	31041.9	100	7.00
6			16-Jan-14	B2	46083.6	46082.7	100	9.00
7		14	21-Jan-14	A3	30630.6	30630	100	6.00
8			21-Jan-14	A4	30703.7	30703.1	100	6.00
9			21-Jan-14	B2	47236.6	47236	100	6.00
10			22-Jan-14	A1	31137.8	31138.8	100	12.00
11			22-Jan-14	A2	31044	31043.7	100	3.00
12			22-Jan-14	B1	46082.5	46081.9	100	6.00

Table K - 8: Analysis of outflow samples within a 8-year simulation

Sample no.	Simulated		Date	Sample container	Mass of filter after the filtration (b) mg	Mass of filter before the filtration (a) mg	The volume of the sample (v) mL	Suspended solids (ρ) mg/L
	Year	Wee						
1	8	15	28-Jan-14	A3	30633.2	30632.6	100	6.00
2			28-Jan-14	A4	30706.5	30705.7	100	8.00
3			28-Jan-14	B2	47238.3	47237.6	100	7.00
4			29-Jan-14	A1	31137.4	31137.2	100	2.00
5			29-Jan-14	A2	31045.1	31044.7	100	4.00
6			29-Jan-14	B1	46084.2	46083.3	100	9.00
7			30-Jan-14	A3	30630.3	30629.8	100	5.00
8			30-Jan-14	A4	30704.1	30703.5	100	6.00
9			30-Jan-14	B2	47237.7	47236.3	100	14.00
10		16	04-Feb-14	A1	31138	31137.3	100	7.00
11			04-Feb-14	A2	31044.6	31043.6	100	10.00
12			04-Feb-14	B1	46084.6	46083.3	100	13.00
13			05-Feb-14	A3	30631.2	30630.2	100	10.00
14			05-Feb-14	A4	30703.9	30703.3	100	6.00
15			05-Feb-14	B2	47237	47236.2	100	8.00
16			06-Feb-14	A1	31139.6	31138.6	100	10.00
17			06-Feb-14	A2	31045.8	31044.7	100	11.00
18			06-Feb-14	B1	46082.6	46081.4	100	12.00

Table K - 9: Analysis of outflow samples within a 9-year simulation

Sample no.	Simulated		Date	Sample container	Mass of filter after the filtration (b) mg	Mass of filter before the filtration (a) mg	The volume of the sample (v) mL	Suspended solids (ρ) mg/L
	Year	Wee						
1	9	17	11-Feb-14	A3	30633.1	30632.4	100	7.00
2			11-Feb-14	A4	30705.2	30704.8	100	4.00
3			11-Feb-14	B2	47239.4	47238.8	100	6.00
4			12-Feb-14	A1	31137.4	31136.6	100	8.00
5			12-Feb-14	A2	31045.2	31044.1	100	11.00
6			12-Feb-14	B1	46083.5	46083.2	100	3.00
7			13-Feb-14	A3	30630.9	30630.5	100	4.00
8			13-Feb-14	A4	30705.5	30704.9	100	6.00
9			13-Feb-14	B2	47239.5	47238.8	100	7.00
10		18	18-Feb-14	A1	31138.3	31137.2	100	11.00
11			18-Feb-14	A2	31043.2	31042	100	12.00
12			18-Feb-14	B1	46082.2	46081.2	100	10.00
13			19-Feb-14	A3	30632.5	30631.1	100	14.00
14			19-Feb-14	A4	30705.1	30704.1	100	10.00
15			19-Feb-14	B2	47239.2	47238	100	12.00
16			20-Feb-14	A1	31138.9	31138.2	100	7.00
17			20-Feb-14	A2	31045.4	31044.6	100	8.00
18			20-Feb-14	B1	46083.1	46082.3	100	8.00

Table K - 10: Analysis of outflow samples within a 10-year simulation

Sample no.	Simulated		Date	Sample container	Mass of filter after the filtration (b) mg	Mass of filter before the filtration (a) mg	The volume of the sample (v) mL	Suspended solids (ρ) mg/L
	Year	Wee						
1	10	19	25-Feb-14	A1	31140.5	31139.4	100	11.00
2			25-Feb-14	A2	31045.7	31045.3	100	4.00
3			25-Feb-14	B1	46082.9	46082.6	100	3.00
4			26-Feb-14	A3	30631.4	30630.4	100	10.00
5			26-Feb-14	A4	30704.9	30704.2	100	7.00
6			26-Feb-14	B2	47238.1	47236.9	100	12.00
7			27-Feb-14	A1	31138.8	31138.3	100	5.00
8			27-Feb-14	A2	31044.3	31043.5	100	8.00
9			27-Feb-14	B1	46083.2	46083	100	2.00
10		20	04-Mar-14	A1	31139.8	31139	100	8.00
11			04-Mar-14	A2	31044.1	31043.1	100	10.00
12			04-Mar-14	B1	46084.4	46083.6	100	8.00
13			05-Mar-14	A3	30632.4	30631.7	100	7.00
14			05-Mar-14	A4	30705.9	30705.5	100	4.00
15			05-Mar-14	B2	47238.4	47237.9	100	5.00

Table K - 11: Analysis of outflow samples within a 11-year simulation

Sample no.	Simulated		Date	Sample container	Mass of filter after the filtration (b) mg	Mass of filter before the filtration (a) mg	The volume of the sample (v) mL	Suspended solids (ρ) mg/L
	Yea	Wee						
1	11	21	11-Mar-14	A1	30632.4	30631.7	100	7.00
2			11-Mar-14	A2	30705.9	30705.5	100	4.00
3			11-Mar-14	B1	47238.4	47237.9	100	5.00
4			12-Mar-14	A1	30633.7	30632.7	100	10.00
5			12-Mar-14	A2	30707.8	30706.4	100	14.00
6			12-Mar-14	B1	47240	47238.6	100	14.00
7			13-Mar-14	A3	31139.5	31138.5	100	10.00
8			13-Mar-14	A4	31044.9	31043.4	100	15.00
9			13-Mar-14	B2	46084.5	46083.3	100	12.00
10			13-Mar-14	A1	30632.7	30631.1	100	16.00
11			13-Mar-14	A2	30706	30704.9	100	11.00
12			13-Mar-14	B1	47238.7	47236.4	100	23.00
13		22	18-Mar-14	A1	30706.7	30705.8	100	9.00
14			18-Mar-14	A2	30632.6	30631.3	100	13.00
15			18-Mar-14	B1	47238.9	47237.8	100	11.00
16			19-Mar-14	A3	31140.3	31139.2	100	11.00
17			19-Mar-14	A4	31046.7	31045.6	100	11.00
18			19-Mar-14	B2	46084.2	46083.5	100	7.00
19			20-Mar-14	A1	30633.4	30633	100	4.00
20			20-Mar-14	A2	30706.1	30705.6	100	5.00
21			20-Mar-14	B1	47239.2	47239	100	2.00

Table K - 12: Analysis of outflow samples within a 12-year simulation

Sample no.	Simulated		Date	Sample container	Mass of filter after the filtration (b) mg	Mass of filter before the filtration (a) mg	The volume of the sample (v) mL	Suspended solids (ρ) mg/L
	Year	Wee						
1	12	23	25-Mar-14	A1	30633.1	30632.6	100	5.00
2			25-Mar-14	A2	30705.6	30705.3	100	3.00
3			25-Mar-14	B1	47238	47237.5	100	5.00
4			26-Mar-14	A3	31140.4	31140.1	100	3.00
5			26-Mar-14	A4	31044.2	31043.7	100	5.00
6			26-Mar-14	B2	46083.8	46083.2	100	6.00
7			27-Mar-14	A1	30633	30632	100	10.00
8			27-Mar-14	A2	30707.2	30706.1	100	11.00
9			27-Mar-14	B1	47238.7	47237.5	100	12.00
10		24	01-Apr-14	A1	31139.1	31138.4	100	7.00
11			01-Apr-14	A2	31045.8	31045.2	100	6.00
12			01-Apr-14	B1	46085.7	46084.8	100	9.00
13			02-Apr-14	A3	30633.3	30632.2	100	11.00
14			02-Apr-14	A4	30706.5	30705.8	100	7.00
15			02-Apr-14	B2	47239.2	47238.3	100	9.00
16			03-Apr-14	A1	31142	31140.6	100	14.00
17			03-Apr-14	A2	31047.4	31046.7	100	7.00
18			03-Apr-14	B1	46085	46084.2	100	8.00

Appendix L Regression Analysis

Pre-sediment phase

Table L - 1: Showing model summary for pre-sediment phase

Model	R	R2	Adjusted R2	Std. Error	Change statistics				
					R2 change	F change	df1	df2	Sig. Fchange
1	0.844	0.712	0.637	1.92	0.712	9.414	5	19	0.000

Table L - 2: Showing ANOVA for pre-sediment phase

Model		Sum of squares	Df	Mean square	F	Sig.
1	Regression	173.715	5	34.743	9.414	0.000
	Residual	70.124	19	3.691		
	Total	243.838	24			

Table L - 3: Showing Coefficients for pre-sediment phase

Model		Unstandardized Coefficients		Standardized Coefficients	t	Sig.	95.0% Confidence Interval for B	
		B	Std. Error	Beta			Lower Bound	Upper Bound
1	(Constant)	-1040.69	543.04		-2.370	.0794	-1569.277	-97.316
	x_4(pre)	-0.12	0.22	0.492	1.071	0.6162	-0.074	.229
	x_2(pre)	14.14	28.0	-0.288	-.493	0.6228	-30.122	18.644
	x_3(pre)	12.14	38.68	0.840	1.693	0.0217	-9.449	89.441
	x_1(pre)	8.75	3.32	0.301	2.285	0.0217	.295	6.738

Post-sediment phase

Table L - 4: Showing model summary for post-sediment phase

Model	R	R2	Adjusted R2	Std. Error	Change statistics				
					R2 change	F change	df1	df2	Sig. Fchange
1	.680	.463	.439	1.9788989	.463	19.387	4	90	0.000

Table L - 5: Showing ANOVA for post-sediment phase

Model		Sum of squares	Df	Mean square	F	Sig.
1	Regression	303.683	4	75.921	19.387	0.000
	Residual	352.444	90	3.916		
	Total	656.127	94			

Table L - 6: Showing Coefficients for post-sediment phase

Model		Unstandardized Coefficients		Standardized Coefficients	t	Sig.	95.0% Confidence Interval for B	
		B	Std. Error	Beta			Lower Bound	Upper Bound
1	(Constant)	-73.78	96.99		-2.097	0.4499	-334.358	-9.044
	x_5(post)	-3806.11	2319.88	0.492	0.849	0.1061	-0.391	0.975
	x_4(post)	6.44	3.91	-0.012	-0.054	0.1043	-9.335	8.840
	x_2(post)	-6.57	4.00	-0.530	-1.567	0.1060	-12.476	1.473
	x_3(post)	-3.79	3.10	0.120	0.513	0.2271	-3.053	5.177
	x_1(post)	4.64	1.23	0.404	4.933	0.0004	2.659	6.245